

**Synthesis and Biological Evaluation of Novel Inhibitors of
Protein Biogenesis at the Endoplasmic Reticulum**

A thesis submitted to The University of Manchester for the degree of
Doctor of Philosophy in the Faculty of Engineering and Physical
sciences

2011

Helen Williams

School of Chemistry

CONTENTS

CONTENTS	2
ABSTRACT	6
DECLARATION	7
COPYRIGHT STATEMENT	7
ACKNOWLEDGEMENTS	9
ABBREVIATIONS	11
CHAPTER 1: INTRODUCTION	15
1.1 Protein biosynthesis and quality control	15
1.2 Protein synthesis at the endoplasmic reticulum.....	17
1.2.1 Protein targeting and translocation at the endoplasmic reticulum	17
1.2.2 Sec61	20
1.3 Protein folding and quality control at the ER.....	21
1.3.1 Chaperones.....	22
1.3.2 <i>N</i> -Glycosylation	22
1.4 Endoplasmic reticulum associated degradation.....	24
1.4.1 Recognition and targeting.....	25
1.4.2 Retro-translocation and ubiquitination.....	26
1.5 The Unfolded Protein Response	29
1.6 ER function and disease	29

1.7 Small molecule inhibitors of ER function.....	30
1.7.1 Eeyarestatins	31
1.7.2 Synthesis of Eeyarestatins	33
1.7.3 Other inhibitors of translocation - Cotransin	39
1.7.4 Synthesis of HUN-7293 and its analogues	40
1.8 Click Chemistry.....	52
1.9 Project aims	56
CHAPTER 2: RESULTS AND DISCUSSION PART I: CHEMISTRY	61
2.1 Synthesis of ESI and ESII	61
2.1.1 ESI.....	61
2.1.2 ESII.....	67
2.2 Synthesis of ESI and ESII analogues.....	68
2.2.1 <i>p</i> -nitrophenyl analogue of ESII.....	68
2.2.2 Synthesis of symmetrical ESI analogues.....	69
2.2.3 Synthesis of unsymmetrical ESI analogues.....	71
2.3 Synthesis of “short form” Eeyarestatins.....	74
2.4 Preparation of acetylene derivative suitable for click chemistry.....	76
2.4.1 Acetylene analogues of ESI.....	76
2.4.2 Synthesis of the acetylenic analogue of ESII.....	79
2.4.3 Synthesis of short click compounds.....	81
2.5 Click reactions with alkyne Eeyarestatins.....	88
2.6 Summary	90
2.7 Synthesis of Cotransin.....	93

2.7.1 Solid phase synthesis.....	93
2.7.2 Solution phase synthesis of Cotransin.....	96
CHAPTER 3: RESULTS AND DISCUSSION PART II: BIOCHEMISTRY	99
3.1 Cytotoxicity of ESI analogues.....	100
3.2 Effect of ES compounds on cell morphology.....	105
3.3 Accumulation of polyubiquitin conjugates	110
3.4 ER protein translocation.....	113
3.4.1 Post-translational translocation.....	114
3.4.2 Cotranslational translocation	116
3.5 Protein secretion	118
3.6 Click chemistry.....	125
3.7 Summary	128
CHAPTER 4: CONCLUSIONS AND FURTHER WORK.	129
4.1 Eeyarestatins.....	129
4.2 Cotransin	132
CHAPTER 5: EXPERIMENTAL.....	134
5.1 General procedures	134
5.2 Preparation of Eeyarestatins	136
5.2.1 Symmetrical Eeyarestatins.....	136
5.2.2 Unsymmetrical Eeyarestatins.....	157
5.2.3 Short form Eeyarestatins.	162

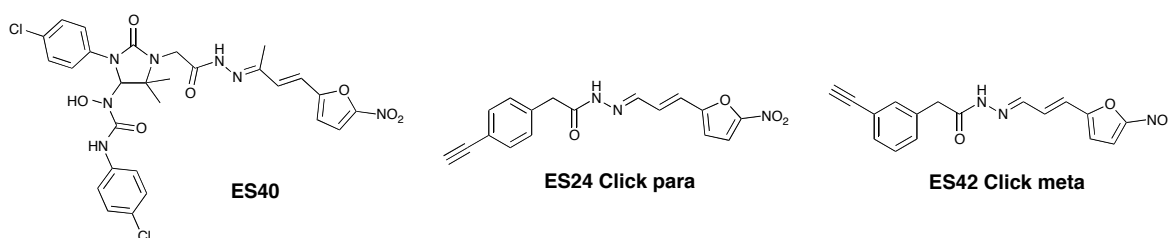
5.2.4 Click Eeyarestatins.....	167
5.2.5 Click chemistry	196
5.3 Synthesis of Cotransin.....	201
5.3.1 Solution phase synthesis of Cotransin.....	201
5.4 Biochemical experiments.	207
5.4.1 General methods	207
5.4.2 Measurement of Cell Viability (MTT assay).....	210
5.3.3 Vacuolisation and accumulation of polyubiquitin conjugates.....	211
5.4.4 <i>In vitro</i> translocation assay	211
5.4.5 Protein secretion from HepG2 cells	213
5.4.6 Click chemistry	214
REFERENCES	215

Word count: 41,120

ABSTRACT

Biosynthesis and folding of proteins entering the secretory pathway of eukaryotic cells is coordinated at the endoplasmic reticulum (ER). Any terminally misfolded proteins are sorted for the endoplasmic reticulum associated degradation (ERAD) pathway for destruction. Eeyarestatin I (ESI) is a potent inhibitor of certain stages of protein biogenesis at the ER including protein translocation across the ER and deubiquitination, a late stage of the ERAD process.

Here several structurally related Eeyarestatins (ES) were synthesised based on key structural requirements shown in ESI and the structural activity relationship of these compounds both *in vivo* and *in vitro* was investigated. Experiments conducted included: cytotoxicity to determine toxicity of ES compounds at several concentrations; cell microscopy to identify vacuole formation frequently exhibited by ESI; SDS page electrophoresis and western blotting for ubiquitin to ascertain the extent of accumulation of ubiquitinated protein and indicator of inhibition of deubiquitination; a translocation block assay looking to determine the inhibitory effect the ES compounds have on translocation of selected proteins across the ER membrane; and finally a secretion assay to determine the ES compound's ability to block overall secretion of proteins from cells. Whilst none of the "new" analogues seem to be equipotent to ESI in all inhibitory activities, inhibitory activity of compounds ES40, ES24 Click meta and ES24 Click para appear to be more specific towards DUBs, with ES40 being the most active.



DECLARATION

No portion of the work referred to in this thesis has been submitted in support of an application for another degree or qualification at this or any other University or other institute of learning.

COPYRIGHT STATEMENT

- i.** The author of this thesis (including any appendices and/or schedules to this thesis) owns certain copyright or related rights in it (the “Copyright”) and she has given The University of Manchester certain rights to use such Copyright, including for administrative purposes.
- ii.** Copies of this thesis, either in full or in extracts and whether in hard or electronic copy, may be made **only** in accordance with the Copyright, Designs and Patents Act 1988 (as amended) and regulations issued under it or, where appropriate, in accordance with licensing agreements which the University has from time to time. This page must form part of any such copies made.
- iii.** The ownership of certain Copyright, patents, designs, trade marks and other intellectual property (the “Intellectual Property”) and any reproductions of copyright works in the thesis, for example graphs and tables (“Reproductions”), which may be described in this thesis, may not be owned by the author and may be owned by third parties. Such Intellectual Property and Reproductions cannot and must not be made available for use without the

prior written permission of the owner(s) of the relevant Intellectual Property and/or Reproductions.

- iv. Further information on the conditions under which disclosure, publication and commercialisation of this thesis, the Copyright and any Intellectual Property and/or Reproductions described in it may take place is available in the University IP Policy (see <http://www.campus.manchester.ac.uk/medialibrary/policies/intellectual-property.pdf>), in any relevant Thesis restriction declarations deposited in the University Library, The University Library's regulations (see <http://www.manchester.ac.uk/library/aboutus/regulations>) and in The University's policy on presentation of Theses.

ACKNOWLEDGEMENTS

I would firstly like to thank Dr Roger Whitehead for his unyielding support during my four years as a PhD student. Particularly during my final 12 months, which were exceptionally troublesome, he allowed me to vent my many frustrations.

Special thanks go to Dr Lisa Swanton and Prof. Stephen High who both allowed me space in their labs to do the biochemistry assays and were always on hand for help deciphering the results and answering the ridiculous amount of questions I must have had throughout the four years.

Many thanks go to Prof. Sabine Flitsch for her help with the solid phase Cotransin synthesis and for her input during collaboration meetings.

I would also like to thank the Whitehead lab group past and present for making my four years enjoyable and for their assistance with difficult procedures. Special thanks go to John who started his PhD at the same time and who I've known since I started university, thanks for the entertaining vents of frustration and the gaming nights to release the stress.

Many thanks go to the Swanton and High labs for help with the biochemistry, particularly Marjo, Peri, Craig, Lydia and Jennifer who all taught me various biochemistry techniques.

I would like to thank Mass Spectrometry department for all their help throughout the years and NMR staff for their help I getting decent ^{13}C NMR for the very insoluble Eeyarestatin products.

And finally special thanks to all of my family and friends for the best 8 years of university I could have hoped for, I love you all.

DEDICATION

For Mum, Dad, Catherine, David, my partner David and nephew Jake

ABBREVIATIONS

Ar: Aryl

ATP: Adenosine triphosphate

BiP: Binding immunoglobulin protein

Bpt: Boiling point

brd: Broad doublet

brm: Broad medium

brs: Broad singlet

brt: Broad triplet

brw: Broad weak

Bref A: Brefeldin A

¹³C NMR: Carbon nuclear magnetic resonance

CFTR: Cystic fibrosis transmembrane conductance regulator

CNX: Calnexin

COPII: Coat protein II

CRT: Calreticulin

δ: Chemical shift

DCM: Dichloromethane

DEPT: Distortionless enhancement by polarization transfer

DGCN: (*R*)-2-hydroxy-4-cyanobutyric acid

DIC: *N,N'*-diisopropylcarbodiimide

DIEA: *N,N*-diisopropylethylamine

DMEM: Dulbecco's modified eagles medium

DMF: Dimethylformamide

DMP: Dess-Martin periodinane

DMSO: Dimethyl sulfoxide

DTT: Dithiothreitol

DUBs: Deubiquitinating enzymes

EDCI: *N*-(3-dimethylaminopropyl)-*N*'-ethylcarbodiimide

EDEMs: ER degradation enhancing mannosidases

EGTA: Ethylene glycol tetraacetic acid (ethylene glycol-bis(2-aminoethylether)-
N,N,N',N'-tetraacetic acid)

ER: Endoplasmic reticulum

ERAD: Endoplasmic reticulum associated degradation

ES: Eeyarestatin

g: Grams

GI: Glucosidase I

GII: Glucosidase II

GT: Glucosyltransferase

GTP: Guanosine-5'-triphosphate

HATU: 2-(7-Aza-1H-benzotriazole-1-yl)-1,1,3,3-tetramethyluronium
hexafluorophosphate

HBTU: 2-(1*H*-Benzotriazole-1-yl)-1,1,3,3-tetramethyluronium
hexafluorophosphate

HEPES: 2-[4-(2-hydroxyethyl)piperazin-1-yl]ethanesulphonic acid

HMQC: Heteronuclear multiple quantum coherence

¹H NMR: Proton nuclear magnetic resonance

HOAt: 3-hydroxytriazolo[4,5-*b*]pyridine

HPLC: High performance liquid chromatography

h: Hour

HRMS: High resolution mass spectrometry

Hsp: Heat shock protein

Hz: Hertz

IB: Immunoblot

IR: Infrared

KHM: Potassium, HEPES, Magnesium buffer

M: Molecular peak (mass spectrum)

Me: Methyl

mg: Milligrams

MHC: Major histocompatibility complex

mL: Millilitre

mmol: Millimoles

MHz: Megahertz

mins: Minutes

MTO: *N*¹-methoxy-*N*-methyl-L-tryptophan

MTT: 3-(4,5-Dimethylthiazol-2-yl)-2,5-diphenyltetrazolium bromide

NMI: *N*-methylimidazole

PBS: Phosphate buffered saline

PDI: Protein disulphide isomerase

PE: Petroleum ether

pCec: Procecropin

ppCec: Pre-procecropin

pPL: Pre-prolactin

PSII: Proteasome inhibitor

RP: Regulatory particle

rt: Room temperature

SDS-PAGE: Sodium dodecyl sulphate polyacrylamide gel electrophoresis

SRP: Signal recognition particle

TBAF: Tetrabutylammonium fluoride

TBS: Tris buffered saline

TBTA: Tris[(1-benzyl-1H-1,2,3-triazol-4-yl)methyl] amine

TCA: Trichloroacetic acid

TCEP: Tris(carboxyethyl)phosphine

TCR α : T-cell receptor α

TEA: Triethylamine

TFA: Trifluoroacetic acid

THF: Tetrahydrofuran

TLC: Thin layer chromatography

Tris: tris(hydroxymethyl)aminomethane

-ve: Negative

+ve: Positive

ν_{\max} : absorption

CHAPTER 1: INTRODUCTION

1.1 Protein biosynthesis and quality control

Proteins are biochemical compounds consisting of one or more polypeptides typically folded into a globular or fibrous form, facilitating a biological function (e.g. enzymatic, structural, mechanical or cell signalling). Like other biological macromolecules such as polysaccharides and nucleic acids, proteins are essential parts of organisms and participate in virtually every process within cells.¹

Cells are made up of many organelles contained within a cell membrane including a nucleus, ribosomes, rough and smooth endoplasmic reticulum, Golgi apparatus and many more, which are separately enclosed in their own lipid bilayers called membranes and the space in between filled with cytosol.²

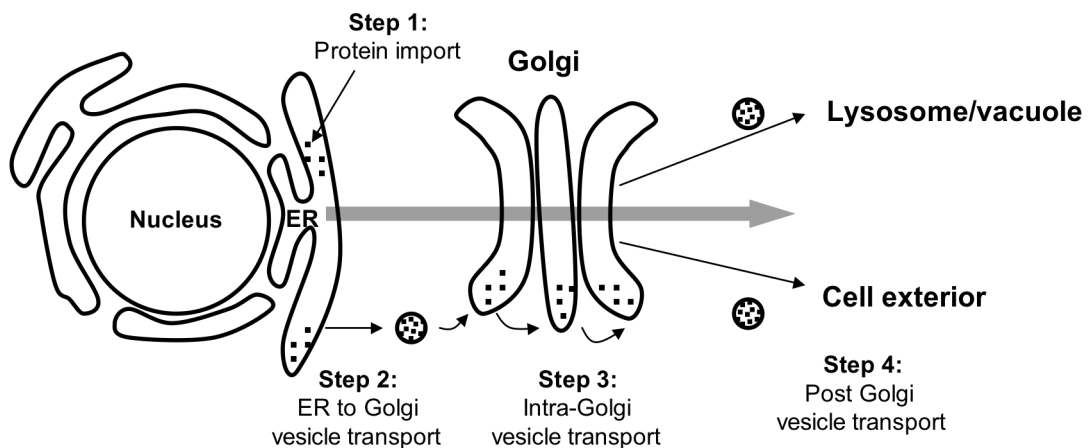


Figure 1.1. Simple overview of the secretory pathway in eukaryotic cells (Taken from Wellesley college³) This process is broken down into four general steps: Step 1 protein import in the ER followed by protein folding; Step 2 ER to Golgi transport in vesicles; Step 3 Intra-Golgi vesicle transport and finally Step 4 Post-Golgi transport to the cell exterior, lysosome or vacuoles. The large arrow shows the overall flow of proteins through the secretory pathway.

Although the protein synthesis (translation) begins on ribosomes located in the

cytosol, proteins can be directed to particular locations within the cell by the presence of specific targeting signals. Approximately one third of the proteome is predicted to have a signal sequence that will result in targeting to the endoplasmic reticulum (ER)⁴. The endoplasmic reticulum is a network of tubules, vesicles and sacs that are interconnected. Proteins may serve specialised functions in the cell including protein synthesis, insertion of membrane proteins, sequestration of calcium and production of steroids amongst others.² Most membrane proteins (i.e. proteins that are inserted into the membrane) and proteins that are destined to be released from cells (secretory proteins) are synthesised at the ER. Once targeted to the ER, these proteins are threaded across the ER membrane (a process called translocation) as linear polypeptide chains, which then must fold into the correct three-dimensional state. Properly folded proteins are recruited into membrane bound vesicles, which bud off from the ER and transport them to the Golgi apparatus (Figure 1.1). The Golgi acts as a sorting station to deliver secretory and membrane proteins to their correct destination within the cell (Figure 1.1).

However, protein biogenesis is surprisingly inefficient. It has been estimated that around 30 % of all newly synthesised proteins are in some way defective and are rapidly degraded.⁵ Errors in transcription and translation can lead to the incorporation of incorrect amino acids leading to a polypeptide that is unable to fold correctly. Even with the correct sequence of amino acids folding is intrinsically error-prone. Furthermore, the efficiency of protein folding can be compromised under various situations, including environmental stress or due to genetic mutation. Effective removal of these defective proteins and the recycling of their constituent amino acids is vital for cellular homeostasis and survival. Defective proteins may compete with their functional equivalents for substrate binding or complex

formation, thereby engaging in harmful non-native interactions and this ultimately can lead to disease.⁶ Misfolded or damaged proteins may also form toxic aggregates. Although the toxicity of aberrant cytosolic proteins is usually restricted to the host cell, secretory and transmembrane proteins are released from the cell or exposed at its surface thereby posing a greater risk. In particular, they have the potential to interfere with cell-to-cell communication, disrupt development and even prevent recognition by the immune system.⁷ This scenario is normally averted by a sequence of quality control steps at the site of secretory and membrane protein biogenesis, the ER.⁸ This quality control system monitors protein folding and assembly and prevents the forward transport of non-native polypeptides.⁹ Proteins that are retained by the ER quality control are typically degraded by a process called ER-associated degradation (ERAD), in which the misfolded protein is transported back into the cytosol and degraded by the proteasome.¹⁰ Thus, ERAD is an essential mechanism to prevent the accumulation of misfolded proteins within the ER.

1.2 Protein synthesis at the endoplasmic reticulum

1.2.1 Protein targeting and translocation at the endoplasmic reticulum

Targeting of secretory proteins to the ER is mediated by a hydrophobic signal peptide that is typically at the *N*-terminus of a polypeptide and is usually 15-30 residues in length.¹¹ Secretory proteins enter the ER lumen through a proteinaceous channel, the Sec61 complex embedded in the ER membrane and *via* either co-translational means (i.e. at the same time as translation is occurring) or post-translational means (i.e. after translation of the polypeptide is completed).^{9, 11, 12}

In mammalian cells most proteins appear to be translocated into the ER co-translationally (Figure 1.2).^{2, 11} The signal recognition particle (SRP) binds to the signal peptide on the *N*-terminus of the nascent polypeptide when it is exposed from the ribosome, causing a pause in translation (Figure 1.2 a).^{2, 12, 13} The SRP bound ribosome then selectively binds to the SRP receptor in the ER membrane (Figure 1.2 b)), SRP is displaced and the ribosome binds to the translocon. The nascent chain is transferred to the Sec61 complex and translation then continues (Figure 1.2 c). As the polypeptide is synthesised it is translocated into the ER lumen through the Sec61 complex using GTP hydrolysis as the energy source to drive protein synthesis.¹⁴ The signal peptide may be cleaved from the nascent polypeptide by a signal peptidase as translation continues, and the mature polypeptide is finally released into the ER lumen.

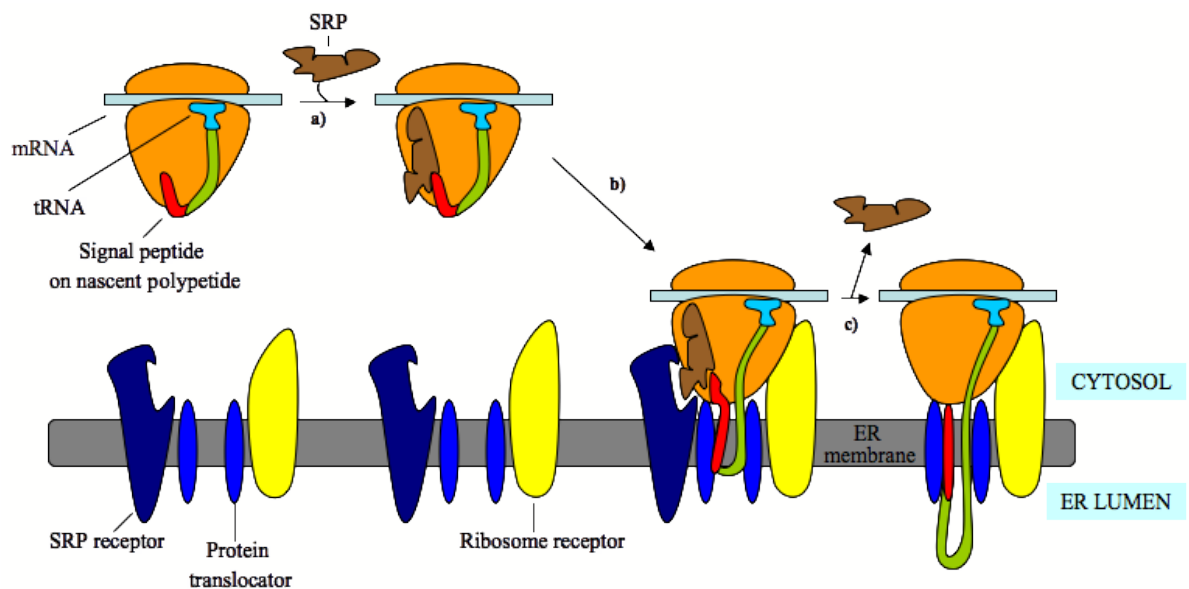


Figure 1.2 Co-translational translocation of polypeptides is mediated by SRP (Modified from Alberts *et al*²). a) SRP binds to the signal peptide on the growing polypeptide chain causing a pause in translation; b) The SRP bound ribosome then binds to the SRP receptor in the ER membrane; c) SRP is displaced and the ribosome binds to the translocon and translation continues.

The simplest transmembrane proteins are targeted in a similar fashion, a signal peptide on the amino terminus initiates translocation, but the polypeptide contains an extra hydrophobic sequence (orange segment in Figure 1.3), which stops translocation across the ER membrane.² When this stop-transfer segment enters the Sec61 translocon and interacts with a putative binding site, translocation stops, the translocator opens up and discharges the protein laterally into the lipid bilayer this process is known as integration.^{2, 11, 14} In this case the signal peptide sequence is usually cleaved after insertion (Figure 1.3).¹⁵

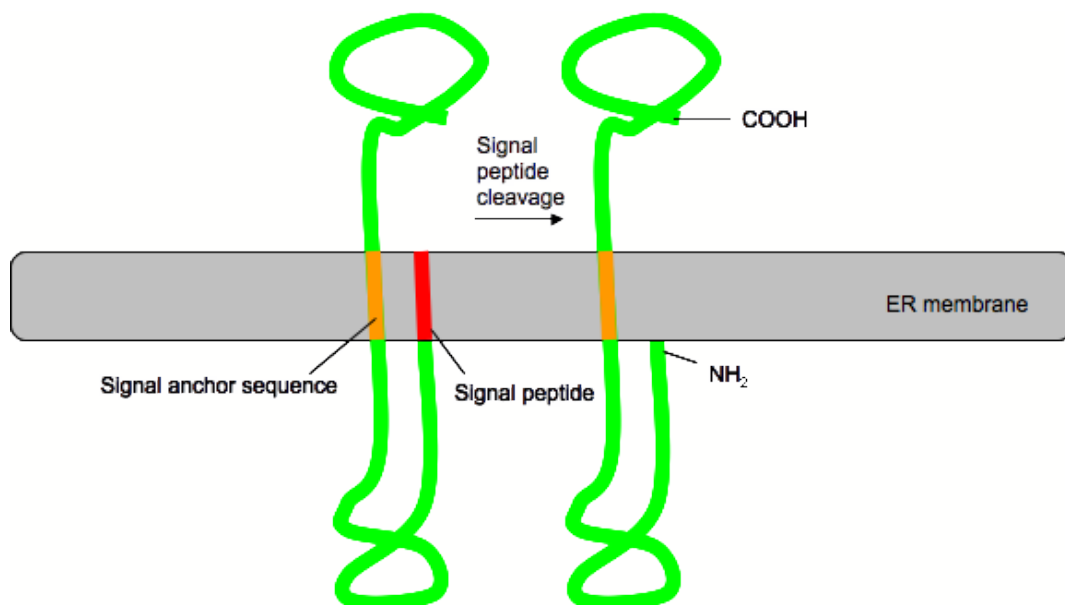


Figure 1.3 Simple transmembrane protein after membrane insertion. (Modified from Alberts *et al*²)

Other transmembrane proteins contain a signal sequence embedded further in the polypeptide chain. This signal is still recognised by the SRP as for *N*-terminus signal peptides, the difference is that when the translocon releases the polypeptide into the lipid bilayer the signal peptide itself serves as the transmembrane anchor. Such signal-anchor proteins can orientate in two ways, one with the carboxyl terminus on

the luminal side of the membrane and *N*-terminus on the cytosolic face and *vice versa* (Figure 1.4).^{2, 16} The topology depends on the orientation of the signal-anchor, which in turn depends on the distribution of nearby charged amino acids.^{2, 16}

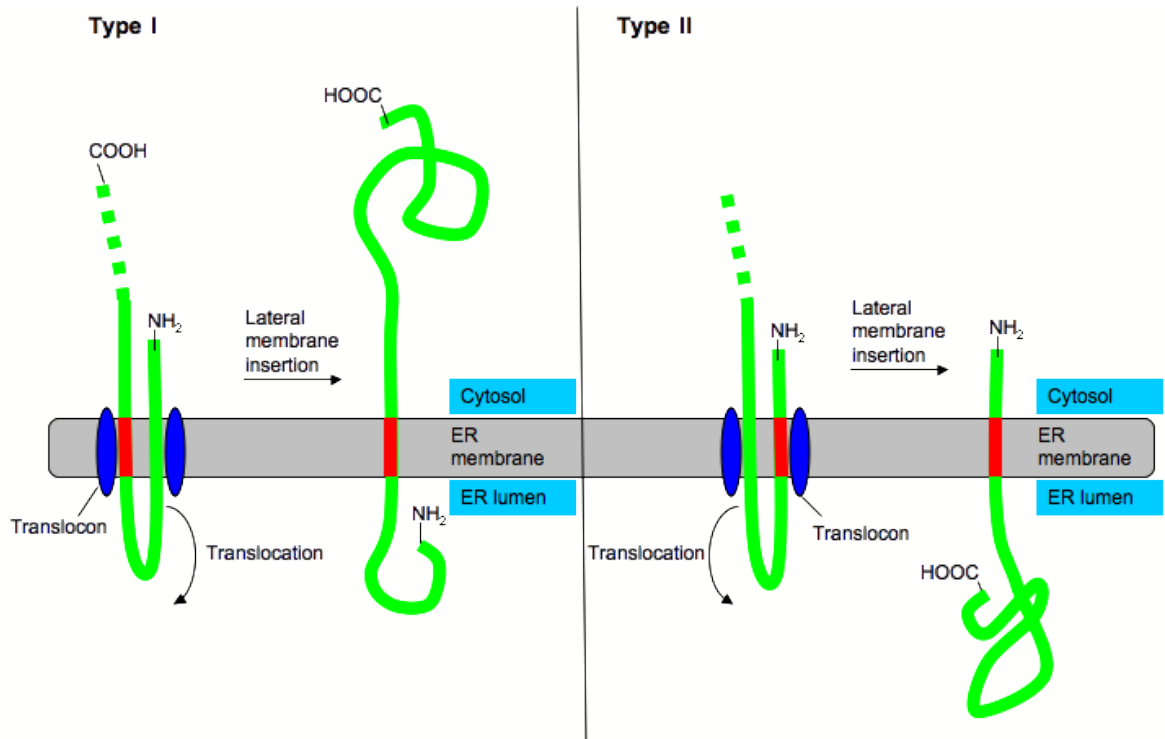


Figure 1.4. Type I and II orientation of signal sequence and final membrane structure after insertion into the ER membrane

Multiple pass transmembrane proteins have several hydrophobic start and stop transfer sequences that allow these proteins to achieve their final orientation in the membrane.¹⁷

1.2.2 Sec61

The Sec61 complex is an ER membrane complex composed of three major subunits (α , β , γ ; heterotrimeric) that forms a pore through the membrane.^{11, 18} Figure 1.5

shows the structure of the equivalent protein translocation channel in the bacterium *Escherichia coli* (*E.Coli*). This complex is well conserved and were two of the components, SecY and SecE, share sequence and functionality with mammalian Sec61 α and Sec61 γ , which together with Sec61 β (equivalent to SecG in *E.Coli*), form the Sec61 translocon in the ER membrane.¹³

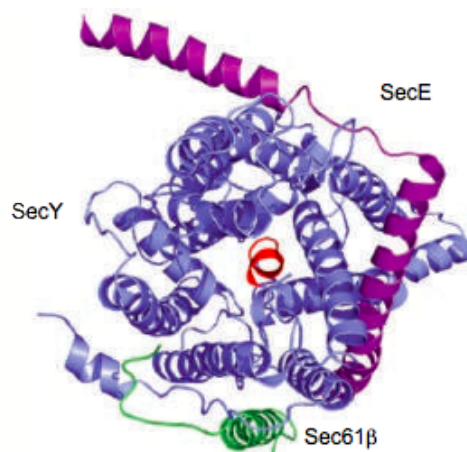


Figure 1.5. A protein translocator in *E. Coli* (Taken from Cross *et al.*¹³)

Sec61 α has a region called the plug that closes the pore when it is inactive (Figure 1.5, red ribbon). This plug is believed to be displaced when a hydrophobic region of a nascent polypeptide interacts with another region of Sec61 denoted the seam, thereby allowing translocation of the polypeptide into the ER lumen.^{2, 14} The plug returns to the centre of the Sec61 complex when the nascent polypeptide chain has left the pore.¹⁴

1.3 Protein folding and quality control at the ER

After proteins have been translocated into the ER lumen they fold and may undergo post-translational modifications, such as the addition of oligosaccharides to specific

Asparagine residues (*N*-glycosylation), disulfide bond formation between cysteine residues and assembly with partner subunits (oligomerisation); before being packaged into vesicles to be transported to the Golgi for sorting to their final destinations.

1.3.1 Chaperones

As the polypeptide is exposed on the luminal side of the ER membrane, molecular chaperones bind to it and initiate protein folding, oligomerisation, maturation and post-translational modifications, which may include *N*-glycosylation and disulfide bond formation.¹⁹ Molecular chaperones are folding catalysts and there are several classes including: Heat shock proteins (Hsp's) including BiP and cofactors, which are ATPases involved in initial folding and recognition of non-native proteins; Oxidoreductases (*e.g.* Protein disulfide isomerase (PDI)), which are involved in the formation of disulfide bond formation or reduction and lectins (*e.g.* Calnexin (CNX)), which are involved in *N*-glycosylation. These chaperones are retained in the ER by the presence of specific amino acid sequences such as KDEL (Lys-Asp-Glu-Leu). Most chaperones bind to unfolded proteins, promote folding, In addition, due to their ability to recognise signals that are present on unfolded proteins, chaperones form an essential part of the quality control system that identifies and retains non-native proteins in the ER (see below).

1.3.2 *N*-Glycosylation

Many proteins are modified by the addition of a core glycan to specific Asparagine residues within the consensus sequence. *N*-linked glycans may be essential for the

protein's function, and also facilitate folding by allowing them to interact with specific chaperone proteins in the ER lumen, including calnexin and calreticulin. The presence of N-glycans also provides a quality control mechanism for identifying proteins that have failed to fold properly.

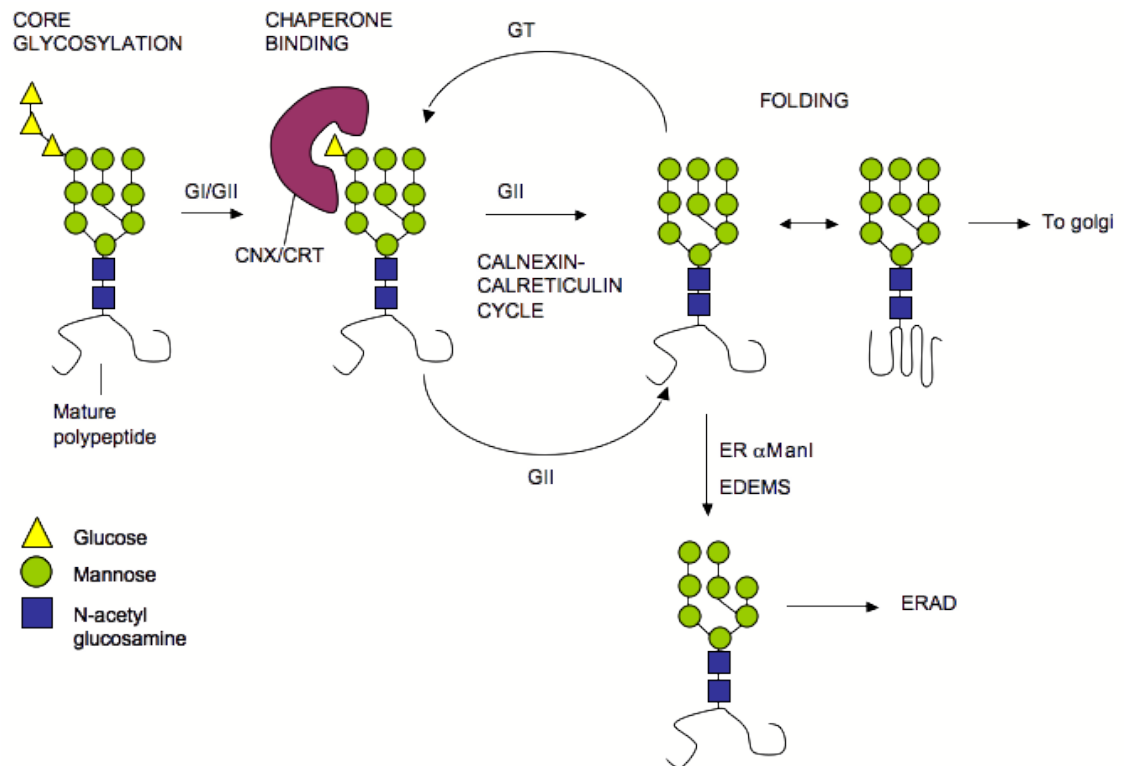


Figure 1.6. N-glycans role in quality control (Modified from Hegde and Ploegh²⁰)

The first glucose on the *N*-glycan is rapidly removed by glucosidase I (GI) and this event is followed by removal of the second glucose by glucosidase II (GII). Lectins, Calnexin (CNX) and Calreticulin (CRT), recognise the resulting mono-glucosylated *N*-glycan and bind to the glycoprotein. GII removes the final glucose residue and if correctly folded the mature protein can leave the calnexin cycle. If the protein is not folded correctly it is recognised by a soluble enzyme known as glycoprotein glucosyltransferase (GT). GT reglucosylates misfolded or incompletely folded

glycoproteins, which can then rebind calnexin and reinitiate the chaperone-mediated protein folding process again.^{6, 21} If misfolding is terminal then an ER-resident mannose trimming enzyme, mannosidase I (ER α ManI), acts upon the core glycan and removes one terminal mannose from *N*-glycans. This generates an 8-mannose ‘degradation signal’ that is recognised by the ER quality control and ERAD machinery.⁶

1.4 Endoplasmic reticulum associated degradation

Proteins that are identified by the quality control system as being non-native are retained in or returned to the ER and are ultimately degraded *via* ERAD. ERAD is not mediated within the ER lumen but by the cytosolic proteasome, which is a multisubunit protease complex and a major pathway for degradation of proteins. It is composed of a barrel shaped core particle, which contains the protease subunits, and two lids that control entry into the proteolytic core.⁴ In order to be degraded by the proteasome, misfolded proteins in the ER must therefore be translocated back across the ER membrane into the cytosol, a process called retro-translocation.²²

The process of selective protein export from the ER to the cytosol followed by proteosomal degradation is known as endoplasmic reticulum associated degradation (ERAD).⁶ This degradation process is responsible for the destruction of both integral membrane and luminal proteins, and is usually selective for non-native proteins. Damaged, unfolded or misfolded proteins are targeted for degradation, correctly folded ones are spared.²³

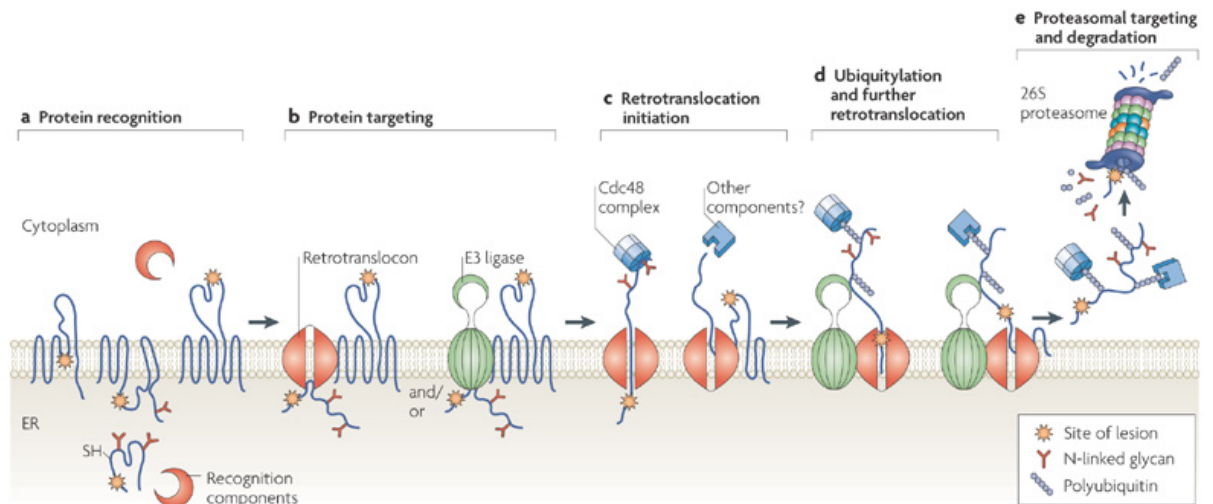


Figure 1.7. Step by step illustration of the ERAD pathway (Taken from Vembar and Brodsky²⁴). **a)** Protein recognition. Misfolded proteins are recognised by molecular chaperones that facilitate their folding; **b)** Protein targeting. ERAD substrates are targeted to the retro-translocation machinery (the retro-translocon) and/or to E3 ligases; **c)** Retro-translocation initiation. Precisely how ERAD substrates are retro-translocated is not known but it is believed that Cdc48(p97) provides the driving force for this process; **d)** Ubiquitylation and further retro-translocation. As proteins exit the retro-translocon they are polyubiquitinated by E3 ubiquitin ligases; **e)** Proteasomal targeting and degradation. Once a polyubiquitinated substrate is displaced into the cytoplasm, it is recognised by receptors in the 19S cap of the 26S proteasome. De-ubiquitinating enzymes (not shown) remove the polyubiquitin tag. The substrate is degraded into peptide fragments by the 20S catalytic core of the proteasome.

The ERAD pathway is a complex multi-step process and intense study over the past 10-15 years has identified a large number of proteins that participate in the degradation of different types of misfolded proteins (or ERAD 'substrates'). In general ERAD can be seen to occur in distinct stages these including: Identification or recognition of terminally misfolded proteins; Protein targeting to retro-translocation machinery; Initiation of retro-translocation and ubiquitylation and finally deubiquitylation followed by proteasomal degradation (Figure 1.7).

In the case of ERAD, small molecule inhibitors of the pathway are needed in order to elucidate the mechanistic detail at the molecular level.

1.4.1 Recognition and targeting

It is widely believed that chaperones help identify any incorrectly folded proteins for ERAD, by the presence of a variety of signals.

ER chaperone-like lectins, calnexin and calreticulin, recognise specific *N*-glycans on glycoproteins, formed when glycosylated proteins cannot fold in the ER. Calnexin and calreticulin bind to and retain immature glycoproteins and facilitate their folding, continuing this cycle until the protein folds correctly. If, however, glycoproteins cannot fold correctly within an appropriate timescale, they are targeted for ERAD.¹⁹

In contrast, BiP recognises hydrophobic regions of peptides, approximately 7 residues in length, that are usually buried inside native proteins, but may be exposed on the surface of misfolded/unfolded proteins.²⁵ BiP recognises non-native proteins and retains them in the ER, and helps target those that are terminally misfolded to the retro-translocation machinery.¹⁹ In some cases subsequent interaction with protein disulfide isomerase (PDI) is required for ERAD, most likely because the reduction of disulfide bonds is required to enable the passage of the misfolded protein back across the ER membrane and back to the cytosol.²⁶

Chaperones also participate in the cellular unfolded protein response; hence if there is an accumulation of unfolded proteins then chaperones bind to them causing a reduction in the concentration of free chaperones. This reduction is detected by the cell and results in the inhibition of global synthesis of new proteins until the 'backlog' is cleared up and the free chaperone concentration again increases.¹⁹

1.4.2 Retro-translocation and ubiquitination

Following identification and targeting, most ERAD substrates require the covalent attachment of a chain of ubiquitin molecules in order to be degraded.²⁷ Ubiquitin is a small protein approximately 8.5 kDa²⁸ that is covalently attached to target proteins by a cascade system of enzymes.²⁹ Polyubiquitination occurs on the cytosolic face of the ER membrane and is usually coupled to retro-translocation of the ERAD

substrate across the ER membrane. It has been suggested that ubiquitination might promote movement of the polypeptide into the cytosol by preventing it slipping back into the ER. However, since ubiquitination takes place primarily in the cytosol it cannot be directly involved in initiating export of soluble proteins from the ER.

Precisely how proteins are extracted from the ER is not known, but the Sec61 complex is one of several possible channels that might mediate protein export out of the ER.²² Hence, a number of ERAD substrates can be isolated together with the Sec61 complex when the ER membrane is solubilised under mild conditions.^{30, 31} For many ERAD substrates ubiquitin modification takes place after the ER-luminal *N*-terminus of the protein has been made accessible to the ubiquitination machinery on the cytosolic face of the ER membrane.⁶ Both membrane and soluble proteins are initially polyubiquitinated and remain membrane associated.

The ubiquitination system typically consists of E1 (ubiquitin-activating), E2 (ubiquitin-conjugating), and E3 (ubiquitin-ligating) enzymes.^{29, 32} In the first step, which is catalysed by an E1, the COOH-terminus of ubiquitin is activated in an ATP dependent step and covalently linked through a thioester bond to an active-site cysteine in the E1. In the second step, ubiquitin is transferred from the E1 to an active site cysteine in one of the at least 13 known E2s in mammals. In the final step, which is accomplished by the action of an E3 ubiquitin-ligase, ubiquitin is covalently linked through an isopeptide bond to a lysine in the target protein or to another ubiquitin that has been linked to the target protein. ERAD substrates need to be ubiquitinated with at least 4 copies of ubiquitin for the proteasome to recognise them for degradation. E3 ligases are generally responsible for determining the substrate specificity of ubiquitination reactions. A number of E3 ligases contribute to ERAD, and these are believed to be associated with or form part of the retro-translocation

machinery.

As it emerges from the ER membrane, the polyubiquitinated ERAD substrate is recognised by a number of ubiquitin-binding accessory proteins that help deliver it to the proteasome for degradation.^{9, 33, 34} These include the ATPase p97, which is believed to provide the driving force to extract the proteins from the ER membrane (Figure 1.8).³⁵⁻³⁷

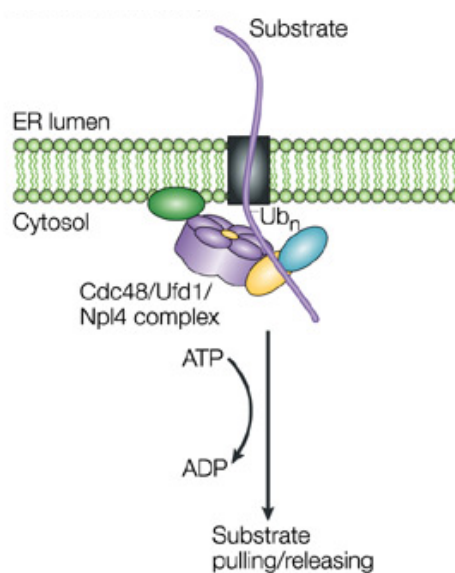


Figure 1.8. Protein extraction from the ER membrane (Taken from Tsai 2002²²)

In order to enter the narrow proteolytic chamber of the proteasome, polyubiquitin chains must be removed from the ERAD substrate. This is achieved by the action of proteases termed deubiquitinating enzymes (DUBs). Several DUBs have been implicated in ERAD³⁸ and two of these appear to be physically associated with p97 (YOD1 and Ataxin-3).^{39, 40} Inhibition of p97-associated DUBs activity can block degradation of ERAD substrates.^{38, 39, 41} In addition, DUBs are also found associated with the 19S regulatory particle (lid) of the proteasome.⁴

The study of ERAD would be helped by the identification of inhibitors, which block

particular stages in the pathway. Currently, only proteasome inhibitors, which block proteasomal degradation only, are available.

1.5 The Unfolded Protein Response

ERAD functions to eliminate misfolded proteins from the ER. However, in some situations (eg. increased synthesis of mutant proteins, adverse environmental conditions, decreased proteasome activity etc.), misfolded or unfolded proteins can accumulate. The presence of high levels of unfolded/misfolded proteins in the ER lumen activates a signalling pathway known as the unfolded protein response (UPR). The function of the UPR is to increase expression of chaperone proteins (thereby promoting protein folding), to decrease overall protein synthesis (thereby reducing the burden of newly synthesised proteins that require folding), and to increase expression of ERAD factors (thereby facilitating degradation of misfolded proteins). Together, these mechanisms help to restore homeostasis to the ER. However, if not successful, prolonged activation of the UPR can lead to programmed cell death.

1.6 ER function and disease

Disruption of ER protein folding, ERAD and UPR signalling pathways have been observed in a large number of important human diseases, including diabetes mellitus, cancer, neurodegeneration, bone and joint disease.^{42, 43} In addition, many genetic diseases are known to be caused by misfolding of particular secretory or membrane proteins leading to their premature degradation. In this way, these proteins will not be deployed to later compartments, as is the case in cystic fibrosis. The most common cause of this disease, is the deletion of phenylalanine at position 508 in the

membrane protein CFTR, which inhibits folding of CFTR, leading to recognition and degradation by the ERAD system.¹⁰

The ubiquitin proteasome system has emerged as a therapeutic target for cancer treatment. For example, the proteasome inhibitor Bortezomib is an anti-cancer drug approved for treatment of multiple myeloma and Mantle cell lymphoma.⁴⁴ Disruption of ER homeostasis (most likely by blocking ERAD) and activation of the UPR is thought to be a major mechanism through which Bortezomib kills cancer cells.^{45, 46} However, because the proteasome functions in many essential cellular pathways, in addition to ERAD, it has many additional side effects.⁴⁷ Thus, there is interest in additional, potentially more selective inhibitors of the ubiquitin proteasome system and ERAD.

1.7 Small molecule inhibitors of ER function

The use of small molecules as specific inhibitors of cellular processes has a well-established potential to provide insights into function and molecular mechanism, and can additionally form the basis for therapeutic intervention in disease.⁴⁸

Compounds that interfere with ERAD include proteasome inhibitors, ER-mannosidase I inhibitors and agents that change the redox potential in the ER.^{6, 49, 50}

Inhibition of ER-mannosidase I stabilises only selected misfolded glycoproteins.⁴⁹

Manipulation of redox potential by addition of alkylating reagents, such as diimide or *N*-ethylmaleimide blocks delivery of misfolded proteins from the ER to the cytosol, but has limited specificity.⁵⁰

1.7.1 Eeyarestatins

In order to identify novel small molecule inhibitors Fiebiger *et al* screened a chemical library for compounds that interfere with the US11 mediated degradation of a class 1 major histocompatibility complex (MHC), the heavy chain-enhanced green fluorescent protein fusion protein (EGFP-HC). Inhibitors of the degradation of fluorescent protein fusion protein (EGFP-HC). Inhibitors of the degradation of EGFP-HC molecules cause them to accumulate and thus, increase fluorescence. This screen of 16,320 compounds identified two structurally related compounds that specifically increased EGFP-HC fluorescence. These were Eeyarestatin I (ESI), **1**, and Eeyarestatin II (ESII), **2** (Figure 1.9); the inhibitory effect of these compounds on ERAD was validated by pulse-chase assays to determine the rate of ER substrate degradation in the presence/absence of compounds.

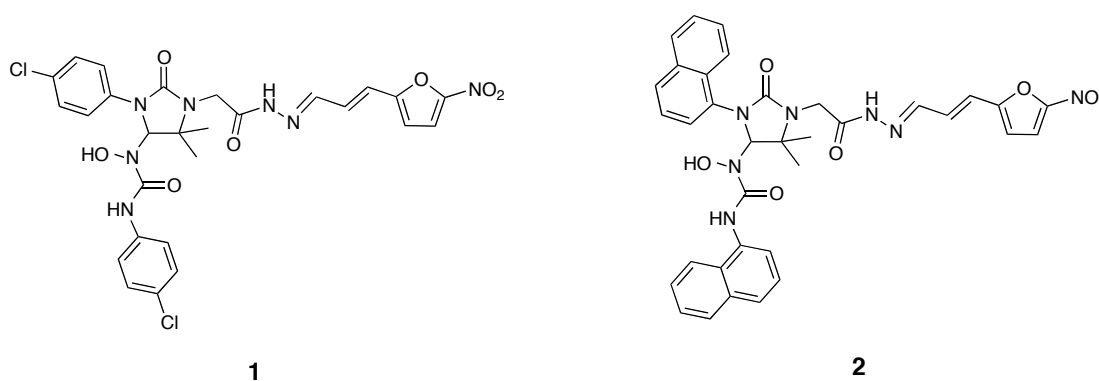


Figure 1.9. Structures of Eeyarestatin I and II

ESI was found to be more potent than ESII and ESI also inhibited the degradation of another ERAD substrate T-cell receptor α (TCR α). Fiebiger *et al.*⁵¹ also showed that degradation of misfolded proteins from the ER was impaired by the addition of ESI, without affecting degradation of cytosolic proteins. This suggested that ES compounds interfere with a step that precedes proteasomal degradation. Further experiments provided evidence that retro-translocation was inhibited by ESI

treatment, suggesting that these compounds block an early stage in the ERAD pathway (Figure 1.7b). This makes it a potentially valuable experimental tool with which to study the poorly characterised early stages in the ERAD pathway. The molecular target of ESI is not known. However, recent studies by Wang and co-workers^{41, 52} and Cross and coworkers⁵³ have identified several ESI inhibitory targets. Wang found that ESI associates with the p97 enzyme and associated DUBs, causing an inhibition of ERAD and an accumulation of polyubiquitinated proteins. They determined that ESI is bifunctional and can be divided into two parts: the aromatic domain on the “western” side and the nitrofurane domain on the “eastern” side. Wang found that the nitrofurane domain interacts with p97 causing the inhibition but the aromatic domain associates with the ER membrane allowing access to the p97 enzyme.⁵² From their observation they concluded that simpler membrane targeting groups could replace the aromatic domain to enhance membrane-targeting specificity. ESI, **1**, also disturbs ER homeostasis and has anticancer activities resembling that of Bortezomib. Because ESI has the ability to cause ER stress and cause the accumulation of polyubiquitinated proteins it therefore has potential as a possible anti-cancer drug.⁵² The study by Cross found that ESI elicits a wide-ranging inhibition of co-translational protein translocation into the ER but does not affect the spontaneous ability of proteins to integrate into the ER membrane. They suggested that because of this, the inhibition of ESI is limited to proteins that require Sec61 for translocation and therefore indicating Sec61 as the target for this compound. They also discovered that ESI prevents the transfer of a nascent polypeptide from the SRP to the Sec61 complex, and suggested that this may be by a direct effect on the Sec61 complex.⁵³ Cross also showed that ESI inhibits protein secretion from cultured mammalian cells by analysing the secretion of pulse-labelled glycoproteins into the

media from HepG2 cells treated with ESI. Strikingly, ESI exhibited almost complete loss of secretory proteins in the media. Recent work in the High lab shows ESI inducing vacuolisation in HeLa cells treated with the compound, however, the reason for this phenomenon is still under debate.⁵⁴

1.7.2 Synthesis of Eeyarestatins

Syntheses of ESI and various analogues have previously been developed in the Whitehead group⁵⁵, which follow the general route shown in Figure 1.10. The first step involves a coupling reaction between glycine methyl ester and 2-chloro-2-methyl-1-nitrosopropane.

The following step involves nucleophilic attack of the amine **1** onto various R-substituted isocyanates to generate a cyclic urea compound. Compounds with R¹ the same as R² were prepared using path **A**, compounds with R¹ different to R² were prepared using path **B**.

Step 3 involves the transformation of ester group on the cyclic urea compounds to the corresponding hydrazide. This was followed by a coupling reaction between the hydrazides and (*E*)-3-(5-nitro-2-furyl) acrylaldehyde.

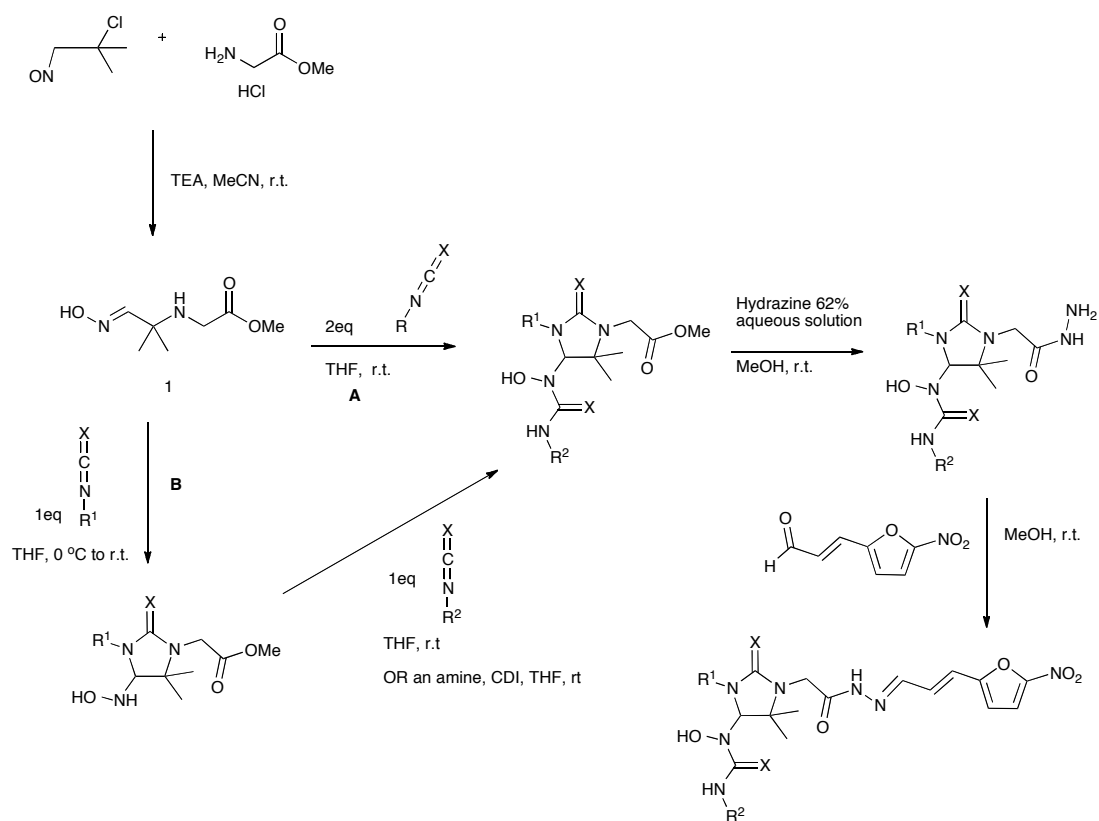


Figure 1.10. General synthesis of Eeyarestatins

All analogues that have been prepared are shown in the tables below, table 1.1 shows the symmetrical analogues previously prepared *via* path **A**, table 1.2 shows the unsymmetrical analogues prepared *via* path **B**. ESI and ESII are compounds **1** and **2** respectively.

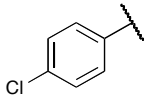
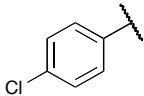
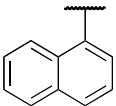
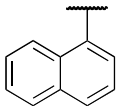
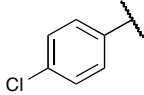
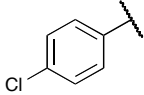
Entry	R ¹	R ²	X
1 (ESI)			O
2 (ESI)			O
3			S

Table 1.1: Analogues produced by path A

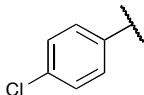
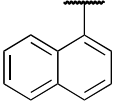
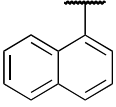
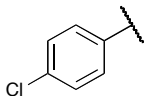
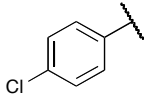
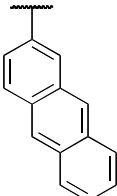
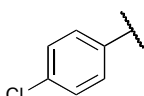
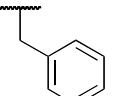
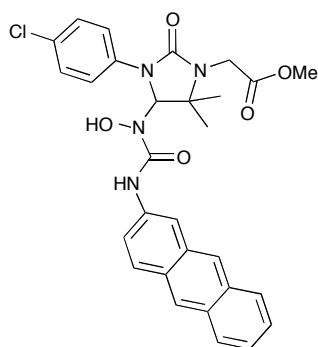
Entry	R ¹	R ²	X
4			O
5			O
6			O
7			O

Table 1.2: Analogues produced by path B

For analogues such as unsymmetrical methyl ester, **6** shown in Figure 1.11, there are no commercially available or readily synthesised isocyanates. They can however be prepared using carbonyl diimidazole and a corresponding amine. Methyl ester **6** was formed *in situ* from 1,1-carbonyldiimidazole and 2-aminoanthracene.



6

Figure 1.11. Methyl ester precursor to anthracenyl Eeyarestatin

A second set of analogues, also prepared from the hydrazide precursor to ESI, **8**, using different aldehydes in the final coupling reaction, is shown in Figure 1.12. Structures for **9**, **10** and **11** are summarised in Table 1.3.

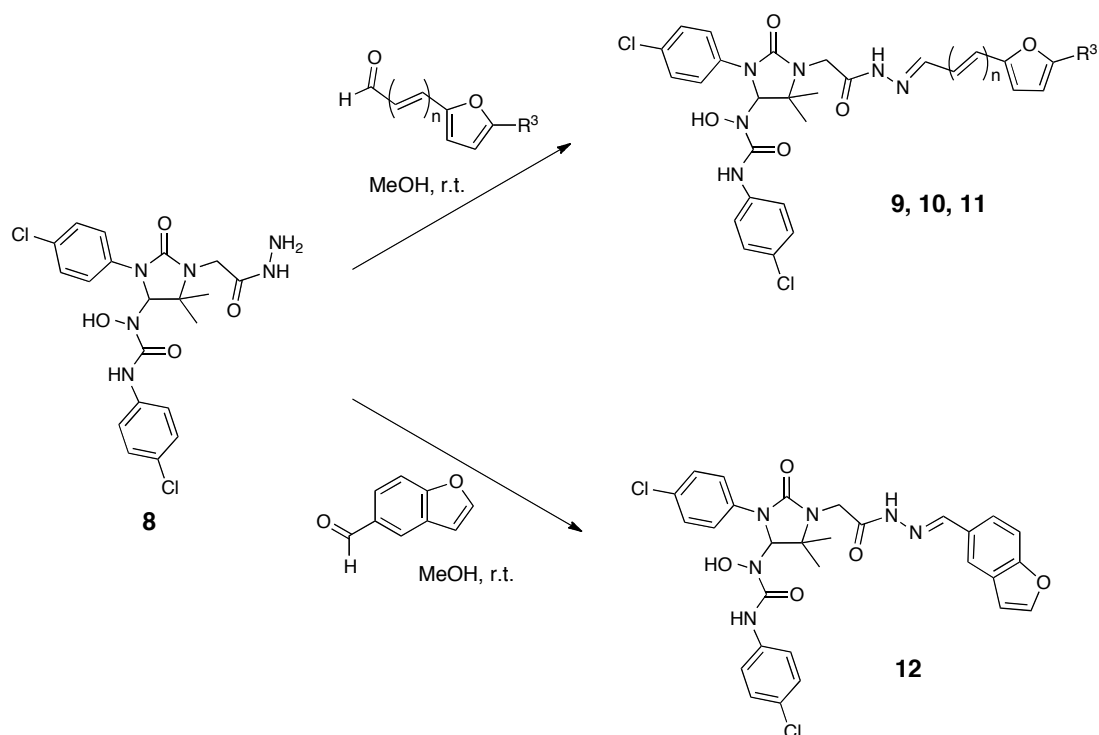


Figure 1.12. Alternative aldehydes to create new inhibitors

Entry	n	R ³
9	1	H
10	0	NO ₂
11	0	H

Table 1.3. Summary of analogues prepared by aldehyde variation

A third set of analogues has also been prepared in the Whitehead group *via* the nucleophilic substitution by the free hydroxyl group, R¹ position in Figure 1.13, of Eeyarestatin I and II on sulfonyl chlorides and biotin. Results are summarised in Table 1.4.

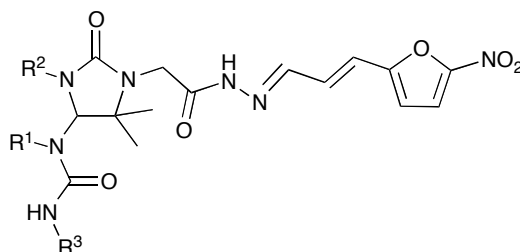


Figure 1.13. Loci for potential structural variation

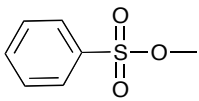
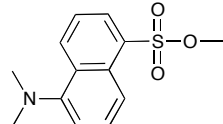
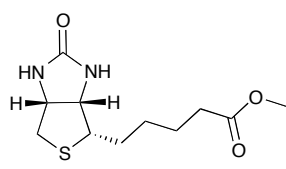
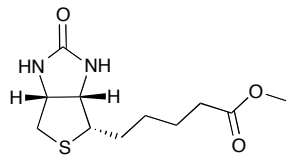
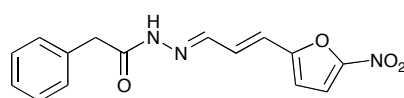
Entry	R ¹	R ²	R ³
13		4-Cl-C ₆ H ₄	4-Cl-C ₆ H ₄
14		4-Cl-C ₆ H ₄	4-Cl-C ₆ H ₄
15		4-Cl-C ₆ H ₄	4-Cl-C ₆ H ₄
16		C ₁₀ H ₇	C ₁₀ H ₇

Table 1.4. Summary of analogues prepared by variation at R¹, R² or R³

A “short form” analogue of the ES compounds has also been prepared (Figure 1.14) which shows similar potency to ESI. It was synthesised from methyl phenyl acetate, which was converted into its corresponding hydrazide and then coupled with (*E*)-3-(5-nitro-2-furyl)acrylaldehyde to give final product **17**.

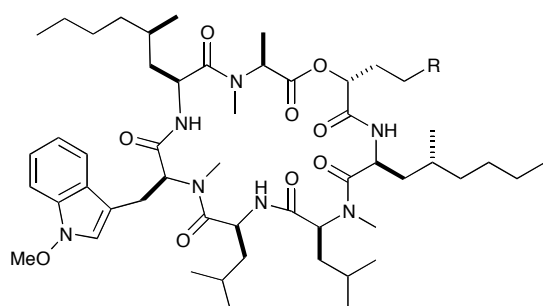


17

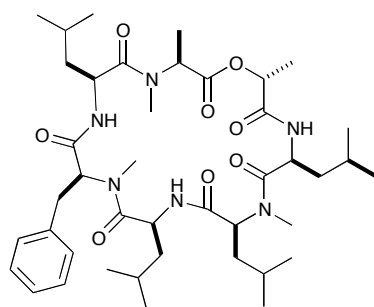
Figure 1.14. “Short form” Eeyarestatin

1.7.3 Other inhibitors of translocation - Cotransin

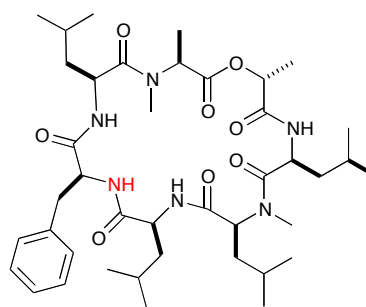
To date only CAM741 (Figure 1.15) has been identified as a selective inhibitor of ER translocation, in the most recent study Harant and co-workers confirmed that CAM741 inhibits translocation through the Sec61 complex.^{56, 57} A similar study by J. L. Garrison and co-workers showed the small molecule Cotransin also inhibits translocation.⁵⁸ The compounds bind directly to the Sec61 complex and block its activity but the effect of CAM741/Cotransin is limited by substrate specificity, only a small subset of precursor proteins are prevented from entering the ER in the presence of CAM741.⁵⁶⁻⁶⁰ Whilst the compounds may bind directly, their inhibitory effect is determined by the properties of the nascent chain signal sequence.^{56, 57}



HUN-7293: R = CN
CAM741: R = COOⁿPr



Cotransin



nor-Cotransin

Figure 1.15. Cyclodepsipeptides

CAM741 and Cotransin are analogues of known compound HUN-7293, a cyclic heptadepsipeptide, which is a potent inhibitor of “vascular cell adhesion molecule-1” (VCAM-1) expression and exhibits anti-inflammatory properties.⁶¹

Cotransin exhibits several interesting features: firstly it contains an unnatural *D*-lactic acid residue and secondly, it contains three *N*-methylated amino acids. Its synthesis has been completed in both solution and solid phases: the solution phase was a modification of the Boger method used to make HUN-7293;^{58, 61, 62} solid phase synthesis was accomplished by Coin and co-workers starting from the unnatural *D*-lactic acid.⁶³ Interestingly it appears that the *N*-methyl group on the Phe residue, highlighted in Figure 1.15, is critical for biological potency since, when removed, the compound apparently becomes inactive towards VCAM 1 expression; this compound is known as nor-Cotransin.⁵⁸

1.7.4 Synthesis of HUN-7293 and its analogues

HUN-7293 is a naturally occurring heptadepsipeptide, which was first isolated in 1992 from a fungal broth.^{61, 62} It contains six *L*-amino acid residues and one *D*- α -hydroxy carboxylic acid residue and its stereochemistry was assigned using a combination of ¹H NMR and X-ray crystallography.⁶⁴ The Boger research group was the first to synthesise this molecule in solution and in the process, they prepared a series of analogues.^{61, 62}

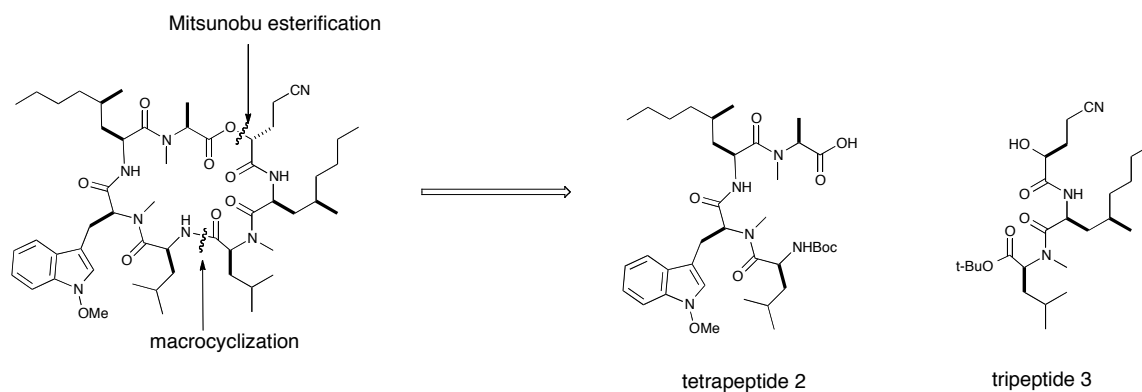


Figure 1.16 Retrosynthetic analysis of HUN-7293

Boger used a convergent synthesis exploiting the use of the Mitsunobu reaction to invert the (*R*)-2-hydroxy-4-cyanobutyric acid (DGCN) α -centre avoiding racemization of the sensitive *N*-Me-Ala residue. The final macrocyclization between *N*-Me-Leu and a Leucine residue to form the secondary amide proved to be unusually effective benefiting from intramolecular *H*-bonding arrangement of the acyclic substrate (Figure 1.16).⁶¹

Boger's synthesis began with the preparation of amino acid constituents (*4R*)-5-propyl-*L*-leucine (PrLeu), an *N*^{1'}-methoxy-*N*-methyl-*L*-tryptophan (MTO) derivative and DGCN. The PrLeu constituent was synthesised from commercially available (*R*)-(+)-citronellol as shown in Figure 1.17.

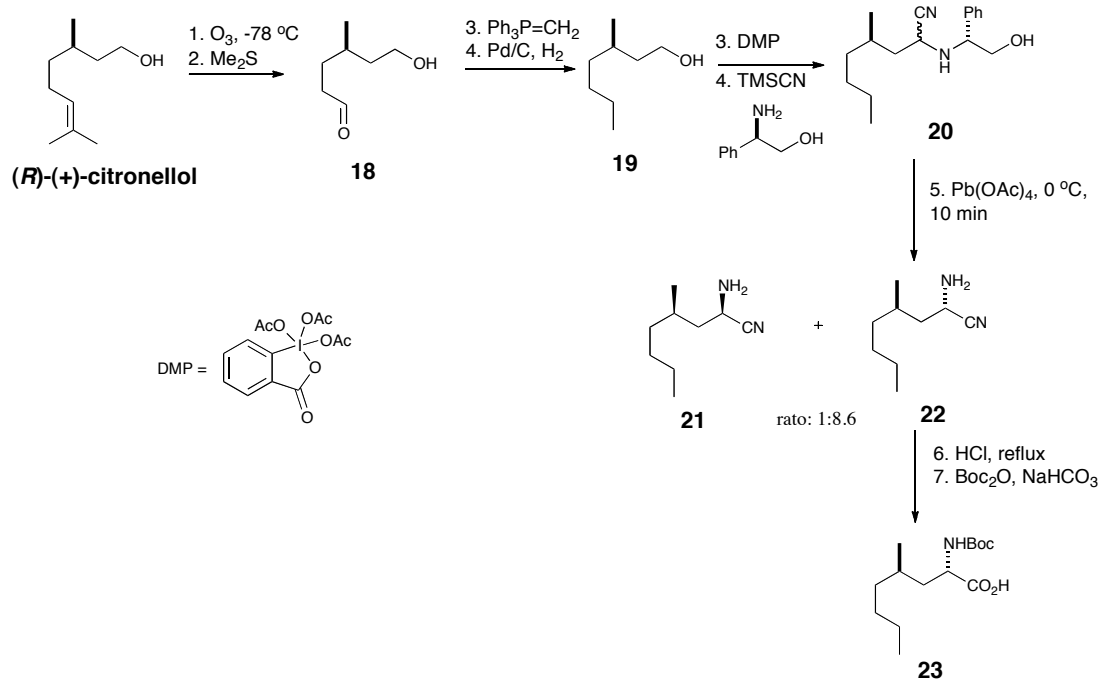


Figure 1.17. Synthesis of PrLeu constituent

Ozonolysis followed by a Wittig reaction with methylenetriphenylphosphorane followed by hydrogenation gave the saturated alcohol **19**. Oxidation with Dess-Martin periodinane (DMP) gave the aldehyde, which then underwent a Strecker reaction without further purification giving an 8.6:1 mixture of (*S*):(*R*) diastereoisomers. It wasn't possible to separate the diastereoisomers at this stage but they found that after oxidative cleavage with lead acetate the free amine **22** could be easily separated from **21** by column chromatography. The stereochemistry was confirmed by synthesis of their Mosher derivatives and comparing ^1H NMR spectra. Hydrolysis of the nitrile to the acid followed by boc protection of the amine under standard conditions gave PrLeu **23**.

The MTO constituent was synthesised in two ways: initially a ten-step process beginning with phenylacetic acid was used utilising an enantiomeric enzymatic hydrolysis of an *N*-acetate by Acylase I from *Aspergillus* sp to get the required

stereochemistry. A shorter more effective synthesis was developed from *L*-Abrine (Figure 1.18) after the original synthesis was completed.

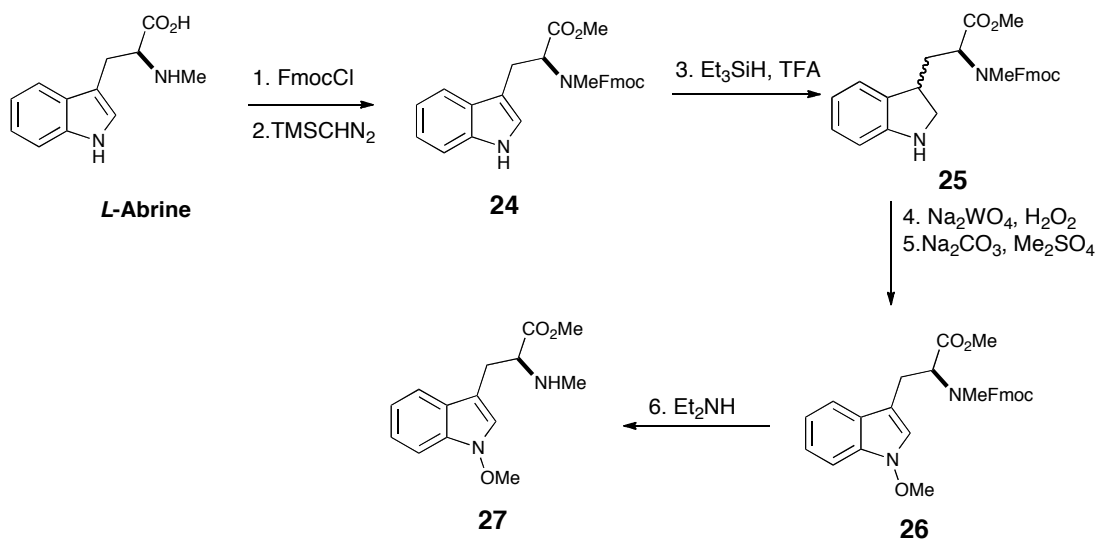


Figure 1.18 Synthesis of MTO constituent

After Fmoc protection and esterification the indole **24** was reduced to the corresponding indoline **25**. The indoline was then *N*-oxidised with *in situ* reoxidation and subsequent *O*-methylation gave indole **26**. Finally Fmoc deprotection gave the MTO derivative **27**.

The (*S*)-2-hydroxy-4-cyanobutyric acid (DGCN) constituent was synthesised as shown in Figure 1.19, the use of Mitsunobu conditions late in the synthesis of HUN-7293 allowed the use of the naturally configured *L*-amino acid as a starting material.

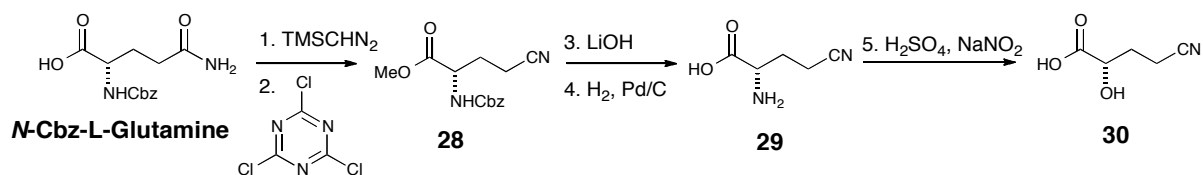


Figure 1.19. Synthesis of the DGCN constituent

The starting material for this sequence was the Cbz protected *L*-Glutamine, which was converted into the methyl ester then dehydrated using the cyanuric chloride to give the desired nitrile **28**. Hydrolysis of the methyl ester and removal of the Cbz *via* hydrogenolysis gave the free amino acid **29**. Upon treatment with H₂SO₄ and NaNO₂ this gave the desired DGCN **30**. It was also found that dehydration of the methyl ester **28** could be accomplished using Ac₂O/py and subsequent hydrogenolysis also gave the free amino acid **29**.

With these constituents in hand attention turned to the synthesis of the tripeptide and the tetrapeptide.

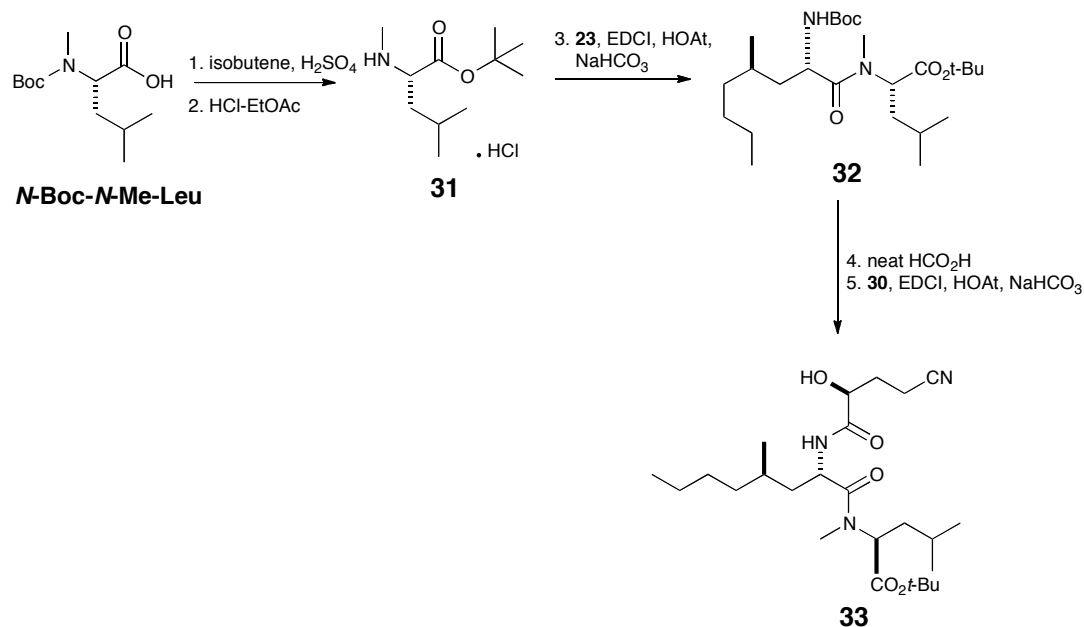


Figure 1.20. Synthesis of the tripeptide

The tripeptide was synthesised as shown in Figure 1.20, from commercially available *N*-Boc-*N*-Me-Leu, which was treated with isobutene and H₂SO₄ in dichloromethane (DCM) to generate the *t*-butyl ester. These conditions simultaneously removed the Boc group after treatment with HCl-EtOAc to give the HCl salt **31**. This was then

coupled to *N*-Boc-PrLeu **23** and the Boc group removed selectively with neat formic acid (30 min at rt). Finally coupling to the DGCN component under the same coupling conditions yielded the tripeptide **33**.

The tetrapeptide was synthesised in a convergent fashion from two dipeptides (Figure 1.21).

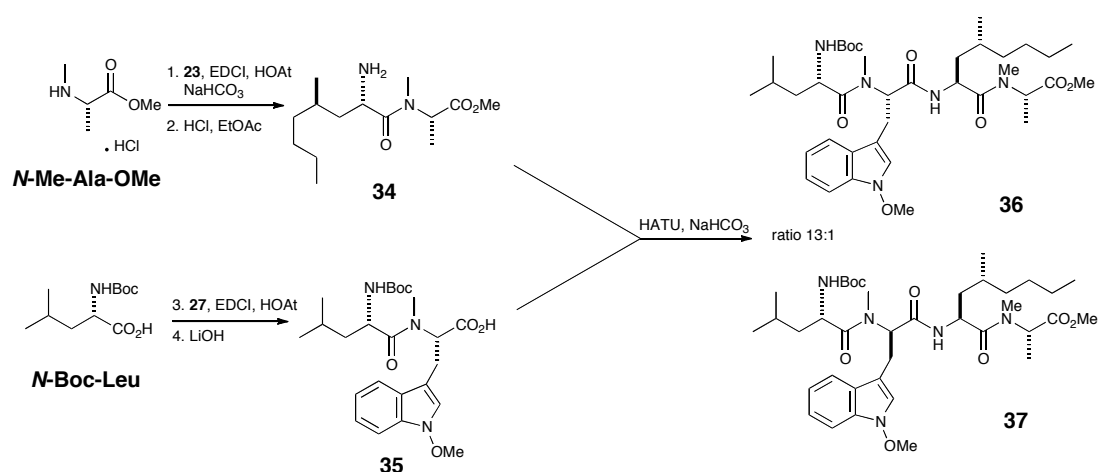


Figure 1.21. Synthesis of the tetrapeptide

The first dipeptide **34** was prepared from *N*-Me-alanine methyl ester (*N*-Me-Ala-OMe), which was obtained using Olsen's procedure to *N*-methylate readily available Boc-Alanine.⁶⁵ Coupling of *N*-Me-Ala-OMe with *N*-Boc-PrLeu **23** followed by deprotection with HCl-EtOAc gave **34**. Dipeptide **35** was prepared by coupling *N*-Boc-leucine (*N*-Boc-Leu) to MTO derivative **27** followed by hydrolysis of the ester with LiOH to give **35**. The final peptide coupling step with HATU gave a 13:1 ratio of diastereoisomers **36:37**, which were separated by semi-preparative high performance liquid chromatography (HPLC). During further studies into the synthesis of analogues for HUN-7293 it was found that using *N*-(3-dimethylaminopropyl)-*N'*-ethylcarbodiimide (EDCI), 3-hydroxytriazolo[4,5-

b]pyridine (HOAt) and 2,6-lutidine in this final step resulted in an increase in ratio from 13:1 to 32:1 in favour of diastereoisomer **36**.⁶²

The final steps of the synthesis, shown in Figure 1.22, involved initial hydrolysis of the free ester **36** followed by a Mitsunobu displacement with tripeptide **33** to give the linear heptadepsipeptide **38**. Finally removal of both the Boc and t-butyl protecting group and macrocyclization using EDCI, HOAt and NaHCO₃ in dimethylformamide (DMF) or HATU and collidine in DCM gave HUN-7293, **39**, in good yield. Interestingly, macrocyclisation with EDCI and HOAt without base present afforded the epimer at the *N*-Me-Leucine center labelled * only.⁶²

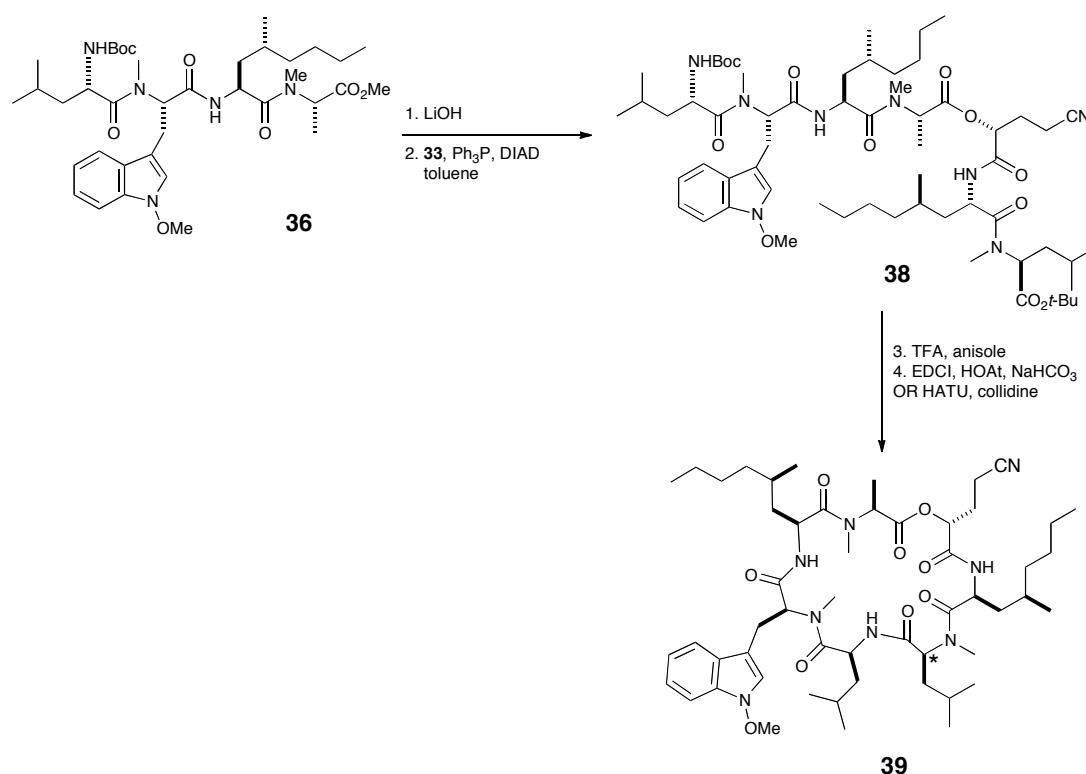


Figure 1.22. Final steps in the synthesis of HUN-7293

As previously mentioned, Boger and co-workers synthesised many analogues of HUN-7293. It is clear from Figure 1.23 that there is a huge potential for variation in its structure.

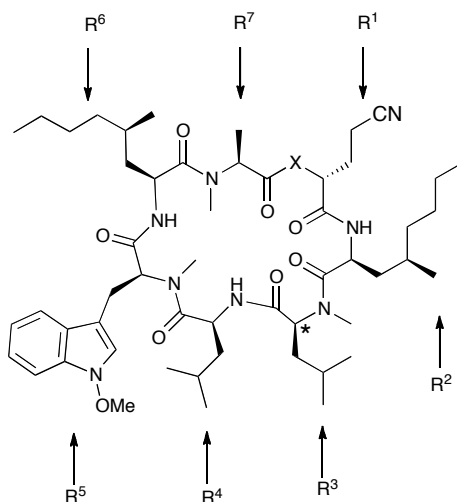


Figure 1.23. Loci for potential structural variation in HUN-7293

All of the analogues synthesised were tested for inhibition of protein expression of both VCAM-1 and inducible cell adhesion molecule-1 (ICAM-1); HUN-7293 exhibited 24-fold selectivity for VCAM-1 over ICAM-1 expression. The first set of analogues to be investigated, shown in Table 1.5, exploited the epimerisation resulting from omission of the base in the macrocyclisation. Introduction of an NH instead of the O at the X position gave *aza*-HUN-7293, however this replacement caused a reduction in potency towards both VCAM-1 and ICAM-1. It was concluded that the stereochemistry of R³ Leucine is important to the properties of HUN-7293. Both epimers **40** and **42** caused a reduction in activity but the epimer **40** only caused a 2-fold reduction in activity compared to the 10-fold loss in potency of **42**.

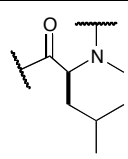
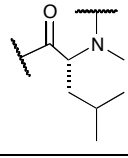
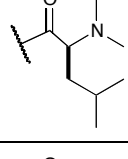
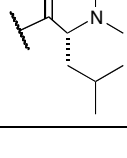
Compound	X	*
39 (HUN-7293)	O	
40	O	
41 (aza-HUN-7293)	NH	
42	NH	

Table 1.5. Summary of analogues prepared by variation at X and/or *

An alanine scan on HUN-7293 was performed to ascertain the significance of each residue on the activity towards inhibition of protein expression of VCAM-1. This involved the replacement of each amino acid side chain with a methyl group whilst preserving the stereochemistry of the backbone. This replacement, in all cases, led to a reduction in potency ranging from 2 fold to 1000 fold. Changes to residue 5 were the most significant and residue 1 the least significant. The study also demonstrated that a change to R¹-R⁴ increased selectivity towards inhibition of VCAM-1 over ICAM-1. Boger suggested that because of these effects then changes to R¹ could be tolerated whereas changes to all other residues would be more challenging especially in the case of R⁵.

The *N*-methyl groups on residues 3, 5 and 7 also appeared to be significant with that on residue 5 the most so. Removal of the *N*-methyl groups resulted in a significant reduction in inhibition (11- and 7-fold in residues 3 and 7 respectively), but the

selectivity for VCAM-1 was greatly improved (54- and 180-fold respectively). Removal of the *N*-methyl group in residue 5 resulted in complete loss of inhibition. The analogues prepared by the Boger group are summarised in Table 1.6.⁶² Variation of the amino acids at R¹, R², R⁵, R⁶ and R⁷ was carried out and R⁵ analogues are shown in Figure 1.23 for clarity.

Compound	R ¹	R ²	R ⁶	R ⁷
39 (HUN-7293)	(CH ₂) ₂ CN	PrLeu	PrLeu	CH ₃
43	(CH ₂) ₃ CN	PrLeu	PrLeu	CH ₃
44	(CH ₂) ₂ CN	(CH ₂) ₅ CH ₃	PrLeu	CH ₃
45	(CH ₂) ₂ CN	CH ₂ CH(CH ₃) ₂	PrLeu	CH ₃
45 epimer	(CH ₂) ₂ CN	CH ₂ CH(CH ₃) ₂	PrLeu	CH ₃
46	(CH ₂) ₂ CN	PrLeu	(CH ₂) ₅ CH ₃	CH ₃
47	(CH ₂) ₂ CN	PrLeu	CH ₂ CH(CH ₃) ₂	CH ₃
48	(CH ₂) ₂ CN	PrLeu	PrLeu	H

Table 1.6. Summary of analogues prepared by variation at R¹, R², R⁶ or R⁷.

The synthesis of **43** involved the incorporation of commercially available (*S*)-5-cyano-2-hydroxypentanoic acid into the final step of the tripeptide synthesis. The analogue showed lower inhibition compared to HUN-7293 but only moderately so. The preparation of **44**, **45** and **45** epimer involved the incorporation of (*S*)-aminooctanoic acid and *L*-leucine into analogues of **32**. Macrocyclisation of the same acyclic heptadepsipetide for **45** with EDCI and HOAt without base present afforded the epimer. **44** and **45** both showed slightly reduced inhibitory potency but slightly enhanced selectivity for VCAM-1. The **44** epimer again had slightly less potency towards inhibition but selectivity towards VCAM-1 was increased. The synthesis of

46 and **47** involved the incorporation of (*S*)-aminooctanoic acid, *L*-leucine and *L*-glycine respectively into analogues of dipeptide **34**. Analogue **46** showed similar potency and selectivity of inhibition of VCAM-1 expression to that of HUN-7293, however shortening the chain as in the case of **47** reduced potency 7-fold. Preparation of **48** simply involved the substitution of *N*-methyl alanine for *N*-methyl glycine. This simplification resulted in only slight reduction in inhibition but increased the selectivity for inhibition of VCAM-1 over ICAM1-1.

Since residue 5 was the site that demonstrated the greatest effect on inhibition a more thorough investigation of this residue was carried out. The analogues prepared are summarised in Figure 1.24.

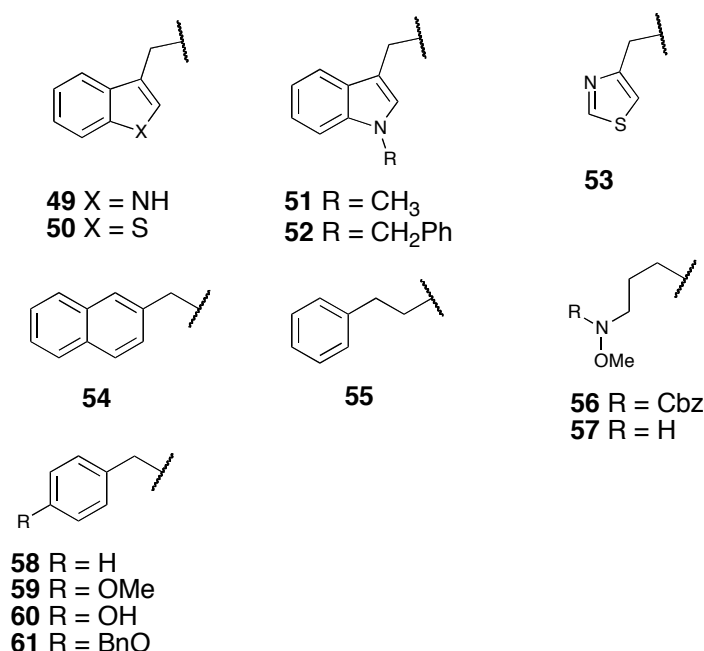


Figure 1.24. Summary of analogues prepared by variation of residue 5

All of these analogues required the synthesis of the corresponding *N*-methyl amino acid precursors, which was carried out using a procedure described by Coggins and Benoiton⁶⁶ (*N*-methylation of the corresponding *N*-Boc carboxylic acid). The *N*-

methyl amino acid methyl ester precursor for **56** was obtained directly by reaction of (*S*)-methyl-2-amino-5-(((benzyloxy)carbonyl)(methoxy)amino)pentanoate with Ag₂O-MeI. The precursors for **50**, **53-55** and **58-61** were all available commercially as their *N*-Boc amino acids or their unprotected amino acids. **51** and **52** were produced by *N*-methylation or *N*-benzylation of the commercially available tryptophan derivatives. Preparation of **56** was accomplished by performing a Mitsunobu displacement of the primary alcohol derived from reduction of Boc-*L*-Glu(*O**t*-Bu)⁶⁷ with CbzNHOMe. **49**, **57** and **60** were products of hydrogenolysis of **39** (HUN-7293), **56** and **61** after macrocyclisation. The coupling of **34** with the modified **35** was accomplished with EDCI, HOAt and 2,6-lutidine in order to reduce epimerisation. Although most of the analogues were less potent than HUN-7293 some had surprisingly similar potency in particular **54**, **55** and **58**. **58** showed only 2-fold less potency than HUN-7293, which led to Boger postulating here that the presence and position of hydrophobic aromatic side chains are important. Introduction of a more polar group into **58** as in the cases **59-61** substantially reduced activity, as did the removal of the methoxy group on HUN-7293 in case **49**. Incorporation of benzothiophene gave an inhibitor (**50**) that was nearly equipotent to HUN-7293.

Boger concluded that many of the side chains could be altered without affecting potency and even, in some instances, induce improvements in selectivity towards VCAM-1 expression inhibition.

Cotransin, a sister compound to HUN-7293, can be prepared using the same synthetic approach to HUN-7293. Garrison and co-workers synthesised Cotransin by changing the amino acids at positions R², R⁵ and R⁶ and using readily available *L*-lactic acid at R¹.⁵⁸

1.8 Click Chemistry.

Photoaffinity labelling is a powerful tool for identifying protein targets of biologically active small molecules, however, the small molecule must retain its biological activity after a photo reactive group has been attached.

MacKinnon *et al* utilised a strategy using a photo-leucine as a photoaffinity label and ‘clicking’ on a rhodamine-azide reporter, which in-gel fluorescent scanning revealed a major rhodamine labelled protein with an apparent MW of ~50 kDa.⁶⁸

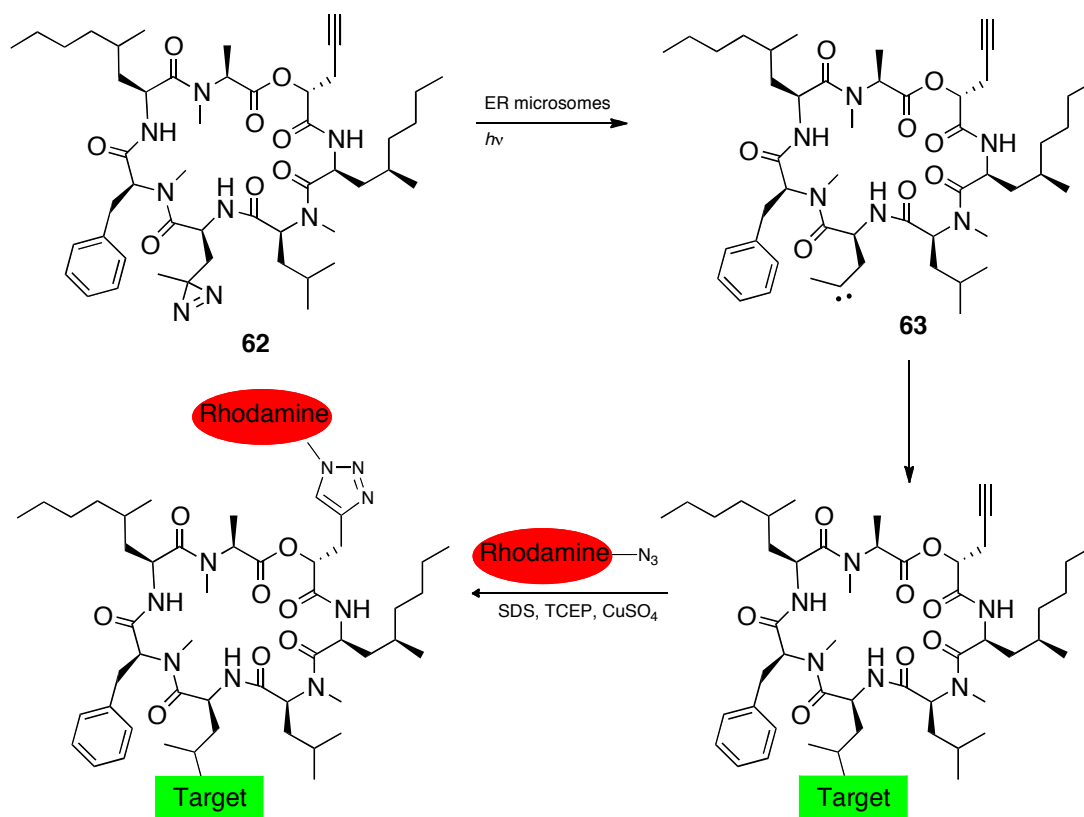


Figure 1.25 Photoaffinity labelling strategy employed by McKinnon *et al* to identify the target of heptadepsipeptide 1 (Taken from McKinnon *et al*⁶⁰): Upon treatment with UV light the photoleucine loses nitrogen to give the corresponding carbene **63**, the carbene photocrosslinks to its target protein, which was detected by “clicking” on rhodamine azide reporter.

The photoaffinity probe after being irradiated forms a highly reactive species that attaches itself irreversibly⁶⁹ to the target that it blocks. Once attached proteins then are denatured: the fluorescent tag is attached using standard “click” chemistry conditions at the propargyl unit and subsequent electrophoresis fluorescent scanning revealed their major fluorescently labelled target (Figure 1.25). This is another possible way to determine the protein channels involved in the ERAD pathway.

Nature shows a preference for the production of carbon-heteroatom bonds over carbon-carbon bonds. Click chemistry takes its cue from nature’s approach employing a set of powerful, highly reliable and selective reactions for the rapid synthesis of new compounds.⁷⁰ There is a strict set of criteria that a process must meet to be grouped in the click chemistry reaction set. The reaction must be widely applicable, be high yielding, have inoffensive side products, which can easily be removed by non-chromatographic means and must also be stereospecific. The process must also have simple reaction conditions, employ readily available starting materials, require the use of no solvent or a benign solvent such as water or a solvent that is removed easily and isolation of the product must be simple. Reactions satisfying all of these criteria are said to be ‘spring loaded’ for the formation of a single product. Carbon-heteroatom bond forming reactions comprise the most common examples, which include:

- Cycloadditions of unsaturated species, 1,3-dipolar cycloadditions especially but also Diels Alder transformations;
- Nucleophilic substitutions, particular ring opening of strained systems such as epoxides;
- Carbonyl chemistry of non-aldol type, such as formation of amides, hydrazones, oximes, and ureas;

- Addition across carbon-carbon multiple bonds, particularly oxidative additions such as epoxide formation but also Michael additions.

The most widely used of all click chemistry reactions is the Huisgen dipolar cycloaddition of azides and alkynes. This reaction unites two unsaturated reactants and provides fast access to 5-membered triazoles. The uncatalyzed azide-alkyne cycloaddition reaction, like all “click” reactions, is thermodynamically very favourable. However, the reaction suffers from two major disadvantages, one being the requirement of high temperature and two being the possibility of forming both 1,4- and 1,5-regioisomers in an equal ratio as shown in Figure 1.26.⁷¹

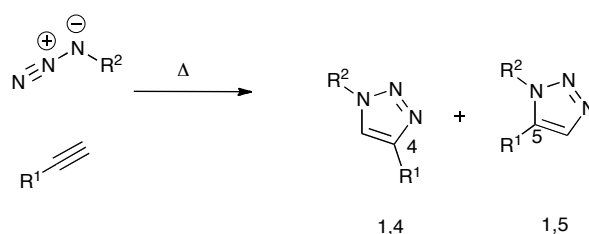


Figure 1.26. Uncatalysed click chemistry

In 2002, the copper-catalyzed azide-alkyne cycloaddition was described by Sharpless⁷¹ and Meldal. The copper catalyst allows the reaction to proceed at rt and proceeds regioselectively, with the 1,4-regioisomer being the only product. It is this copper catalysed cycloaddition that will be utilised in this project, an example of which is shown below in Figure 1.27.

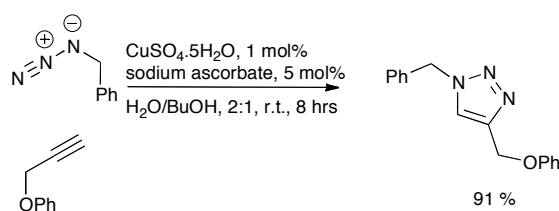


Figure 1.27. Copper catalysed click reaction

This copper catalysed azide cycloaddition has been utilised in several drug syntheses: Kabiramide C, **64**, the triazole analogue of which **65**, shown in Figure 1.28, was found to be as toxic as the precursor itself towards human cervical carcinoma cells.⁷² The alcohol was substituted by an azide and subsequent cycloaddition with propargylamine produced the new analogue.

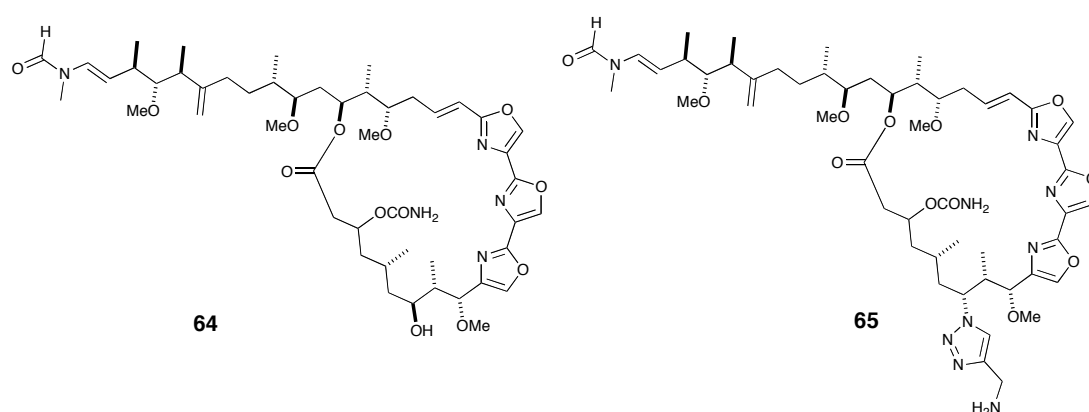


Figure 1.28. Structures of Kabiramide C and its triazole analogue

The “click” cycloaddition has also been used for structural variation of Vancomycin, an effective way of overcoming the problem of emerging Vancomycin-resistant strains of bacteria.⁷³

Although the “click” cycloaddition reaction is generally very successful many chemists are often reluctant to use it due to the fact that potentially explosive azides have to be used. Sharpless *et al* make a note of a general rule of 6: there must be six or more carbons or other atoms of similar size per energetic functional group, in this case the azide, to make the compound “relatively” safe. It is also noted that azides attached directly to olefinic, aromatic or carbonyl moieties are much less stable than aliphatic azides.⁷⁰ It is relatively safe to prepare, use and store azides providing

common sense is applied.

Copper(I) species are powerful catalysts for the formation of 1,2,3-triazoles from azides and alkynes. The general thermodynamic instability of Cu(I) however, results in easy oxidation to Cu(II) and/or disproportionation to Cu(0) and Cu(II). TBTA, tris-[(1-benzyl-1H-1,2,3-triazol-4-yl)methyl]amine, is a stabilizing ligand for Cu(I) and was developed by the Sharpless group in an attempt to improve catalytic activity.⁷⁴

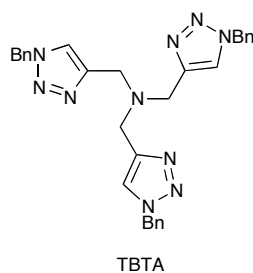


Figure 1.29. Structure of TBTA

TBTA, shown in Figure 1.29, protects Cu(I) from oxidation and disproportionation, while enhancing its catalytic activity. Reactions are typically carried out with 1-2 mol % Cu(I) and TBTA without having to exclude oxygen and water.

1.9 Project aims

Previous work by Cross *et al*⁵³ and Wang *et al*⁵² showed that “eastern” part of the structure was essential for activity, ES35 a compound without this arm was inactive in all assays. In contrast, a truncated version, **17**, lacking the “western” regions was able to inhibit translocation in *in vitro* assays, confirming that this portion of ESI is responsible for at least some of the biological activity of ESI. In order to determine the structure-activity relationship due to changes to this section of ESI, a series of

analogues will be prepared. Previous work in the lab has shown that **17** inhibits translocation in *in vitro* assays but not when added to live cells, suggesting that it is unable to cross the plasma membrane of live cells. The preparation of more hydrophobic analogues of **17** will be investigated and any changes in the ability of these analogues to cross the cell membrane is increased will be determined.

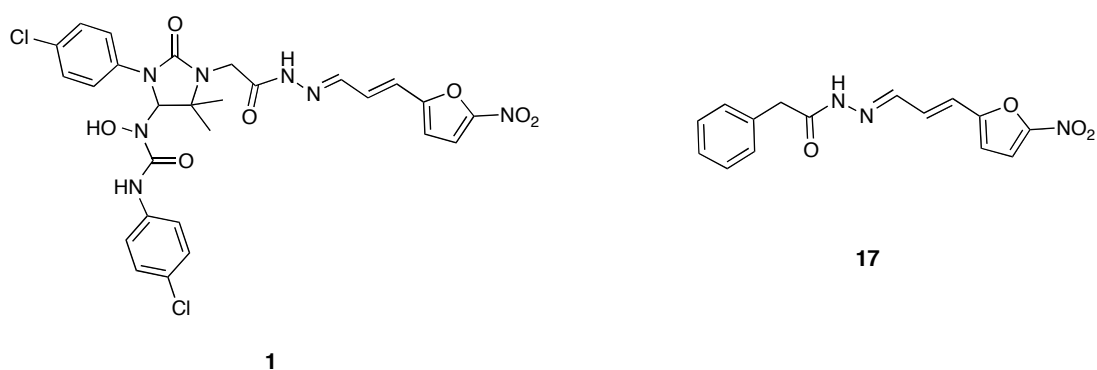


Figure 1.30. Structures of the most potent Eeyarestatins in previous studies

As some of the inhibitory effects of ESI are already known, upon completion of synthesis, inhibitory activity of some if not all of the analogues will be investigated. Bioassays will include: cytotoxicity to determine toxicity of ES compounds at several concentrations; cell microscopy to identify vacuole formation frequently exhibited by ESI; SDS page electrophoresis and western blotting for ubiquitin to ascertain the extent of accumulation of ubiquitinated protein and indicator of inhibition of DUBs; a translocation block assay looking to determine the inhibitory effect the ES compounds have on translocation of selected proteins across the ER membrane; and finally a secretion assay to determine the ES compound's ability to block overall secretion of proteins from cells.

To identify protein targets of the ES compounds, exploiting photoaffinity labelling, the ES compound must retain its biological activity after modification for use with

click chemistry fluorophores. A series of ES compounds containing an alkyne for click chemistry will be synthesised and subjected to bioassay to determine their inhibitory effect before attempting to ascertain which proteins are linked to the degradation pathway by photoaffinity labelling.

Finally, to study the translocation of proteins more closely, Cotransin will be synthesised either by solid phase⁶³ methods or using a modification of the Boger method. This compound is much less complex to prepare, as the majority of the side chains are commercially available as the *N*-Boc amino acids.

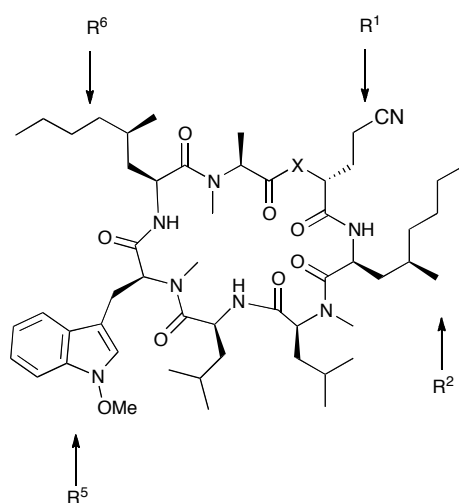


Figure 1.31. Residues of HUN-7293 altered during the synthesis of Cotransin

Cotransin, in a similar manner to HUN-7293, can be prepared in 3 stages. The first stage, the preparation of fragment 1 (Figure 1.32) involves the exchange of Boc-PrLeu at the R² position for Boc-Leucine and DGCN for *L*-lactic acid in the final step.

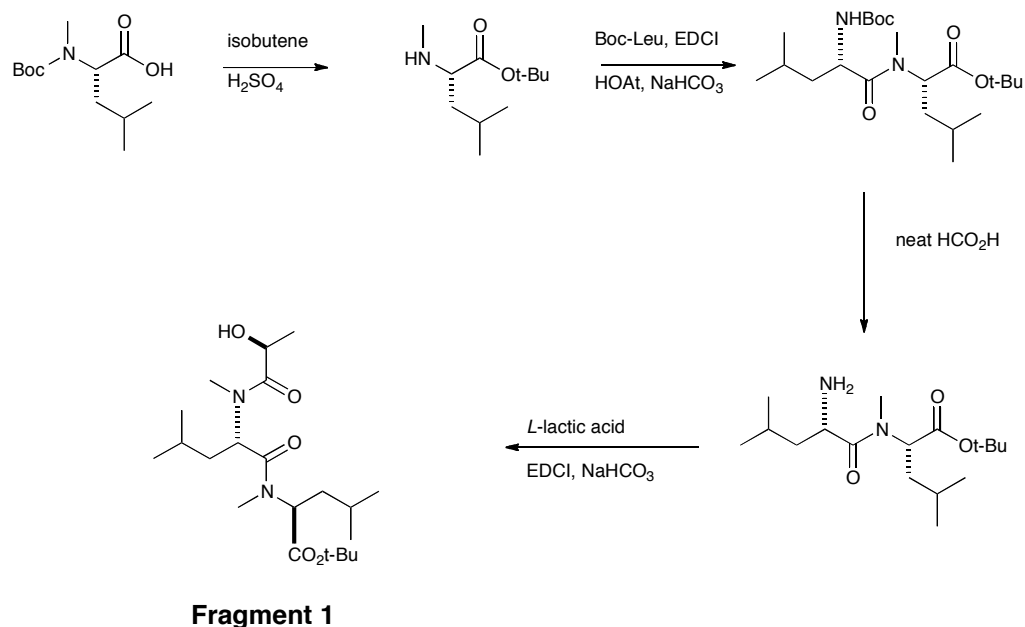


Figure 1.32. Proposed synthesis of fragment 1

The second stage, the synthesis of fragment 2 (Figure 1.33), exchanges Boc-PrLeu at the R⁶ position for Boc-Leu during the synthesis of dipeptide 1 and *N*-Me-Phe-OMe for R⁵ MTO derivative during the synthesis of dipeptide 2.

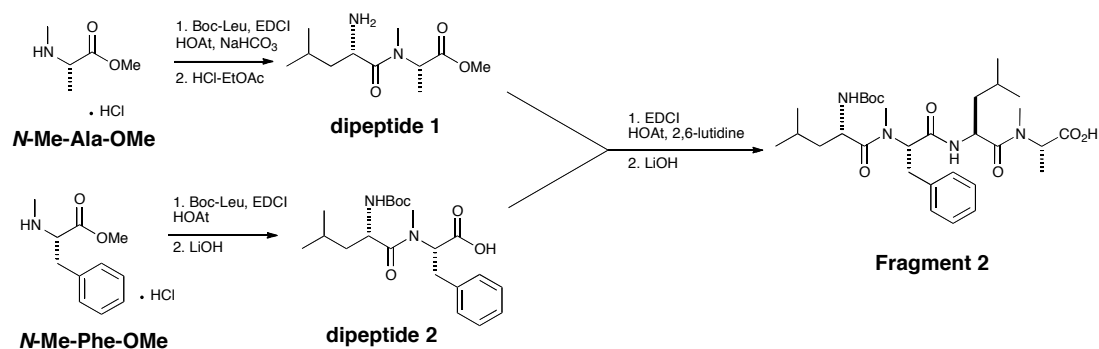


Figure 1.33. Proposed synthesis of fragment 2

The final steps in the synthesis, shown in Figure 1.34, will be similar to those for HUN-7293 although more optimisation may be necessary.

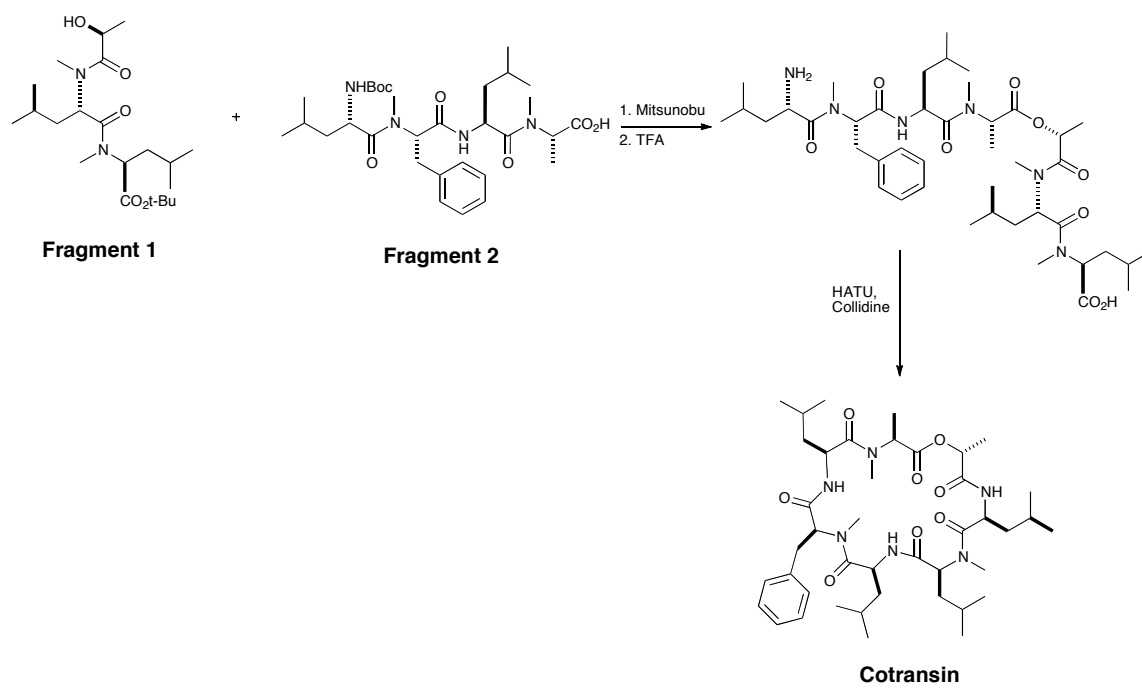


Figure 1.34. Final steps of Cotransin synthesis

CHAPTER 2: RESULTS AND DISCUSSION PART

I: CHEMISTRY

2.1 Synthesis of ESI and ESII.

2.1.1 ESI

The synthesis of ESI starts with the generation of 2-chloro-2methyl-1-nitrosopropane, **66**, prepared according to a literature procedure⁷⁵ by reaction of 2-methylpropene with isoamyl nitrite at $-15\text{ }^{\circ}\text{C}$ and slowly adding concentrated HCl. This procedure gave **66** in a 40% yield.

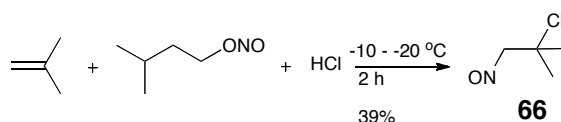


Figure 2.1. Synthesis of nitrosyl chloride

The next step is a substitution reaction of the chlorine with glycine methyl ester to yield the coupled product, **67**, in an 80% yield.

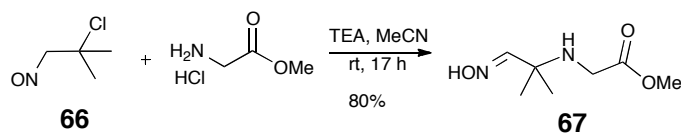


Figure 2.2. Synthesis of glycine methyl ester adduct

The next step involves the reaction of the amine, **67**, with 2 equivalents of 4-chlorophenyl isocyanate in tetrahydrofuran (THF) at room temperature (rt); the mechanism is shown in Figure 2.3.

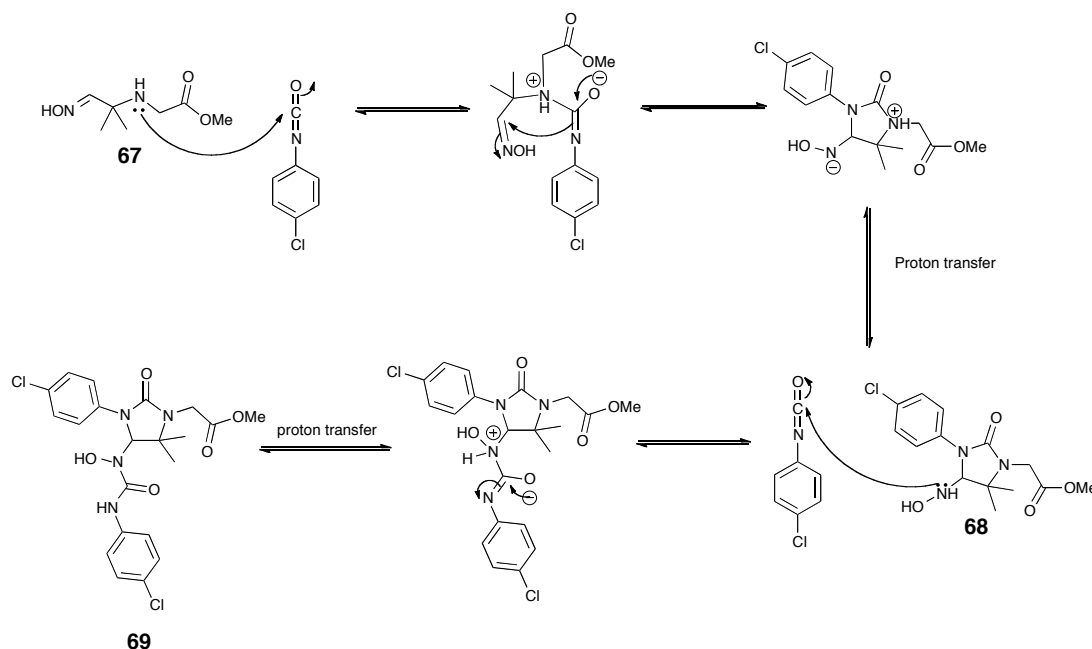


Figure 2.3. Mechanism for formation of symmetrical disubstituted methyl ester

This reaction happens in similar systems under basic conditions, the imide deriving from the isocyanate attacks the oxime to generate the cyclic urea compound **68** after proton transfer.⁷⁶ The second reaction in this case happens so quickly that the linear compound is never isolated. The cyclic urea formation occurs *in situ* and without any basic conditions.

The nucleophilic attack of the hydroxylamine of the cyclic urea **68** is very rapid and even the use of 1 equivalent of isocyanate yielded a mixture of mono- and di-substituted products. This is, inadvertently, a positive result as the disubstituted product is required to continue the synthesis of ESI.

Once the disubstituted product, **69**, had been obtained the next step was to convert the methyl ester into its corresponding hydrazide. This was readily accomplished using a standard procedure often used in peptide synthesis.⁷⁷ A 62% aqueous solution of hydrazine was used as it had been found in earlier work that this gave the best results.⁵⁵ The reaction was carried out in methanol (MeOH) at rt and gave hydrazide **8** (Figure 2.5) in a 63% yield.

With the hydrazide in hand, the final step was the coupling with (*E*)-3-(5-nitro-2-furyl)acrylaldehyde, **70**. Before this could be carried out, however, it was necessary to prepare the conjugated aldehyde. This was accomplished in a 70% yield *via* an *E*-selective Wittig reaction between 5-nitro-2-furfural and (triphenylphosphanyliden)acetaldehyde in THF at rt.

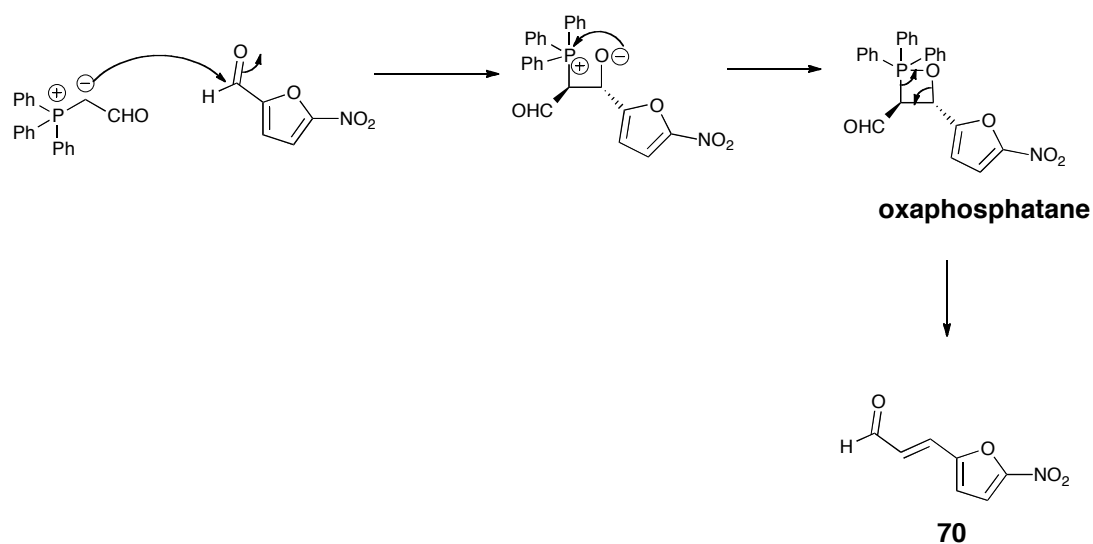


Figure 2.4. Wittig reaction for aldehyde formation

The ylid in the above reaction is stabilised further by the conjugation with the aldehyde. The reason for *E*-stereoselectivity is still debated amongst chemists but some argue that the reaction leading to oxaphosphatane in these types of ylids is

reversible. This suggests that reversal to starting materials can provide a mechanism where *anti* and *syn* diastereoisomers of the oxaphosphetane can interconvert. The *trans*-diastereoisomer is thermodynamically more stable with the bulky groups on opposing sides of the ring, elimination of $\text{Ph}_3\text{P}=\text{O}$ from this oxaphosphetane gives the *E*-alkene. Furthermore, the rate of elimination to the *E*-alkene should be faster than elimination to give the *Z*-alkene due to the difference steric crowding in their respective transition states. The equilibration of both oxaphosphetane diastereoisomers *via* starting materials will replenish supply of the *anti* diastereoisomer and will ultimately give the *E*-alkene as the major stereoisomer.⁷⁸

With the aldehyde **70** in hand, the final step in the synthesis of ESI was undertaken, which involved the condensation of **70** with hydrazide **8** in MeOH at rt, which proceeded in an 81% yield.

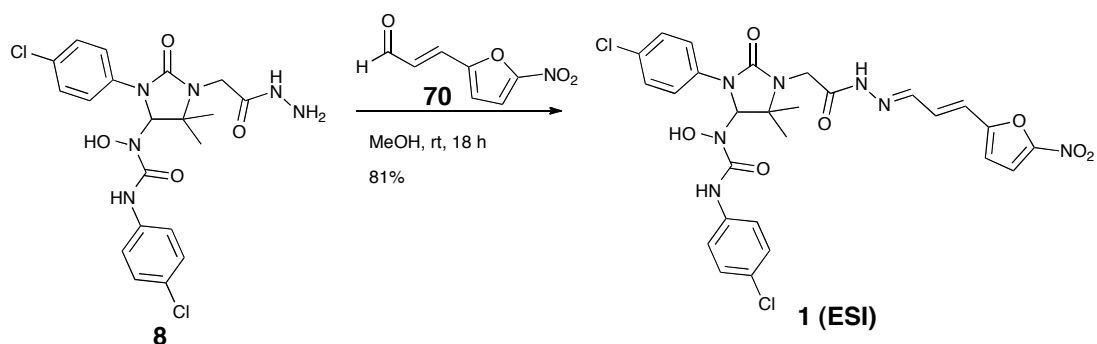


Figure 2.5. Final condensation in the synthesis of ESI

ESI was relatively easy to characterise, however, it is very insoluble and acquisition of ^{13}C NMR data in deuterated chloroform (CDCl_3) was impossible. It was more soluble in dimethyl sulfoxide (DMSO) and it was possible to obtain ^{13}C data but in

this solvent the compound apparently undergoes *cis-trans* isomerism, making the spectra excessively difficult to assign.

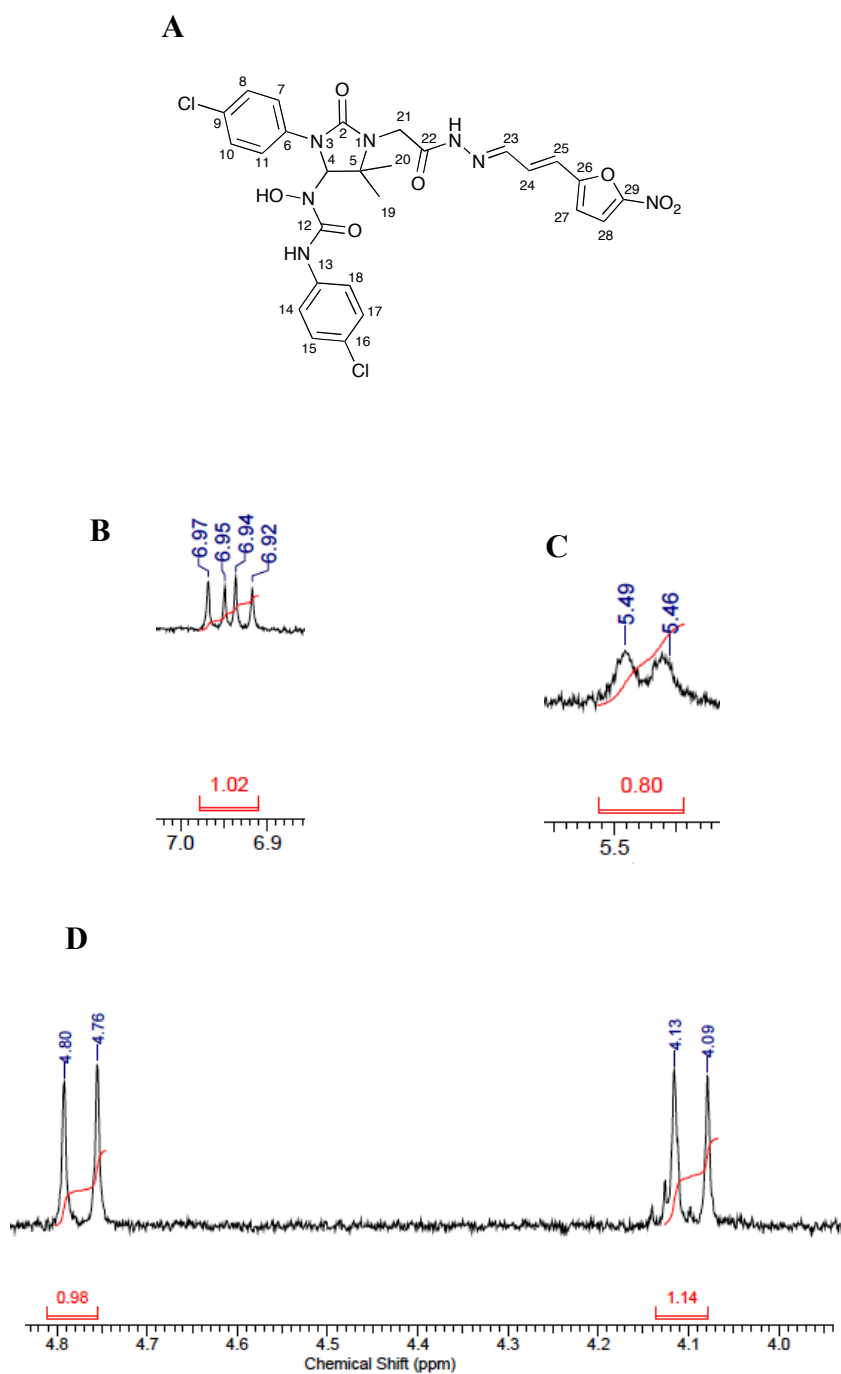


Figure 2.6. Some proton signals of ESI in CDCl_3 : A) numbered structure of ESI; B) proton signal at carbon 24; C) proton signal at carbon 25; D) methylene AB quartet

Figure 2.6 shows proton signals at alkene carbons 24 (Figure 2.6A) and 25 (Figure 2.6B) and the CH₂ at carbon 21 (Figure 2.6C). It is evident from the *J* values from alkene carbons 24 and 25 (15.5 & 9.4 for C(24)H and 15.5 for C(25)H) the structure is predominantly *trans*, however, there is a small indication of the *cis* isomer partially obscured by the doublet at ~4.1 ppm.

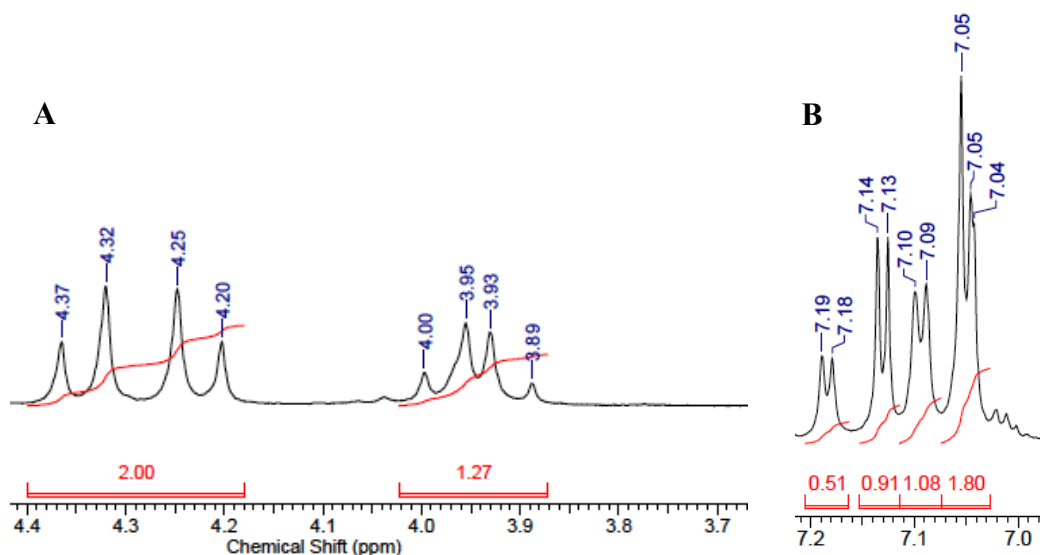


Figure 2.7. Proton signals of ESI in DMSO: A) methylene AB quartet showing *cis-trans* dynamics; B) alkene signals

If the solvent is changed to DMSO, as shown in Figure 2.7A, the relative amount of the *cis* isomer increases suggesting that this system is dynamic. It is not immediately obvious which isomer dominates in *d*₆-DMSO, as Figure 2.7B shows, the alkene signals at carbons 24 and 25 are covering each other making it difficult to determine *J* values for one isomer over the other.

2.1.2 ESII

The synthesis of ESII is almost identical to ESI, the glycine methyl ester adduct, **67**, synthesised earlier was reacted with 2 equivalents of 1-naphthylisocyanate in THF at rt. This gave a 61% yield of the disubstituted ester, **71**.

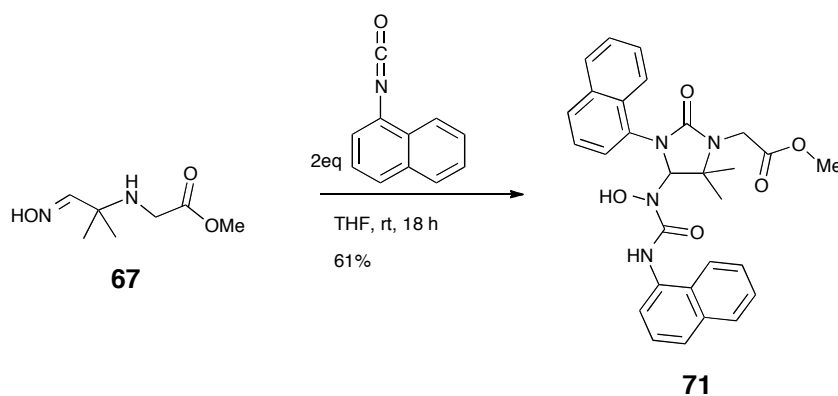


Figure 2.8. Synthesis of methyl ester precursor to ESII

This was then converted into its corresponding hydrazide by reacting, **71**, with 62% hydrazine solution in MeOH at rt with a 55% yield.

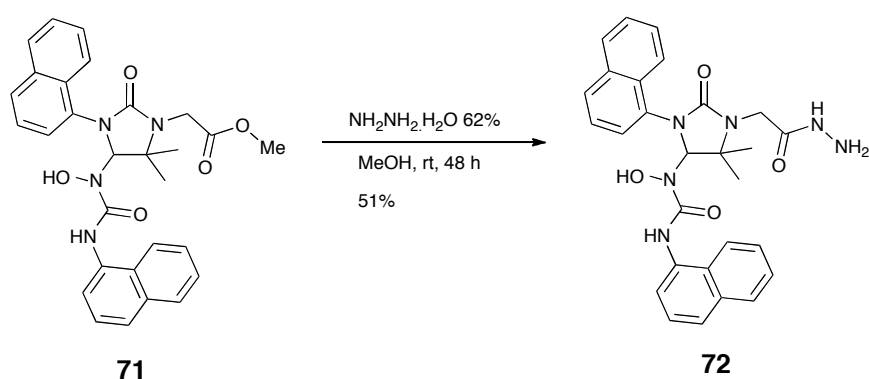


Figure 2.9. Hydrazide precursor to ESII

The hydrazide was then coupled to the (*E*)-3-(5-nitro-2-furyl)acrylaldehyde, **70**, previously synthesised in MeOH at rt; this gave ESII in an 83% yield.

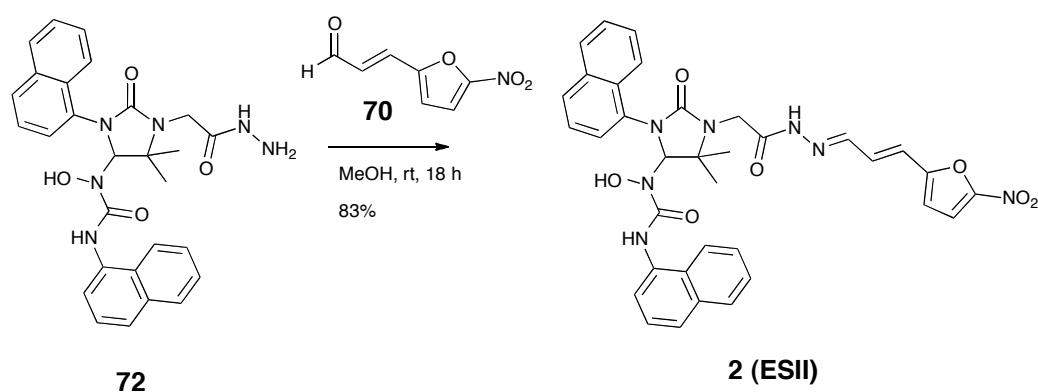


Figure 2.10. Final aldehyde condensation to form ESII

ESII proved much more difficult to analyse by NMR spectroscopy, it is apparent that ESII is less stable than ESI in chloroform with both *cis* and *trans* isomers being present giving a complicated spectrum. A well-resolved proton NMR was difficult to acquire, even though several solvents were used including *d*₆-acetone and *d*₆-DMSO. Eventually, a spectrum of the *trans* isomer as a single entity was finally obtained after the addition of a drop of *d*₅-pyridine to CDCl₃. Other analytical techniques such as mass spectrometry (MS), melting point (Mp) and infra-red (IR) were used to confirm the identity of the structure.

2.2 Synthesis of ESI and ESII analogues.

2.2.1 *p*-nitrophenyl analogue of ESII

The *p*-nitrophenyl analogue of ESII, shown in Figure 2.11, was prepared using the same hydrazide used to prepare ESII. The final step was the reaction of this hydrazide with *p*-nitrophenylcinnamaldehyde to give analogue **73**.

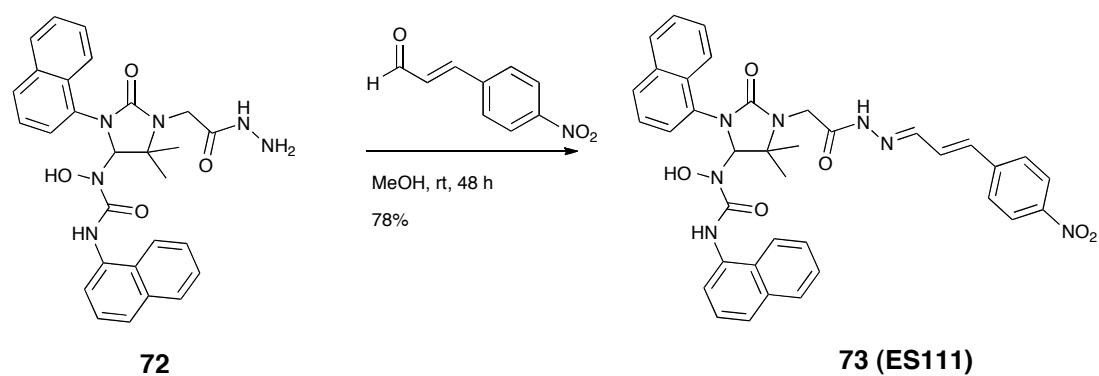


Figure 2.11. Synthesis of *p*-nitrophenyl ESI

2.2.2 Synthesis of symmetrical ESI analogues

The focus of this project was mainly targeted toward ESI due to its enhanced activity towards ERAD inhibition. The first set of analogues prepared involved small changes to the nitrofuran side chain. Figure 2.12 shows the 4 analogues synthesised in this context, which were prepared by reacting the hydrazide precursor **8**, with their corresponding commercially available aldehydes (The ketone precursor for analogue **74** was prepared using a Wittig reaction).

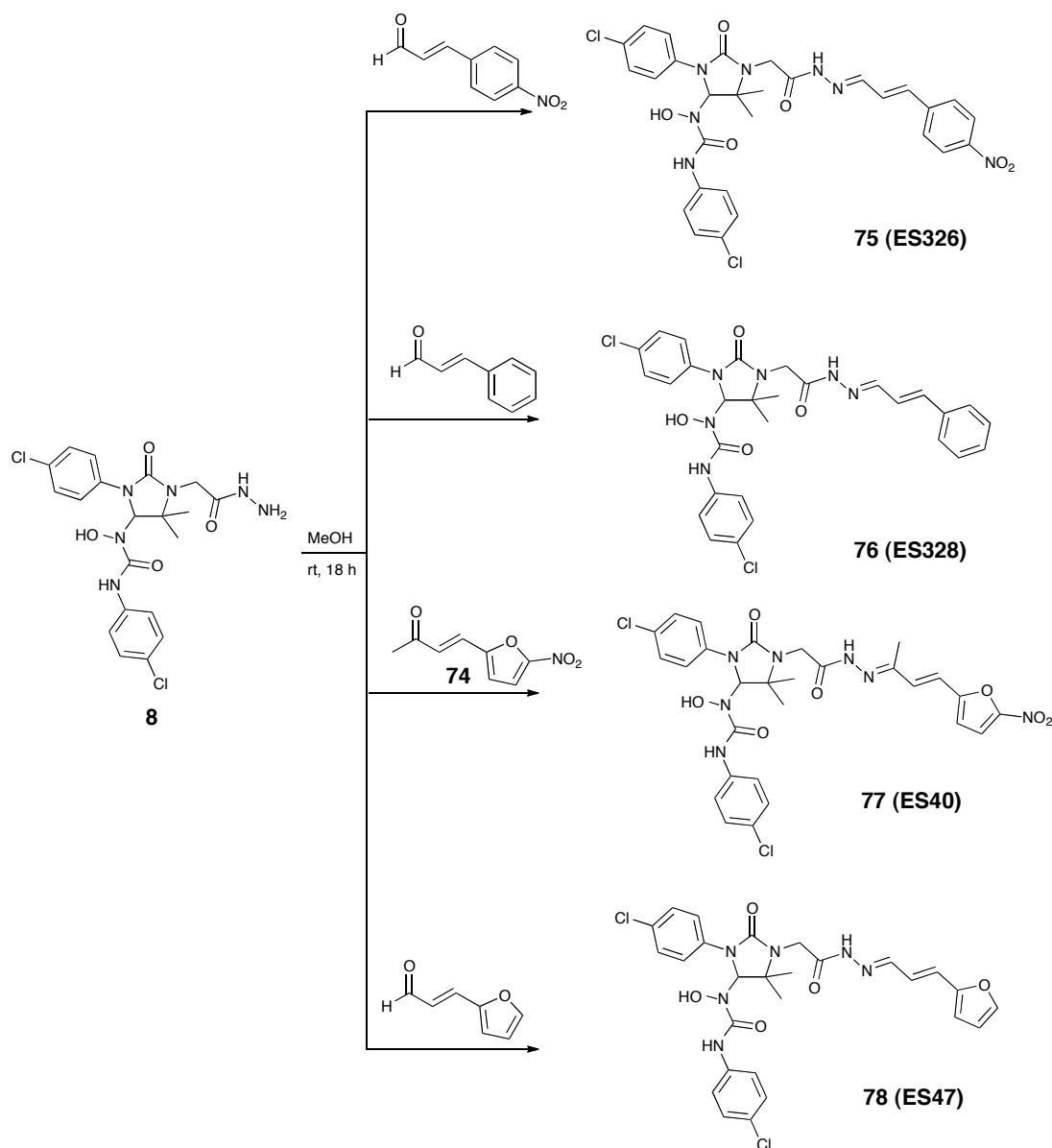


Figure 2.12 Preparation of ESI analogues by aldehyde variation

The *p*-nitrophenyl analogue of ESI, **75 (ES326)**, was obtained in 54% yield by reaction of hydrazide **8** with *p*-nitrocinnamaldehyde. The phenyl analogue **76 (ES328)** was obtained after reaction of hydrazide **8** with cinnamaldehyde in a 47% yield. The furan analogue **78 (ES47)** was prepared by reaction of hydrazide **8** with 2-furanacrolein in 51% yield. The ketone **74** required for the preparation of analogue **77** was synthesised *via* a Wittig reaction between 1-(triphenylphosphoranylidene)propan-2-one and 5-nitro-2-furaldehyde shown in

Figure 2.13. When this ketone was coupled to the hydrazide **8**, analogue **77** was obtained in a 51% yield.

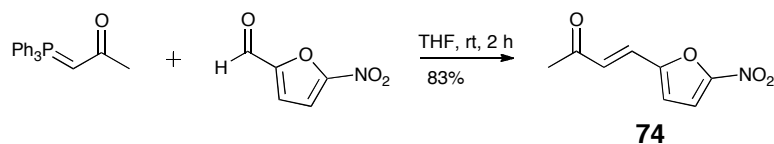


Figure 2.13. Preparation of ketone

All of the analogues exhibited similar dynamics in DMSO to ESI and the ¹H NMR spectrum of *p*-nitrophenyl analogue was unobtainable in CDCl₃ due to poor solubility.

2.2.3 Synthesis of unsymmetrical ESI analogues

In order to prepare and unsymmetrical disubstituted analogues it was necessary to prepare the mono substituted intermediate, **68** (Figure 2.14). Using one equivalent of isocyanate this reaction yields a mixture of mono- and di-substituted products and reaction conditions needed to be optimised. Earlier work had showed that reasonable conditions for the preparation of a mono-substituted product required one equivalent of isocyanate and glycine methyl ester in THF at 0 °C until the glycine methyl ester had dissolved followed by warming to rt.⁵⁵ This gave a ratio of 5.5/1/0 mono/di/**67** respectively, easily distinguished between in a ¹H NMR spectrum. All of the protons are shifted slightly differently, however, the C(3)H is shifted significantly in the two molecules. In the mono substituted derivative it is at δ 4.65 whereas in the disubstituted derivative it is around δ 6.18. Purification by flash column chromatography gave the mono-substituted intermediate as a single product in

average yield of 50%. The maximum yield of 70% was obtained by reacting **68** in THF at 0 °C for a further hour after the glycine methyl ester had dissolved then warming the reaction to rt.

Once the mono substituted product had been prepared, it was necessary to introduce a second R group in order to yield an unsymmetrical methyl ester; the easiest way to accomplish this is to use the appropriate “R-isocyanate”, however, only the corresponding amines were available. An unsymmetrical synthesis, not using an isocyanate, had been carried out previously in the group using 1,1-carbonyldiimidazole and an aminoanthracene. (The general mechanism is shown in Figure 2.14).⁵⁵

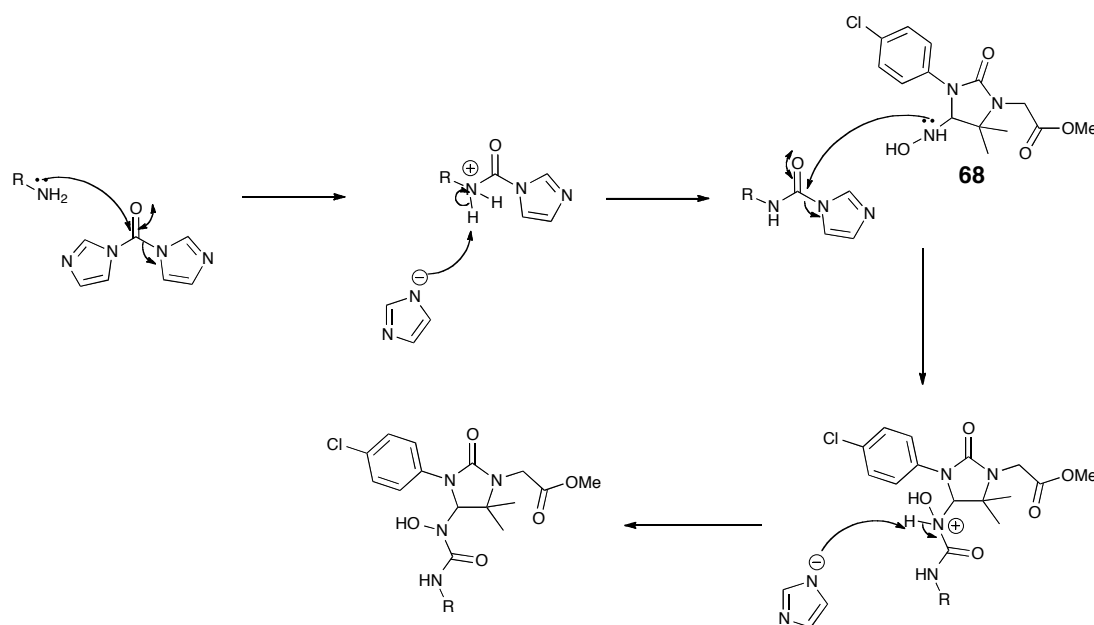


Figure 2.14. CDI mediated introduction of a second R group

Addition of a benzyl amino group under these conditions described was initially attempted (Figure 2.15). This, however, proved unsuccessful with the reaction never reaching completion and yielding mainly the mono-substituted product at the end of

the reaction. Even changing to rt conditions in DCM, as reported by Asato *et al*⁷⁹, and carrying out the reaction at -20 °C in acetonitrile (MeCN) as reported by Bhowruth *et al*⁸⁰, failed to yield the desired methyl ester **79**.

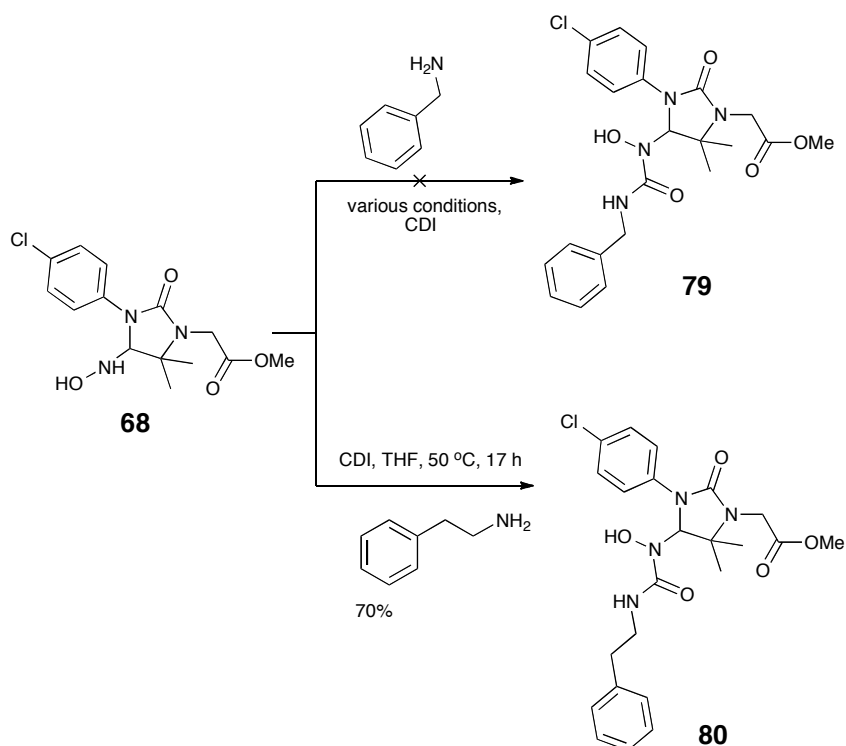


Figure 2.15. Synthesis of unsymmetrical methyl esters

Initial attempts to attach a phenethyl group by carrying out the reaction in THF at 50 °C for 17 h, gave the desired methyl ester **80** in 70% yield. This reaction required the use of 2:1 equivalents of phenethylamine:**68** for reaction to go to completion but any excess phenethylamine could be readily removed by flash chromatography (2:1, petroleum ether (PE):ethyl acetate (EtOAc)). On scale up, a drop in yield to 44% was observed even after increasing both the reaction time and the temperature. This yield was still workable, however, so the conversion into the corresponding hydrazide using the same conditions as for the symmetrical ES compounds gave **81** in 55%

yield. The final coupling proceeded smoothly to give analogue **82** (Figure 2.16) in 50% yield.

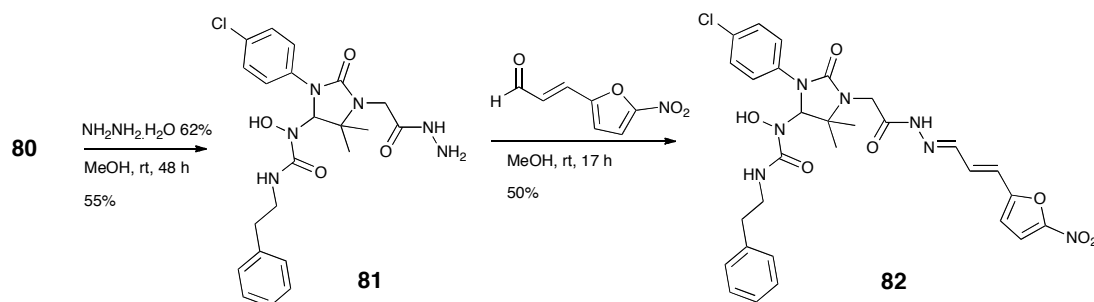


Figure 2.16 Synthesis of “phenethyl Eeyarestatin”

2.3 Synthesis of “short form” Eeyarestatins.

The synthesis of the “short form” analogues of the ESI commences with the conversion of commercially available methyl phenyl acetate into its corresponding hydrazide as shown in Figure 2.17. This was accomplished using a 62% aqueous hydrazine solution in MeOH at rt, to give 2-phenylacetohydrazide, **83**, in 65% yield. This was then coupled to (E) -3-(5-nitro-2-furyl)acrylaldehyde in MeOH at rt to give the short form analogue **17** (ES24), in 66% yield.

It is essential that the hydrazide used in this reaction is pure as impurities remain in the end product after the final reaction. Since the end product, like ESI and ESII, is unstable in solution for prolonged periods of time, it cannot be purified by column chromatography or recrystallisation.

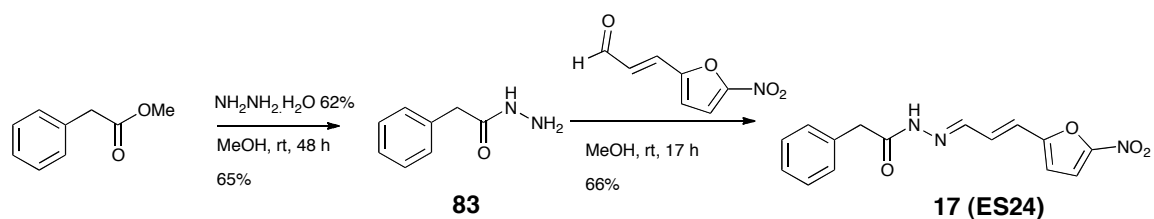


Figure 2.17 Synthesis of a “short form” analogue of ESI (**ES24**)

Syntheses of the short form analogues, **84** and **85** (shown in Figure 2.18) were accomplished by reaction of phenylacetohydrazide **83** with commercially available aldehydes 4-nitrocinnamaldehyde and 2-nitrocinnamaldehyde to give **84** and **85** respectively in identical yields of 89%.

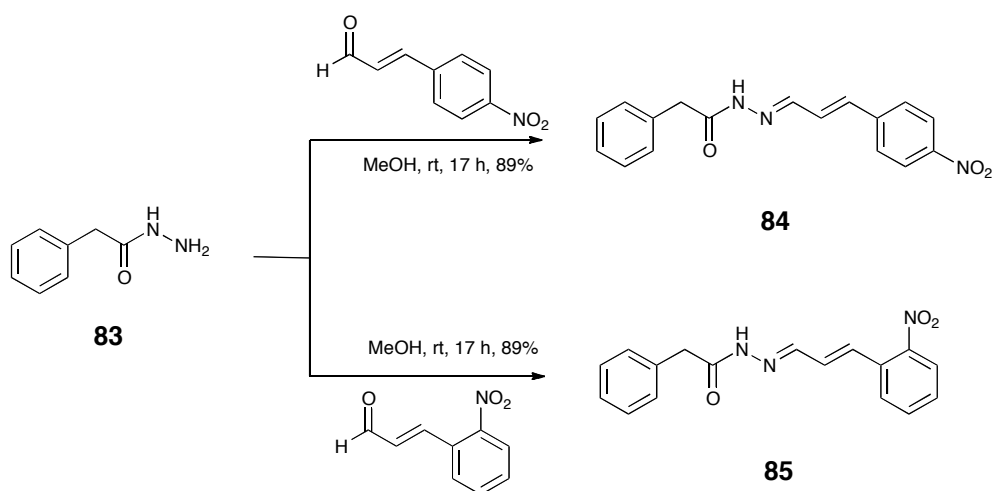


Figure 2.18 Synthesis of analogues of “short form” Eeyarestatin

The synthesis of benzoyl analogue **86** (Figure 2.19) was readily accomplished in a 53% yield by reacting (*E*)-3-(5-nitro-2-furyl)acrylaldehyde with commercially available benzoylhydrazine.

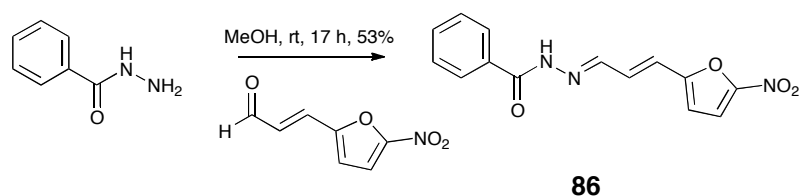


Figure 2.19. Synthesis of “short form” benzoyl analogue of ESI

2.4 Preparation of acetylene derivative suitable for click chemistry

2.4.1 Acetylene analogues of ESI

As has been previously discussed, Click chemistry can be used to remove proteins from a cellular system with a small molecule that is known to interact with them. Having detailed a working synthesis of unsymmetrical analogues, it was possible to prepare a series of acetylenic compounds for application in click chemistry. Three were synthesised (from precursors shown in Figure 2.20), in order to assess whether they were effective in “removing” proteins *in vitro*.

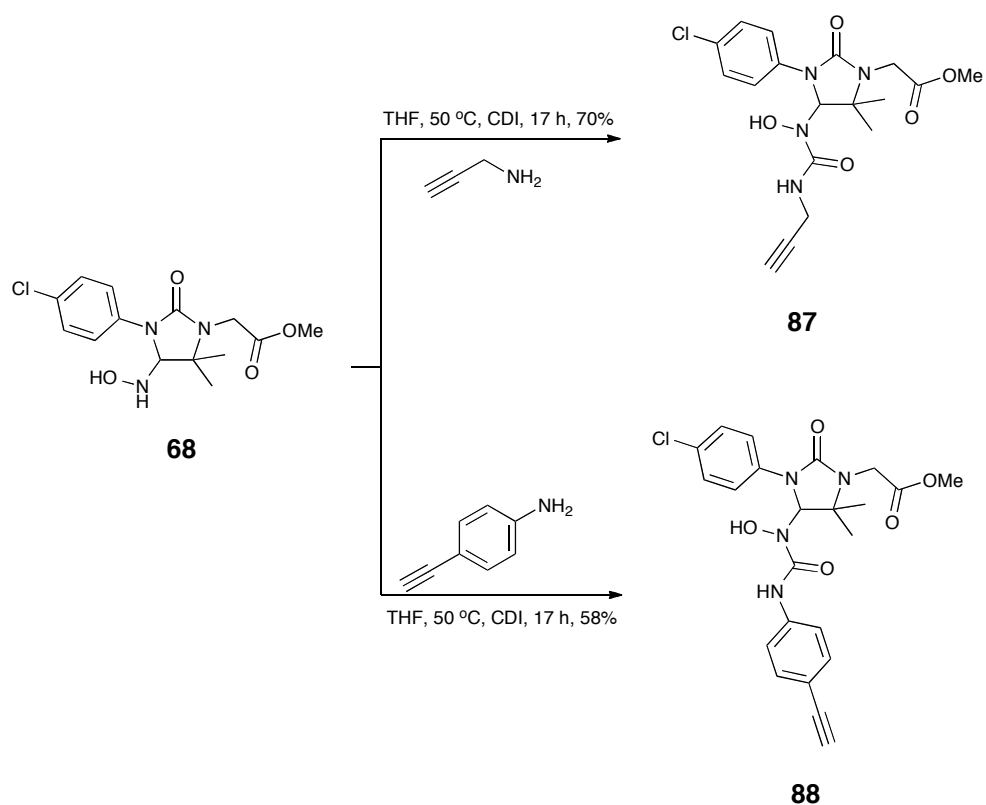


Figure 2.20. Synthesis of acetylenic methyl ester precursors

The synthesis of all three analogues was accomplished by initial reaction of the appropriate amine (propargyl amine for **87** and 4-ethynylaniline for **88**) with cyclic urea **68** and CDI, under similar conditions to those used for the unsymmetrical ES compounds. Flash column chromatography yielded the unsymmetrical disubstituted products **87** and **88** containing the acetylene unit in 70% and 58% yields respectively. The conversion into their corresponding hydrazides was attempted with a 62% aqueous solution of hydrazine. The hydrazides were obtained in a pure state with careful monitoring by TLC. It was found that 2.5 h was sufficient to allow isolation of hydrazide **89** in 98% yield. Only 1.5 h was required to give the corresponding hydrazide **90** in 94% yield: a longer reaction time resulted in the appearance of impurities by TLC analysis.

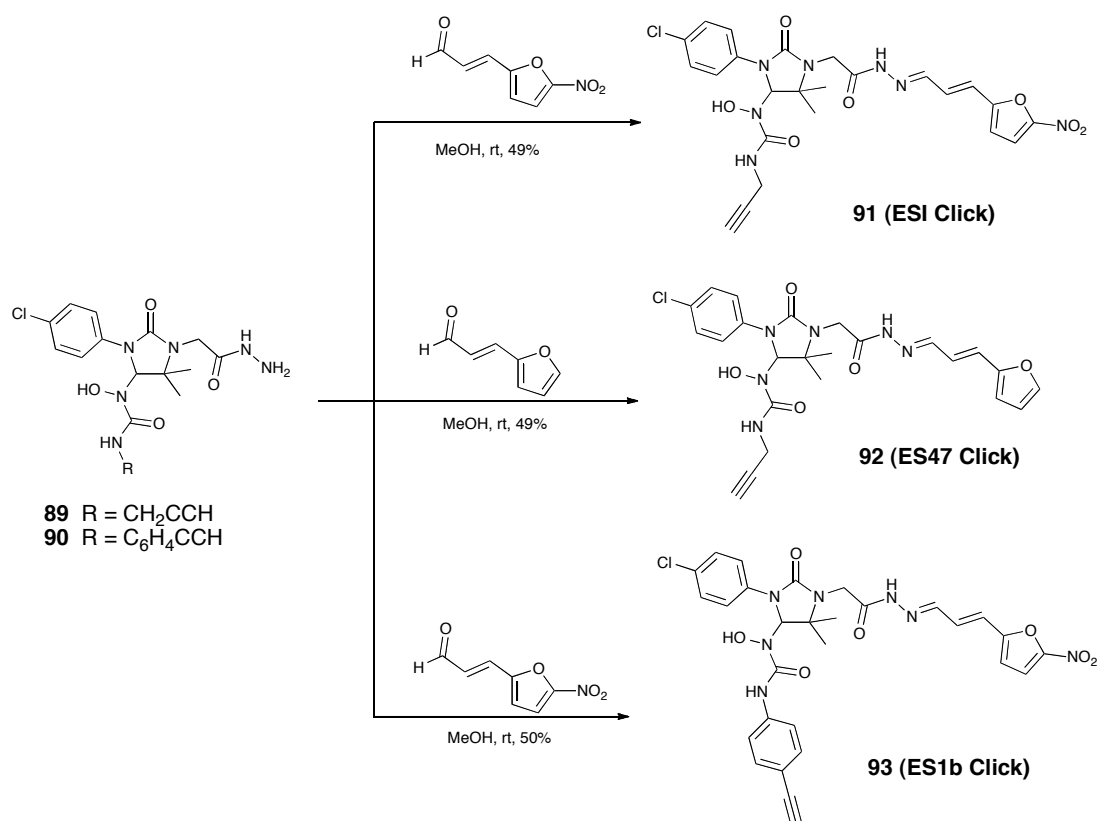


Figure 2.21. Synthesis of acetylenic unsymmetrical Eeyarestatins

The final coupling of hydrazide **89** with aldehydes (*E*)-3-(5-nitro-2-furyl)acrylaldehyde and 2-furanacrolein gave analogues **91** and **92** in identical yields (49%). Coupling of hydrazide **90** with (*E*)-3-(5-nitro-2-furyl)acrylaldehyde gave acetylenic analogue **93** in a 50% yield.

A synthesis of the analogue containing a propargyl unit in the “north west” quadrant (**94** in Figure 2.22) of the ES skeleton was also investigated. Several attempts were made under a variety of conditions, including different temperatures, and molar ratios of CDI and amine, to obtain the monosubstituted methyl ester **94** (Figure 2.22), however, all failed. This may mean that the range of ES compounds accessible is limited by the number of available isocyanates.

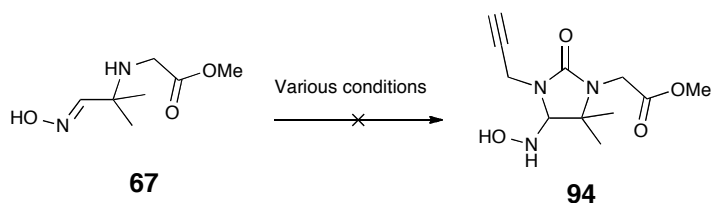
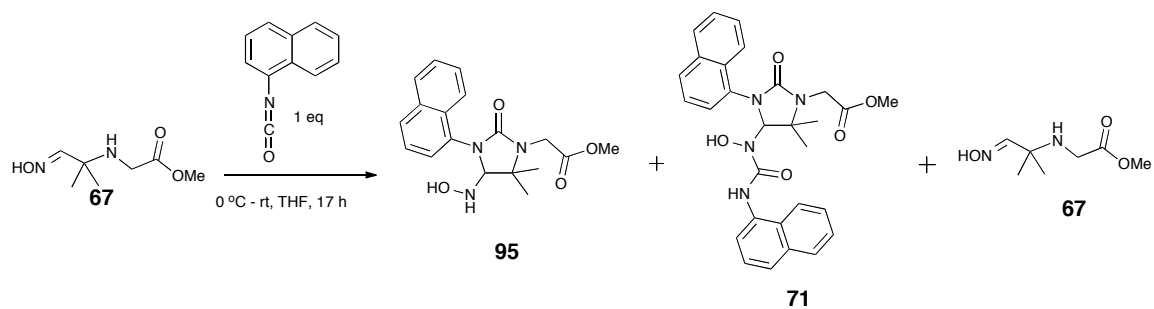


Figure 2.22 Introduction of an acetylenic R-group in the “north west” quadrant of the Eeyarestatins failed

Attempts to prepare this target and other related analogues of this type were abandoned.

2.4.2 Synthesis of the acetylenic analogue of ESII

The first step of the reaction sequence leading to the acetylenic analogue of ESII involved the reaction of the amine, **67**, with one equivalent of 1-naphthyl isocyanate to give mono-substituted compound, **95** (Figure 2.23). This reaction, in the first instance, was carried out at 0 °C to minimise the formation of the disubstituted product, **71**. The first attempt at this reaction resulted in no product formation at all and stirring the reaction mixture at 0 °C for a relatively short time only resulted in the formation of the disubstituted product with some remaining starting material. In the second attempt, the reaction mixture was left at 0 °C for 4 h before allowing it to warm slowly to rt and this greatly improved the yield of product, **96** to 44%. When the reaction was left for longer at 0 °C, this resulted in no improvements in yield. Inevitably, some of the undesirable disubstituted product, **72**, was formed and careful purification by flash column chromatography was necessary.



a) 0 °C for 20 mins then warmed to rt	0%	:	50%	:	50%
b) 0 °C for 4 hrs then warmed to rt	44%	:	19%	:	18%

Figure 2.23. Preparation of the monosubstituted naphthyl methyl ester

After finally obtaining the desired product, **95**, it was necessary to introduce the propargyl unit onto the hydroxylamine. This was accomplished, as described previously, using CDI and propargylamine to give methyl ester, **96**, in a 44% yield after purification by flash column chromatography.

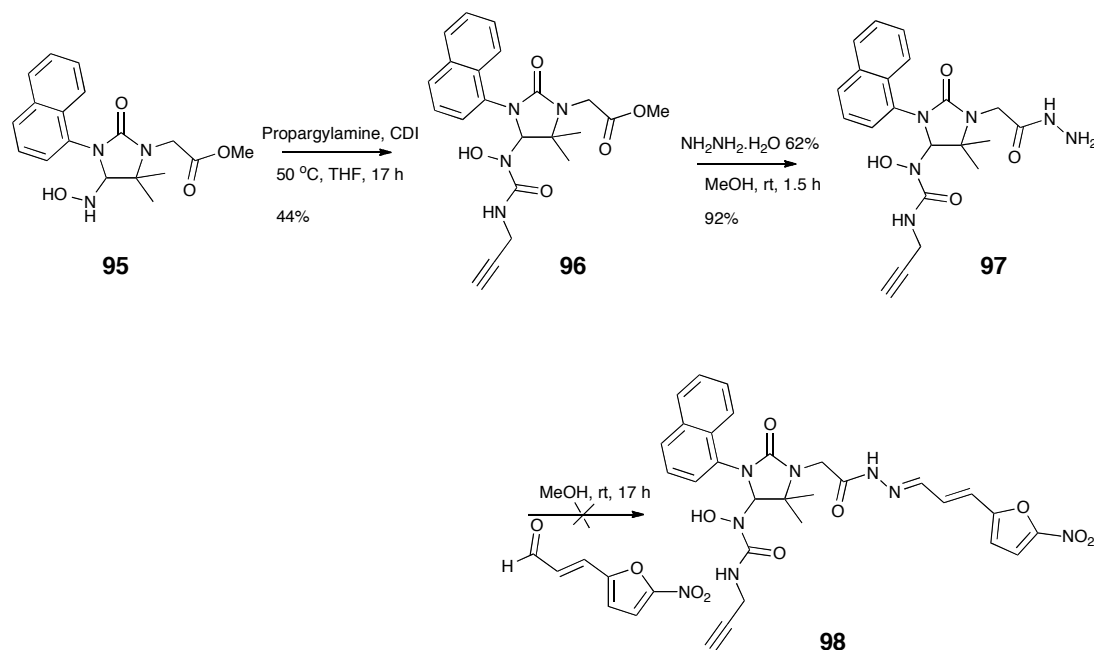


Figure 2.24. Synthesis of acetylenic analogue of ESII

The next step in the reaction sequence was the conversion of methyl ester, **96**, into its corresponding hydrazide, **97**, which was accomplished using a 62% aqueous hydrazine solution in a 92% yield. Careful monitoring by TLC showed that a reaction time of 1.5 h was sufficient to allow the isolation of the pure hydrazide.

The final step in the reaction sequence was the coupling of hydrazide, **97**, with (*E*)-3-(5-nitro-2-furyl)acrylaldehyde. Despite numerous attempts, this reaction proved to be unsuccessful. During initial attempts a solid precipitate formed but unfortunately neither the precipitate nor the filtrate showed any sign of the product **98** when analysed by NMR or mass spectrometry. The mass spectrum showed peaks at 334 and 632 by negative ion electrospray, 238 mass units below and 60 mass units above the anticipated mass respectively. Additional attempts at this reaction were unsuccessful and only starting material was recovered, therefore, this part of the project was abandoned.

2.4.3 Synthesis of short click compounds

There were two questions to be answered by preparing and assaying “short form” acetylenic compounds;

1. Do the “short form” analogues interact with the same proteins as ESI or do they have a different effect?
2. ES24 has trouble getting across the ER membrane. Could adding extra hydrophobic groups increase the effect these shorter compounds have on cells?

After discussion with collaborators compounds **99** and **100** (Figure 2.25) were selected due to their extra hydrophobicity and the alkyne that could also potentially be used in click chemistry.



Figure 2.25. Selected acetylenic “short form” compounds

Both compounds should be accessible from a Sonogashira reaction using their corresponding aryl halides.⁸¹ With this in mind the commercially available 3-bromo and the 4-bromophenylacetic acids were chosen to attempt the synthesis of these analogues. Since many of the final compounds had been found to be unstable when stored for long periods of time in solution and some hydrazides had been difficult to purify, it was decided that the Sonogashira coupling would be attempted on the methyl ester precursor.

The synthesis commenced with esterification of the 3-bromophenylacetic acid **101** under standard conditions as reported by Davies *et al*⁸² to give **102** in a 99% yield.

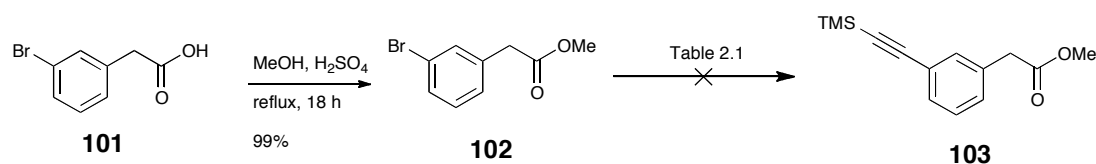


Figure 2.26 Attempted synthesis of methyl 2-(3-((trimethylsilyl)ethynyl)phenyl)acetate

The Sonogashira reaction of 3-bromo methyl ester **103** proved to be a lot more difficult than initially anticipated: Table 2.1 outlines all of the conditions investigated. Entry 1 used a procedure by Iwanowicz *et al*⁸³ who used the same aryl bromide as ourselves. This reaction never reached completion, presumably due the absence of Cu(I) in the Iwanowicz procedure, CuI catalyses the introduction of the

acetylene on the palladium catalyst by substituting for the halide during the transmetallation step. Further attempts using the same conditions but with the addition of CuI (Entry 2 in table 2.1) did not produce any better results. Following this lack of success it was suggested that the temperature may have been too high and either product breakdown was occurring or one or both catalysts were being adversely affected. Lowering the temperature, however, and changing the molar ratio of TMS-acetylene (Entries 3 and 4 in table 2.1) did not improve yields. Eventually, the catalyst was changed to the standard $\text{Pd}(\text{PPh}_3)_2\text{Cl}_2$ and this resulted in an improved ratio of product to starting material but the reaction still lay heavily in favour of the latter. Ahmed *et al* reported that the use of aqueous ammonia as the activator instead of TEA furnished cross-coupling reactions in good to excellent yields.⁸⁴ The addition of aqueous NH_3 in this case, however, (entry 6) never afforded the desired product and after further increasing catalyst loading as well as other reaction variables it was concluded that the C-Br on this molecule was resistant to cross-coupling conditions.

Entry	Mass of ester	Mol% of catalyst	Catalyst	Activator	CuI mol%	Solvent	°C	Equivalents of TMS-acetylene	Ratio of 103:102
1	50 mg	10	Pd(PPh ₃) ₂ (OAc) ₂	TEA	0	Toluene	100	1.5	1:8
2	50 mg	10	Pd(PPh ₃) ₂ (OAc) ₂	TEA	10	Toluene	100	1.5	1:5
3	50 mg	10	Pd(PPh ₃) ₂ (OAc) ₂	TEA	10	THF	rt	1.5	1:4
4	50 mg	10	Pd(PPh ₃) ₂ (OAc) ₂	TEA	10	THF	rt	2	1:5
5	50 mg	10	Pd(PPh ₃) ₂ Cl ₂	TEA	10	THF	rt	1.5	1:3
6	50 mg	10	Pd(PPh ₃) ₂ Cl ₂	NH ₃ (aq)	10	THF	rt	1.5	1:5
7	50 mg	20	Pd(PPh ₃) ₂ Cl ₂	TEA	10	THF	rt	1.5	1:5
8	50 mg	20	Pd(PPh ₃) ₂ Cl ₂	TEA + Vol inc	20	THF	rt	2	1:5

Table 2.1. Conditions investigated for the Sonogashira reaction of methyl 2-(3-bromophenyl)acetate

It was then decided to investigate an aromatic Finkelstein reaction in an attempt to convert the aryl bromide into the corresponding aryl iodide.⁸⁵ This reaction again did not proceed, the GC trace of the reaction mixture indicating only the presence of starting material (Figure 2.27). Following this failure, it was decided to purchase 3-iodophenylacetic acid in order to investigate the Sonogashira reaction further.

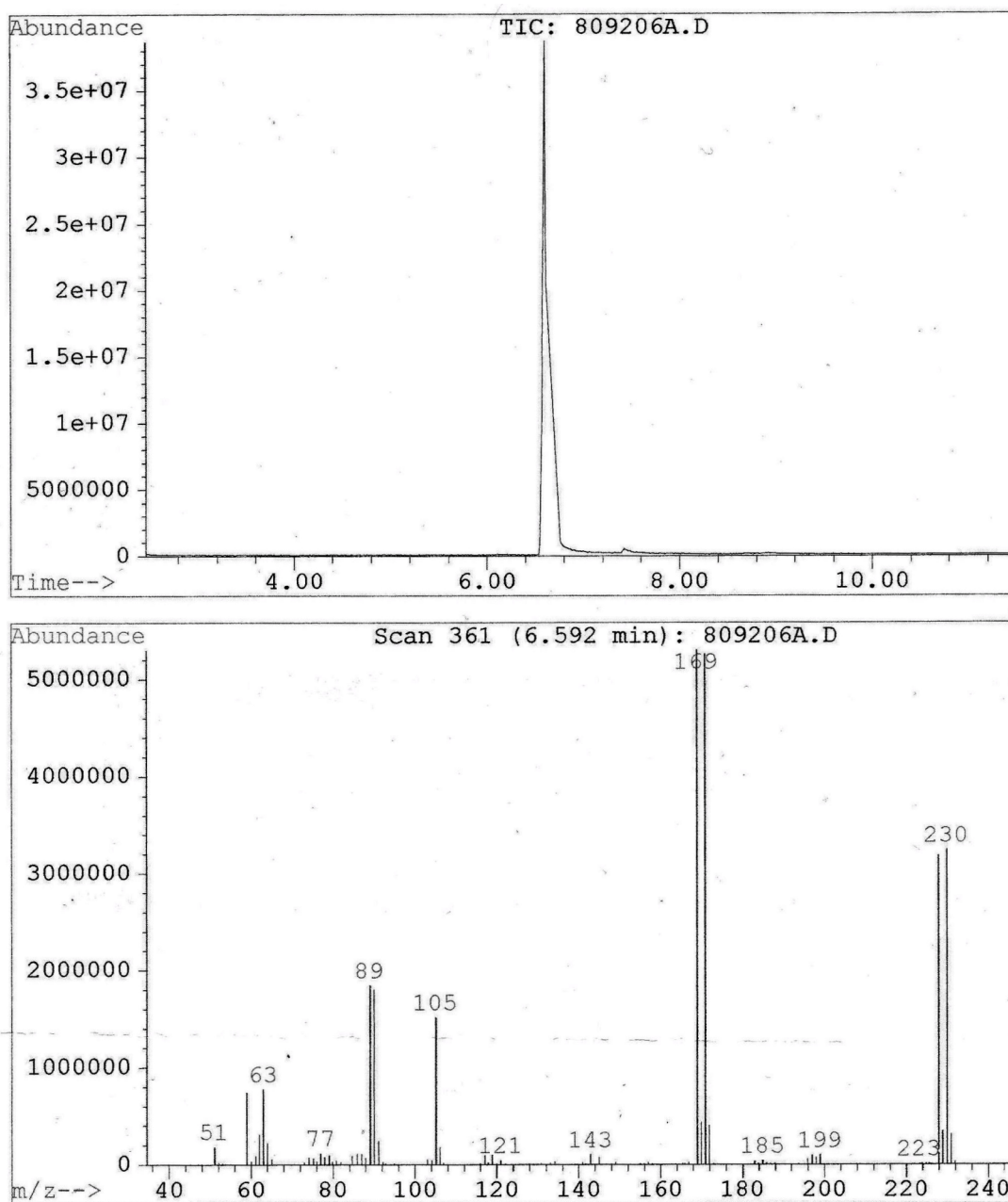


Figure 2.27 GC trace of the reaction mixture of the attempted aromatic Finkelstein

The new synthesis began with the esterification of 3-iodophenylacetic acid, **104**, which proceeded smoothly to give methyl ester **105** in a 95% yield. This was followed by the Sonogashira reaction, which was carried out at rt for 18 h. On this occasion the reaction was successful and gave an excellent yield of 97% of methyl ester **103**. This reaction proceeded smoothly using either of the palladium catalysts

investigated previously and provided similar yields in both cases and never went to completion in the absence of CuI.

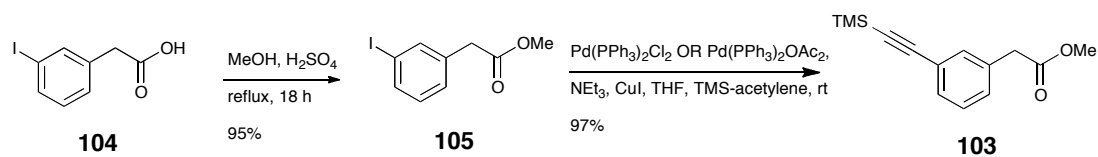


Figure 2.28. Sonogashira reaction on the iodo methyl ester

The next step in the synthesis was the removal of the TMS protecting group, which was accomplished using tetrabutylammonium fluoride (TBAF) in THF to give **106** in a 74% yield. The procedure was that reported by Nagarajan *et al* who had used this on the corresponding *para* isomer of **103**.⁸⁶ The methyl ester was then converted into its corresponding hydrazide **107** using the same conditions as before, however in this step an impurity remained even after flash chromatography. This impurity like the hydrazide was soluble in MeOH so it was proposed that it might be removed in the final step as the ES analogue was expected to precipitate out of solution as the reaction proceeded. The final coupling to (*E*)-3-(5-nitro-2-furyl)acrylaldehyde proceeded smoothly yielding the ES analogue **99** in a 53% yield, with no impurities apparent in the ¹H NMR spectrum, confirming that the impurity in the hydrazide could be removed through washing with MeOH during work-up.

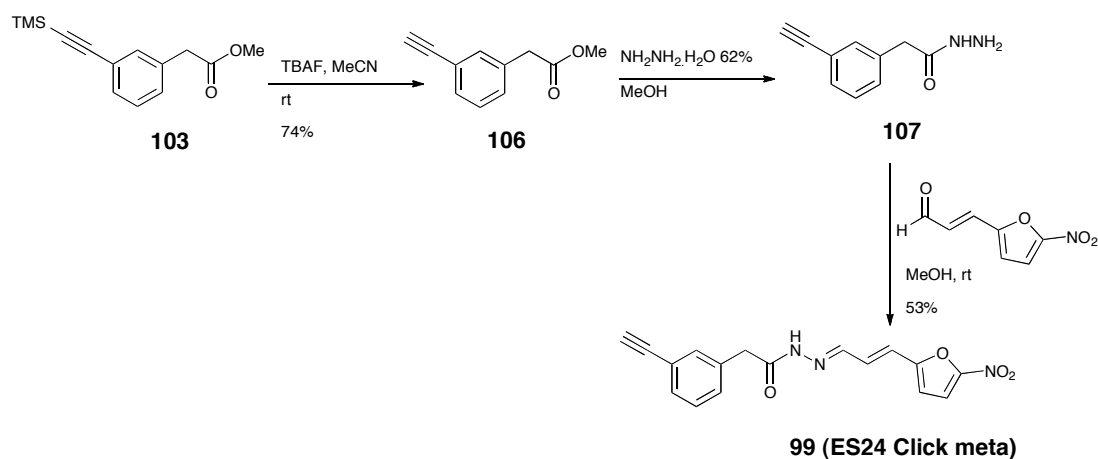


Figure 2.29. Synthesis of ES24 Click meta

The 4-acetylenic analogue was obtained in a slightly different manner commencing with the iodination of methylphenylacetate, **108**, as described for phenylacetic acid by Waybright *et al.*⁸⁷ A test iodination on the methylphenylacetate directly was carried out, however, it was found that yield of product was very low so phenylacetic acid was then used as starting material.

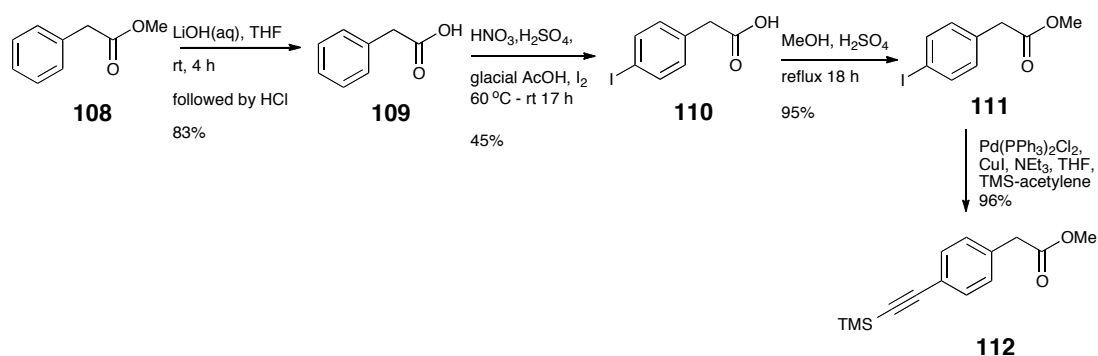


Figure 2.30. Synthesis of the *para* acetylenic moiety

The first step of the sequence was the hydrolysis of methylphenylacetate, **108**, using an aqueous solution of LiOH in THF to give phenylacetic acid, **109**.⁸⁸ This was followed by the iodination reaction following Waybright's procedure; this proceeded smoothly giving the 4-iodophenylacetic acid, **110**, as a single isomer in a 45% yield.

The methyl ester **111** was obtained in 95% yield after esterification with MeOH and H₂SO₄ at reflux for 18 h and the subsequent Sonogashira reaction afforded TMS-acetylene **112** in a 96% yield.

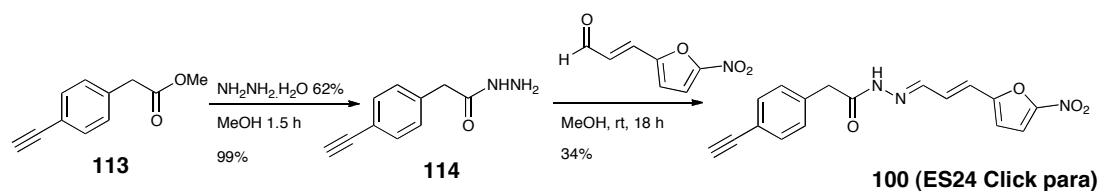


Figure 2.31 Synthesis of para acetylenic “short form” analogue

Removal of the TMS group with TBAF gave acetylene **113** in an 83% yield and subsequent conversion to the hydrazide **114** followed by coupling to the (*E*)-3-(5-nitro-2-furyl)acrylaldehyde proceeded as expected in 99 and 34% yields respectively, to give analogue **100**.

2.5 Click reactions with alkyne Eeyarestatins.

The click reaction requires a stable azide to react with the alkyne previously synthesised. The Webb group previously prepared a suitable azide, the triethylene glycol azide **117** (TEG-N₃).⁸⁹ The first step in their synthesis was the conversion of triethylene glycol, **115**, into the monotosylate, **116** using tosyl chloride, silver oxide and potassium iodide in DCM at 0 °C.⁸⁹ Further searching of the literature revealed a procedure by Feizi *et al*⁹⁰ which gave the monotosylate in a better yield 60 – 70% (Compared to 50% in the Webb group), therefore, this procedure was used in preference. Thus, reaction of triethylene glycol with tosyl chloride in pyridine at 0 °C followed by purification by flash column chromatography gave the desired product in a 61% yield.

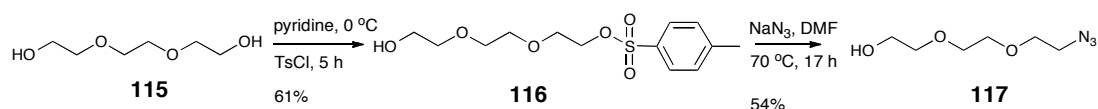


Figure 2.32. Synthesis of triethyleneglycol azide

The next step of the synthesis was the nucleophilic substitution of the tosylate with the azide, which was accomplished using sodium azide in DMF at elevated temperature and furnished triethylene glycol azide (TEG-N₃), **117**, in a 54% yield. With the organic azide now in hand the click reactions of the methyl ester, **87** and the alkyne ES, **91**, were then attempted. For the more soluble methyl ester **87**, a modified procedure by Sharpless *et al*⁷¹ was followed using copper sulphate and sodium ascorbate to give the 1,4-triazole **118** as the only product. Two equivalents of the azide were required for the reaction to go to completion, and after purification by flash column chromatography the triazole **118** was obtained in a 93% yield.

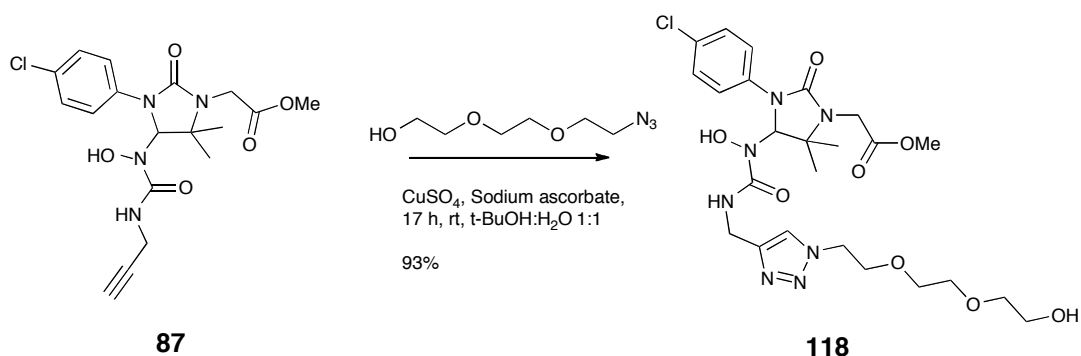


Figure 2.33. Click reaction on methyl ester

For the methyl ester, **87**, it was found that 17 h was sufficient for the reaction to go to completion: for the alkyne ES, **91**, however, an extended period of time was

required, however, after 42 h the reaction was complete and compound **119** was isolated in a 90% yield.

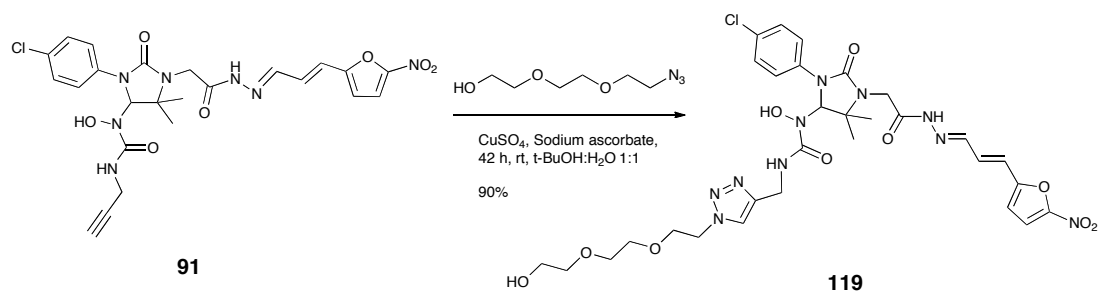
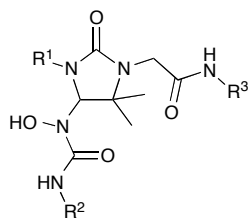


Figure 2.34. Click reaction on alkyne Eeyarestatin

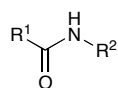
2.6 Summary

Tables 2.2 and 2.3 summarise all of the analogues prepared in this project. ES40, ES47, ES326, ES328, ES111 were all prepared to determine the effect changes to the nitro-furan chain had on inhibition. ESI Click and ES Ib Click were both prepared in preparation for photoaffinity labelling in an attempt to identify proteins affected by these compounds. ES24 Click para and ES24 Click meta were prepared in an attempt to improve hydrophobicity so that the “short form” analogues may be able to cross the cell membrane. All other analogues were prepared to investigate the activity of other “short form” analogues in comparison to activity observed with ES24.



Eeyarestatin	R ¹	R ²	R ³
1 (ESI)			
2 (ESII)			
73 (ES111)			
75 (ES326)			
76 (ES328)			
77 (ES40)			
78 (ES47)			
91 (ESI Click)			
92 (ES47 Click)			
93 (ESIb Click)			

Table 2.2. Summary of ESI and ESII analogues prepared



“Short form” Eeyarestatin	R ¹	R ²
17 (ES24)		
84		
85		
86		
99 (ES24 Click meta)		
100 (ES24 Click para)		

Table 2.3, Summary of “short form” Eeyarestatins prepared

With the synthesis of all of these ES compounds completed and the confirmation that the click reaction on the alkyne ES proceeds as expected they were then used in biological assays to determine their inhibitory activity on ERAD and protein translocation. Unfortunately due to time constraints not all of the analogues synthesised could be tested, a small selection of compounds that were most similar to ESI and ES24 were decided upon and are shown in Chapter 3. The alkyne ES

compounds were also used in an attempt to determine which proteins are affected by these compounds using a similar click chemistry strategy employed by MacKinnon *et al.*⁶⁰

2.7 Synthesis of Cotransin

2.7.1 Solid phase synthesis

The synthesis of Cotransin can be approached in two ways, either by using the solid phase procedure described by Coin⁶³ or in solution by using a modification of the Boger method for the synthesis of HUN-7293.^{58, 62} It was decided that the synthesis would be first attempted using solid phase as it was predicted to be less time-consuming. Figure 2.35 outlines the reaction sequence as reported by Coin this was followed in our approach to the target.

The first step of the synthesis involved coupling of unnatural lactic acid to 2-chlorotriethylchloride resin using *N,N*-diisopropylethylamine (DIEA) in DCM. This resin is usually selected due to its high level of substitution (ideal for shorter polypeptides), acid lability and its ability to minimise diketopiperazine (DKP) formation.^{91, 92} They elected to first attach unnatural lactic acid to the resin due to the consideration that it cannot form an oxazolone when activated, which would be beneficial in the final cyclisation.^{63, 93} The coupling of lactic acid was followed by ester formation with *N*-Me-alanine using *N,N'*-diisopropylcarbodiimide (DIC) activation and *N*-methylimidazole (NMI) as a catalyst. This was then followed by Fmoc removal with 20% piperidine in DMF and coupling of Fmoc-leucine with HATU. The optimal conditions for subsequent removal of the Fmoc group with minimal DKP formation had been found to involve two sequential reactions with 0.15 M TBAF in DMF, for 1 minute each, followed by immediate washing with MeOH and DCM for 15 seconds. This was followed by the immediate coupling to Fmoc-*N*-Me-Phe that had been pre-activated with HBTU and DIEA in DMF giving the tetradepsipeptide **123**. The final three couplings were all accomplished by initial removal of the Fmoc group with 20% piperidine in DMF followed by amide bond formation with HATU or HBTU. Fmoc removal followed by acidic cleavage from the resin and reverse phase HPLC (90:10 H₂O:MeOH) gave linear Cotransin **127** in only a 3% yield compared to the 23% yield reported by Coin *et al*. Further runs were monitored by mass spectrometry confirming that all resin-bound intermediates were the correct products (NMR cannot be used on the scale used in this procedure). Resin loadings were consistent with Coin *et al* and were confirmed by quantifying the piperidine-dibenzylfulvene adduct formed during Fmoc removal using its absorbance at 301 nm and entering it into resin loading equation (Eq 1).⁹⁴ This is achieved by

weighing a small amount of resin (W) and reacting with 1 mL of 20% piperidine in DMF solution. A small volume (v) of this solution is diluted in 1 mL of 20% piperidine in DMF (V) and the UV absorbance at 301 nm taken.

$$\text{Resin loading (mmol/g)} = \frac{\text{Absorbance} \times V \times 10^3}{\epsilon \times v \times W \text{ (mg)} \times \text{cell length (cm)}}$$

$\epsilon = 7800 \text{ M}^{-1} \text{ cm}^{-1}$ at 301 nm

V = dilution volume in μL

v = Volume of solution diluted in μL

W = mass of dried resin

Eq 1. Resin loading equation (Taken from Kay *et al*⁹⁴)

It was concluded that HPLC purification after the acidic cleavage of the linear Cotransin from the resin was very inefficient and low yielding. It was therefore decided that a solution phase synthesis would be attempted as inexpensive natural lactic acid could be used as a starting material and the progress of the reaction sequence could be readily monitored by NMR.

2.7.2 Solution phase synthesis of Cotransin

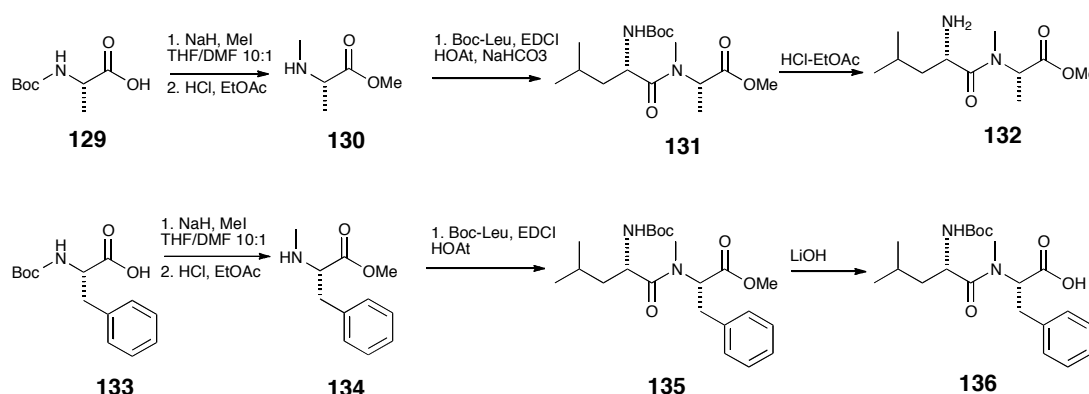


Figure 2.36. Synthesis of dipeptides

The solution phase synthesis of Cotransin commenced with the preparation of the *N*-methyl amino acids *N*-Me-Ala-OMe (**130**) and *N*-Me-Phe-OMe (**134**) from commercially available Boc-alanine, **129**, and Boc-phenylalanine, **133**, respectively. A slightly modified procedure reported by Coggins and Benoiton⁶⁶ was followed using NaH and MeI for methylation followed by HCl in EtOAc (In preference to HBr in acetic acid) for removal of the Boc group. Dipeptide **132** was afforded upon reaction of **130** with Boc-leucine, EDCI and HOAt in the presence of NaHCO₃ and subsequent removal of the Boc group with HCl-EtOAc. Dipeptide **135** was prepared from **134** using Boc-leucine, EDCI and HOAt and subsequent hydrolysis of the ester using LiOH gave dipeptide **136**. Both dipeptides **132** and **136** were used in the next reaction without further purification to generate fragment 2 (Figure 2.37) as a mixture of diastereoisomers, separation by HPLC was necessary but due to time constraints purification by HPLC was not completed.

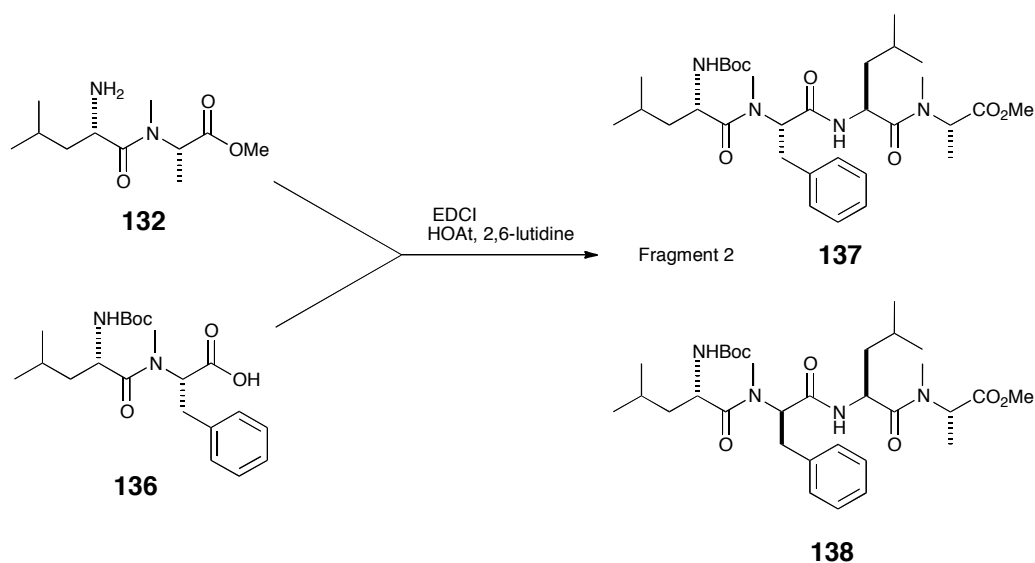


Figure 2.37. Synthesis of fragment 2

Unfortunately, due to time constraints it was not possible to investigate the synthesis of fragment 1 from commercially available *N*-Boc-*N*-Me-leucine (Figure 2.38) and all remaining steps in the solution phase synthesis were never completed (See conclusions and further work for further details).

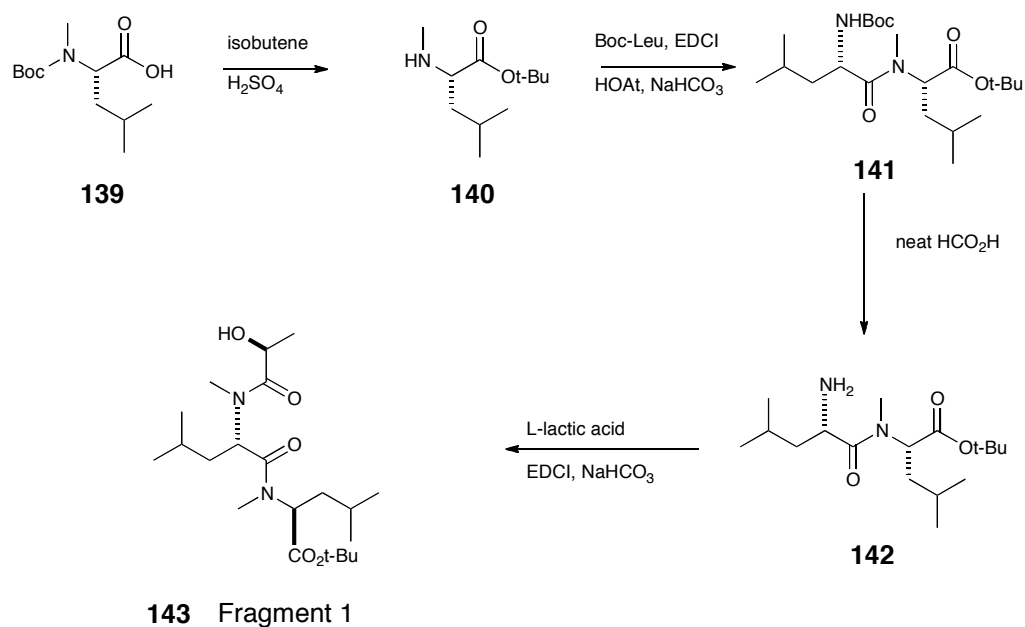


Figure 2.38. Synthesis of fragment 1

CHAPTER 3: RESULTS AND DISCUSSION PART

II: BIOCHEMISTRY

All biological assays were conducted on a selection of compounds previously described in Chapter 2 the majority being shown in Figure 3.1 (See section 3.5 for the others). Previous work by Cross *et al*⁵³ and Wang *et al*⁵² showed that the right hand part of the structure was essential for activity. ES35 a compound without the “eastern” arm was inactive in all assays. In contrast, a truncated version lacking the left hand regions was able to inhibit translocation in *in vitro* assays, confirming that this portion of ESI is responsible for at least some of the biological activity of ESI. In order to determine the structure-activity relationships due to changes to this section of ESI the series of analogues shown in Figure 3.1 was prepared (Structural changes compared to ESI are circled in red). Previous work in the lab has shown that ES24 inhibits translocation in *in vitro* assays but not when added to live cells, suggesting that it is unable to cross the plasma membrane of live cells. The two “short form” analogues prepared by the addition of an alkyne are ideal for investigating any changes in activity observed if the ability of these analogues to cross the cell membrane is increased (Structural changes compared to ES24 are circled in blue).

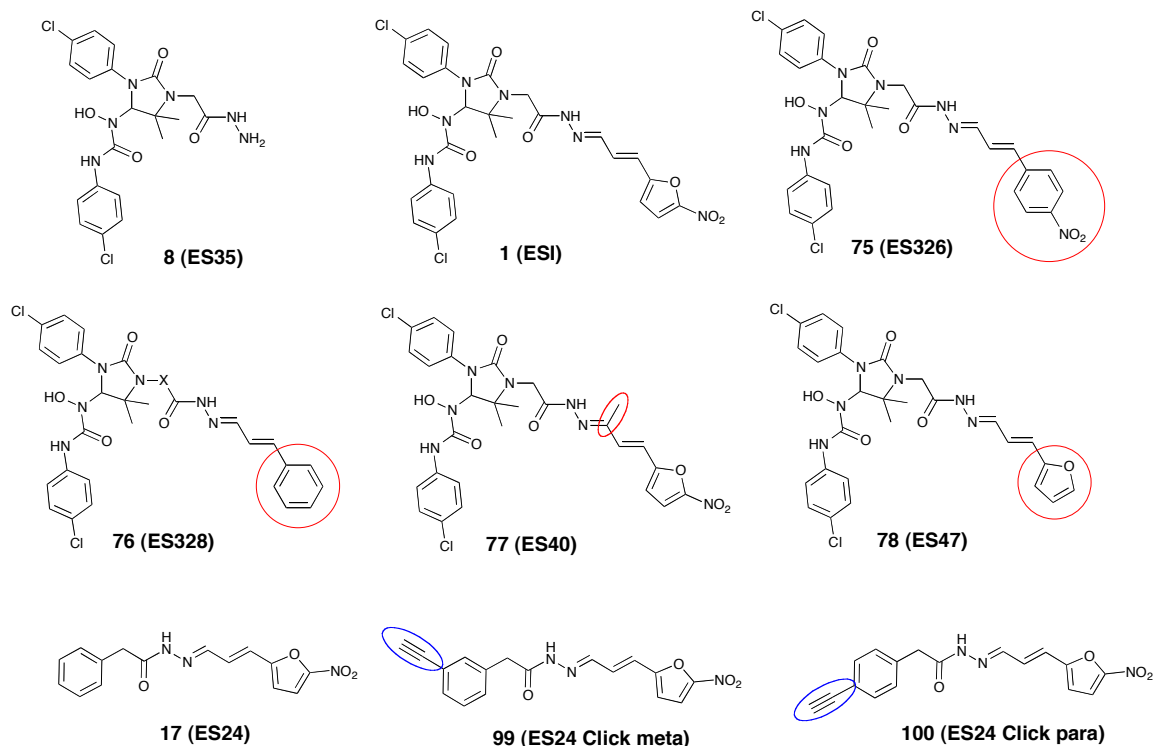


Figure 3.1. Selected compounds for biological testing

3.1 Cytotoxicity of ESI analogues

Cell viability assays can be used to determine the cytotoxicity of potential medicinal agents and toxic materials, since those agents would stimulate or inhibit the cell viability and growth. The MTT assay is a colorimetric assay developed by Mosmann⁹⁵ for measuring the activity of enzymes that reduce MTT (3-(4,5-dimethylthiazol-2-yl)-2,5-diphenyl tetrazolium bromide) to formazan dyes, giving a purple colour (Shown in Figure 3.2), the absorbance of which can be measured at 570 nm.

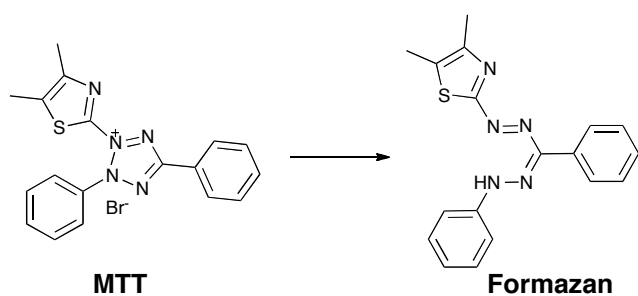


Figure 3.2. Reduction of MTT to formazan

These reductions can only take place when the reductase enzymes are active, and therefore conversion is used as a measure of viable (living) cells. This assay was used to determine the relative cytotoxicity of the different ES compounds. HeLa cells were treated with 2, 4, 8, 16, 32 and 64 μM concentrations of ES35, ESI, ES40, ES326, ES328, ES24, ES24 Click para and ES24 Click meta for 18 h and cell viability determined by MTT. ES35 and ESI were used as negative and positive controls respectively for all biochemical experiments. The same averaged ESI data are shown in each graph for comparison.

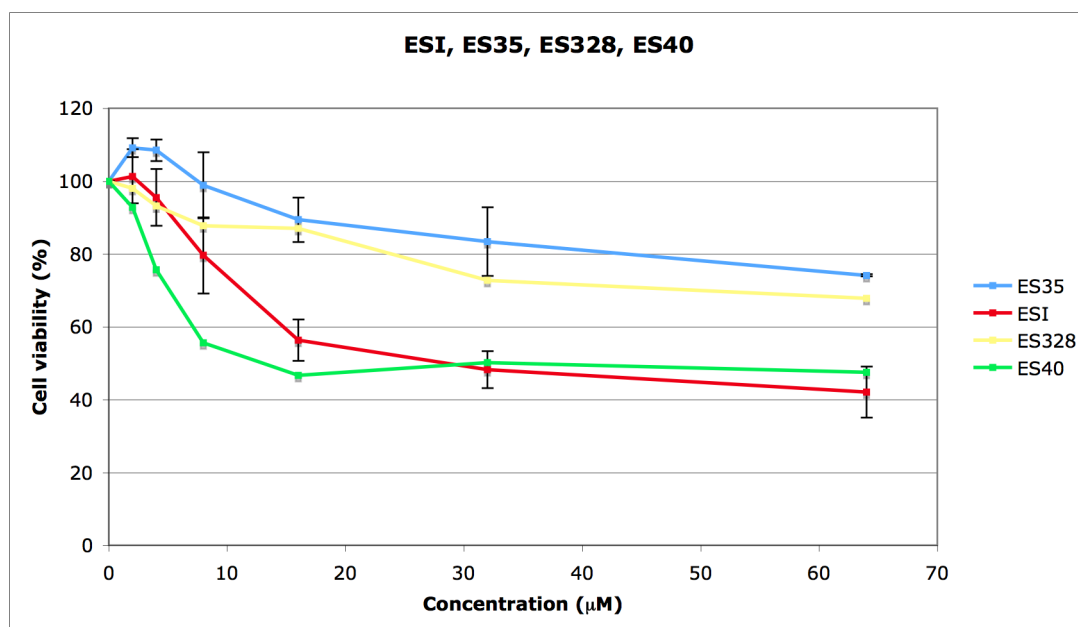


Figure 3.3. Cytotoxicity of ESI, ES35, ES328 and ES40. In a 96-well dish HeLa cells were treated with ESI, ES35 and ES40 at concentrations of 2, 4, 8, 16, 32 and 64 μM in triplicate and three lanes of DMSO controls at 64 μM and cell viability was determined by MTT. This was repeated with ES40 replaced with ES328. The graph shows the quantification normalised against DMSO plus the ESI and ES35 result from 3 independent experiments (mean \pm SD, $n = 3$).

ESI reduced the viability of cells at 8 and 16 μM to 79 and 58% respectively. Increasing the concentration to 32 and 64 μM cell viability had a minor additional effect on cell viability (48 and 42% respectively; Figure 3.3, red line). In contrast, ES35 showed little cytotoxicity, and even at 64 μM cell viability was only reduced to 74% (Figure 3.3, light blue line). ES328 (Has a phenyl ring instead of a nitrofuran) resembled ES35, and showed only a slight toxicity even at 64 μM , when cell viability was only reduced to 67% (Figure 3.3, yellow line). In contrast, ES40 (containing a methyl on the nitrofuran arm) was more potently cytotoxic than ESI, and caused a greater reduction in cell viability at lower concentrations (Figure 3.3, light green line). Even at 4 μM , cell viability was reduced to 74%, whilst at 8 and 16 μM a reduction of cell viability to 55 and 46% respectively was observed. Again, a levelling off of the cytotoxic effect was observed at concentrations of 32 and 64 μM . This levelling off indicates that not all of the HeLa cells die after the 18 h period, and

indicates that even at the maximum concentrations used, cell viability does not reach zero.

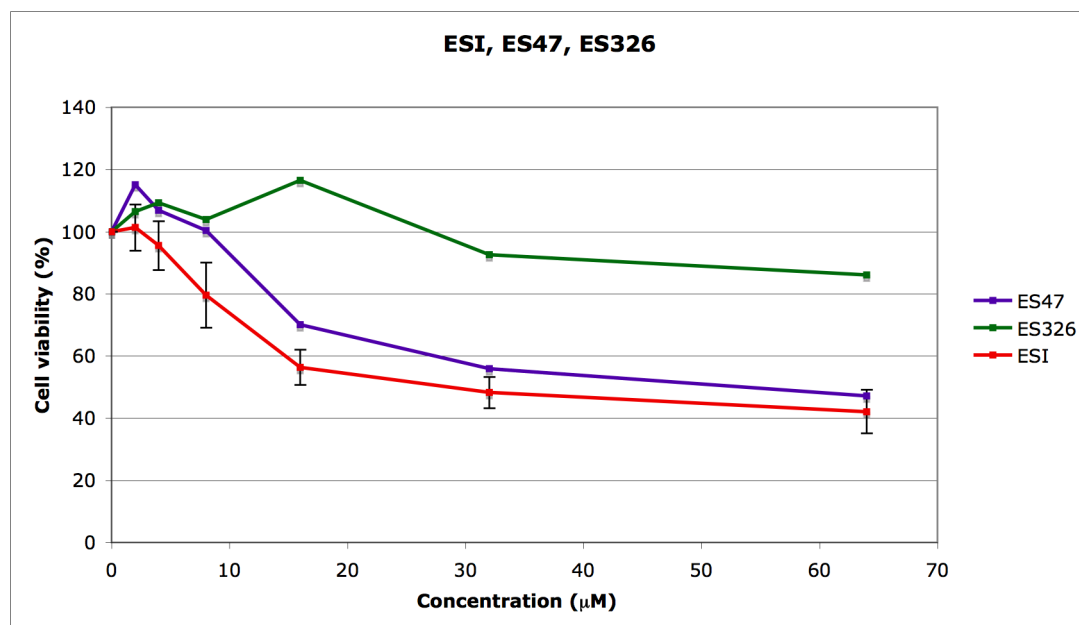


Figure 3.4. Cytotoxicity of ES47 and ES326. In a 96-well dish HeLa cells were treated with ESI, ES35 and ES47 at concentrations of 2, 4, 8, 16, 32 and 64 μM in triplicate and three lanes of DMSO controls at 64 μM and cell viability was determined by MTT. This was repeated with ES47 replaced with ES326 the graph shows the quantification normalised against DMSO plus the ESI result from 3 independent experiments (mean \pm SD, $n = 3$). The ES35 result has been omitted for clarity.

ES326 exhibited a similarly low toxicity compared to ES35, and even at 64 μM of this compound, cell viability remained at 86% (Figure 3.4, green line). Although ES47 showed little toxicity at low concentrations ($< 8 \mu\text{M}$), higher concentrations ($\geq 16 \mu\text{M}$) did affect cell viability (Figure 3.4 purple line), and at 32 and 64 μM , ES47 exhibited cell toxicity similar to ESI and ES40. Thus, the dose response curve of ES47 was shifted to the right by comparison with ESI (Figure 3.4, red line.).

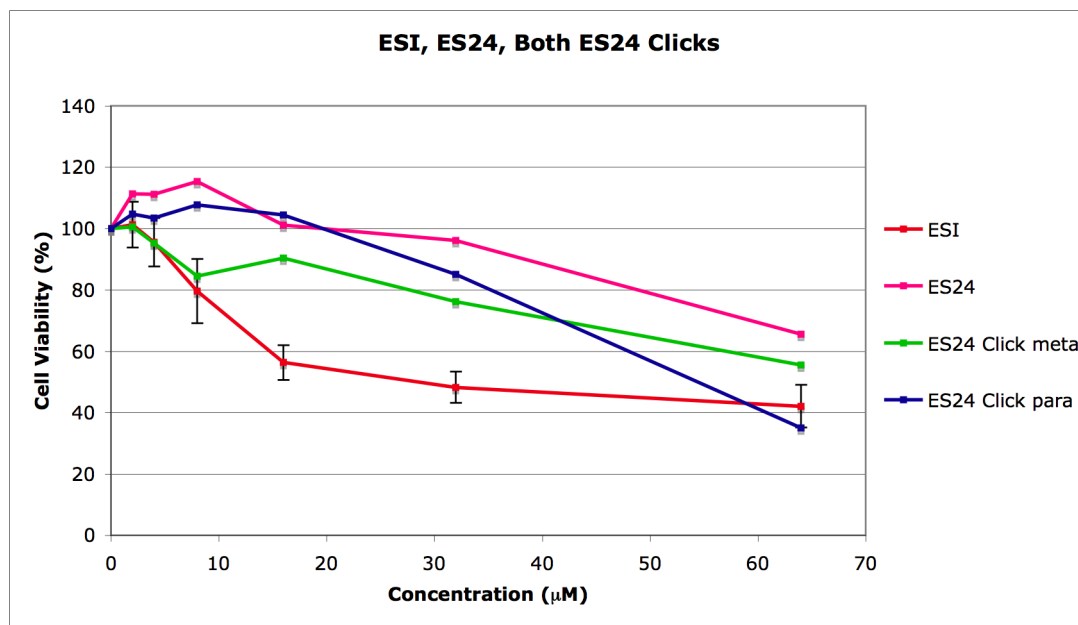


Figure 3.5, Cytotoxicity of ES24, ES24 Click meta and ES24 Click para. In a 96-well dish HeLa cells were treated with ESI, ES35 and ES24 at concentrations of 2, 4, 8, 16, 32 and 64 μM in triplicate and three lanes of DMSO controls at 64 μM and cell viability was determined by MTT. This was repeated with ES24 and ES35 replaced by ES24 Click para and ES24 Click meta. The graph shows the quantification normalised against DMSO plus the ESI result from 3 independent experiments (mean \pm SD, $n = 3$). The ES35 result has been omitted for clarity.

Next, the three “short form” compounds (ES24, ES24 Click para and ES24 Click meta) were examined. ES24 is essentially the nitrofuranyl arm of ESI with a hydrophobic group attached to allow cell permeability. As previously discussed it inhibits translocation in *in vitro* assays but not when added to live cells, suggesting that it is unable to cross the plasma membrane of live cells. By comparison to ESI, ES24 showed little cytotoxicity. However, at highest concentrations, there was some loss of cell viability. The click versions, ES24 Click meta and para were both slightly more toxic to cells, with ES24 Click meta having the largest effect (Figure 3.5, light green line) and ES24 being the least potent (Figure 3.5, pink line). At 32 μM cell viability was slightly affected by all three compounds again with ES24 Click meta being slightly more potent and ES24 being the least potent. At 64 μM cell viability was dramatically reduced in all 3 compounds but in the case of ES24 Click

para in particular cell viability was reduced to 35%, which was lower than ESI at the same concentration.

In summary, ES40 was more toxic than ESI, particularly at lower concentrations (i.e. dose response curve shifted to left). ES47 was relatively non-toxic at lower concentration, but showed similar toxicity to ESI at concentrations above 16 μM . All three “short form” compounds showed no toxicity at low concentrations but had high toxicity above 64 μM and finally ES326, ES328 and ES35 all showed little or no toxicity at all concentrations investigated.

3.2 Effect of ES compounds on cell morphology

Previous experiments in the High group revealed that treatment with ESI causes dramatic changes in the subcellular morphology of HeLa cells. In particular, the ER forms large vacuolar structures throughout the cytoplasm.⁵⁴ This vacuolisation can be visualised by phase contrast microscopy, thus providing a simple assay for the cellular activity of ESI compounds. Although the underlying causes of the changes in ER structure are not known, the vacuolisation resembles paraptosis, a system of programmed cell death in which empty spaces form in the cell cytoplasm and the mitochondria swells, causing the cell to lose viability.⁹⁶ Interestingly, paraptosis can be induced by perturbing the ubiquitin proteasomal system⁹⁷ such as that caused by treatment with DUB inhibitors. Therefore, vacuolisation may reflect the ability of ESI to induce ER-stress and/or to disrupt the ubiquitin proteasome system.

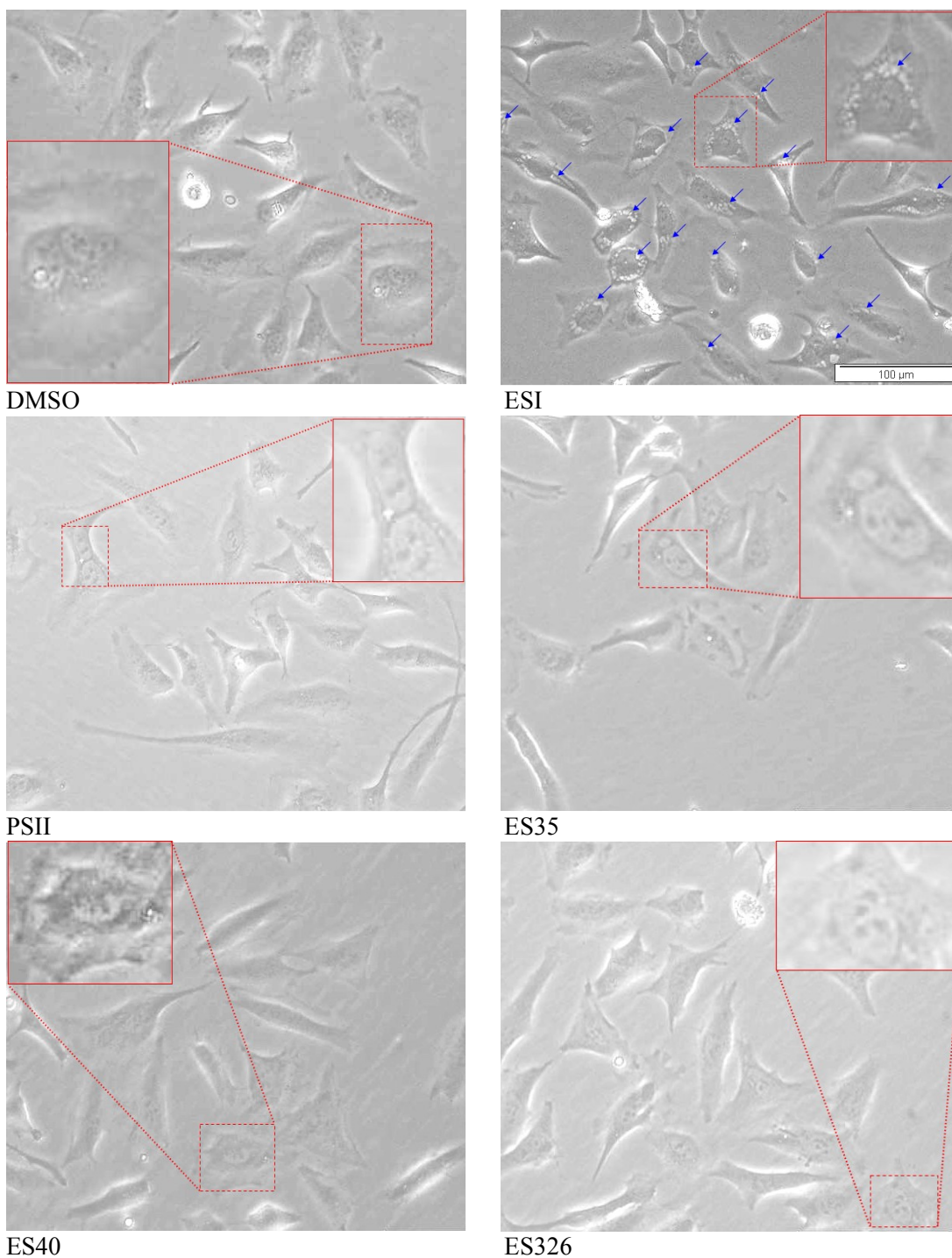
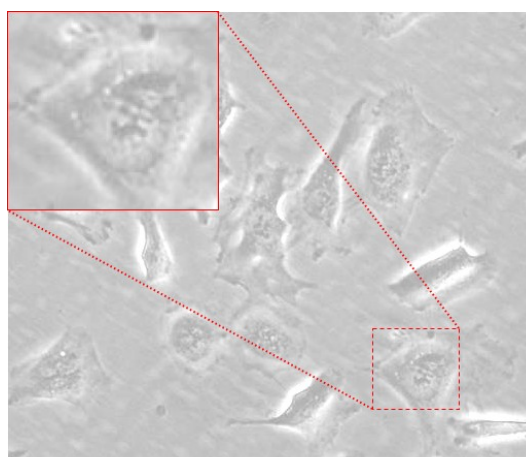
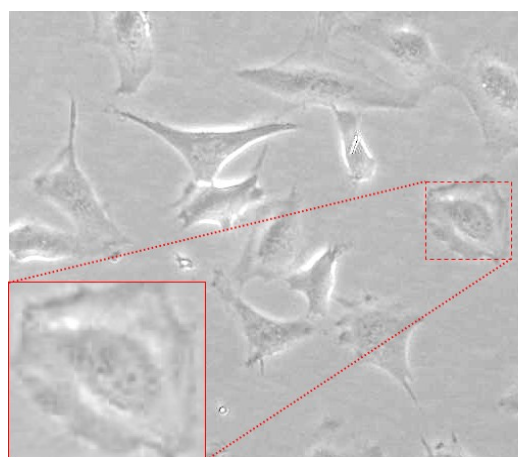


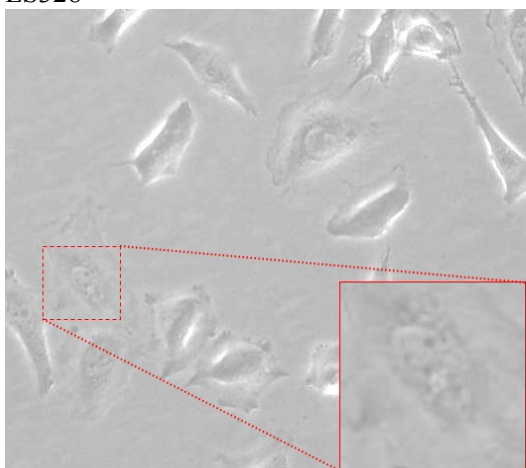
Figure 3.6. Effect of ES compounds on subcellular morphology images from Eeyarestatin treated HeLa cells: HeLa cells were plated into 6-well dishes and treated with PSII (10 µM), ESI, ES35, ES40, ES326, ES328, ES47, ES24, ES24 Click para or ES24 Click meta at 8 µM at 37 °C for 8 h. After this time pictures of the live cells were taken using an Olympus IX51 Inverted microscope. Blue arrows indicate vacuole formation.



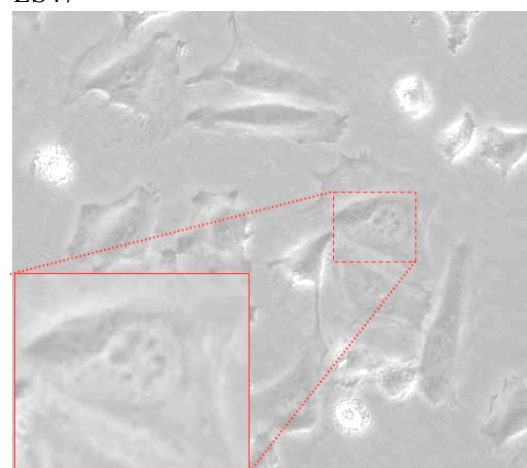
ES328



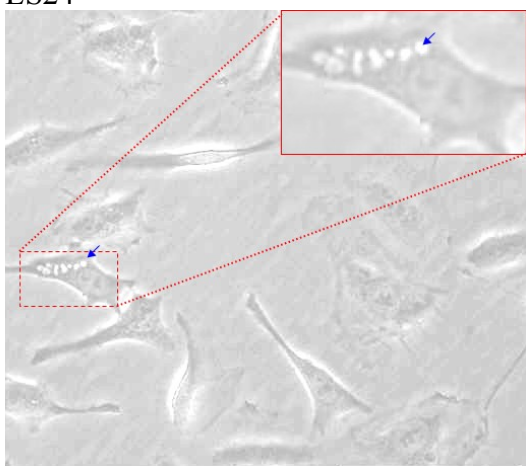
ES47



ES24



ES24 Click meta



ES24 Click para

Figure 3.6 continued. Effect of ES compounds on subcellular morphology images from Eeyarestatin treated HeLa cells: HeLa cells were plated into 6-well dishes and treated with PSII (10 μ M), ESI, ES35, ES40, ES326, ES328, ES47, ES24, ES24 Click para or ES24 Click meta at 8 μ M at 37 $^{\circ}$ C for 8 h. After this time pictures of the live cells were taken using an Olympus IX51 Inverted microscope. Blue arrows indicate vacuole formation.

In the presence of the solvent control, DMSO, HeLa cells displayed a typical appearance by phase contrast microscopy, with the nucleus, plasma membrane and

various organelles being visible (Figure 3.6, top left panel). When cells were treated with ES35, the cells showed no evidence of vacuolisation therefore providing a comparison for inactive *versus* active compounds (Figure 3.6, row 2, right panel). However, treatment with 8 μ M ESI for 8 h, resulted in the appearance of prominent vacuoles in most of the cells (Figure 3.6, top right panel, blue arrows). In contrast, the majority of compounds did not cause vacuolisation in HeLa cells (Figure 3.6, rows 3, 4 and 5). Surprisingly, even ES40, which was more toxic than ESI in the MTT assay, did not induce vacuolisation after 8 h treatment (Figure 3.6, row 3 left panel). In fact, only ES24 Click para of the “short form” analogues showed any evidence of vacuolisation after 8 h, but this was only observed in a very small proportion of the cells.

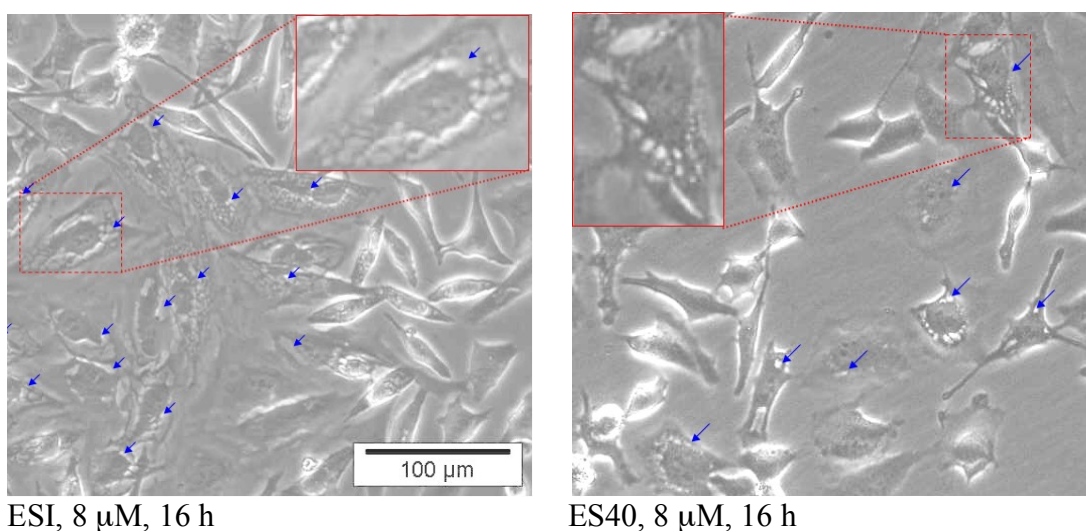
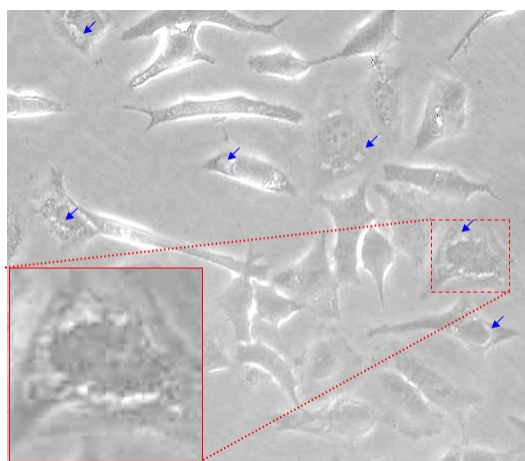


Figure 3.7. Vacuole formation after 16 hour treatment: HeLa cells were plated into 6-well dishes and treated with ESI, ES40, ES24, ES24 Click para or ES24 Click meta at 8 μ M at 37°C for 16 h. After this time pictures of the live cells were taken using an Olympus IX51 Inverted microscope (images from ES24 and both ES24 Click compounds are omitted). Blue arrows indicate vacuole formation.

The lack of effect of the compounds was unexpected given their cytotoxicity, particularly so for ES40, which showed greater toxicity than ESI in the MTT assays.

Since the MTT assays were performed after 16 h of treatment, the morphology of the cells was also examined after 16 h treatment with the compounds in case vacuolisation occurred after more prolonged treatment. However, only ES40 showed increased evidence of vacuoles after this time (Figure 3.7, right panel), and this effect was minor compared to ESI, with vacuoles observed only in approximately 20% of cells treated with ES40 for 16 h.



ES47 16 μ M

Figure 3.8. Vacuolisation was observed in ES47 treated cells at 16 μ M: HeLa cells were plated into 6-well dishes and treated with ES47 at 16 μ M at 37 °C for 8 h. After this time pictures of the live cells were taken using an Olympus IX51 Inverted microscope (images from ES24 and both ES24 Click compounds are omitted). Blue arrows indicate vacuole formation.

ES47 showed a dramatic decrease in cell viability at concentrations greater than 16 μ M thus a further experiment was run at 16 μ M to determine if this was a factor in this ES compound's ability to induce vacuolisation. The increase of concentration to 16 μ M induced vacuolisation in HeLa cells (Figure 3.8) but not as severe as in ESI treated cells.

Thus, the ability to induce vacuolisation was not apparent for most of the ES analogues, even under conditions (concentration and length of treatment) when they caused substantial loss of cell viability. Interestingly, ES40, which was more toxic to cells than ESI at 8 μ M, induced less vacuolisation and this occurred more slowly

than when cells were treated with ESI. These results suggest that vacuolisation is not simply a result of cell death, and may be related to particular action(s) of ESI in cells.

3.3 Accumulation of polyubiquitin conjugates

ESI has been shown to inhibit the activity of one or more DUBs that function to remove ubiquitin chains from ubiquitinated proteins.⁴¹ As a result, treatment of cells with ESI leads to the accumulation of polyubiquitinated proteins that can be detected by SDS-PAGE and Western blotting with anti-ubiquitin antibodies.⁴¹ This provides an assay to assess the ability of ESI and the new ES compounds to inhibit DUBs.

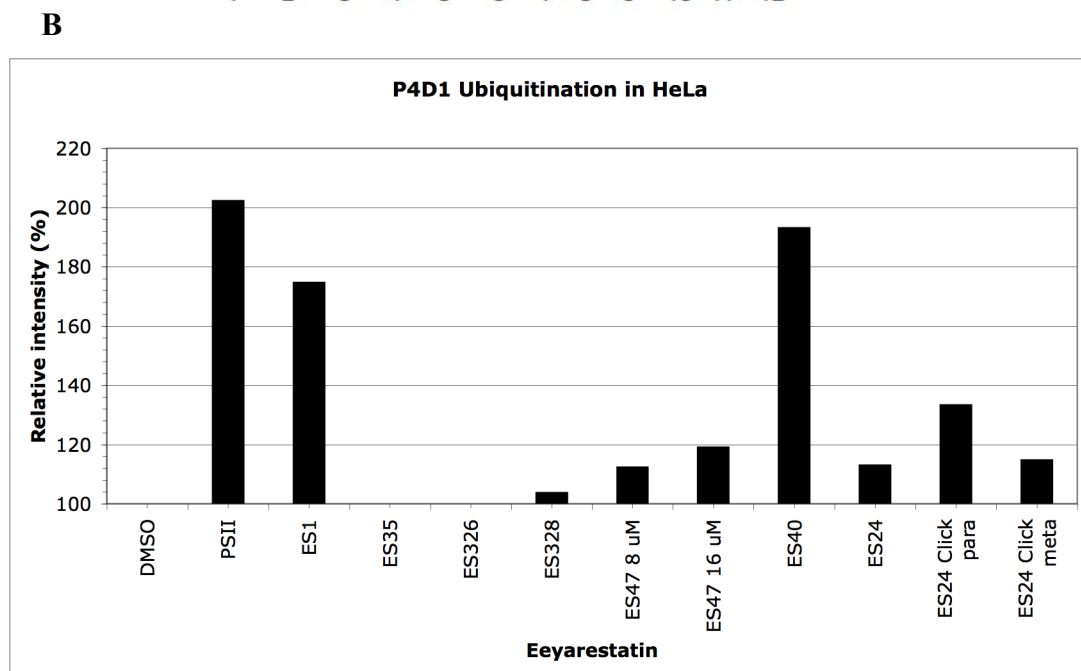
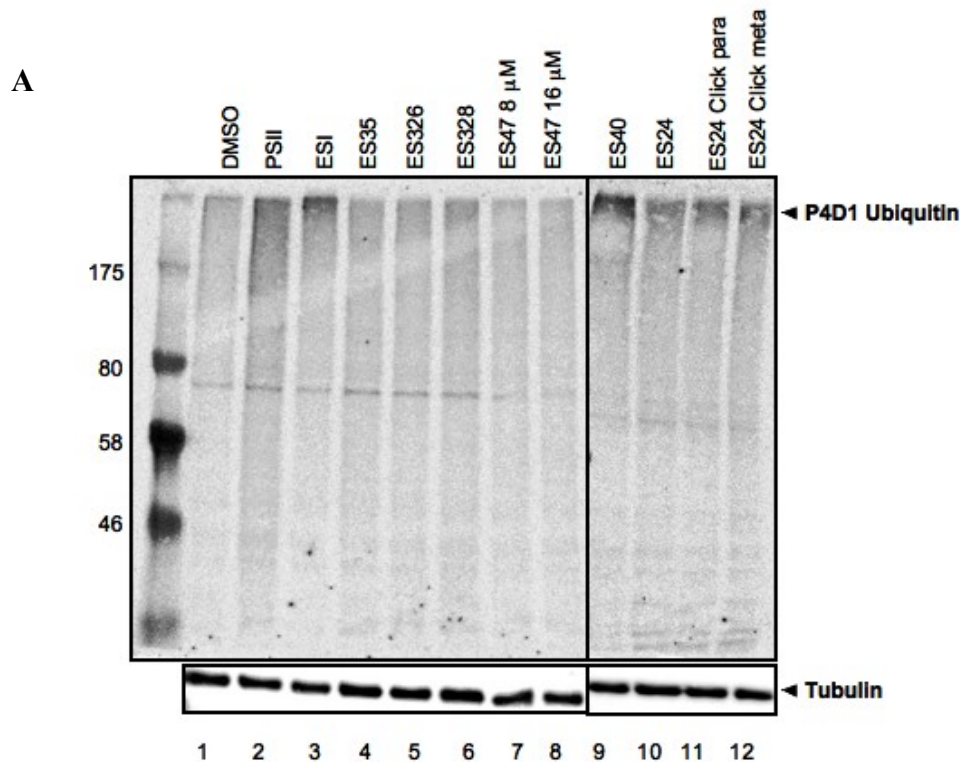


Figure 3.9. Accumulation of Ubiquitinated proteins in HeLa cells treated with Eeyarestatins: Top left panel: Confluent HeLa cells were treated for 8 h with ES compounds at 8 μ M or 16 μ M as indicated, and lysates analysed by SDS-PAGE and immunoblotting with anti-polyubiquitin and anti tubulin antibodies followed by infra-red labelled secondary antibodies; Top right panel: due to a blemish on original immunoblot the same cell samples that had been treated with ES40, ES24, ES24 Click para and ES24 Click meta at 8 μ M were analysed again by SDS-PAGE and immunoblotting; Bottom panels: Levels of α -Tubulin were specifically analysed by immunoblotting of cell samples; (B) The intensity of the ubiquitin signal was quantified using pixel counting in the Odyssey software and normalised relative to the intensity of the tubulin loading control. The normalised ubiquitin signal was then expressed as a percentage of that in the DMSO treated control cell lysate.

In lysates of cells treated with DMSO as a solvent control, very little polyubiquitinated material was detected (Figure 3.9 A, top panel, lane 1). Similarly, ES35 treated cells contained low levels of high molecular weight ubiquitinated material. By contrast, treatment of cells with PSII, a proteasomal inhibitor,⁹⁸ caused a marked accumulation of a range of high molecular weight polyubiquitinated proteins that were visible as a smear at the top of the polyacrylamide gel (Figure 3.9 A, top panel, lane 2). ESI treatment for 8 h also causes an accumulation of polyubiquitinated material (Figure 3.9 A top panel, lane 3). In line with its effect on cell viability and ER vacuolisation, ES40 also resulted in a large accumulation of polyubiquitin conjugates (Figure 3.9 A, top panel, lane 9). In fact, at 8 μ M, ES40 appeared to have a greater effect on accumulation of polyubiquitinated protein than ESI. Although less dramatic, treatment with ES24, ES24 Click para and ES24 Click meta also increased levels of polyubiquitinated proteins (Figure 3.9 A, right panel, lanes 10 – 12). This was also apparent when the signal intensity of the polyubiquitin conjugates was quantified and expressed relative to that of the DMSO control (Figure 3.9 B). This analysis also revealed that ES328 and ES47 both caused a slight accumulation of polyubiquitinated proteins (Figure 3.9 A, top panel, lanes 6, 7 and 8). The effect of ES47 was concentration dependent, ES326 did not appear to cause any accumulation of polyubiquitinated proteins above what was seen in DMSO treated cells (Figure 3.9 A, top panel, lanes 5, 7 and 8).

Again, the general SAR / trend observed in the cytotoxicity and vacuolisation assays was also seen in the ability of ES compounds to induce accumulation of polyubiquitinated proteins. Thus, ES40 was the most active of the analogues, whilst ES326 and ES328 were essentially inactive in this assay. ES47 again exhibited some activity, that was concentration dependent, and the short form ES24, ES24 Click para

and ES24 Click meta all caused a slight accumulation of polyubiquitin conjugates, with ES24 Click para being the most effective. Interestingly, ES40 induced even greater accumulation of polyubiquitin conjugates than ESI, suggesting that this version of ES may be a more effective DUB inhibitor. In contrast, ES40 had a less pronounced effect on vacuolisation, suggesting that vacuolisation may not be directly related to target inhibition of DUBS in the ubiquitin proteasome system.

3.4 ER protein translocation

In addition to inhibiting the activity of DUB enzyme(s), ESI has been shown to block Sec61 mediated protein translocation across the ER membrane.⁵³ Two separate assays were employed in order to determine the ability of the new ESI compounds to block post-translational and co-translational translocation. In both cases, HeLa cells were first treated with the ES compounds for 1 h before being semi-permeabilising with low concentrations of digitonin. Semi-permeabilisation selectively permeabilises the plasma membrane, leaving the cellular organelles, such as the ER and Golgi network intact.⁹⁹ These semi-permeabilised cells were then used as a source of ER membranes for *in vitro* translocation of radiolabelled substrate proteins.

3.4.1 Post-translational translocation

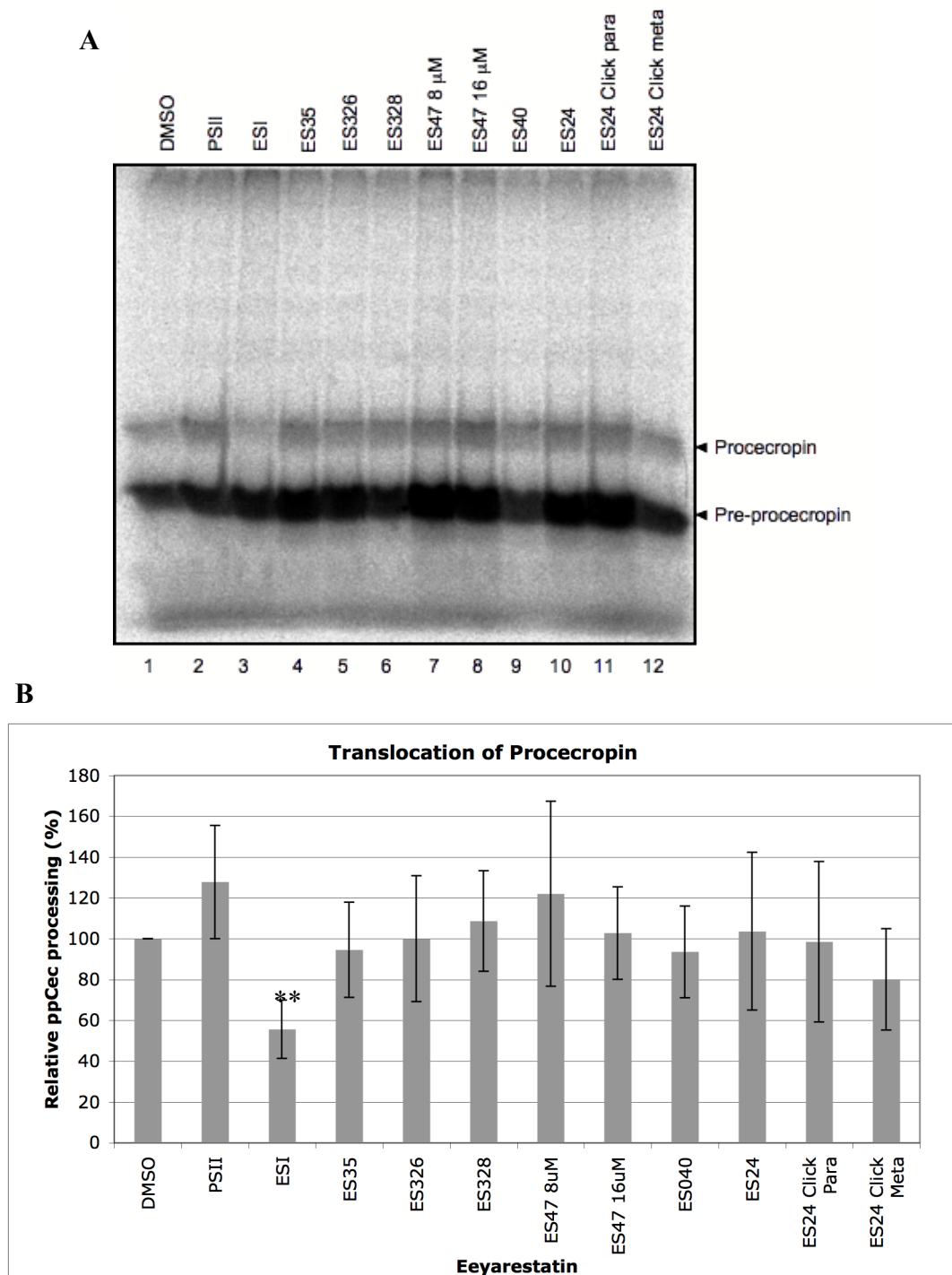


Figure 3.10. Post-translational translocation of procecropin (ppCec) in HeLa cells treated with Eeyarestatins: (A) *In vitro* translated ^{35}S Methionine/Cysteine labelled ppCec was added to semi-permeabilised cells that had been treated with ES compounds at $8\ \mu\text{M}$ for 1 h. The cells were washed and the ^{35}S Methionine/Cysteine labelled ppCec was analysed by SDS-PAGE and phosphorimaging; (B) Quantification by pixel counting using AIDA software was used to determine the relative processing of pCec normalised relative to the intensity of ppCec. The normalised signal was then expressed as a percentage of that in the DMSO treated control cell lysate (mean \pm SEM, $n = 3$). Differences in the block of post-translational translocation of ppCec were assessed for statistical significance using 2-tailed t-tests with equal variance assumed ($p < 0.05$ ** very significant).

The first experiment investigated the effect on post-translational translocation of procecropin (ppCec), which due to its small size is translocated across the ER membrane in a post-translational manner.¹⁰⁰ Thus, ³⁵S ppCec was translated *in vitro*, and then the radiolabelled protein added to semi-permeabilised cells that had been treated with the various compounds. Translocation was determined by the amount of *N*-glycosylated procecropin, since the addition of *N*-linked oligosaccharides to proteins occurs in the lumen of the ER. Thus, a reduction in the amount of the *N*-glycosylated form generated is indicative of an inhibition of translocation of ppCec across the ER. Translation of ppCec was completed in the presence of ³⁵S labelled Methionine/Cysteine and the translation reaction was added to ES-treated semi-permeable HeLa cells. In untreated cells a major band of un-glycosylated ppCec is observed with a minor band of a higher molecular weight form, which represents *N*-glycosylated pCec. Treatment with DMSO or PSII did not alter the amount of *N*-glycosylated pCec produced (Figure 3.10 A, lanes 1 and 2), showing that these compounds did not affect translocation of ppCec. In cells treated with ESI however, there was a clear decrease in the amount of *N*-glycosylated pCec that was generated more than 50% of the ppCec was prevented from translocating into the ER (Figure 3.10 A, lane 3). Quantification of the amount of *N*-glycosylated protein produced revealed that the *N*-glycosylated pCec levels were 50% lower in ESI treated cells, consistent with previous observations.⁵³ Interestingly, ES40 showed no significant block in translocation of this substrate (Figure 3.10 A, lane 9). ES35, ES326, ES328, ES24, ES24 Click para and ES47 at 8 μ M and 16 μ M did not cause a block in translocation of this substrate (Figure 3.10 A, lanes 4 – 8, 10 and 11). ES24 Click meta caused a slight block of approximately 20% in translocation of this substrate (Figure 3.10 A, lane 12).

3.4.2 Cotranslational translocation

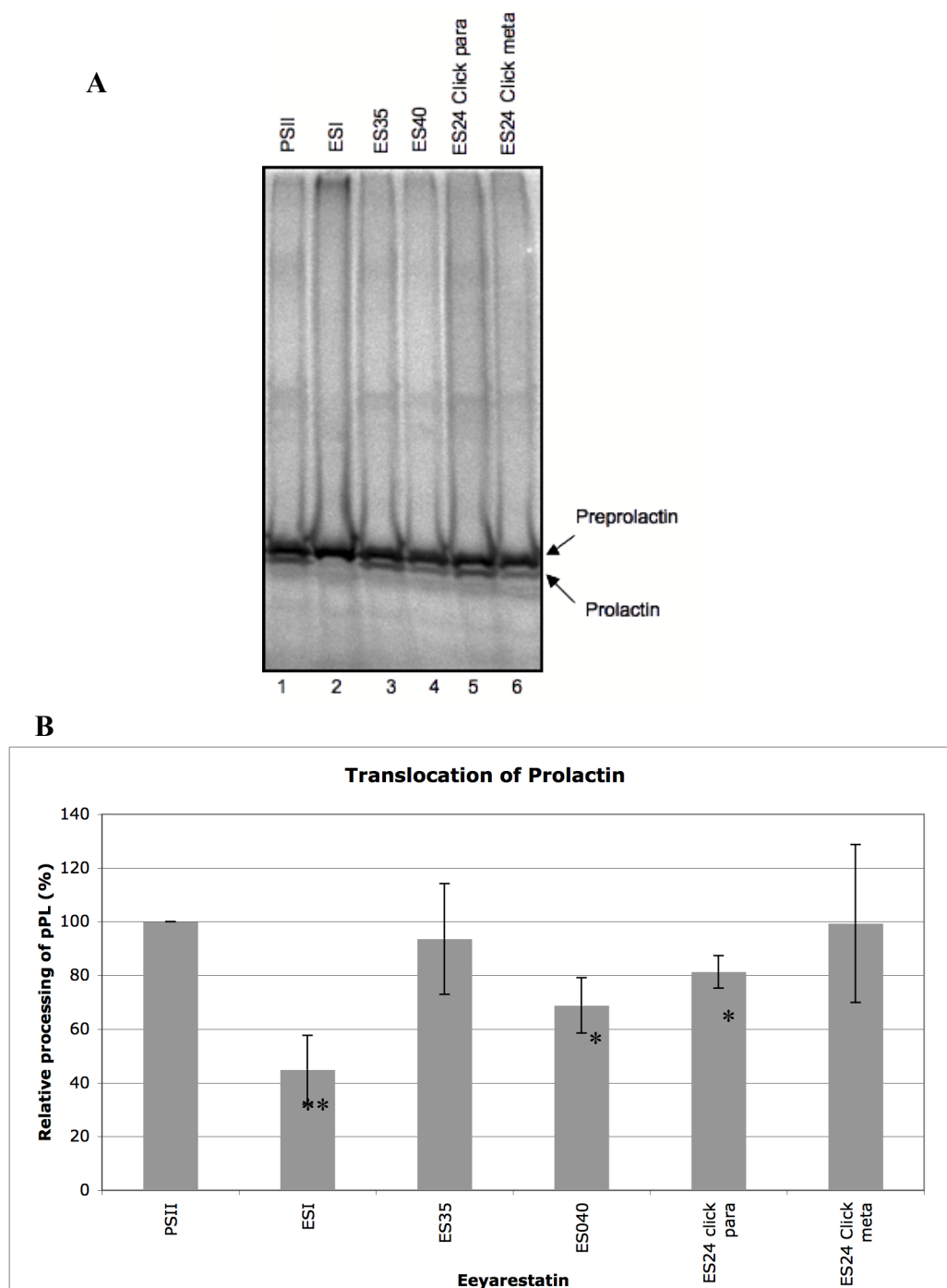


Figure 3.11. Co-translational translocation of prolactin in HeLa cells treated with Eeyarestatins: (A) Pre-prolactin (pPL) was translated *in vitro* in the presence of semi-permeabilised HeLa cells that had been treated with ES compounds at 8 μ M for 1 h. The cells were harvested and analysed by SDS-PAGE and phosphorimaging; (B) Quantification by pixel counting using AIDA software was used to determine the relative processing of cleaved prolactin normalised relative to the non-cleaved pPL. The normalised signal was then expressed as a percentage of that in the DMSO treated control cell lysate (mean \pm SEM, n = 3). Differences in the block of post-translational translocation of ppCec were assessed for statistical significance using 2-tailed t-tests with equal variance assumed ($p < 0.05$ * significant, ** very significant).

Co-translational translocation was determined by measuring the cleavage of a second protein, preprolactin (pPL). Following translocation across the ER, the signal sequence of pPL is removed, leading to the production of a smaller protein, providing a marker for entry into the ER. In order to allow co-translational translocation, mRNA encoding pPL was translated in the presence of ES-treated semi-permeabilised cells. In this way, the radiolabelled pPL could be translocated across the ER membranes as it was being translated. This assay is more challenging and therefore only the most interesting compounds were used in this case. PSII and ESI were used as the negative and positive controls respectively. In cells treated with PSII there was a major band representing pPL, and also a more rapidly migrating product that represents PL lacking its signal sequence, and had therefore been translocated across the ER membrane. Treatment with ES35 did not alter the extent of pPL processing, showing that it did not block co-translational translocation of pPL into the ER (Figure 3.11 A, lane 3). In contrast, ESI reduced the level of pPL cleavage by approximately 65%, consistent with previous work showing that this compound effectively inhibits translocation of pPL into the ER (Figure 3.11 A, lane 2). In addition, ES40 and to a lesser extent the ES24 Click para caused a slight block in co-translational translocation of this substrate (Figure 3.11 A, lanes 4 – 6). ES24 Click meta did not cause a block in co-translational translocation of this substrate. In summary, none of the compounds were as effective as ESI in inhibiting translocation *in vitro*. This was unexpected, particularly for ES40 given its apparently activity in terms of cytotoxicity and accumulation of polyubiquitin conjugates.

3.5 Protein secretion

The ER is a major site of synthesis for both membrane integrated and secretory proteins. Thus, an alternative way to observe the inhibitory effect of these compounds on protein import/translocation at the ER was to measure how they affect the overall secretion of proteins from cells. It has previously been shown that ESI inhibits the secretion of proteins from HepG2 cells.⁵³ This hepatocyte (liver) derived cell line secretes a large number of abundant glycoproteins, which can be detected by metabolic labelling with ³⁵S. In this assay, HepG2 cells were incubated with ³⁵S-methione/cysteine to allow synthesis of ³⁵S labelled proteins being translated (the 'pulse' period). The ³⁵S-methione/cysteine was removed and cells were grown for a further 1.5 h in the presence of non-radioactive amino acids. During this time (the 'chase' period), ³⁵S labelled secretory proteins synthesised during the pulse were trafficked through the secretory pathway, and released into the media. Radiolabelled proteins in the cells and media were visualised by SDS-PAGE and phosphorimaging. HepG2 cells treated with DMSO as a solvent control during both the pulse and chase periods secreted a large number of radiolabelled proteins in the media. This was taken to represent a profile of proteins normally secreted from the cells (Figure 3.12A, lower panel, lane 1). A similar profile of protein secretion was observed in cells treated with 8 μ M ES35 (Figure 3.12A, lower panel, lane 3). In contrast, when cells were treated with Brefeldin A (Bref A), a fungal metabolite which blocks ER-Golgi trafficking,¹⁰² very few proteins were secreted (Figure 3.12A, lower panel, lane 2), despite efficient labelling of total cellular proteins (Figure 3.12A, upper panel, lane 2). Consistent with previous work, treatment of cells with ESI also markedly reduced the quantity of several secretory proteins in the media.⁵³ Treatment with ES40 and ES24 Click meta, also resulted in the reduction of several secretory

proteins in the media (Figure 3.12A, lower panel, lanes 5 and 11), without obviously altering the labelling of total cellular proteins (Figure 3.12A, upper panel, lanes 5 and 11). However, the effect of these compounds was not as dramatic as ESI. In contrast, ES326, ES328, ES47, ES24 and ES24 Click para had no detectable effect on secretion of radiolabelled proteins (Figure 3.12A, lower panel, lanes 6 – 10)

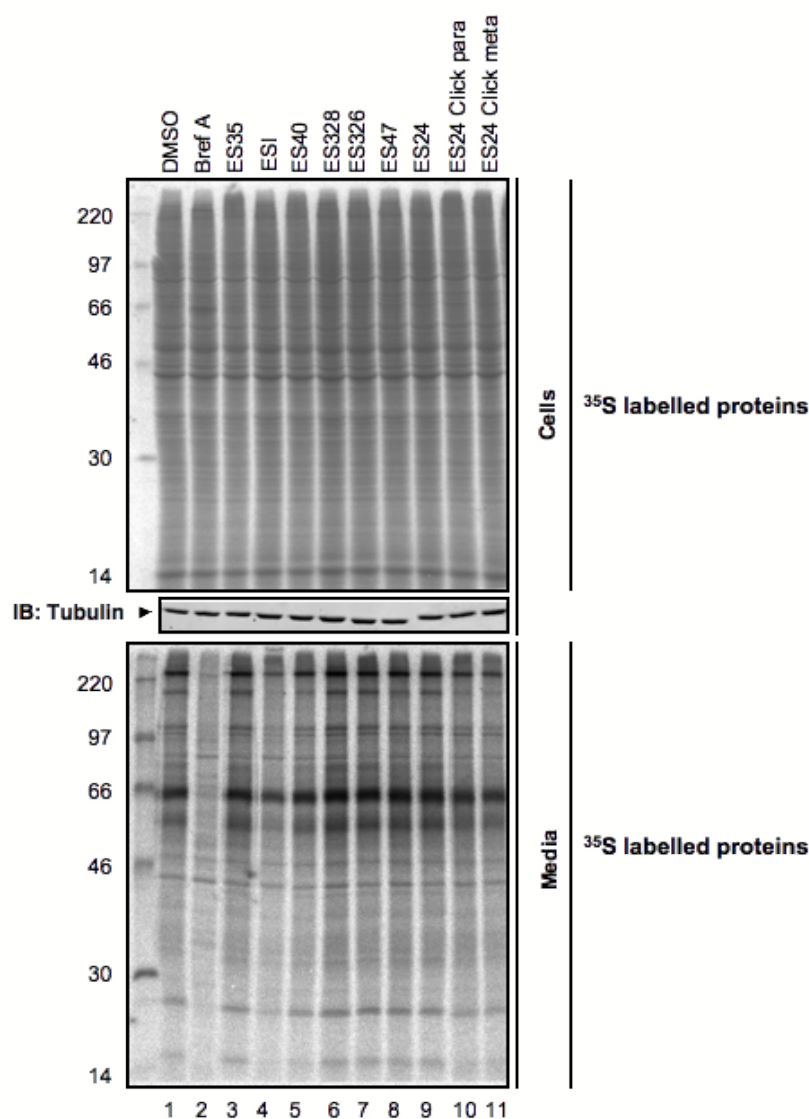


Figure 3.12A Protein secretion from HepG2 cells that have been treated with Eysarestatins: Upper panel: Confluent HepG2 cells were pulse-labelled with ^{35}S met/cys for 60 min in the presence of 8 μM , ESI compounds, 5 $\mu\text{g}/\text{mL}$ Bref A or 10 μM DMSO. They were then chased in absence of ^{35}S for 1.5 h. At the end of the chase, the media was retained and TCA precipitated and the cells lysed in SDS-PAGE sample buffer. Samples of the cell lysate (upper panel) and TCA precipitated media (lower panel) were analysed by SDS-PAGE and phosphorimaging. Levels of α -Tubulin in cell lysates were analysed by immunoblotting (middle panel).

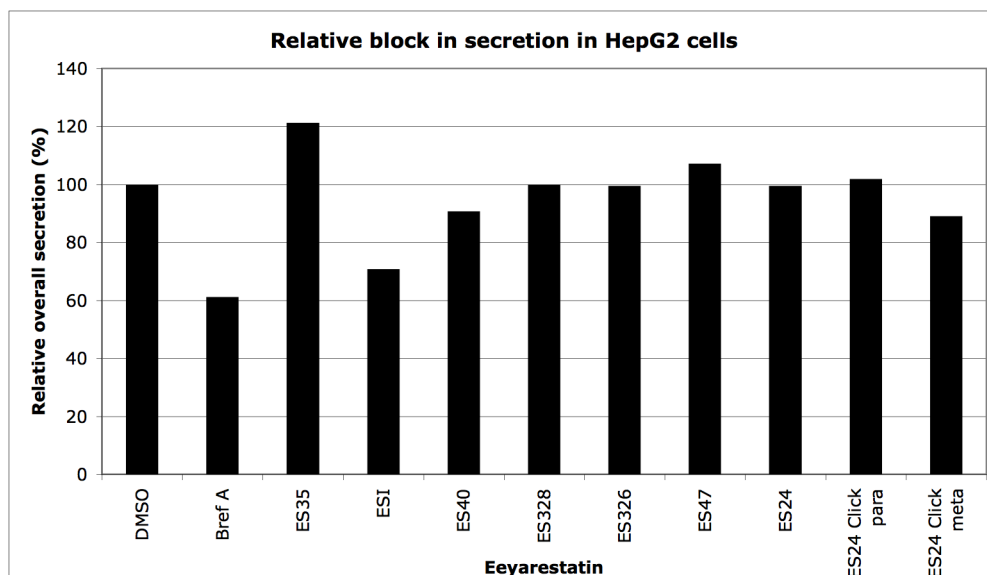


Figure 3.12B Quantification of protein secretion from HepG2 cells that have been treated with Eeyarestatins: Each lane of the TCA precipitated media was quantified by pixel counting using AIDA software and then normalised to the corresponding signal from the cell extract this signal was the expressed as a percentage relative to the DMSO control;

In order to analyse the secretion of specific proteins directly, the TCA precipitated media of the treated HepG2 cultures was subjected to western blotting with antibodies to two well-characterised secretory proteins α 1-anti-trypsin (α 1-AT) and albumin. Significant amounts of both proteins were secreted by DMSO treated cells (Figure 3.13A, upper and middle panels, lane 1), whilst treatment with Bref A resulted in a dramatic reduction in the levels of α 1-AT and albumin secreted into the media (Figure 3.13A, upper and middle panels, lane 2).⁵³ In line with its effect on global protein secretion, ES40 also inhibited secretion of α 1-AT and albumin, albeit to a lesser extent than ESI (Figure 3.13A, upper and middle panels, lane 5). Strikingly, cells treated with ES24 Click para and ES24 Click meta effectively blocked α 1-AT secretion, to a similar extent as ESI (Figure 3.13A, upper panel lanes 3, 10 and 11), with the para compound showing slightly lower effect than the meta compound. However, the effect of these compounds on albumin secretion was not as strong compared to ESI (Figure 3.13A, middle panel, lanes 3, 10 and 11).

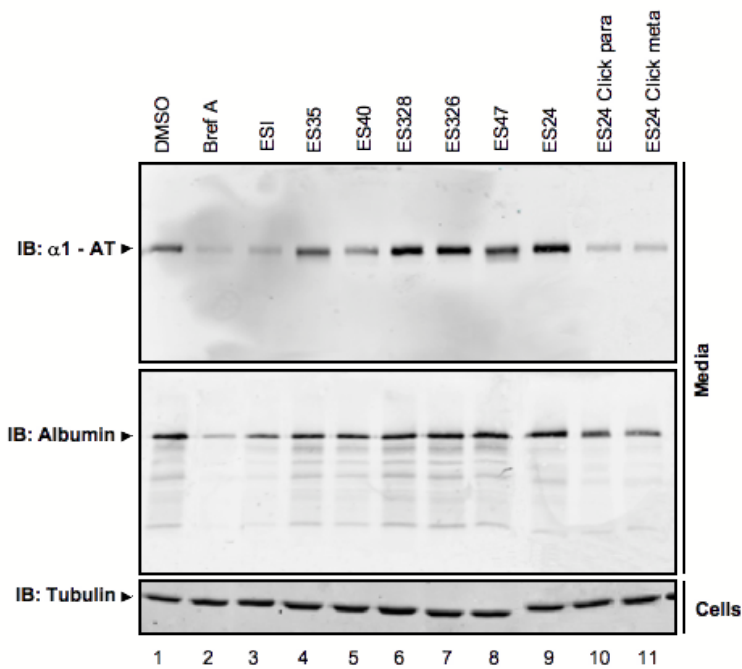


Figure 3.13A Secretion of α 1-AT and albumin from HepG2 cell. TCA precipitated media was analysed by SDS-PAGE and western blotting with anti- α 1-AT (upper panel), anti-albumin (middle panel). To control for cell number, cell lysates were western blotted with anti-tubulin (lower panel).

Although ES326, ES328, ES47, ES24 did not obviously reduce secretion of these proteins (Figure 3.13 A, upper and middle panels, lanes 6, 7, 8 and 9), quantification of the signal intensity showed that whilst they do not affect the secretion of α 1-AT (Figure 3.13B), but ES326, ES328, ES47 and ES24 all slightly reduced secretion of albumin Figure 3.13C).

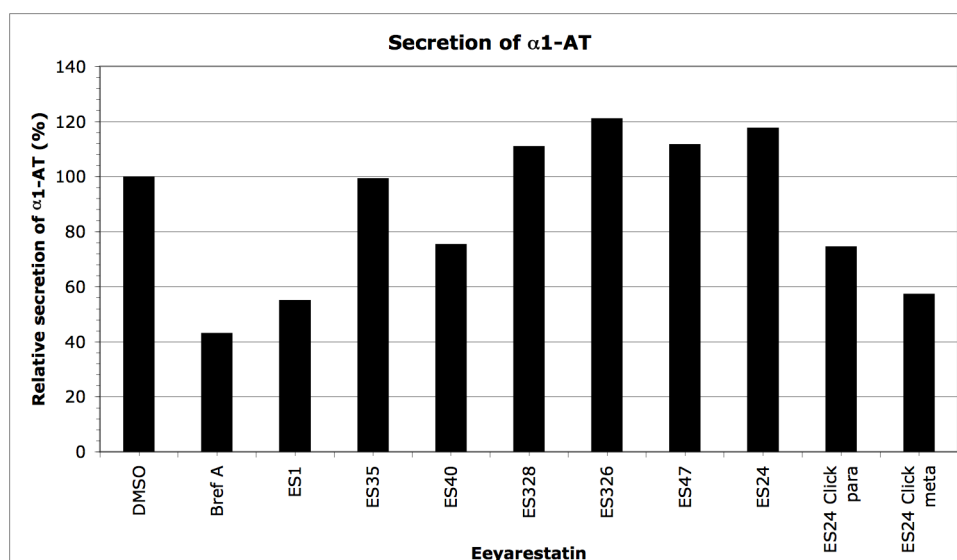


Figure 3.13B Secretion of α 1-AT from HepG2 cell. The bands for α 1-AT, as indicated, were quantified by pixel counting using Odyssey software and then normalised to tubulin signal this signal was the expressed as a percentage relative to the DMSO control.

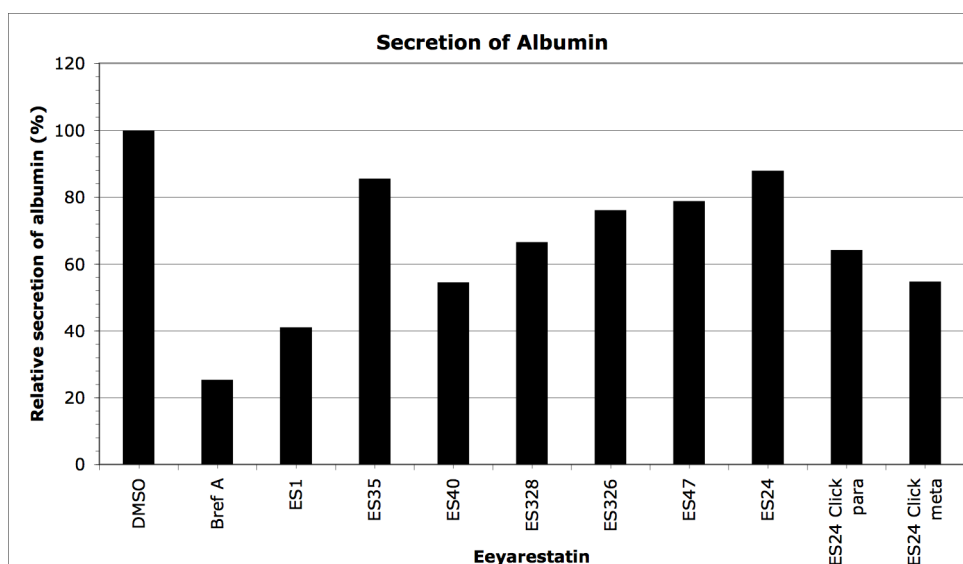


Figure 3.13C Quantification of the secretion of albumin from HepG2 cell. The phosphorimage bands for albumin, as indicated, were quantified by pixel counting using Odyssey software and then normalised to the tubulin signal. This signal was then expressed as a percentage relative to the DMSO control.

Importantly, the metabolic labelling of total cellular proteins did not appear to be affected by treatment with any of the compounds (Figure 3.12A, top panel, all lanes). Thus, an effect on protein synthesis is unlikely to account for the reduction of proteins found secreted into the media. Together these results suggest that ES40,

ES24 Click para, ES24 Click meta all induce a wide-ranging inhibition of protein secretion from cultured HepG2. In contrast, ES326, ES328, ES47 and ES24 appear to have little if any effect. Thus, the structure-activity relationship observed in this assay was generally similar to that observed for polyubiquitination, with ES40 being the most active (after ESI) and the click 24s having a smaller effect. ES40 seems to be less active than ESI in terms of blocking secretion and translocation but more effective in inducing accumulation of polyubiquitin conjugates. Therefore, the effect of these compounds to induce accumulation of polyubiquitins in HEPG2 cells was investigated.

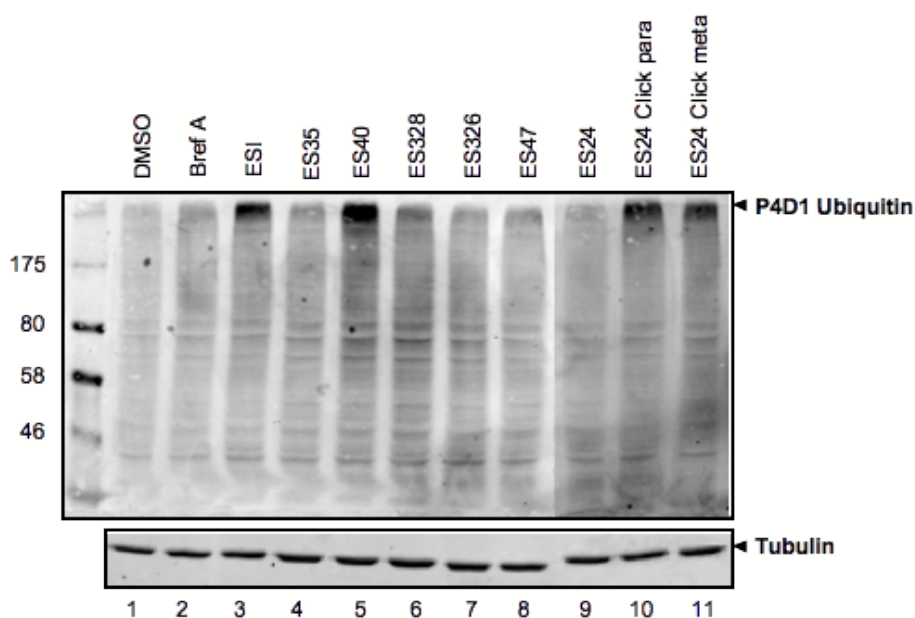


Figure 3.14A. Accumulation of polyubiquitinated proteins in HepG2 cells: Top panel: HepG2 cells treated with ES compounds at 8 μ M for 8 h were harvested and ubiquitin levels analysed by SDS-PAGE and immunoblotting; lower panel: Levels of tubulin were specifically analysed by immunoblotting of cell samples.

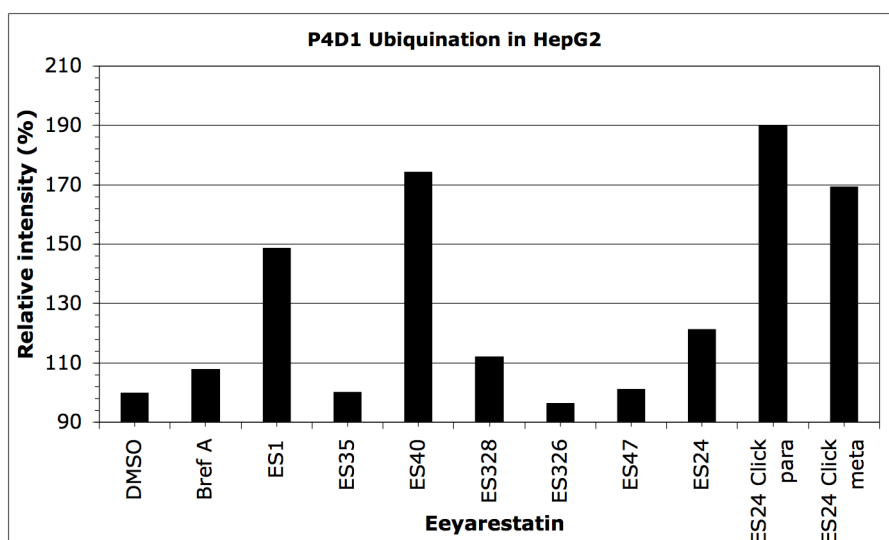


Figure 3.14B. Quantification of the accumulation of polyubiquitinated proteins in HepG2 cells: Ubiquitin bands were quantified by pixel counting using Odyssey software and normalised to the Tubulin signal this was expressed as a percentage compared to the DMSO control

In order to ascertain whether the compounds cause accumulation of polyubiquitinated proteins in other cell lines the same ubiquitin assay described previously was repeated on this cell line. Using the same cells from the secretion assay ubiquitin levels were analysed by SDS-PAGE and immunoblotting.

In cells treated with DMSO as a solvent control and Bref A there was no accumulation of polyubiquitinated proteins as expected (Figure 3.14A, top panel, lanes 1 and 2). ESI as expected caused an accumulation of high molecular weight polyubiquitinated proteins (Figure 3.14A top panel, lane 3). ES40 caused a greater accumulation of polyubiquitinated proteins compared to ESI (Figure 3.14A, top panel, lane 5). However, in HepG2 cells, both ES24 Click compounds caused a larger accumulation of polyubiquitinated proteins than ESI, in contrast to what was observed in HeLa cells (Figure 3.14A, top panel, lanes 10 and 11).

In summary, the results were similar to those observed in HeLa cells, with ESI causing a marked accumulation of polyubiquitin conjugates compared to ES35. It was again observed that ES40 was more effective than ESI.

3.6 Click chemistry

As previously discussed in Chapter 1, MacKinnon *et al* rhodamine labelled a protein with an apparent MW of ~50 kDa using a photo-leucine as a photoaffinity label and ‘clicking’ on a rhodamine-azide reporter to an alkyne on the same small molecule that had bound its target (Figure 1.25).

This is a useful way to determine targets associated with small molecule inhibitors, thus a series of click compounds were prepared in an attempt to determine targets associated with the ES compounds (Figure 3.16)

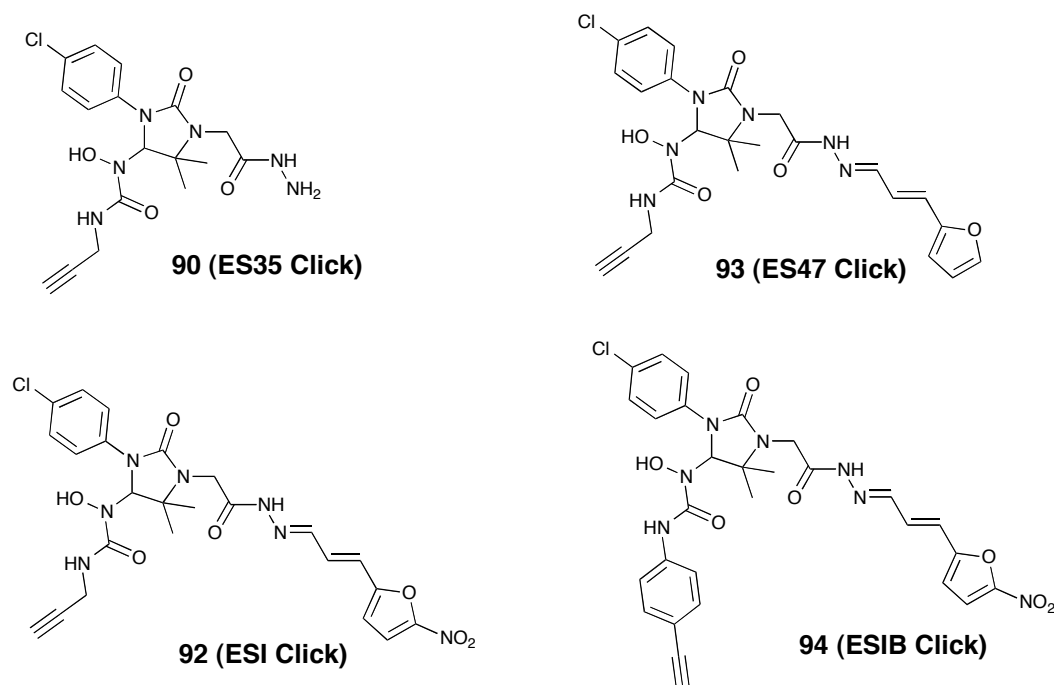


Figure 3.16. Structures of Eeyarestatins for use in biological click chemistry assay

ESI Click was initially tested by the High lab for its ability to inhibit cotranslational translocation of signal peptide peptidase (SPP) when added directly to ER derived microsomal membranes. The results showed that *in vitro* treatment of microsomes

with ESI Click resulted in a similar level of inhibition of translocation to ESI (Figure 3.17, lane 8).

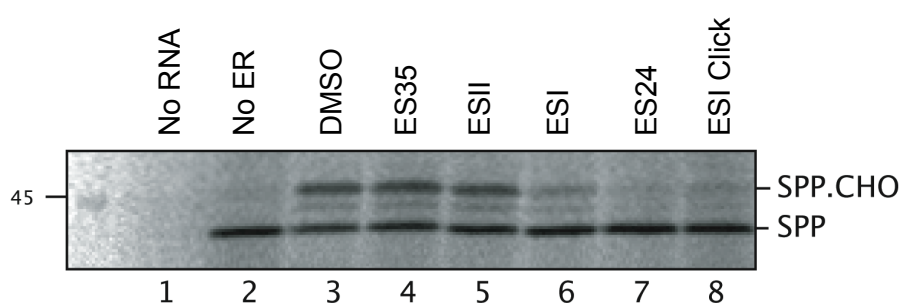


Figure 3.17. Translocation of SPP in ER microsomes treated with Eeyarestatins (Provided by McKibbin *et al*⁵⁴): *In vitro* translated ³⁵S Methionine/Cysteine labelled SPP was added to ER microsomes that had been treated with 500 μ M of the compounds ES35, ESI, ESII, ES24, or ESI Click for 1 h on ice. The ER microsomes were washed and the ³⁵S Methionine/Cysteine labelled SPP was analysed by SDS-PAGE and phosphorimaging;

Thus, this compound could potentially be used to identify the molecular targets of ESI. As a first step towards this, the ability of several different ES Click compounds (ES35 Click, ESI Click, ES47 Click or ESIB Click; Structures in Figure 3.16) to covalently bind to proteins in ER derived microsomes was examined. ER microsomes were treated with the different ES compounds, and incubated for 1 h to allow them to react with potential target protein(s) in the microsomes. Subsequently, cycloaddition using the commercially available Alexa 488 azide fluorophore (Shown in Figure 3.19) was performed, in order to allow visualisation of the ESI. Samples were separated by SDS-PAGE and the Alexa 488 fluorescence visualised using fluorescence scanning.

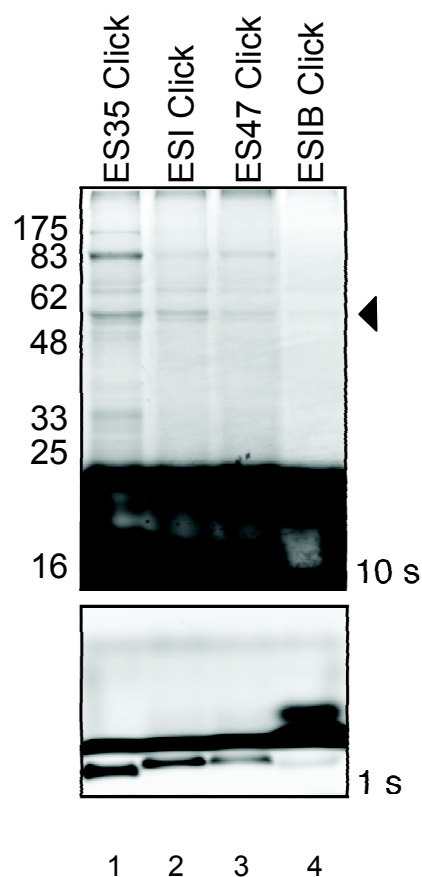


Figure 3.18. Click reaction in Eeyarestatin treated ER microsomes: ER microsomes were treated with 250 μ M ES35 Click, ESI Click, ES47 Click or ESIB Click for 1 h on ice before performing cycloaddition of Alexa Fluor 488 azide *in situ* for 1 h at rt. After the addition of 6 \times sample buffer the reactions were analysed by SDS-PAGE and fluorescence scanning. Top panel 10 s exposure indicates “clicked” proteins; Lower panel 1 s exposure indicates click reaction completion.

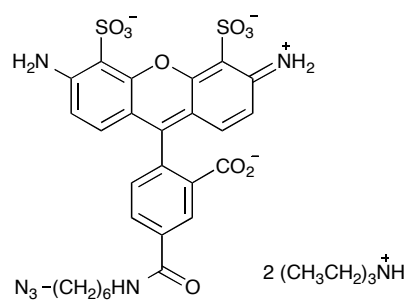


Figure 3.19. Alexa 488 azide

A range of different Alexa 488 labelled species were observed in microsomes treated with ES35 Click (Figure 3.18, upper panel, lane 1). These most likely represent

proteins that had been modified with ES35, and thus labelled with the fluorophore following the click reaction.

ESI Click and ES47 Click also appeared to target a similar range of proteins, though with noticeably lower efficiency (Figure 3.18, lanes 2 and 3). Thus, under these *in vitro* conditions (ER derived membranes and high concentrations of ESI compounds) it is impossible to determine which proteins might be targeted by ESI. ESIB Click did not clearly label any species (Figure 3.18, lane 4), this may be due to the lower reactivity of the alkyne. Since the phenyl alkyne Click reaction is significantly slower than for an aliphatic alkyne, it is possible that no reaction with the fluorophore occurred in this time frame, thus, none of the targets of this compounds could be identified. ES35 actually seems to modify more proteins than ESI, suggesting that the experimental conditions need to be altered in order to selectively detect the ESI specific targets (Eg The use of live cells may be required).

3.7 Summary

Compound	Assay							
	MTT	Vacuolisation	Poly-ubiquitin	Translocation		Secretion		
				Post-translational	Co-translational	Overall	α 1-AT	Albumin
ES35	–	–	–	–	–	–	–	+
ESI	+++	+++	+++	+++	+++	+++	+++	+++
ES40	+++	+	+++	+	+	+	++	++
ES326	–	–	–	–	✘	–	–	+
ES328	–	–	–	–	✘	–	–	+
ES47 8 μ M	–	–	+	–	✘	–	–	+
ES47 16 μ M	+	+	+	+	✘	✘	✘	✘
ES24	+	–	+	+	✘	–	–	+
ES24 Click para	+	–	++	+	+	–	++	++
ES24 Click meta	+	–	++	+	+	+	++	++
CAM741	✘	✘	✘	✘	✘	–	–	–

Table 3.2. Summary of results of all biological assays investigated: – negative results, + slightly positive result, ++ positive result, +++ exceptionally positive result, ✘ assay not completed.

CHAPTER 4: CONCLUSIONS AND FURTHER

WORK.

4.1 Eeyarestatins

None of the new analogues investigated were equipotent with or more potent than ESI in all inhibitory activities, however ES40 appeared to be more potent than ESI in terms of cytotoxicity and inducing accumulation of polyubiquitin conjugates and both ES24 Click compounds displayed similar activity to ESI when inducing accumulation of polyubiquitin conjugates. Interestingly, none of the 'new' ES compounds appeared to induce vacuolisation as observed ESI treated cells. Even ES40, which had exhibited the most potent activity of all the new analogues, did not show any significant vacuolisation. Some compounds affected secretion of albumin but not α 1-AT, which was unexpected as it indicates that there may be some selectivity in the ability of ES326, ES328 and ES24 to inhibit translocation. ES326 and ES328 (containing phenyl rings instead of furan rings) only had a slight effect on the secretion of albumin confirming that the nitrofurans are a vital structural requirement for activity of the ES compounds (although other possibilities could be explored). ES47 without the nitro group showed a concentration effect in the accumulation of polyubiquitin and vacuolisation assays but this effect was not as significant as ESI at 8 μ M suggesting that the nitro group may also be a structural requirement for activity of the ES compounds. ES40 was more toxic than ESI towards HeLa cells and caused a higher accumulation of polyubiquitin conjugates compared to ESI in both HeLa and HepG2 cells but was less effective at blocking translocation *in vitro*, or protein secretion from live cells. The structure-activity

The results observed in the “short form” ES compounds were particularly interesting. In previous work ES24 had difficulty crossing the cell membrane, however, the addition of hydrophobic groups increased the ability of these “short form” compounds to induce accumulation of polyubiquitin conjugates particularly in HepG2 cells. The changes to ES24 structure were only minor thus new targets can be synthesised to explore ES24 activity in more detail. Some examples of possible targets are shown in Figure 4.2 and are currently under study in the Whitehead lab. These analogues were selected to further investigate the addition of different functional groups on activity **149** and **150** to investigate further addition of hydrophobic groups, **151** to investigate the addition of electronegative groups and finally **152** to investigate the addition of a pyridine.

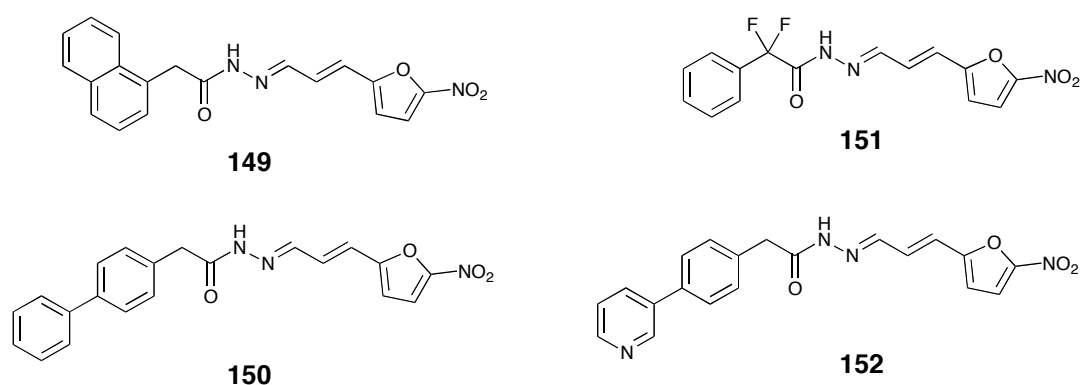


Figure 4.2. Possible targets to explore “short form” activity in more detail

The IC₅₀ values would give an exact toxicity of these compounds and the MTT assay could be used again to determine these. To achieve this drug treatments need to occur over a longer time period, such as 72 h, so that cell viability reaches zero and over a wider range of concentrations.

As previously discussed the click chemistry reaction needs to be repeated to optimise the conditions for confirmation of the result. If optimisation is successful then the proteins that interact with the ES compounds can be determined.

4.2 Cotransin

As previously discussed the synthesis of fragment 1 of Cotransin was not completed. Further work would involve the esterification of *N*-Boc amino acid **139** with isobutene to give ester **140**. This would then be followed by the amino acid coupling to Boc-Leu under standard conditions to give the dipeptide **141**. The final two steps would involve the selective removal of the Boc group using neat formic acid followed by the coupling to the natural lactic acid using EDCI and NaHCO₃ to give fragment 1, **143**.

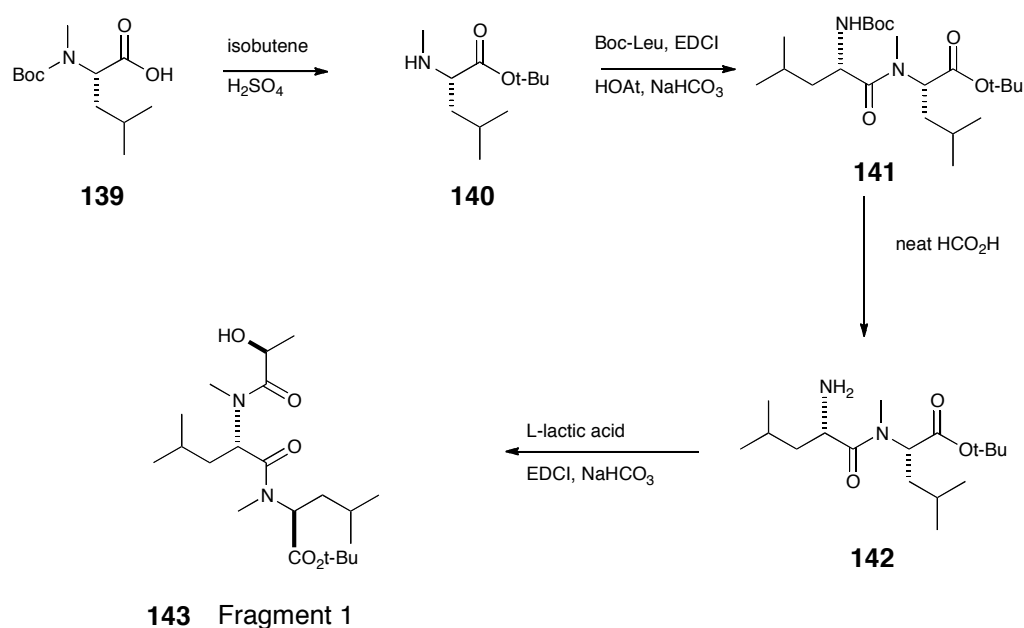


Figure 4.3. Synthesis of fragment 1 a precursor to Cotransin

The HPLC of fragment 2 and the hydrolysis using LiOH to give **137** would need to be completed for the coupling of fragment 1 to fragment 2 *via* the Mitsunobu reaction. This reaction would invert the stereochemistry of the lactic acid to give the required linear heptadepsipeptide **153**. Then reaction with TFA to remove both the Boc and *t*-Butyl protecting groups and final cyclisation with either EDCI, HOAt and NaHCO₃ or HATU and collidine would hopefully furnish Cotransin.

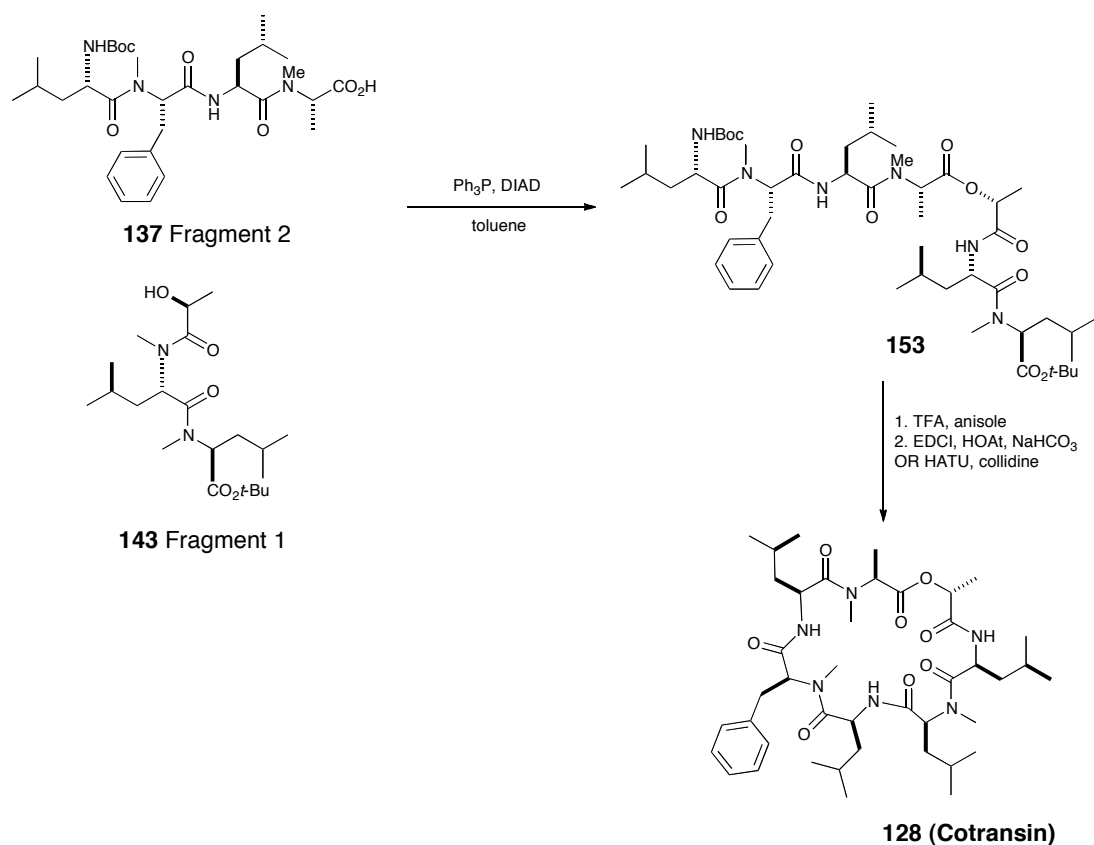


Figure 4.4 Final steps in the synthesis of Cotransin

Once complete Cotransin can then be used in the assays completed here to determine its inhibitory activity compared to ESI and CAM741.

CHAPTER 5: EXPERIMENTAL

5.1 General procedures

Structures

All chemical structures and chemical names were generated using ChemDraw Ultra v12.0.

Chromatography

Column chromatography was performed using silica gel (Sigma-Aldrich) 40 – 63 μm 60 \AA treated with solvent system used in individual procedures. The eluents are specified in individual procedures.

Infra – Red Spectroscopy

Recorded as KBr discs using an ATI Mattson genesis series FT-IR instrument or Perkin Elmer FT-IR system or taken as a solid state on Perkin Elmer FT-IR or Bruker Alpha P FT-IR instrument. Absorption maxima (ν_{max}) are recorded in wavenumbers (cm^{-1}).

Mass spectrometry

Mass spectrometry was carried out by the staff in the Mass Spectrometry Laboratory, School of Chemistry, at the University of Manchester, using Micromass Platform II (ES and LCMS), Waters QTOF (HRMS and LCMS) and Thermo Finnigan MAT95XP (HRMS and GCMS) spectrometers. Only molecular ions, fractions from molecular ions and other major peaks are reported as mass/charge (m/z) ratios. Reported mass values are within ± 5 ppm mass units for electrospray and ± 10 ppm for HRMS.

Melting Points

Recorded on a Sanyo Gallenkamp MPD350 heater.

Nuclear Magnetic Resonance

^1H and ^{13}C NMR spectra were acquired using Bruker Avance 500, Bruker Avance 400, and Bruker Avance 300 spectrometers. ^1H and ^{13}C assignments were supported by ^1H COSY, DEPT and HMQC.

Chemical shifts (δ_{H}) are quoted in parts per million (ppm) to the nearest 0.01 ppm and referenced to TMS to the nearest 0.1 Hz. Data is reported in the format: Chemical shift, integration, multiplicity. Chemical shifts (δ_{C}) are reported in ppm to the nearest 0.01 ppm and referenced to the solvent peak.

Optical rotation

$[\alpha]_{\text{D}}$ measurements are given in units of $10^{-1} \text{ deg cm}^2 \text{ g}^{-1}$ and were recorded on an AA-100 polarimeter (Optical activity limited).

Solvents

DCM was dried over calcium hydride; THF was distilled from sodium benzophenone ketyl under nitrogen atmosphere; PE Bp 40-60 °C was distilled before use. Deionised water was obtained from a Millipore Elix 5.

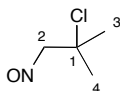
Solvents were evaporated on a Büchi RE111 rotary evaporator equipped with a Büchi 461 water bath.

All chemicals were handled in accordance with safety instructions. All reactions were carried out with exclusion of water in an inert nitrogen atmosphere using a nitrogen balloon. All glassware was pre-dried in an oven at 110 °C and cooled in a dessicator prior to use.

5.2 Preparation of Eeyarestatins.

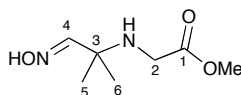
5.2.1 Symmetrical Eeyarestatins.

2-Chloro-2-methyl-1-nitrosopropane. (66)



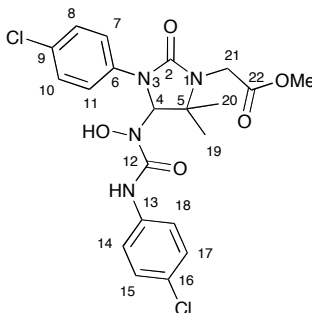
2-methylpropene (16 mL, 10 g, 178.2 mmol) was condensed into a 3-necked round bottomed flask cooled to $-30\text{ }^{\circ}\text{C}$ and equipped with a cold finger at $-78\text{ }^{\circ}\text{C}$. The temperature was allowed to rise until $-15\text{ }^{\circ}\text{C}$ and then *iso*-amyl nitrite (24 mL, 178.2 mmol) was added. Cold concentrated HCl (15 mL) was then added drop-wise and the mixture allowed to stir for 2 h at $-10\text{ }^{\circ}\text{C}$. After this time the bath was cooled to $-20\text{ }^{\circ}\text{C}$ without stirring. The resulting precipitated solid was collected by filtration, washed with cold MeOH ($-15\text{ }^{\circ}\text{C}$, 30 mL) and dried under vacuum to give the title compound as a colourless solid (8.67 g, 39%). Mp $100\text{--}101.8\text{ }^{\circ}\text{C}$ [lit.¹⁰¹ $104\text{--}105\text{ }^{\circ}\text{C}$]; ν_{max} (evaporated film)/ cm^{-1} 3030 (w), 2981 (w, C-H), 2963 (w, C-H), 2863 (w, C-H), 1460 (m, N=O); ^1H NMR (300 MHz, CDCl_3) δ 4.70 (2H, s, C(2)H₂), 1.76 (6H, s, C(3)H₃ & C(4)H₃); ^{13}C NMR (125 MHz, CDCl_3) δ 66.3 (C(2)), 65.8 (C(1)), 31.2 (C(3) & C(4)),

Methyl-2-[(2-hydroxyamino-1,1-dimethylethyl)amino]acetate. (67)



Glycine methyl ester hydrochloride (5.17 g, 41 mmol) was added, under an atmosphere of nitrogen, to a solution of 2-chloro-2-methyl-1-nitrosopropane, **66** (5.0 g, 41 mmol) in freshly distilled MeCN (82 mL). Freshly distilled triethylamine (8.3 mL, 82 mmol) was then added drop-wise. The reaction mixture was allowed to stir at rt for 17 h and then quenched by the addition of a saturated aqueous solution of sodium bicarbonate (40 mL). The organic material was extracted into DCM (4 × 50 mL) and the combined organic layers were washed with brine (40 mL), dried over magnesium sulfate and concentrated under reduced pressure to yield the title compound as a colourless solid (5.747 g, 80%). Mp 86.0–86.9 °C; ν_{\max} (evaporated film)/ cm^{-1} 3292 (m, O-H), 3163 (m, N-H), 3081 (m, C-H), 2977 (m, C-H), 2874 (m, C-H), 2798 (m, C-H), 1750 (s, C=O); ^1H NMR (300 MHz, CDCl_3) δ 7.28 (1H, s, C(4)H), 3.73 (3H, s, CO_2CH_3), 3.39 (2H, s, C(2)H₂), 1.27 (6H, s, C(5)H₃ & C(6)H₃); ^{13}C NMR (125 MHz, CDCl_3) δ 172.7 (C(1)), 154.8 (C(4)), 54.1 (C(3)), 52.0 (CO_2CH_3), 44.7 (C(2)), 25.2 (C(5) & C(6)); m/z (+ve ion electrospray) 197 ($[\text{M}+\text{Na}]^+$, 100%), (Found 197.0899, $\text{C}_7\text{H}_{14}\text{N}_2\text{NaO}_3$ ($[\text{M}+\text{Na}]^+$), requires 197.0897).

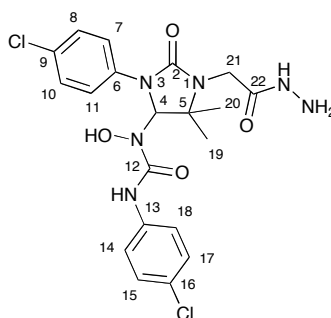
Methyl 2-(3-(4-chlorophenyl)-4-(3-(4-chlorophenyl)-1-hydroxyureido)-5,5-dimethyl-2-oxoimidazolidin-1-yl)acetate. (69)



A solution of 4-chlorophenyl isocyanate (1.01 g, 5.75 mmol) in freshly distilled THF (2 mL) was added under an atmosphere of nitrogen to a solution of oxime, **67** (0.57 g, 2.87 mmol) also in freshly distilled THF (14 mL). The resulting solution was stirred at rt for 17 h and was then concentrated under reduced pressure. The product was crystallised from DCM, collected by filtration, washed with diethyl ether (20 mL) and dried. The filtrate was concentrated under reduced pressure and the crystallisation procedure was repeated a further three times. Combination of the four batches of crystallised product gave the title compound as a colourless solid (1.03 g, 65%). Mp 217.5–218.8 °C; ν_{\max} (solid state)/cm⁻¹ 3320 (m, O-H), 3285 (m, N-H), 2980 (w, C-H), 1735 (s, C=O), 1695 (s, C=O), 1672 (s, C=O), 1590 (m, Ar C=C), 1526 (s, Ar C=C), 1494 (s, Ar C=C); ¹H NMR (500 MHz, CDCl₃) δ 8.14 (1H, brs, NH or OH), 7.94 (1H, brs, NH or OH), 7.66 (2H, d, *J* 8.8 Hz, 2 × Ar-CH), 7.53 (2H, d, *J* 8.8 Hz, 2 × Ar-CH), 7.28–7.24 (4H, m, 4 × Ar-CH), 6.18 (1H, s, C(4)H) 4.40 (1H, d, *J* 18.1 Hz, , C(21)H_aH_b), 3.59 (1H, d, *J* 18.1 Hz, , C(21)H_aH_b), 3.58 (3H, s, CO₂CH₃), 1.36 (3H, s, C(19)H₃ or C(20)H₃), 1.30 (3H, s, C(19)H₃ or C(20)H₃); ¹³C NMR (75 MHz, CDCl₃, some signals are coincident) δ 172.6 (C(22)), 156.8 (C(2) or

$\underline{C}(12)$), 155.8 ($\underline{C}(2)$ or $\underline{C}(12)$), 137.2 (Ar- \underline{C}), 136.9 (Ar- \underline{C}), 129.1 (Ar- \underline{CH}), 128.9 (Ar- \underline{C}), 128.8 (Ar- \underline{CH}), 128.2 (Ar- \underline{C}), 121.0 (Ar- \underline{CH}), 120.3 (Ar- \underline{CH}), 74.7 ($\underline{C}(4)$), 59.0 (C(5)), 53.0 (CO₂ \underline{CH}_3), 40.6 ($\underline{C}(21)$), 26.4 ($\underline{C}(19)$ or $\underline{C}(20)$), 19.3 ($\underline{C}(19)$ or $\underline{C}(20)$); *m/z* (-ve ion electrospray) 483.4 ([M-H]⁻, (³⁷Cl, ³⁷Cl), 15%), 481.4 ([M-H]⁻, (³⁵Cl, ³⁷Cl), 83 %), 479.5 ([M-H]⁻, (³⁵Cl, ³⁵Cl), 100%), (+ve ion electrospray) 507 ([M+Na]⁺, (³⁷Cl, ³⁷Cl), 10%), 505 ([M+Na]⁺, (³⁵Cl, ³⁷Cl), 60%), 503 ([M+Na]⁺, (³⁵Cl, ³⁵Cl), 100%); (Found 503.0847, C₂₁H₂₂³⁵Cl₂N₄NaO₅ ([M+Na]⁺), requires 503.0859).

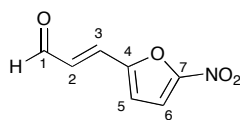
3-(4-Chlorophenyl)-1-(3-(4-chlorophenyl)-1-(2-hydrazinyl-2-oxoethyl)-5,5-dimethyl-2-oxoimidazolidin-4-yl)-1-hydroxyurea. (8)



An aqueous solution of hydrazine (62%, 1.18 mL, 24 mmol) was added to a solution of imidazolidinone, **69** (0.567 g, 1.18 mmol) in MeOH (6 mL). The reaction mixture was stirred at rt for 48 h and then cooled to 0 °C. The resulting precipitate was collected by filtration, washed sequentially with cold MeOH (10 mL) and diethyl ether (10 mL) and dried to yield the title compound as a colourless solid (0.358 g, 63%). Mp 197.5–199 °C; ν_{\max} (solid state)/cm⁻¹ 3304 (m, O-H), 3085 (m, N-H), 3029 (m, C-H), 1700 (s, C=O), 1649 (m, Ar C=O), 1647 (m, Ar C=O), 1591, (m, Ar

C=C), 1527 (s, Ar C=C), 1493 (s, Ar C=C); ¹H NMR (500 MHz, CD₃OD) δ 7.68 (2H, d, *J* 8.8 Hz, 2 × Ar-CH), 7.46 (2H, d, *J* 8.8 Hz, 2 × Ar-CH), 7.33 (2H, d, *J* 8.8 Hz, 2 × Ar-CH), 7.28 (2H, d, *J* 8.8 Hz, 2 × Ar-CH) 6.12 (1H, s, C(4)H), 4.08 (1H, d, *J* 17.3 Hz, C(21)H_aH_b), 3.82 (1H, d, *J* 17.3 Hz, C(21)H_aH_b), 1.41 (3H, s, C(19)H₃ or C(20)H₃), 1.35 (3H, s, C(19)H₃ or C(20)H₃); ¹³C NMR (125 MHz, CD₃OD, some signals are coincident) δ 171.5 (C(22)), 159.0 (C(2) or C(12)), 158.5 (C(2) or C(12)), 138.8 (Ar-C), 138.4 (Ar-C), 130.3 (Ar-C), 130.0 (Ar-C), 129.9 (Ar-CH), 129.8 (Ar-CH), 123.4 (Ar-CH), 122.6 (Ar-CH), 77.1 (C(4)), 61.1 (C(5)), 42.4 (C(21)), 25.7 (C(19) or C(20)), 19.4 (C(19) or C(20)); *m/z* (-ve ion electrospray) 483 ([M-H]⁻, (³⁷Cl, ³⁷Cl), 10%) 481 ([M-H]⁻, (³⁵Cl, ³⁷Cl), 65%) 479 ([M-H]⁻, (³⁵Cl, ³⁵Cl), 100%), (+ve ion electrospray) 507 ([M+Na]⁺, (³⁷Cl, ³⁷Cl), 8%), 505 ([M+Na]⁺, (³⁵Cl, ³⁷Cl), 55%), 503 ([M+Na]⁺, (³⁵Cl, ³⁵Cl), 100%); (Found 479.0998, C₂₀H₂₁³⁵Cl₂N₆O₄ ([M-H]⁻), requires 479.1007).

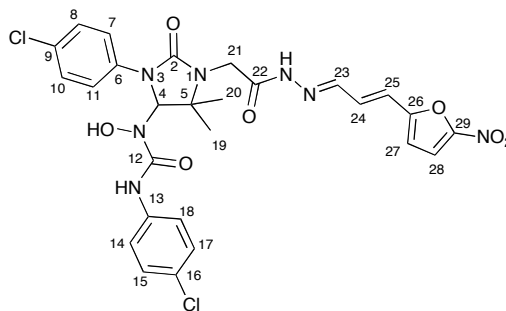
(E)-3-(5-Nitro-2-furyl)acrylaldehyde. (70)



A solution of 5-nitrofuran-2-carbaldehyde (1.067 g, 7.56 mmol) in freshly distilled THF (1 mL) was added drop-wise under an atmosphere of nitrogen to a solution of (triphenylphosphanylidene)acetaldehyde (2.3 g, 7.56 mmol) in freshly distilled THF (50 mL) at rt. The reaction mixture was allowed to stir at rt for 2 h and then concentrated under reduced pressure. Purification by flash column chromatography

(SiO₂; Et₂O:PE, 3:1) yielded the title compound as an orange solid (1.056 g, 70%). Mp 114–116 °C [lit.¹⁰² 110–116 °C]; ν_{\max} (evaporated film)/cm⁻¹ 3150 (w, C-H), 3133 (w, C-H), 1686 (s, C=O), 1629 (m, C=C), 1519 (s, C=C), 1470 (s, C=C); ¹H NMR (300 MHz, *d*₆-DMSO) δ 9.70 (1H, d, *J* 7.6 Hz, CHO), 7.79 (1H, d, *J* 4.0 Hz, C(6)H), 7.7 (1H, d, *J* 15.9 Hz, C(3)H), 7.43 (1H, d, *J* 4.0 Hz, C(5)H), 6.75 (1H, dd, *J* 15.9 & 7.6 Hz, C(2)H); ¹³C NMR (100 MHz, *d*₆-DMSO) δ 193.6 (C(1)), 152.3 (C(7)), 152.3 (C(4)), 136.4 (C(3)), 130.4 (C(2)), 118.1 (C(5)), 114.6(C(6)).

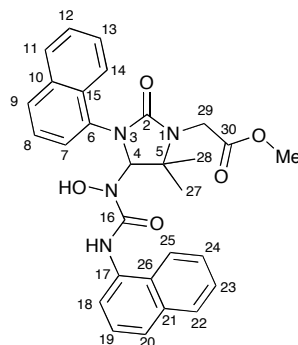
3-(4-Chlorophenyl)-1-[3-(4-chlorophenyl)-5,5-dimethyl-1-(2-((*E*)-2-((*E*)-3-(5-nitrofuran-2-yl)allylidene)hydrazinyl)-2-oxoethyl)-2-oxoimidazolidin-4-yl)-1-hydroxyurea (ESI). (1)



(*E*)-3-(5-nitro-2-furyl)acrylaldehyde (63 mg, 0.377 mmol) was added under an atmosphere of nitrogen to a solution of acyl hydrazide, **8** (0.180 g, 0.377 mmol) in freshly distilled MeOH (2 mL). The resulting solution was stirred at rt for 17 h and then concentrated under reduced pressure. The product was crystallised from DCM, collected by filtration, washed with cold DCM (10 mL) and pentane (10 mL) and dried yielding the title compound as a yellow solid (0.191 g, 81%). Mp 211–213 °C;

ν_{\max} (solid state)/ cm^{-1} 3382 (w, O-H), 3124 (w, N-H), 2983 (m, C-H), 2890 (w, C-H), 1707 (m, C=O), 1669 (s, C=O), 1519 (s, C=C), 1494 (s, C=C); ^1H NMR (500 MHz, CDCl_3) δ 9.85 (1H, brs, NH or OH), 9.42 (1H, brs, NH or OH), 7.68 (2H, d, J 8.8 Hz, 2 \times Ar- CH), 7.65 (1H, brs, NH or OH), 7.38 (2H, d, J 9.1 Hz, 2 \times Ar- CH), 7.30–7.26 (3H, m, C(23) H & 2 \times Ar- CH), 7.18 (1H, d, J 3.7 Hz, C(28) H), 7.16 (2H, d, J 8.8 Hz, 2 \times Ar- CH), 6.95 (1H, dd, J 15.5 & 9.4 Hz, C(24) H), 6.34 (1H, d, J 3.7 Hz, C(27) H), 6.13 (1H, s, C(4) H), 5.47 (1H, brd, J 15.5 Hz, C(25) H), 4.78 (1H, d, J 18.3 Hz, C(21) H_aH_b), 4.11 (1H, d, J 18.3 Hz, C(21) H_aH_b), 1.43 (3H, s, C(19) H_3 or C(20) H_3), 1.30 (3H, s, C(19) H_3 or C(20) H_3); ^{13}C NMR (100 MHz, d_6 -DMSO, two isomers, some signals are coincident) δ 169.8 ($\text{C}=\text{O}$), 165.3 ($\text{C}=\text{O}$), 161.0 ($\text{C}=\text{O}$), 156.9 (Ar- C), 156.4 (Ar- C), 155.7 (Ar- C), 155.6 (Ar- C), 154.9 (Ar- C), 154.8 (Ar- C), 151.4 (Ar- C), 151.4 (Ar- C), 147.0 (Ar- C), 143.8(Ar- CH), 138.3 (Ar- C), 138.1 (Ar- C), 138.0 (Ar- C), 130.1 (Ar- CH), 128.6 (Ar- CH), 128.4 (Ar- CH), 128.3 (Ar- CH), 128.3 (Ar- CH), 126.5 (Ar- C), 126.3 (Ar- C), 126.2 (Ar- C), 124.0 (Ar- CH), 123.9 (Ar- CH), 123.3 (Ar- CH), 121.5 (Ar- CH), 121.3 (Ar- CH), 120.1 (Ar- CH), 120.0 (Ar- CH), 119.8 (Ar- CH), 119.2 (Ar- CH), 115.4 (Ar- CH), 115.4 (Ar- CH), 113.4 (Ar- CH), 74.4 ($\text{C}(4)\text{H}$, major isomer), 74.3 ($\text{C}(4)\text{H}$, minor isomer), 58.8 ($\text{C}(5)$, minor isomer), 58.6 ($\text{C}(5)$, major isomer), 40.25 ($\text{C}(21)$), 26.8 ($\text{C}(19)$ or $\text{C}(20)$, major isomer), 26.4, ($\text{C}(19)$ or $\text{C}(20)$, minor isomer) 19.3 ($\text{C}(19)$ or $\text{C}(20)$, major isomer), 19.1 ($\text{C}(19)$ or $\text{C}(20)$, minor isomer); m/z (–ve ion electrospray) 632 ($[\text{M}-\text{H}]^-$, (^{37}Cl , ^{37}Cl), 15%), 630 ($[\text{M}-\text{H}]^-$, (^{35}Cl , ^{37}Cl), 70%), 628 ($[\text{M}-\text{H}]^-$, (^{35}Cl , ^{35}Cl), 100%), (+ve ion electrospray); (Found 628.1123, $\text{C}_{27}\text{H}_{24}^{35}\text{Cl}_2\text{N}_7\text{O}_7$ ($[\text{M}-\text{H}]^-$), requires 628.1120).

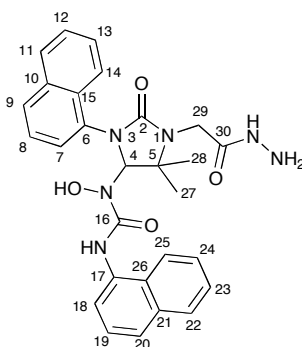
Methyl 2-(4-(1-hydroxy-3-(naphthalen-1-yl)ureido-5,5-dimethyl-3-(naphthalen-1-yl)-2-oxoimidazolidin-1-yl)acetate. (71)



A solution of 1-naphthyl isocyanate (1.01 g, 5.75 mmol) in freshly distilled THF (2 mL) was added under an atmosphere of nitrogen to a solution of oxime, **67** (0.57 g, 2.87 mmol) also in freshly distilled THF (14 mL). The reaction mixture was stirred at rt for 15 h when residual solvent was removed under reduced pressure. The product was crystallised from DCM, collected by filtration, washed with diethyl ether (20 mL) and dried under vacuum. The filtrate was concentrated under reduced pressure and the crystallisation procedure was repeated a further three times. Combination of the crystallised material yielded the title compound as a colourless solid (0.921 g, 61%). Mp 199–200 °C; ν_{\max} (solid state)/cm⁻¹ 3436 (w, O-H), 3054 (brw, N-H), 2839 (brw, C-H), 1749 (s, C=O), 1658 (s, C=O), 1535 (s, C=C); ¹H NMR (500 MHz, CDCl₃) δ 8.17 (1H, brs, NH or OH), 8.08 (1H, brd, *J* 7.9 Hz, Ar-CH), 7.99 (1H, brs, NH or OH), 7.92 (1H, brd, *J* 6.7 Hz, Ar-CH), 7.87–7.78 (4H, m, 4 × Ar-CH), 7.61–7.59 (2H, m, 2 × Ar-CH), 7.52–7.55 (1H, m, Ar-CH), 7.50–7.44 (5H, m, 5 × Ar-CH), 7.35–7.32 (1H, m, Ar-CH), 6.19 (1H, s, C(4)H), 4.69 (1H, d, *J* 18.2 Hz, C(29)H_aH_b), 3.88 (3H, s, CO₂CH₃), 3.79 (1H, d, *J* 18.2 Hz, C(29)H_aH_b), 1.71 (3H, s, C(27)H₃ or C(28)H₃), 1.49 (3H, s, C(27)H₃ or C(28)H₃);

^{13}C NMR (125 MHz, CDCl_3 , some signals are coincident) δ 173.9 ($\underline{\text{C}}(30)$), 156.1 ($\underline{\text{C}}(2)$ and $\underline{\text{C}}(16)$ coincident), 134.6 (Ar- $\underline{\text{C}}$), 134.0 (Ar- $\underline{\text{C}}$), 132.1 (Ar- $\underline{\text{C}}$), 131.1 (Ar- $\underline{\text{C}}$), 128.6 (Ar- $\underline{\text{CH}}$), 128.5 (Ar- $\underline{\text{CH}}$), 128.4 (Ar- $\underline{\text{CH}}$), 127.4 (Ar- $\underline{\text{C}}$), 126.7 (Ar- $\underline{\text{CH}}$), 126.0 (Ar- $\underline{\text{CH}}$), 125.8 (Ar- $\underline{\text{CH}}$), 125.6 (Ar- $\underline{\text{CH}}$), 125.5 (Ar- $\underline{\text{CH}}$), 125.1 (Ar- $\underline{\text{CH}}$), 120.9 (Ar- $\underline{\text{CH}}$), 120.0 (Ar- $\underline{\text{CH}}$), 77.6 ($\underline{\text{C}}(4)$), 59.2 ($\underline{\text{C}}(5)$), 53.2 ($\text{CO}_2\underline{\text{C}}\text{H}_3$), 40.5 ($\underline{\text{C}}(29)$), 25.8 ($\underline{\text{C}}(27)$ or $\underline{\text{C}}(28)$), 20.3 ($\underline{\text{C}}(27)$ or $\underline{\text{C}}(28)$); m/z (-ve ion electrospray) 511 ($[\text{M}-\text{H}]^-$, 100%); (+ve ion electrospray) 535 ($[\text{M}+\text{Na}]^+$, 100%). (Found 535.1949, $\text{C}_{29}\text{H}_{28}\text{N}_4\text{NaO}_5$ ($[\text{M}+\text{H}]^+$), requires 535.1952).

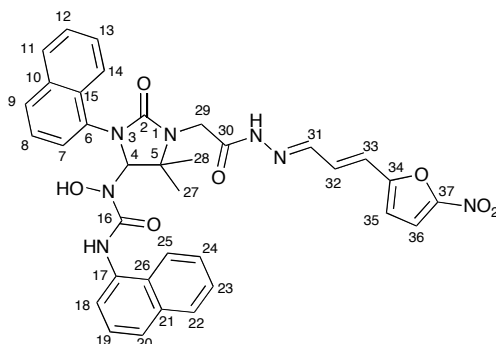
1-(1-(2-Hydrazinyl-2-oxoethyl)-5,5-dimethyl-3-(naphthalen-1-yl)-2-oxoimidazolidin-4-yl)-1-hydroxy-3-(naphthalen-1-yl)urea. (72)



An aqueous solution of hydrazine (62%, 0.88 mL, 23 mmol) was added to a solution of imidazolidinone **71** (451 mg, 0.88 mmol) in MeOH (4.5 mL). The reaction mixture was stirred at rt for 48 h and then cooled to 0 °C. The resulting precipitated solid was collected by filtration and washed sequentially with cold MeOH (10 mL) and diethyl ether (10 mL). The filtrate was concentrated under reduced pressure and the residual solid was recrystallised at rt from DCM/diethyl ether (1:1), washed with

cold MeOH and diethyl ether and then combined with the first batch of precipitate to yield the title compound as a colourless solid (248 mg, 55%). Mp 195–197 °C; ν_{max} (evaporated film)/ cm^{-1} 3390 (m, O-H), 3271 (brm, N-H), 3054 (m, N-H), 2971 (m, C-H), 2857 (brw, C-H), 1686 (s, C=O), 1596 (m, C=C), 1520 (m, C=C), 1495 (s, C=C); ^1H NMR (500 MHz, CD_3OD) δ 8.12 (1H, brs, NH or OH), 7.98 – 7.95 (3H, m, 3 \times Ar- CH), 7.80 (1H, d, J 8.2 Hz, Ar- CH), 7.68 (1H, d, J 8.2 Hz, Ar- CH), 7.61–7.52 (4H, m, 4 \times Ar- CH), 7.45–7.30 (5H, m, 5 \times Ar- CH), 6.99 (1H, d, J 7.2 Hz, Ar- CH), 6.10 (1H, s, C(4) H), 4.12 (1H, d, J 16.9 Hz, C(29) H_aH_b), 3.96 (1H, d, J 16.9 Hz, C(29) H_aH_b), 1.70 (3H, s, C(27) H_3 or C(28) H_3), 1.61 (3H, s, C(27) H_3 or C(28) H_3); ^{13}C NMR (CD_3OD : 75 MHz, some signals are coincident) 171.8 ($\text{C}(30)$), 161.3 ($\text{C}(2)$ or $\text{C}(16)$), 160.7 ($\text{C}(2)$ or $\text{C}(16)$), 136.2 (Ar- C), 135.7 (Ar- C), 134.0 (Ar- C), 132.7 (Ar- C), 131.0 (Ar- C), 129.9 (Ar- CH), 129.8 (Ar- CH), 129.2 (Ar- CH), 128.0 (Ar- CH), 127.6 (Ar- CH), 127.5 (Ar- CH), 127.2 (Ar- CH), 127.1 (Ar- CH), 126.9 (Ar- CH), 126.4 (Ar- CH), 124.3 (Ar- CH), 123.6 (Ar- CH), 79.7 ($\text{C}(4)$), 61.5 ($\text{C}(5)$), 42.6 ($\text{C}(29)$), 26.5 ($\text{C}(27)$ or $\text{C}(28)$), 20.5 ($\text{C}(27)$ or $\text{C}(28)$); m/z – (–ve ion electrospray) 511 ($[\text{M}-\text{H}]^-$, 100%), (+ve ion electrospray) 535 ($[\text{M}+\text{Na}]^+$, 100%); (Found 535.2065, $\text{C}_{28}\text{H}_{28}\text{N}_6\text{NaO}_4$ ($[\text{M}+\text{Na}]^+$), requires 535.2064).

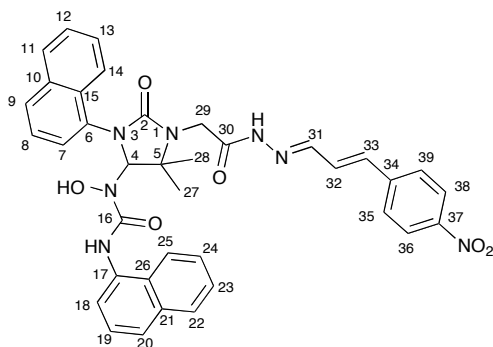
1-(5,5-Dimethyl-3-(naphthalen-1-yl)-1-(2-((E)-2-((E)-3-(5-nitrofuran-2-yl)allylidene)hydrazinyl-2-oxoethyl)-2-oxoimidazolidin-4-yl)-1-hydroxy-3-(naphthalen-1-yl)urea (ESII). (2)



(*E*)-3-(5-nitro-2-furyl)acrylaldehyde (20 mg, 0.120 mmol) was added under nitrogen to a solution of acyl hydrazide, **72** (70 mg, 0.137 mmol) in freshly distilled MeOH (1 mL). The reaction mixture was stirred at rt for 48 h and then concentrated under reduced pressure. The residue was recrystallised at rt from EtOAc/diethyl ether (1:2), yielding the title compound as a yellow solid (75 mg, 83%). Mp 213–215 °C; ν_{\max} (solid state)/cm⁻¹ 3410 (w, O-H), 3267 (m, N-H), 3013 (brm, N-H), 2862 (w, C-H), 1739 (brs, C=O) 1702 (s, C=O), 1655 (s, C=O), 1626 (m, C=C), 1537 (s, C=C); ¹H NMR (400 MHz, CDCl₃ and one drop of *d*₅-Pyridine) δ 11.6 (1H, brs, NH or OH), 7.97–7.95 (3H, m, 3 × Ar-CH), 7.89–7.87 (1H, m, Ar-CH), 7.81–7.76 (1H, m, Ar-CH), 7.71–7.65 (2H, m, 2 × Ar-CH), 7.53–7.45 (10H, m, 10 × Ar-CH), 7.28 (1H, d, *J* 2.9 Hz, C(36)H), 6.86 (1H, dd, *J* 15.4 & 8.9 Hz, C(32)H), 6.48 (1H, d, *J* 2.9 Hz, C(35)H), 6.32 (1H, s, C(4)H), 5.55 (1H, brs, NH or OH), 5.36 (1H, d, *J* 17.0 Hz, C(29)H_aH_b), 4.59 (1H, d, *J* 17.0 Hz, C(29)H_aH_b) 1.67 (3H, s, C(27)H₃ or C(28)H₃), 1.52 (3H, s, C(27)H₃ or C(28)H₃); ¹³C NMR (75 MHz, CDCl₃ plus *d*₅-Pyridine,

some signals are coincident) δ 171.5 (C(30)), 166.2 (C(2) or C(16)), 157.3 (C(2) or C(16)), 154.0 (C(34)), 147.9 (Ar-C), 133.9 (Ar-C), 133.7 (Ar-C), 132.5 (Ar-C), 130.0 (Ar-C), 128.8 (Ar-C), 128.0 (Ar-CH), 127.6 (Ar-CH), 126.2 (Ar-CH), 125.9 (Ar-CH), 125.3 (Ar-CH) 125.0 (Ar-CH), 122.4 (Ar-CH), 121.5 (Ar-CH), 113.0 (Ar-CH), 110.5 (Ar-CH), 77.2 (C(4)), 59.1 (C(5)), 41.9 (C(29)), 25.8 (C(27) or C(28)), 19.5 (C(27) or C(28)); m/z (-ve ion electrospray) 660 ($[M-H]^-$, 100%), (+ve ion electrospray) 684 ($[M+Na]^+$, 100%); (Found 660.2199, $C_{35}H_{30}N_7O_7$ ($[M-H]^-$), requires 660.2212).

1-(5,5-Dimethyl-3-(naphthalen-1-yl)-1-(2-((E)-2-((E)-3-(4-nitrophenyl)allylidene)hydrazinyl-2-oxoethyl)-2-oxoimidazolidin-4-yl)-1-hydroxy-3-(naphthalen-1-yl)urea (ES111). (73)

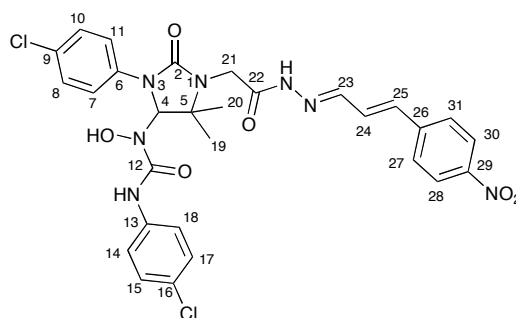


p-Nitrocinnamaldehyde (40 mg, 0.227 mmol) was added under an atmosphere of nitrogen to a solution of acyl hydrazide, **72** (116 mg, 0.16 mmol) in freshly distilled MeOH (2 mL). The reaction mixture was stirred at rt for 48 h and concentrated under reduced pressure. The resulting solid was collected by filtration, washed with diethyl ether (10 mL) and pentane (10 mL) to yield the title compound as a yellow solid

(117 mg, 78%). Mp 191.5–193.5 °C; ν_{\max} (evaporated film)/cm⁻¹ 3390 (brw, O-H), 3195 (brm, N-H), 3048 (m, N-H), 2952 (m, C-H), 2886 (m, C-H), 1685 (s, C=O), 1597 (m, C=C), 1517 (s, C=C); ¹H NMR (400 MHz, *d*₆-DMSO, two isomers) δ 11.6 (brs, NH or OH), 9.2 (brs, NH or OH minor isomer), 9.2 (s, NH or OH major isomer), 8.31 – 8.21 (m, Ar-CH), 8.12 – 7.84 (m, Ar-CH), 7.76 – 7.54 (m, Ar-CH), 7.49 – 7.10 (m, Ar-CH), 6.94 (dd, *J* 16.3 & 9.8 Hz, C(32)H minor isomer), 5.93, (brs, C(4)H major isomer & C(4)H minor isomer), 5.60 (d, *J* 16.3 Hz, C(33)H minor isomer), 4.46 (d, *J* 17.9 Hz C(29)H_aH_b major isomer), 4.31 (d, *J* 17.9 Hz, C(29)H_aH_b major isomer), 4.07 (partly obscured by solvent peak at 4.04, C(29)H_aH_b minor isomer), 3.97 (d, *J* 11.1 Hz, C(29)H_aH_b minor isomer), 1.60 (s, C(27)H₃ or C(28)H₃ major isomer & C(27)H₃ or C(28)H₃ minor isomer), 1.52 (s, C(27)H₃ or C(28)H₃ major isomer & C(27)H₃ or C(28)H₃ minor isomer); ¹³C NMR (100 MHz, *d*₆-DMSO, two isomers, some signals are coincident) δ 170.4 (C=O), 158.7 (Ar-C), 148.7 (Ar-C), 148.7 (Ar-C), 147.0 (Ar-C), 146.9 (Ar-C), 146.9 (Ar-C), 142.7 (Ar-C), 142.6 (Ar-C), 134.1 (Ar-C), 134.1 (Ar-C), 134.0 (Ar-C), 133.7 (Ar-C), 133.7 (Ar-C), 133.6 (Ar-C), 131.6 (Ar-C), 131.6 (Ar-C), 131.5 (Ar-C), 131.3 (Ar-C), 131.2 (Ar-C), 131.2 (Ar-C), 131.1 (Ar-C), 129.8 (Ar-CH), 129.8 (Ar-CH), 129.1 (Ar-CH), 128.6 (Ar-CH), 128.5 (Ar-CH), 128.5 (Ar-CH), 128.4 (Ar-CH), 128.1 (Ar-CH), 128.0 (Ar-CH), 127.9 (Ar-CH), 127.8 (Ar-CH), 126.7 (Ar-C), 126.1 (Ar-C), 126.0 (Ar-C), 125.9 (Ar-CH), 125.9 (Ar-CH), 125.8 (Ar-CH), 125.7 (Ar-CH), 125.7 (Ar-CH), 125.6 (Ar-CH), 125.5 (Ar-CH), 124.2 (Ar-CH), 124.1 (Ar-CH), 123.0 (Ar-CH), 122.6 (Ar-CH), 77.0 (C(4)), 59.6 (C(5) minor isomer), 59.2 (C(5) major isomer), 40.6 (C(29) minor isomer), 40.3 (C(29) major isomer), 26.4 (C(27) or C(28) minor isomer), 26.3 (C(27) or C(28) major isomer), 20.5 (C(27) or C(28) minor

isomer), 20.4 (C(27) or C(28) major isomer); m/z (-ve ion electrospray) 670 ($[M-H]^-$, 100%), (+ve ion electrospray) 694 ($[M+Na]^+$, 100%); (Found 694.2385, $C_{37}H_{33}N_7NaO_6$ ($[M+Na]^+$), requires 694.2385).

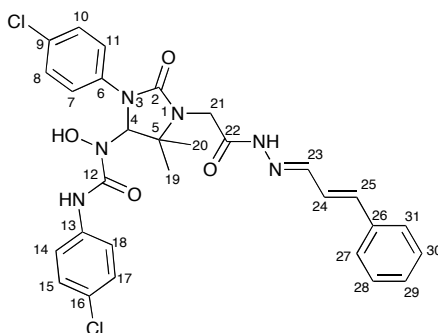
3-(4-Chlorophenyl)-1-[3-(4-chlorophenyl)-5,5-dimethyl-1-(2-((E)-2-((E)-3-(4-nitrophenyl)allylidene)hydrazinyl)-2-oxoethyl)-2-oxoimidazolidin-4-yl]-1-hydroxyurea (ES326). (75)



p-Nitrocinnamaldehyde (30 mg, 0.17 mmol) was added under an atmosphere of nitrogen to a solution of acyl hydrazide, **8** (75 mg, 0.16 mmol) in freshly distilled MeOH (1 mL). The reaction mixture was stirred at rt for 18 h and then concentrated under reduced pressure. The product was crystallised from DCM, collected by filtration and washed with cold DCM (10 mL) and pentane (10 mL) yielding the title compound as a yellow solid (54 mg, 54%). Mp 210.5–211 °C; ν_{\max} (evaporated film)/ cm^{-1} 3206 (w), 3166 (w), 3098 (w), 1674 (s), 1590 (m), 1515 (s), 1495 (s); ^1H NMR (400 MHz, d_6 -DMSO) δ 9.78 (brs, NH or OH minor isomer), 9.76 (brs, NH or OH major isomer), 9.33 (brs, NH or OH major isomer & NH or OH minor isomer), 8.35 (d, J 8.7 Hz, Ar- CH), 8.28 (d, J 8.7 Hz, Ar- CH), 8.09, (d, J 8.7 Hz, Ar-

CH), 7.94 (d, J 9.1 Hz, Ar-CH), 7.76 – 7.70 (m, Ar-CH), 7.46 – 7.36 (m, Ar-CH),
 7.33 – 7.25 (m, Ar-CH), 6.16 (brs, C(4)H major isomer & C(4)H minor isomer),
 4.41, (d, J 18.2 Hz, C(21)H_aH_b major isomer), 4.29 (d, J 18.2 Hz, C(21)H_aH_b major
 isomer), 4.04 (d, J 16.9 Hz, C(21)H_aH_b minor isomer), 3.96 (d, J 16.9 Hz, C(21)H_aH_b
 minor isomer), 1.41 (s, C(19)H₃ or C(20)H₃ minor isomer), 1.39 (s, C(19)H₃ or
 C(20)H₃ major isomer), 1.35 (C(19)H₃ or C(20)H₃ major isomer); ¹³C NMR (100
 MHz, *d*₆-DMSO, two isomers, some signals are coincident) δ 175.5 (C=O), 157.8
 (Ar-C), 157.7 (Ar-C), 157.5 (Ar-C), 156.5 (Ar-C), 156.4 (Ar-C), 150.6 (Ar-C), 142.0
 (Ar-C), 140.3 (Ar-C), 138.3 (Ar-C), 138.1 (Ar-C), 138.0 (Ar-CH), 137.6 (Ar-CH),
 128.4 (Ar-CH), 128.3 (Ar-CH), 128.2 (Ar-CH), 128.1 (Ar-CH), 127.9 (Ar-CH),
 126.3 (Ar-C), 126.3 (Ar-C), 126.2 (Ar-C), 124.2 (Ar-CH), 124.1 (Ar-CH), 124.0
 (Ar-CH), 121.5 (Ar-CH), 121.3 (Ar-CH), 120.1 (Ar-CH), 120.0 (Ar-CH), 119.9 (Ar-
 CH), 119.8 (Ar-CH), 74.4 (C(4) major isomer), 74.4 (C(4) minor isomer), 58.6
 (C(5)), 40.3 (C(21)), 26.9 (C(19) or C(20) minor isomer), 26.8 (C(19) or C(20) major
 isomer), 19.3 (C(19) or C(20) major isomer), 19.2 (C(19) or C(20) minor isomer);
m/z (–ve ion electrospray) 641 ([M–H][–], (³⁵Cl, ³⁷Cl), 30%), 639 ([M–H][–], (³⁵Cl,
³⁵Cl), 97%); (+ve ion electrospray) 664 ([M+Na]⁺, (³⁵Cl, ³⁷Cl), 50%) 662 ([M+Na]⁺,
(³⁵Cl, ³⁵Cl), 100%); (Found 662.1289, C₂₉H₂₇³⁵Cl₂N₇NaO₆, ([M+Na]⁺), requires
662.1292).

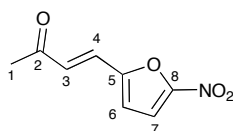
3-(4-Chlorophenyl)-1-(3-(4-chlorophenyl)-5,5-dimethyl-2-oxo-1-(2-oxo-2-((E)-2-((E)-3-phenylallylidene)hydrazinyl)ethyl)imidazolidin-4-yl)-1-hydroxyurea
(ES328). (76)



By using the similar procedure described for **75**, acyl hydrazide, **8** (150 mg, 0.312 mmol) and cinnamaldehyde (83 mg, 0.628 mmol) provided the title compound as a pale yellow solid (86.3 mg, 47%). Mp 166 – 168 °C; ν_{\max} (solid state)/ cm^{-1} 3555 (brw, O-H), 3494 (brw, N-H), 3321 (w, N-H), 3233 (brw), 3057 (w, C-H), 2840 (brw, C-H), 1704 (s, C=O), 1668 (s, C=O), 1650 (m, C=O), 1624 (w, C=C), 1593 (w, C=C), 1522 (s, C=C), 1494 (s, C=C); ^1H NMR (300 MHz, CDCl_3) δ 9.78 (1H, brs, NH or OH), 9.37 (1H, brs, NH or OH), 7.66 (2H, d, J 8.9 Hz, $2 \times \text{Ar-CH}$), 7.53 (1H, t, J 4.2 Hz, NH), 7.36 (2H, d, J 8.9 Hz, $2 \times \text{Ar-CH}$), 7.31 – 7.19 (6H, m, $5 \times \text{Ar-CH}$ & C(23)H), 7.09 – 7.02 (4H, m, $4 \times \text{Ar-CH}$), 6.73 (1H, dd, J 16.2 & 9.4 Hz, C(24)H), 6.12 (1H, s, C(4)H), 6.00 (1H, d, J 16.2 Hz, C(25)H), 4.76 (1H, d, J 18.5 Hz, C(21)H_aH_b), 4.11 (1H, d, J 18.5, C(21)H_aH_b), 1.41 (3H, s, C(19)H₃ or C(20)H₃), 1.32 (3H, s, C(19)H₃ or C(20)H₃); ^{13}C NMR (75 MHz, d_6 -DMSO, two isomers, some signals are coincident) δ 169.7 (C=O), 157.4 (Ar-C), 156.6 (Ar-C), 156.5 (Ar-C), 155.9 (Ar-C), 155.9 (Ar-C), 155.8 (Ar-C), 155.8 (Ar-C), 149.2 (Ar-C), 149.1

(Ar-C), 146.0 (Ar-CH), 139.3 (Ar-CH), 139.2 (Ar-CH), 139.2 (Ar-CH), 138.8 (Ar-CH), 138.3 (Ar-CH), 138.1 (Ar-C), 137.9 (Ar-CH), 135.9 (Ar-C), 135.9 (Ar-C), 135.8 (Ar-C), 128.9 (Ar-CH), 128.6 (Ar-CH), 128.5 (Ar-CH), 128.5 (Ar-CH), 128.4 (Ar-CH), 128.4 (Ar-CH), 127.7 (Ar-CH), 127.7 (Ar-CH), 127.2 (Ar-CH), 127.1 (Ar-CH), 126.7 (Ar-CH), 127.1 (Ar-CH), 126.7 (Ar-C), 126.6 (Ar-C), 126.5 (Ar-C), 126.4 (Ar-C), 125.4 (Ar-CH), 125.2 (Ar-CH), 125.2 (Ar-CH), 121.7 (Ar-CH), 121.5 (Ar-CH), 120.3 (Ar-CH), 120.2 (Ar-CH), 120.2 (Ar-CH), 74.5 (C(4) major isomer), 74.5 (C(4) minor isomer), 58.9 (C(5) minor isomer), 58.6 (C(5) major isomer), 40.6 (C(21)), 26.8 (C(19) or C(20) major isomer), 26.3 (C(19) or C(20) minor isomer), 19.4 (C(19) or C(20) major isomer), 19.0 (C(19) or C(20) minor isomer); *m/z* (–ve ion electrospray) 595 ([M–H][–], (³⁷Cl, ³⁷Cl), 15%), 595 ([M–H][–], (³⁵Cl, ³⁷Cl), 75%), 593 ([M–H][–], (³⁵Cl, ³⁵Cl), 100%), (+ve ion electrospray) 621 ([M+Na]⁺, (³⁷Cl, ³⁷Cl), 45%), 619 ([M+Na]⁺, (³⁵Cl, ³⁷Cl), 45%), 617 ([M+Na]⁺, (³⁵Cl, ³⁵Cl), 100%); (Found 595.1629, C₂₉H₂₉³⁵Cl₂N₆O₄, ([M+H]⁺), requires 595.1622).

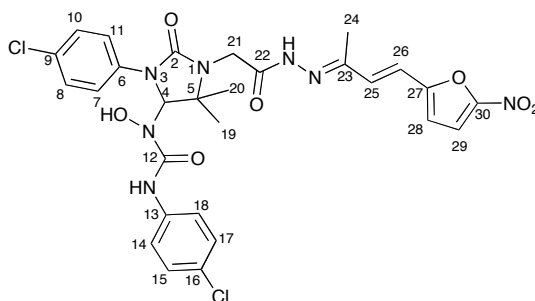
(E)-4-(5-Nitrofuran-2-yl)but-3-en-2-one. (74)



A solution of 5-nitrofuran-2-carbaldehyde (1.067 g, 7.56 mmol) in freshly distilled THF (1 mL) was added drop-wise under an atmosphere of nitrogen to a solution of (acetylmethylene)triphenylphosphorane (2.41 g, 7.57 mmol) in freshly distilled THF

(50 mL) at rt. The reaction mixture was allowed to stir at rt for 2 h and then concentrated under reduced pressure. Purification by flash column chromatography (SiO₂; Et₂O:PE, 3:1) yielded the title compound as orange crystals (1.048 g, 83%). Mp 115–116 °C, [lit¹⁰³ 114–115 °C]; ν_{\max} (evaporated film)/cm⁻¹ 3147 (w, C-H), 3124 (w, C-H), 3111 (w, C-H), 3054 (w, C-H), 3040 (w, C-H), 1689 (s, C=O), 1616 (s, C=C), 1563 (m, C=C), 1523 (m, C=C), 1506 (w); ¹H NMR (400 MHz, CDCl₃) δ 7.30 (1H, d, *J* 3.8 Hz, C(7)H), 7.20 (1H, d, *J* 16.0 Hz, C(3)H), 6.83 (1H, d, *J* 16.0 Hz, C(4)H), 6.79 (1H, d, *J* 3.8 Hz, C(6)H), 2.31 (3H, s, C(1)H₃); ¹³C NMR (100 MHz, CDCl₃) δ 196.9 (C(2)), 152.8 (C(5) and C(8)), 129.6 (C(4)), 126.9 (C(3)), 116.3 (C(6)), 113.4 (C(7)), 28.8 (C(1)); *m/z* (+ve ion electrospray) 180 ([M-H]⁻, 100%); (Found (by +EI) 181.0376, C₈H₇NO₄, ([M]⁺, requires 181.0370).

3-(4-Chlorophenyl)-1-(3-(4-chlorophenyl)-5,5-dimethyl-1-(2-((E)-2-((E)-4-(5-nitrofur-2-yl)but-3-en-2-ylidene)hydrazinyl)-2-oxoethyl)-2-oxoimidazolidin-4-yl)-1-hydroxyurea (ES40). (77)

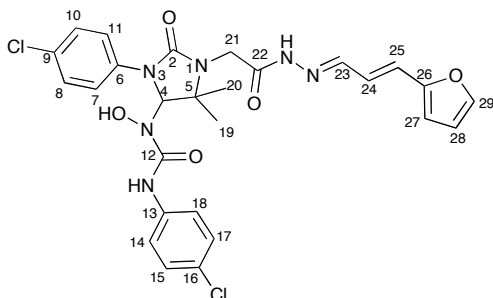


Ketone **74** (41 mg, 0.229 mmol) was added to a solution of acyl hydrazide, **8** (100 mg, 0.208 mmol) dissolved in MeOH under an atmosphere of nitrogen. The reaction

mixture was allowed to stir at rt for 18 h or until TLC showed completion. The resulting precipitate was filtered and washed with cold MeOH giving the title compound as a yellow solid (68 mg, 51%). Mp 178 – 180 °C; ν_{\max} (evaporated film)/cm⁻¹ 3218 (brw, O-H), 3142 (brw, N-H), 2970 (w, C-H), 2873 (w, C-H), 2830 (w, C-H), 1700 (s, C=O), 1684 (s, C=O), 1667 (s, C=O), 1664 (s, C=C), 1653 (s, C=C), 1589 (w, C=C), 1559 (w, C=C), 1522 (s, C=C), 1496 (s, C=C); ¹H NMR (400 MHz, CDCl₃) δ 8.68 (1H, brs, NH or OH), 8.45 (1H, brs, NH or OH), 8.20 (1H, brs, NH or OH), 7.66 (2H, d, *J* 9.0 Hz, Ar-CH), 7.53 (2H, d, *J* 9.0 Hz, Ar-CH), 7.37 (1H, d, *J* 3.8 Hz, C(29)H), 7.25 (4H, m, partly obscured by CDCl₃, 4 × Ar-CH), 7.08 (1H, d, *J* 16.4 Hz, C(25)H), 6.72 (1H, d, *J* 16.4 Hz, C(26)H), 6.64 (1H, d, *J* 3.8 Hz, C(28)H), 6.19 (1H, s, C(4)H), 4.73 (1H, d, *J* 18.2 Hz, C(21)H_aH_b), 4.15 (1H, d, *J* 18.2 Hz, C(21)H_aH_b), 1.96 (3H, s, C(24)H₃), 1.43 (3H, s, C(19)H₃ or C(20)H₃), 1.32 (3H, s, C(19)H₃ or C(20)H₃); ¹³C NMR (75 MHz, *d*₆-DMSO, two isomers, some signals are coincident) δ 170.6 (C=O), 166.0 (C=O), 162.4 (C=O), 156.7 (Ar-C), 156.5 (Ar-C), 152.6 (Ar-C), 151.3 (Ar-C), 151.2 (Ar-C), 148.1 (Ar-C), 134.1 (Ar-C), 134.1 (Ar-C), 134.0 (Ar-C), 128.5 (Ar-CH), 128.4 (Ar-CH), 128.3 (Ar-CH), 126.5 (Ar-C), 126.4 (Ar-C), 126.3 (Ar-C), 121.5 (Ar-CH), 121.4 (Ar-CH), 120.3 (Ar-CH), 120.2 (Ar-CH), 120.1 (Ar-CH), 119.0 (Ar-CH), 115.5 (Ar-CH), 115.5 (Ar-CH), 115.3 (Ar-CH), 113.1 (Ar-CH), 113.1 (Ar-CH), 74.5 (C(4) minor isomer), 74.5 (C(4) major isomer), 58.6 (C(5) minor isomer), 58.6 (C(5) major isomer), 40.9 (C(21) major isomer), 40.8 (C(21) minor isomer), 26.9 (C(19) or C(20) major isomer), 26.2 (C(19) or C(20) minor isomer), 19.3 (C(19) or C(20) major isomer), 19.3 (C(19) or C(20) minor isomer), 11.5 (C(24)); *m/z* (-ve ion electrospray)

646 ([M-H]⁻, (³⁷Cl, ³⁷Cl), 25%), 644 ([M-H]⁻, (³⁵Cl, ³⁷Cl), 70 %), 642 ([M-H]⁻, (³⁵Cl, ³⁵Cl), 100%), (+ve ion electrospray) 670 ([M+Na]⁺, (³⁷Cl, ³⁷Cl), 20%), 668 ([M+Na]⁺, (³⁵Cl, ³⁷Cl), 70%), 666 ([M+Na]⁺, (³⁵Cl, ³⁵Cl), 100%); (Found 666.1251, C₂₈H₂₇³⁵Cl₂N₇NaO₇, ([M+Na]⁺), requires 666.1241).

3-(4-Chlorophenyl)-1-(3-(4-chlorophenyl)-1-(2-((E)-2-((E)-3-(furan-2-yl)allylidene)hydrazinyl)-2-oxoethyl)-5,5-dimethyl-2-oxoimidazolidin-4-yl)-1-hydroxyurea (ES47). (78)

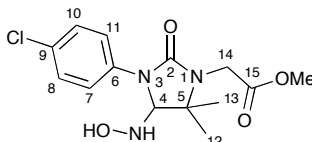


By using the similar procedure described for **75**, acyl hydrazide, **8** (150 mg, 0.312 mmol) and 2-furanacrolein (76 mg, 0.622 mmol) provided the title compound as a pale yellow solid (92.6 mg, 51%). Mp 203 – 204 °C; ν_{\max} (solid state)/cm⁻¹ 3395 (w, O-H), 3222 (brw, N-H), 3145 (brw, N-H), 3132 (brw), 3039 (w, C-H), 2979 (w, C-H) 2974 (w, C-H), 2930 (w, C-H), 1699 (m, C=O), 1680 (s, C=O), 1661 (s, C=O), 1633 (m, C=C), 1588 (w, C=C), 1550 (s, C=C), 1512 (m, C=C), 1492 (w, C=C); ¹H NMR (300 MHz, CDCl₃) δ 9.66 (1H, brs, NH or OH), 8.30 (1H, brs, NH or OH), 7.77 (1H, brs, NH or OH), 7.65 – 7.43 (3H, m, 3 × Ar-CH), 7.41 – 7.14 (9H, m, 9 × Ar-CH), 6.61 (1H, dd, *J* 16.1 & 9.9 Hz, C(24)H), 6.35 (1H, dd, *J* 23.6 & 3 Hz,

C(28)H), 6.10 (1H, s, C(4)H), 5.79 (1H, d, J 16.1 Hz, C(25)H), 4.75 (1H, d, J 18.7 Hz, C(21)H_aH_b), 4.09 (1H, d, J 18.7 Hz, C(21)H_aH_b), 1.40 (3H, s, C(19)H₃ or C(20)H₃) 1.31 (3H, s, C(19)H₃ or C(20)H₃); ¹³C NMR (100 MHz, *d*₆-DMSO, two isomers, some signals are coincident) δ 169.5 (C=O), 160.0 (C=O), 156.5 (Ar-C), 155.7 (Ar-C), 155.6 (Ar-C), 153.1 (Ar-C), 151.8 (Ar-C), 151.7 (Ar-C), 148.4 (Ar-C), 148.2 (Ar-C), 145.3 (Ar-CH), 145.3 (Ar-CH), 145.2 (Ar-CH), 144.4 (Ar-CH), 144.3 (Ar-CH), 144.2 (Ar-CH), 138.3 (Ar-C), 138.1 (Ar-C), 128.4 (Ar-CH), 128.3 (Ar-CH), 128.3 (Ar-CH), 128.3 (Ar-CH), 126.3 (Ar-C), 126.2 (Ar-C), 125.7 (Ar-CH), 122.9 (Ar-CH), 121.3 (Ar-CH), 120.0 (Ar-CH), 119.9 (Ar-CH), 119.8 (Ar-CH), 112.5 (Ar-CH), 111.6 (Ar-CH), 111.6 (Ar-CH), 74.4 (C(4) both isomers), 58.6 (C(5) both isomers), 40.2 (C(21)), 26.8 (C(19) or C(20) major isomer), 26.2 (C(19) or C(20) minor isomer) 19.3 (C(19) or C(20) major isomer), 18.9 (C(19) or C(20) minor isomer); m/z (-ve ion electrospray) 587 ([M-H]⁻, (³⁷Cl, ³⁷Cl), 10%), 585 ([M-H]⁻, (³⁵Cl, ³⁷Cl), 65%), 583 ([M-H]⁻, (³⁵Cl, ³⁵Cl), 100%), (+ve ion electrospray) 611 ([M+Na]⁺, (³⁷Cl, ³⁷Cl), 10%) 609 ([M+Na]⁺, (³⁵Cl, ³⁷Cl), 60%), 607 ([M+Na]⁺, (³⁵Cl, ³⁵Cl), 100%); (Found 607.1244, C₂₇H₂₆³⁵Cl₂N₆NaO₅, ([M+Na]⁺), requires 607.1234).

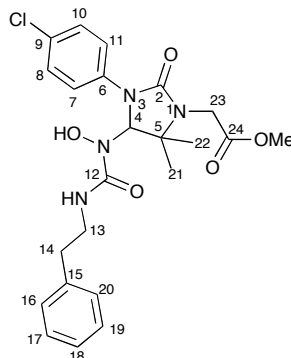
5.2.2 Unsymmetrical Eeyarestatins.

Methyl 2-(3-(4-chlorophenyl)-4-(hydroxyamino)-5,5-dimethyl-2-oxoimidazolidin-1-yl)acetate. (68)



A solution of 4-chlorophenyl isocyanate (768 mg, 5 mmol) in freshly distilled THF (6 mL) at 0 °C, was added drop-wise under an atmosphere of nitrogen, to a solution of oxime, **67** (870 mg, 5 mmol) also in freshly distilled THF (44 mL) at 0°C. The reaction mixture was stirred at rt for 17 h and then concentrated to afford a mixture of compounds **68** and **69** (5:1 ratio; ¹HNMR). The crude product was purified by flash column chromatography (SiO₂, PE:EtOAc 2:1) yielding title compound as colourless crystals (766 mg, 50%). Mp 147–149 °C; ν_{\max} (evaporated film)/cm⁻¹ 3366 (brm, O-H), 3248 (m, N-H), 2969 (brm, C-H), 1751 (m, C=O), 1685 (s, C=O), 1490 (s, C=C); ¹H NMR (500 MHz, CDCl₃) 7.56 (2H, d, *J* 9.1 Hz, 2 × Ar-CH), 7.32 (2H, d, *J* 9.1 Hz, 2 × Ar-CH), 5.51 (1H, brs, NH), 4.74 (1H, brs, OH), 4.65 (1H, s, C(4)H), 4.13 (1H, d, *J* 17.9 Hz, C(14)H_aH_b), 3.83 (1H, d, *J* 17.9 Hz, C(14)H_aH_b), 3.76 (3H, s, CO₂CH₃), 1.42 (3H, s, C(12)H₃ or C(13)H₃), 1.33 (3H, s, C(12)H₃ or C(13)H₃); ¹³C NMR (100 MHz, CDCl₃, some signals are coincident) 170.8 (C(15)), 156.2 (C(2)), 136.9 (Ar-C), 129.5 (Ar-C), 129.0 (Ar-CH), 122.9 (Ar-CH), 80.6 (C(4)), 58.6 (C(5)), 52.4 (CO₂CH₃), 40.6 (C(14)), 26.3 (C(12) or C(13)), 19.7 (C(12) or C(13)); *m/z* (+ve ion electrospray) 352.1 ([M+Na]⁺, (³⁷Cl), 30%) 350.1 ([M+Na]⁺, (³⁵Cl), 100%); (Found 350.0874, C₁₄H₁₈³⁵ClN₃NaO₄ ([M+Na]⁺), requires 350.0878).

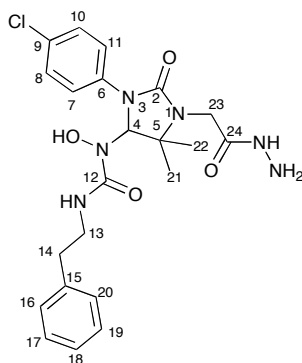
Methyl 2-(3-(4-chlorophenyl)-4-(1-hydroxy-3-phenethylureido)-5,5-dimethyl-2-oxoimidazolidin-1-yl)acetate. (80)



1,1-Carbonyldiimidazole (495 mg, 3.05 mmol) was added under an atmosphere of nitrogen to a solution of phenethylamine (369 mg, 3.05 mmol) in freshly distilled THF (10 mL). The reaction mixture was stirred at 50 °C for 1.5 h then mono-adduct, **68** (500 mg, 1.52 mmol) was added. The reaction mixture was stirred for a further 17 h at 50 °C then allowed to cool to rt. Diethyl ether (10 mL) was added and the precipitated solid was collected by filtration, washed with diethyl ether (20 mL) and pentane (20 mL) and dried under vacuum to yield crude product as a colourless solid (526 mg). Purification by flash column chromatography (SiO₂, PE:EtOAc, 2:1) yielded the title compound as a colourless solid (318 mg, 44%). Mp 182–183 °C; ν_{\max} (evaporated film)/cm⁻¹ 3420 (w, O-H), 3330 (w, N-H), 3027 (w, C-H), 2951 (w, C-H), 2868 (w, C-H), 1757 (m, C=O), 1739 (m, C=O), 1705 (s, C=O), 1656 (m, C=C), 1597 (w, C=C), 1525 (s, C=C), 1496 (s, C=C); ¹H NMR (300 MHz, CDCl₃) δ 7.50 (2H, d, *J* 9.1 Hz, 2 × Ar-CH), 7.22 (1H, brt, NH or OH), 7.20–7.13 (5H, m, 5 × Ar-CH), 7.05 (2H, d, *J* 6.6 Hz, 2 × Ar-CH), 6.08 (1H, s, C(4)H), 6.03 (1H, t, *J* 6 Hz, NH), 4.24 (1H, d, *J* 18 Hz, C(23)H_aH_b), 3.75 (1H, d, *J* 18 Hz, C(23)H_aH_b), 3.73 (3H,

s, CO₂CH₃), 3.51–3.42 (2H, m, C(13)H₂), 2.81–2.70 (2H, m, C(14)H₂), 1.33 (3H, s, C(21)H₃ or C(22)H₃), 1.29 (3H, s, C(21)H₃ or C(22)H₃); ¹³C NMR (100 MHz, CDCl₃) δ 171.9 (C(24)), 158.8 (C(2) or C(12)), 156.7 (C(2) or C(12)), 138.8 (Ar-C), 137.1 (Ar-C), 128.7 (5 × Ar-CH), 128.4 (2 × Ar-CH), 126.3 (Ar-C), 121.0 (2 × Ar-CH), 75.3 (C(4)), 58.9 (C(5)), 52.7 (CO₂CH₃), 41.0 (C(13)), 40.4 (C(23)), 36.1 (C(14)), 25.5 (C(21) or C(22)), 19.2 (C(21) or C(22)); *m/z* (-ve ion electrospray) 475 ([M-H]⁻, (³⁷Cl), 30%), 473 ([M-H]⁻, (³⁵Cl), 100%), (+ve ion electrospray) 499 ([M+Na]⁺, (³⁷Cl), 20%), 497 ([M+Na]⁺, (³⁵Cl), 100%); (Found 475.1743, C₂₃H₂₈³⁵ClN₄O₅ ([M+H]⁺), requires 475.1740).

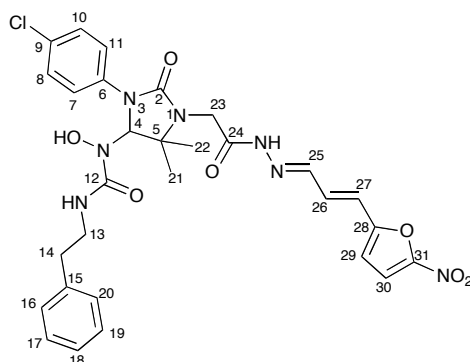
1-(3-(4-Chlorophenyl)-1-(2-hydrazinyl-2-oxoethyl)-5,5-dimethyl-2-oxoimidazolidin-4-yl)-1-hydroxy-3-phenethylurea. (81)



An aqueous solution of hydrazine (62%, 0.88 mL, 23 mmol) was added to a solution of imidazolidinone, **80** (451 mg, 0.88 mmol) in MeOH (4.5 mL). The reaction mixture was stirred at rt for 48 h and then cooled to 0 °C. The precipitated solid was collected by filtration and washed with cold MeOH and diethyl ether. The filtrate was concentrated under reduced pressure and the residue recrystallised at rt from

DCM/diethyl ether (1:1). The resulting solid was collected by filtration, washed with cold MeOH and diethyl ether and dried under vacuum. Combination of both batches yielded the title compound as a colourless solid (248 mg, 55%). Mp 88–90 °C, ν_{\max} (evaporated film)/ cm^{-1} 3321 (brm, O-H), 3078 (w, N-H), 3062 (w, N-H), 3030 (w, N-H), 2970 (w, C-H), 2925 (w, C-H), 2873 (w, C-H), 1699 (s, C=O), 1683 (s, C=O), 1667 (s, C=O), 1652 (s, C=C), 1524 (s, C=C), 1495 (s, C=C); ^1H NMR (500 MHz CD_3OD) δ 7.60 (2H, d, J 8.8 Hz, 2 \times Ar-CH), 7.28 (2H, d, J 8.8 Hz, 2 \times Ar-CH), 7.21 (2H, d, J 6.9 Hz, 2 \times Ar-CH), 7.14 (3H, brd, J 7.9 Hz, 3 \times Ar-CH), 6.99 (1H, brt, J 5.9 Hz, NHCH₂CH₂Ph), 6.00 (1H, s, C(4)H), 4.60 (1H, brs, NOH), 4.07 (1H, d, J 17.3 Hz, C(23)H_aH_b), 3.85 (1H, d, J 17.3 Hz, C(23)H_aH_b), 3.38–3.29 (2H, m, C(13)H₂), 2.68 (2H, t, J 7.3 Hz, C(14)H₂), 1.29 (6H, 2 \times s, C(21)H₃ & C(22)H₃); ^{13}C NMR (100 MHz, CD_3OD) δ 171.6 (C(24)), 161.6 (C(2) or C(12)), 158.5 (C(2) or C(12)), 140.6 (Ar-C), 138.8 (Ar-C), 130.3 (Ar-C), 130.0 (2 \times Ar-CH), 129.9 (2 \times Ar-CH), 129.6 (2 \times Ar-CH), 127.5 (C(18)), 122.9 (2 \times Ar-CH), 77.3 (C(4)), 61.1 (C(5)), 42.6 (C(13)), 42.4 (C(23)), 37.3 (C(14)), 25.7 (C(21) or C(22)), 19.4 (C(21) or C(22)); m/z (–ve ion electrospray) 475 ([M–H][–], (^{37}Cl), 25%), 473 ([M–H][–], (^{35}Cl), 100%), (+ve ion electrospray) 499 ([M+Na]⁺, (^{35}Cl), 30%), 497 ([M+Na]⁺, (^{35}Cl), 100%); (Found 497.1684, $\text{C}_{22}\text{H}_{27}^{35}\text{ClN}_6\text{NaO}_4$ ([M+Na]⁺), requires 497.1675).

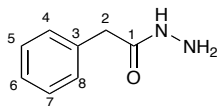
1-(3-(4-Chlorophenyl)-5,5-dimethyl-1-(2-((E)-2-((E)-3-(5-nitrofuran-2-yl)allylidene)hydrazinyl)-2-oxoethyl)-2-oxoimidazolidin-4-yl)-1-hydroxy-3-phenethylurea. (82)



(*E*)-3-(5-nitro-2-furyl)acrylaldehyde (25 mg, 0.147 mmol) was added under nitrogen to a solution of acyl hydrazide, **81** (60 mg, 0.77 mmol) in anhydrous MeOH (0.6 mL). The reaction mixture was stirred at rt for 17 h or until a yellow precipitate formed. Diethyl ether was added to allow further precipitation to occur. The solid was filtered and washed with Et₂O and pentane yielding the title compound as a yellow solid (8 mg, 50%). Mp 131–133 °C (dec); ν_{\max} (evaporated film)/cm⁻¹ 3421 (brm, O-H), 3190 (brm, N-H), 3059 (m, N-H), 2975 (m, C-H), 2929 (m, C-H), 1684 (s, C=O), 1597 (m, C=C), 1559 (m, C=C), 1520 (s, C=C); *m/z* (–ve ion electrospray) 624 ([M–H]⁻, (³⁷Cl), 25%), 622 ([M–H]⁻, (³⁵Cl), 100 %), (+ve ion electrospray) 626 ([M+H]⁺, (³⁷Cl), 30%), 624 ([M+H]⁺, (³⁵Cl), 100%); (Found 624.1966, C₂₉H₃₁³⁵ClN₇O₇ ([M+H]⁺), requires 624.1968).

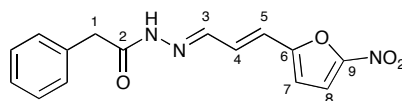
5.2.3 Short form Eeyarestatins.

2-Phenylacetohydrazide. (83)



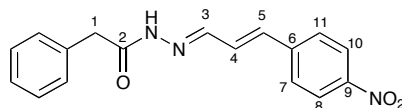
An aqueous solution of hydrazine (62%, 3.23 mL, 67 mmol) was added to a solution of methyl phenylacetate (500 mg, 3.33 mmol) in MeOH (4 mL). The reaction mixture was stirred at rt for 48 h then solvent evaporated under reduced pressure. The product was crystallised from diethyl ether, collected by filtration and washed with cold MeOH and diethyl ether. The filtrate was concentrated under reduced pressure and the crystallisation procedure was repeated a further 3 times. Combination of the four batches of crystallised product gave title compound as a colourless crystalline solid (323 mg, 65%). Mp 115–117 °C [lit.¹⁰⁴ 116 °C]; ν_{\max} (evaporated film)/cm⁻¹ 3293 (s, N-H), 3180 (m, N-H), 3031 (m, C-H), 1644 (s, C=O), 1530 (m, C=C); ¹H NMR (500 MHz, CDCl₃) δ 7.38–7.33 (2H, m, 2 × Ar-CH), 7.33–7.28 (1H, m, Ar-CH), 7.28–7.24 (2H, m, 2 × Ar-CH), 6.77 (1H, brs, NH), 3.85 (2H, brs, NH₂), 3.58 (2H, s, C(2)H₂); ¹³C NMR (400 MHz, CD₃OD) δ 173.3 (C(1)), 136.8 (C(6)), 130.2 (2 × Ar-CH), 129.7 (2 × Ar-CH), 128.1 (C(3)), 41.9 (C(2)); *m/z* (–ve ion electrospray) 149.2 ([M–H]⁻, 100%), (+ve ion electrospray) 173.1 ([M+Na]⁺, 100%); (Found 173.0694, C₈H₁₀N₂NaO ([M+Na]⁺), requires 173.0685).

2-{2-[3-(5-Nitro-2-furyl)-2-propen-1-ylidene]hydrazino}-2-oxoethylbenzene. (17)



(*E*)-3-(5-nitro-2-furyl)acrylaldehyde (128 mg, 0.77 mmol) was added under nitrogen to a solution of acyl hydrazide, **83** (173 mg, 1.15 mmol) in anhydrous MeOH (4 mL). The reaction mixture was stirred at rt for 17 h until a yellow precipitate formed. The solid was filtered and washed with pentane (3 × 5 mL) yielding the title compound (152 mg, 66%) as a yellow solid. Mp 202–204 °C; ν_{\max} (evaporated film)/cm⁻¹ 3137 (w, N-H), 3040 (w, C-H), 2971 (brw, C-H), 2857 (brw, C-H), 1747 (w, C=O), 1667 (s, C=C), 1587 (m, C=C), 1557 (m, C=C), 1504 (s, C=C); ¹H NMR (300 MHz, CDCl₃) δ 9.04 (1H, brs, NH), 7.53 (1H, d, *J* 9.5 Hz, C(3)H), 7.37 – 7.34 (6H, m, C(8)H and 5 × ArCH), 7.16 (1H, dd, *J* 15.5 & 9.5 Hz, C(4)H), 6.65 (1H, d, *J* 15.5 Hz C(5)H), 6.64 (1H, brs, C(7)H), 4.03 (2H, s, C(1)H₂); ¹³C NMR (100 MHz, *d*₆-DMSO, two isomers, some signals are coincident) δ 172.4 (C=O major isomer), 166.8 (C=O minor isomer), 154.9 (Ar-C), 151.3 (Ar-C), 146.7 (Ar-CH), 143.5 (Ar-CH), 135.4 (Ar-C), 130.6 (Ar-CH), 130.3 (Ar-CH), 129.5 (Ar-CH), 129.1 (Ar-CH), 128.3 (Ar-CH), 128.2 (Ar-CH), 126.6 (Ar-CH), 126.4 (Ar-CH), 123.7 (Ar-CH), 123.1 (Ar-CH), 115.4 (C(7) minor isomer), 115.4 (C(7) minor isomer), 113.4 (C(8) major isomer), 113.4 (C(8) minor isomer), 41.2 (C(1) minor isomer), 38.5 (C(1) major isomer); *m/z* (–ve ion electrospray) 298 ([M–H]⁻, 100%), (+ve ion electrospray) 322 ([M+Na]⁺, 100%); (Found 322.0798, C₁₅H₁₃N₃NaO₄ ([M+Na]⁺), requires 322.0809).

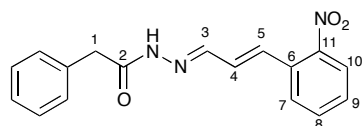
(10E)-N'-((E)-3-(4-Nitrophenyl)allylidene)-2-phenylacetohydrazide. (84)



p-Nitrocinnamaldehyde (39 mg, 0.2 mmol) was added under nitrogen to a solution of 2-phenylacetohydrazide (30 mg, 0.2 mmol) in anhydrous MeOH (1 mL). The reaction mixture was stirred at rt overnight and then Et₂O (5 mL) was added to allow further precipitation to occur. The solid was filtered and washed with Et₂O (10 mL) and pentane (10 mL) yielding the title compound (55 mg, 89%) as a yellow solid. Mp 231–233 °C; ν_{\max} (evaporated film)/cm⁻¹ 3061 (brw, N-H), 2947 (m, C-H), 2879 (w, C-H), 2837 (w, C-H), 1661 (s, C=O), 1593 (m, C=C), 1575 (m, C=C), 1516 (s, C=C); ¹H NMR (400 MHz, *d*₆-DMSO, two isomers) δ 11.65 (s, NH minor isomer), 11.46 (s, NH major isomer), 8.33 – 8.26 (m, Ar-CH), 8.21 (d, *J* 8.7 Hz, Ar-CH), 8.02 (d, *J* 8.7 Hz, Ar-CH), 7.90 – 7.85 (m, Ar-CH), 7.32 – 7.12 (Ar-CH), 3.91 (s, C(1)H₂ major isomer), 3.54 (s, C(1)H₂ minor isomer); ¹³C NMR (100 MHz, *d*₆-DMSO, two isomers some signals are coincident) δ 172.2 (C=O major isomer), 166.7 (C=O minor isomer), 147.6 (Ar-CH), 146.7 (Ar-CH), 146.7 (Ar-CH), 144.6 (Ar-CH), 144.2 (Ar-CH), 142.5 (Ar-CH), 142.8 (Ar-C), 136.3 (Ar-C), 136.2 (Ar-C), 135.7 (Ar-C), 135.4 (Ar-C), 135.4 (Ar-C), 130.0 (Ar-CH), 129.7 (Ar-CH), 129.4 (Ar-CH), 129.1 (Ar-CH), 129.0 (Ar-CH), 128.3 (Ar-CH), 128.3 (Ar-CH), 128.1 (Ar-CH), 128.1 (Ar-CH), 127.9 (Ar-CH), 127.9 (Ar-CH), 126.6 (Ar-CH), 126.5 (Ar-CH), 126.4 (Ar-CH), 126.3 (Ar-CH), 124.0 (Ar-CH), 124.0 (Ar-CH), 123.9 (Ar-CH), 41.0 (C(1))

minor isomer), 38.4 (C(1) major isomer); m/z (-ve ion electrospray) 308 ([M-H]⁻, 100%), (+ve ion electrospray) 332 ([M+Na]⁺, 100%); (Found 332.1022, C₁₇H₁₅NaN₃O₃, ([M+Na]⁺), requires 332.1006).

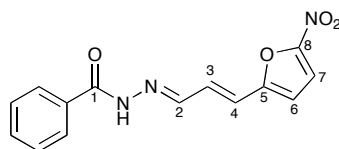
(10E)-N'-((E)-3-(2-Nitrophenyl)allylidene)-2-phenylacetohydrazide. (85)



2-Nitrocinnamaldehyde (118 mg, 0.73 mmol) was added under nitrogen to a solution of 2-phenylacetohydrazide (100 mg, 0.67 mmol) in anhydrous MeOH (1 mL). The reaction mixture was stirred at rt overnight and then Et₂O (5 mL) was added to allow further precipitation to occur. The solid was filtered and washed with Et₂O (10 mL) and pentane (10 mL) yielding the title compound (215 mg, 89%) as a yellow solid. Mp 218–220 °C; ν_{\max} (evaporated film)/cm⁻¹ 3332 (brw, N-H), 2967 (w, C-H), 1659 (s, C=O), 1615 (m, C=C), 1569 (w, C=C), 1553 (m, C=C), 1518 (m, C=C); ¹H NMR (400 MHz, *d*₆-DMSO, two isomers) δ 11.63 (s, NH minor isomer), 11.43 (s, NH major isomer), 8.04 – 7.94 (m, Ar-CH), 7.86 (d, *J* 9.3 Hz, Ar-CH), 7.71 (t, *J* 7.6 Hz, Ar-CH), 7.59 – 7.53 (m, Ar-CH), 7.33 – 7.22 (m, Ar-CH), 7.09 – 7.01 (m, C(4)H major isomer & C(4)H minor isomer), 3.91 (s, C(1)H₂ major isomer), 3.55 (s, C(1)H₂ minor isomer); ¹³C NMR (100 MHz, *d*₆-DMSO, two isomers, some signals are coincident) δ 171.2 (C=O major isomer), 166.7 (C=O minor isomer), 147.8 (Ar-CH), 147.7 (Ar-CH), 147.7 (Ar-CH), 144.6 (Ar-CH), 140.9 (Ar-C), 135.6 (Ar-C), 135.5

(Ar-C), 135.5 (Ar-C), 134.6 (Ar-CH), 133.7 (Ar-CH), 133.5 (Ar-CH), 133.5 (Ar-CH), 132.5 (Ar-CH), 132.0 (Ar-CH), 130.4 (Ar-CH), 130.1 (Ar-CH), 129.9 (Ar-CH), 129.5 (Ar-CH), 129.4 (Ar-CH), 129.2 (Ar-CH), 128.3 (Ar-CH), 128.2 (Ar-CH), 126.6 (Ar-CH), 126.4 (Ar-CH), 124.5 (Ar-CH), 41.1 (C(1) minor isomer), 38.5 (C(1) major isomer); *m/z* (-ve ion electrospray) 308.1 ([M-H]⁻, 100%), (+ve ion electrospray) 332.1 ([M+Na]⁺, 100%); (Found 310.1187, C₁₇H₁₆N₃O₃, ([M+H]⁺), requires 310.1186).

(9E)-N'-(E)-3-(5-Nitrofur-2-yl)allylidene)benzohydrazide. (86)

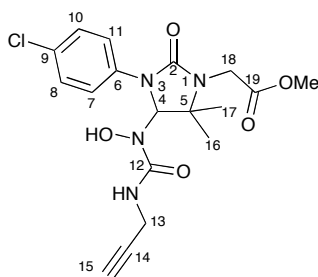


(*E*)-3-(5-nitro-2-furyl)acrylaldehyde (123 mg, 0.74 mmol) was added under nitrogen to a solution of benzhydrazide (100 mg, 0.74 mmol) in anhydrous MeOH (1 mL). The reaction mixture was stirred at rt overnight and then Et₂O (5 mL) was added to allow further precipitation to occur. The solid was filtered and washed with Et₂O (10 mL) and pentane (10 mL) yielding the title compound (112 mg, 53%) as a yellow solid. Mp 226–227 °C; ν_{\max} (evaporated film)/cm⁻¹ 3339 (brw, N-H), 2965 (w, C-H), 1652 (s, C=O), 1631 (m, C=C), 1597 (w, C=C), 1574 (w, C=C), 1548 (w, C=C), 1532 (m, C=C), 1509 (w, C=C); ¹H NMR (400 MHz, *d*₆-DMSO) δ 11.98 (1H, s, NH), 8.26 (1H, d, *J* 8.1 Hz, C(2)H), 7.90 (2H, d, *J* 7.3 Hz, 2 × Ar-CH), 7.76 (1H, d, *J* 3.9 Hz, C(7)H), 7.62 – 7.51 (3H, m, 3 × Ar-CH), 7.17 (1H, d, *J* 3.9 Hz, C(6)H), 7.14 – 7.07 (2H, m, C(3)H & C(4)H); ¹³C NMR (100 MHz, *d*₆-DMSO, some signals are

coincident) δ 163.2 (C(1)), 154.9 (C(8)), 151.4 (C(5)), 147.9 (C(2)), 133.1 (Ar-C), 132.0 (Ar-CH), 130.7 (C(3)), 128.5 (Ar-CH), 127.7 (Ar-CH), 123.9 (C(4)), 115.4 (C(7)), 113.5 (C(6)); m/z (-ve ion electrospray) 284 (100%, [M-H]⁻), (+ve ion electrospray) 286 ([M+H]⁺, 70%), 308 ([M+Na]⁺, 100%); (Found 286.0834, C₁₄H₁₂N₃O₄, ([M+H]⁺), requires 286.0822).

5.2.4 Click Eeyarestatins

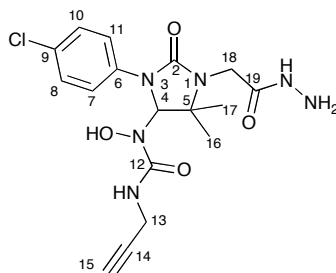
Methyl 2-(3-(4-chlorophenyl)-4-(1-hydroxy-3-(prop-2-ynyl)ureido)-5,5-dimethyl-2-oxoimidazolidin-1-yl)acetate. (87)



1,1-Carbonyldiimidazole (495 mg, 3.05 mmol) was added under an atmosphere of nitrogen to a solution of propargylamine (168 mg, 3.05 mmol) in freshly distilled THF (10 mL). The reaction mixture was stirred at 50 °C for 1.5 h then the mono-adduct, **68** (500 mg, 1.53 mmol) was added. The reaction mixture was stirred for a further 17 h at 50 °C then allowed to cool to rt. Diethyl ether (10 mL) was added and precipitated solid was collected by filtration, washed with diethyl ether (20 mL) and pentane (20 mL) and then dried to give the crude product as a cream solid (619 mg). Purification by flash column chromatography (SiO₂, PE:EtOAc, 2:1) yielded the title

compound as a colourless solid (434 mg, 69%). Mp 177–179 °C; ν_{\max} (evaporated film)/ cm^{-1} 3291 (brm, O-H), 3238 (m, N-H), 2962 (m, C-H), 2933 (m, C-H), 2857 (m, C-H), 1738 (s, C=O), 1703 (s, C=O), 1644 (s, C=C), 1524 (s, C=C), 1495 (s, C=C); ^1H NMR (300 MHz, CDCl_3) δ 7.59 (2H, d, J 7.0 Hz, 2 \times Ar-CH), 7.50 (1H, brs, NH or OH), 7.24 (2H, d, J 7.0 Hz, 2 \times Ar-CH), 6.31 (1H, t, J 5.7 Hz, NH), 6.05 (1H, s, C(4)H), 4.39 (1H, d, J 18.1 Hz, C(18)H_aH_b), 3.99 (2H, dd, J 5.7 & 2.5 Hz, C(13)H), 3.67 (3H, s, CO_2CH_3), 3.60 (1H, d, J 18.1 Hz, C(18)H_aH_b), 2.20 (1H, t, J 2.5 Hz, C(15)H), 1.32 (3H, s, C(17)H₃ or C(18)H₃), 1.27 (3H, s, C(17)H₃ or C(18)H₃); ^{13}C NMR (75 MHz, CDCl_3 , some signals are coincident) δ 172.4 (C(19)) 158.3 (C(2) or C(12)), 156.7 (C(2) or C(12)) 136.9 (Ar-C) 128.8 (Ar-C) 128.7 (Ar-CH), 121.4 (Ar-CH), 80.2 (C(14)), 75.2 (C(4)), 70.7 (C(15)), 58.9 (C(5)), 52.9 (CO_2CH_3), 40.2 (C(18)), 29.5 (C(13)), 25.4 (C(16) or C(17)), 19.2 (C(16) or C(17)), m/z (–ve ion electrospray) 409 ($[\text{M}-\text{H}]^-$, (^{37}Cl), 35%), 407 ($[\text{M}-\text{H}]^-$, (^{35}Cl), 100%), (+ve ion electrospray) 433 ($[\text{M}+\text{Na}]^+$, (^{37}Cl), 25%) 431 ($[\text{M}+\text{Na}]^+$, (^{35}Cl), 100%); (Found 431.1106, $\text{C}_{18}\text{H}_{21}^{35}\text{ClN}_4\text{NaO}_5$ ($[\text{M}+\text{Na}]^+$), requires 431.1093).

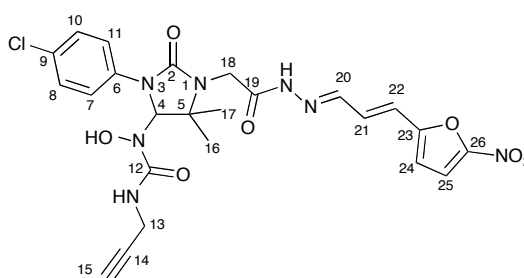
1-(3-(4-Chlorophenyl)-1-(2-hydrazinyl-2-oxoethyl)-5,5-dimethyl-2-oxoimidazolidin-4-yl)-1-hydroxy-3-(prop-2-ynyl)urea. (89)



Hydrazine solution 62% in water (0.6 mL, 619 mg, 12.37 mmol) was added to a solution of methyl ester, **87** (200 mg, 0.489 mmol) in anhydrous MeOH (2 mL). The reaction mixture was stirred at rt for 2.5 h. Then EtOAc (20 mL) and water (10 mL) were added and two phases were separated. The product was extracted further from aqueous layer using EtOAc (2 x 20 mL). The combined organic layers were washed with water several times and dried over Na₂SO₄ then filtered and concentrated under reduced pressure. This yielded the title product (196 mg, 98%) as a white solid. Mp 100–102 °C; ν_{\max} (evaporated film)/cm⁻¹ 3297 (brm, O-H), 2971 (w, C-H), 2933 (w, C-H), 2876 (brw, C-H), 1668 (s, C=O), 1495 (s, C=C); ¹H NMR (500 MHz, CD₃OD) δ 7.64 (2H, d, *J* 8.8 Hz, 2 × Ar-CH), 7.32 (2H, d, *J* 8.8 Hz, 2 × Ar-CH), 6.01 (1H, s, C(4)H), 4.05 (1H, d, *J* 17.4 Hz, C(18)H_aH_b), 3.93–3.92 (2H, m, C(13)H₂), 3.80 (1H, d, *J* 17.4 Hz, C(18)H_aH_b), 2.50 (1H, brs, C(15)H), 1.36 (3H, s, C(16)H₃ or C(17)H₃), 1.32 (3H, s, C(16)H or C(17)H); ¹³C NMR (75 MHz, CD₃OD) δ 171.5 (C(19)), 161.3 (C(2) or C(12)), 158.5 (C(2) or C(12)), 138.8 (Ar-C), 130.2 (Ar-C), 129.9 (Ar-CH), 125.4 (Ar-C), 122.6 (Ar-CH), 86.5 (C(14)), 77.4 (C(4)), 71.9 (C(15)), 61.1 (C(5)), 42.4 (C(18)), 30.4 (C(13)), 25.7 (C(16) or C(17)), 19.3 (C(16) or C(17)); *m/z* (-ve ion electrospray) 409 ([M-H]⁻, (³⁷Cl), 50%) 407 ([M-H]⁻, (³⁵Cl), 100%), (+ve

ion electrospray) 433 ($[M+Na]^+$, (^{37}Cl), 40%) 431 ($[M+Na]^+$, (^{35}Cl), 100%); (Found 431.1195, $C_{17}H_{21}^{35}ClN_6NaO_4$ ($[M+Na]^+$), requires 431.1205).

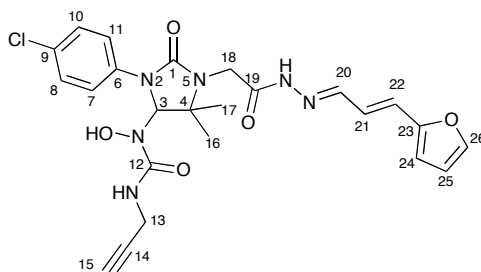
1-(3-(4-Chlorophenyl)-5,5-dimethyl-1-(2-((E)-2-((E)-3-(5-nitrofuranyl)allylidene)hydrazinyl)-2-oxoethyl)-2-oxoimidazolidin-4-yl)-1-hydroxy-3-(prop-2-ynyl)urea. (91)



(*E*)-3-(5-nitro-2-furyl)acrylaldehyde (25 mg, 0.147 mmol) was added under nitrogen to a solution of acyl hydrazide, **89** (60 mg, 0.77 mmol) in anhydrous MeOH (0.6 mL). The reaction mixture was stirred at rt overnight until a yellow precipitate forms. Ether (5 mL) was added to allow further precipitation to occur. The solid was filtered and washed with Et₂O and pentane yielding the title compound (33.5 mg, 49%) as a yellow solid. Mp 159–161 °C; ν_{\max} (evaporated film)/cm⁻¹ 3293 (brm, O-H), 3148 (brm, N-H), 2971 (m, C-H), 2908 (m, C-H), 2848 (m, C-H), 1673 (s, C=O), 1663 (s, C=O), 1516 (m, C=C), 1493 (s, C=C); ¹H NMR (500 MHz, CDCl₃) δ 9.90 (1H, brs, NH or OH), 8.92 (1H, brs, NH or OH), 7.60 (2H, d, *J* 8.9 Hz, 2 × Ar-CH), 7.37 (2H, d, *J* 8.9 Hz, 2 × Ar-CH), 7.33 (1H, d, *J* 3.6 Hz, C(25)H), 7.26 (1H, m, obscured by chloroform peak at 7.27, C(20)H), 6.92 (1H, dd, *J* 15.9 and 9.8 Hz, C(21)H), 6.52 (1H, d, *J* 3.6 Hz, C(24)H), 6.01 (1H, s, C(4)H), 5.84 (1H, t, *J* 5.7 Hz, NH), 5.53 (1H, brd, *J* 15.9 Hz, C(22)H), 4.71 (1H, d, *J* 18.5 Hz, C(18)H_aH_b), 4.07 (1H, d, *J* 18.5 Hz,

C(18)H_aH_b), 3.91 (2H, m, C(13)H), 2.09 (1H, brs, C(15)H), 1.38 (3H, s, C(16)H₃ or C(17)H₃), 1.25 (3H, s, C(16)H₃ or C(17)H₃); ¹³C NMR (100 MHz, *d*₆-DMSO, two isomers, some signals are coincident) δ 169.8 (C=O), 165.4 (C=O), 159.0 (C=O), 158.9 (Ar-C), 157.0 (Ar-C), 155.6 (Ar-C), 154.8 (Ar-C), 154.7 (Ar-C), 154.6 (Ar-C), 151.4 (Ar-C), 151.3 (Ar-C), 147.2 (Ar-CH), 143.7 (Ar-CH), 138.2 (Ar-C), 138.0 (Ar-C), 130.2 (Ar-CH), 130.1 (Ar-CH), 128.4 (Ar-CH), 128.3 (Ar-CH), 128.3 (Ar-CH), 126.5 (Ar-C), 126.1 (Ar-C), 124.2 (Ar-CH), 124.0 (Ar-CH), 123.2 (Ar-CH), 120.1 (Ar-CH), 120.0 (Ar-CH), 115.4 (C(24) major isomer), 115.4 (C(24) minor isomer), 113.6 (C(25) minor isomer), 113.4 (C(25) major isomer), 82.3 (C(14) major isomer), 81.9 (C(14) minor isomer), 74.9 (C(4) major isomer), 74.8 (C(4) minor isomer), 72.5 (C(15) major isomer), 72.2 (C(15) minor isomer), 58.8 (C(5) minor isomer), 58.6 (C(5) major isomer), 41.5 (C(18) minor isomer), 40.2 (C(18) major isomer), 28.9 (C(13) minor isomer), 28.8 (C(13) major isomer), 26.9 (C(16) or C(17) major isomer), 26.2 (C(16) or C(17) minor isomer), 19.2 (C(16) or C(17) major isomer), 18.7 (C(16) or C(17) minor isomer); *m/z* (-ve ion electrospray) 558 ([M-H]⁻, (³⁷Cl), 65%), 556 ([M-H]⁻, (³⁵Cl), 100%), (+ve ion electrospray) 582 ([M+Na]⁺, (³⁷Cl), 30%), 580 ([M+Na]⁺, (³⁵Cl), 100%); (Found 580.1326, C₂₄H₂₄³⁵ClNaN₇O₇, [M+Na]⁺, requires 580.1318).

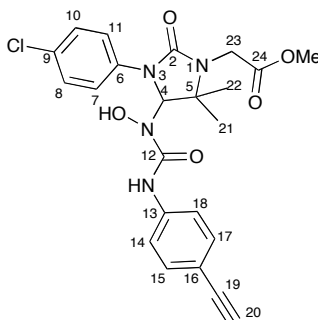
1-(3-(4-Chlorophenyl)-1-(2-((E)-2-((E)-3-(furan-2-yl)allylidene)hydrazinyl)-2-oxoethyl)-5,5-dimethyl-2-oxoimidazolidin-4-yl)-1-hydroxy-3-(prop-2-yn-1-yl)urea. (92)



By using the similar procedure described for **91**, acyl hydrazide **89** (134 mg, 0.312 mmol) and 2-furanacrolein (80 mg, 0.622 mmol) provided the title compound as a pale yellow solid (82.7 mg, 49%). Mp 177.4 °C (dec); ν_{\max} (solid state)/cm⁻¹ 3415 (w, O-H), 3270 (w, N-H), 3132 (brw, N-H), 3125 (brw, C-H), 3079 (brw, C-H), 2928 (w, C-H), 2882 (w, C-H), 1698 (m, C=O), 1662 (s, C=O), 1645 (w, C=O), 1605 (w, C=C), 1526 (m, C=C), 1496 (s, C=C); ¹H NMR (400 MHz, CDCl₃) δ 9.54 (1H, brs, NH or OH), 8.98 (1H, brs, NH or OH), 7.58 (2H, d, *J* 9.0 Hz, 2 × Ar-CH), 7.44 (1H, d, *J* 1.7 Hz, C(26)H), 7.33 (2H, d, *J* 9.0 Hz, 2 × Ar-CH), 7.29 (1H, m, partly obscured by chloroform peak, C(20)H), 6.61 (1H, dd, *J* 15.8 & 9.6 Hz, C(21)H), 6.45 (1H, dd, *J* 3.3 & 1.7 Hz, C(25)H), 6.42 (1H, d, *J* 3.3 Hz, C(24)H), 6.00 (1H, s, C(4)H), 5.93 (1H, brt, *J* 5.6 Hz, NHCH₂CCH), 5.87 (1H, d, *J* 15.8 Hz, C(22)H), 4.74 (1H, d, *J* 18.4, C(18)H_aH_b), 4.06 (1H, d, *J* 18.4, C(18)H_aH_b), 3.99 (2H, dd, *J* 5.6 & 2.5 Hz, C(13)H), 2.09 (1H, t, *J* 2.5 Hz, C(15)H), 1.36 (3H, s, C(16)H₃ or C(17)H₃), 1.26 (3H, s, C(16)H₃ or C(17)H₃); ¹³C NMR (100 MHz, *d*-DMSO, two isomers, some signals are coincident) δ 169.5 (C=O), 165.0 (C=O),

164.5 (C=O), 159.0 (Ar-C), 158.9 (Ar-C), 157.1 (Ar-C), 157.1 (Ar-C), 157.0 (Ar-C), 155.7 (Ar-C), 155.7 (Ar-C), 151.8 (Ar-C), 151.7 (Ar-C), 157.7 (Ar-C), 157.6 (Ar-C), 148.6 (Ar-CH), 145.2 (Ar-CH), 145.2 (Ar-CH), 144.5 (Ar-CH), 144.4 (Ar-CH), 144.3 (Ar-CH), 138.3 (Ar-C), 138.1 (Ar-C), 128.4 (Ar-CH), 128.3 (Ar-CH), 126.5 (Ar-CH), 126.5 (Ar-CH), 126.1 (Ar-CH), 125.7 (Ar-CH), 122.9 (Ar-CH), 122.9 (Ar-CH), 122.8 (Ar-CH), 120.1 (Ar-CH), 119.9 (Ar-CH), 112.6 (C(24) minor isomer), 112.5 (C(24) major isomer), 112.0 (C(25) major isomer), 111.7 (C(25) minor isomer), 82.4 (C(14) major isomer), 82.0 (C(14) minor isomer), 74.9 (C(4) major isomer), 74.8 (C(4) minor isomer), 72.7 (C(15) major isomer), 72.3 (C(15) minor isomer), 58.9 (C(5) minor isomer), 58.6 (C(5) major isomer), 41.6 (C(18) minor isomer), 40.2 (C(18) major isomer), 28.9 (C(13) minor isomer), 28.9 (C(13) major isomer), 27.0 (C(16) or C(17) major isomer), 26.1 (C(16) or C(17) minor isomer), 19.3 (C(16) or C(17) major isomer), 18.6 (C(16) or C(17) minor isomer); *m/z* (-ve ion electrospray) 513 ([M-H]⁻, (³⁷Cl), 100%), 511 ([M-H]⁻, (³⁵Cl), 100%); (Found 511.1505, C₂₄H₂₄³⁵ClN₆O₅, ([M-H]⁻), requires 511.1497).

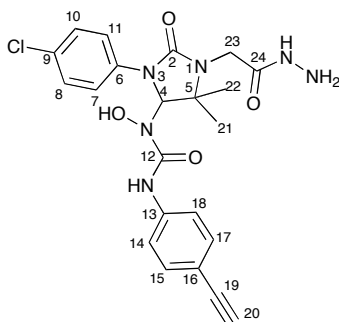
Methyl 2-(3-(4-chlorophenyl)-4-(3-(4-ethynylphenyl)-1-hydroxyureido)-5,5-dimethyl-2-oxoimidazolidin-1-yl)acetate. (88)



1,1-Carbonyldiimidazole (495 mg, 3.05 mmol) was added under nitrogen to a solution of 4-ethynylaniline (358 mg, 3.05 mmol) in freshly distilled THF (6 mL). The reaction mixture was stirred at 50 °C for 1.5 h then **68** (500 mg, 1.53 mmol) was added. The reaction mixture was stirred for 17 h at 50 °C then cooled down to rt. The solvent was then removed under reduced pressure to give a crude yellow solid. The product was purified by flash column chromatography 2:1 PE:EtOAc yielding title compound as a white solid (321 mg, 45%). Mp 179–181 °C; ν_{\max} (evaporated film)/ cm^{-1} 3295 (brm, O-H), 2977 (w, C-H), 2965 (w, C-H), 2868 (w, C-H), 1737 (m, C=O), 1695 (s, C=O), 1674 (s, C=O), 1582 (m, C=C), 1520 (s, C=C), 1497 (s, C=C); ^1H NMR (400 MHz, CDCl_3) δ 8.35 (1H, brs, NH or OH), 8.01 (1H, brs, NH or OH), 7.69 (2H, d, J 8.8 Hz, 2 \times Ar-CH), 7.63 (2H, d, J 8.6 Hz, 2 \times Ar-CH), 7.45 (2H, d, J 8.6 Hz, 2 \times Ar-CH), 7.24 (2H, d, J 8.8 Hz, 2 \times Ar-CH), 6.20 (1H, s, C(4)H), 4.37 (1H, d, J 18.2 Hz, C(23)H_aH_b), 3.56 (1H, d, J 18.2 Hz, C(23)H_aH_b), 3.48 (3H, s, CO_2CH_3), 3.04 (1H, s, C(20)H), 1.35 (C(21)H₃ or C(22)H₃), 1.27 (C(21)H₃ or C(22)H₃); ^{13}C NMR (100 MHz, CDCl_3) δ 171.2 (C(24), 156.8 (C(2) or

C(12)), 155.7 (C(2) or C(12)), 139.3 (2 × Ar-C), 136.8 (2 × Ar-C), 132.9 (2 × Ar-CH), 128.7 (2 × Ar-CH), 121.0 (2 × Ar-CH), 118.5 (2 × Ar-CH), 83.7 (C(19)), 76.4 (C(20)), 74.5 (C(4)), 59.1 (C(5)), 52.9 (CO₂CH₃), 40.2 (C(23)), 25.3 (C(21) or C(22)), 19.2 (C(21) or C(22)) *m/z* (-ve ion electrospray) 471 ([M-H]⁻, (³⁷Cl), 25%), 469 ([M-H]⁻, (³⁵Cl), 100%), (+ve ion electrospray) 495 ([M+Na]⁺, (³⁷Cl), 40%), 493 ([M+Na]⁺, (³⁵Cl), 100%); (Found 493.1260, C₂₃H₂₃³⁵ClNaN₄O₅, ([M+Na]⁺), requires 493.1249).

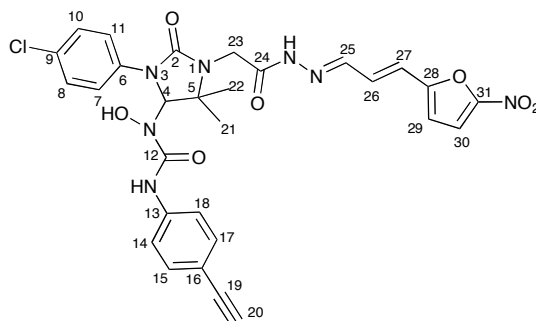
1-(3-(4-Chlorophenyl)-1-(2-hydrazinyl-2-oxoethyl)-5,5-dimethyl-2-oxoimidazolidin-4-yl)-1-hydroxy-3-(4-ethynylphenyl)urea. (90)



Hydrazine solution 62% in water (0.278 mL, 287 mg, 5.74 mmol) was added to a solution of methyl ester, **88** (90 mg, 0.191 mmol) in anhydrous MeOH (1 mL). The reaction mixture was stirred at rt for 1.5 h. Then EtOAc (10 mL) and water (10 mL) were added and two phases were separated. The product was extracted further from aqueous layer using EtOAc (2 x 10 mL). The combined organic layers were washed with water several times and dried over MgSO₄ then filtered and concentrated under reduced pressure. This yielded the title product (85 mg, 94%) as a white solid. Mp

188–190 °C; ν_{\max} (evaporated film)/ cm^{-1} 3288 (brw, O-H), 3218 (w, N-H), 3154 (w, N-H), 2110 (w, C \equiv C), 1699 (m, C=O), 1683 (s, C=O), 1672 (s, C=O), 1583 (w, C=C), 1519 (s, C=C), 1495 (s, C=C); ^1H NMR (400 MHz, CD_3OD) δ 7.70 (2H, d, J 8.8 Hz, 2 \times Ar-CH), 7.50 (2H, d, J 8.8 Hz, 2 \times Ar-CH), 7.40 (2H, d, J 8.8 Hz, 2 \times Ar-CH), 7.33 (2H, d, J 8.8 Hz, 2 \times Ar-CH), 6.14 (1H, s, C(4)H), 4.09 (1H, d, J 17.1 Hz, C(23)H_aH_b), 3.82 (1H, d, J 17.1 Hz, C(23)H_aH_b), 2.42 (1H, s, C(20)H), 1.41 (3H, s, C(21)H₃ or C(22)H₃), 1.35 (3H, s, C(21)H₃ or C(22)H₃); ^{13}C NMR (100 MHz, CD_3OD) δ 171.5 (C(24)), 158.7 (C(2) or C(12)), 158.4 (C(2) or C(12)), 141.2 (Ar-C), 140.2 (Ar-C), 138.8 (Ar-C), 133.9 (Ar-C), 133.7 (2 \times Ar-CH), 129.9 (2 \times Ar-CH), 122.5 (2 \times Ar-CH), 121.4 (2 \times Ar-CH), 84.4 (C(19)), 78.1 (C(20)), 77.0 (C(4)), 61.1 (C(5)), 42.4 (C(23)), 25.7 (C(21) or C(22)), 19.4 (C(21) or C(22)); m/z (–ve ion electrospray) 471 ($[\text{M}-\text{H}]^-$, (^{37}Cl) 30%), 469 ($[\text{M}-\text{H}]^-$, (^{35}Cl), 100%); (Found 493.1371, $\text{C}_{22}\text{H}_{23}^{35}\text{ClN}_6\text{NaO}_4$, ($[\text{M}+\text{Na}]^+$), requires 493.1362).

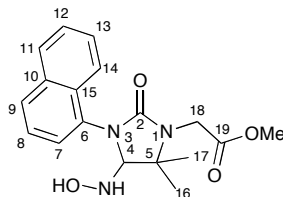
1-(3-(4-Chlorophenyl)-5,5-dimethyl-1-(2-((E)-2-((E)-3-(5-nitrofuranyl)allylidene)hydrazinyl)-2-oxoethyl)-2-oxoimidazolidin-4-yl)-3-(4-ethynylphenyl)-1-hydroxyurea. (93)



(*E*)-3-(5-nitro-2-furyl)acrylaldehyde (33 mg, 0.198 mmol) was added under nitrogen to a solution of acyl hydrazide, **90** (85 mg, 0.198 mmol) in anhydrous MeOH (1 mL). The reaction mixture was stirred at rt for 17 h until a yellow precipitate formed. The solid was filtered and washed with pentane (3 × 5 mL) yielding the title compound as a yellow solid (56.5 mg, 50%). Mp 275 °C (dec); ν_{\max} (evaporated film)/cm⁻¹ 3292 (brm, O-H), 3281 (m, N-H), 3245 (m, N-H), 2919 (w, C-H), 1674 (s, C=O), 1581 (m, C=C), 1556 (w, C=C), 1520 (s, C=C), 1497 (s, C=C); ¹H NMR (400 MHz, CDCl₃) δ 9.93 (1H, brs, NH or OH), 9.46 (1H, brs, NH or OH), 7.73 (1H, brs, NH or OH), 7.69 (2H, d, *J* 9.1 Hz, 2 × Ar-CH), 7.38 (2H, d, *J* 9.1 Hz, 2 × Ar-CH), 7.30 (4H, m, 4 × Ar-CH), 7.25 (1H, m, obscured by chloroform peak at 7.27, C(25)H), 7.16 (1H, d, *J* 3.8 Hz, C(30)H), 6.94 (1H, dd, *J* 15.8 & 9.6 Hz, C(26)H), 6.32 (1H, d, *J* 3.8 Hz, C(29)H), 6.13 (1H, s, C(4)H), 5.47 (1H, d, *J* 15.8 Hz, C(27)H), 4.77 (1H, d, *J* 18.5 Hz, C(23)H_aH_b), 4.11 (1H, d, *J* 18.5 Hz, C(23)H_aH_b), 3.04 (1H, s, C(20)H), 1.43 (3H, s, C(21)H₃ or C(22)H₃), 1.30 (3H, s,

C(21)H₃ or C(22)H₃); ¹³C NMR (100 MHz, *d*₆-DMSO, two isomers, some signals are coincident) δ 169.9 (C=O), 165.4 (C=O), 156.4 (Ar-C), 156.3 (Ar-C), 155.8 (Ar-C), 155.7 (Ar-C), 154.9 (Ar-C), 154.8 (Ar-C), 151.4 (Ar-C), 151.4 (Ar-C), 147.1 (Ar-CH), 143.9 (Ar-CH), 139.8 (Ar-C), 139.6 (Ar-C), 138.3 (Ar-C), 138.1 (Ar-C), 132.1 (Ar-CH), 130.4 (Ar-CH), 130.2 (Ar-CH), 128.5 (Ar-CH), 128.4 (Ar-CH), 127.7 (Ar-C), 126.6 (Ar-C), 126.3 (Ar-C), 124.1 (Ar-CH), 123.3 (Ar-CH), 120.2 (Ar-CH), 120.0 (Ar-CH), 119.7 (Ar-CH), 119.5 (Ar-CH), 115.6 (C(29) minor isomer), 115.5 (C(29) major isomer), 113.6 (C(30) minor isomer), 113.6 (C(30) major isomer), 83.8 (C(19) , 79.7 (C(20) minor isomer), 79.7 (C(20) major isomer), 74.4 (C(4) major isomer), 74.4, (C(4) minor isomer) 58.9 (C(5) minor isomer), 58.7 (C(5) major isomer), 41.6 (C(23) minor isomer), 40.3 (C(23) major isomer), 26.8 (C(21) or C(22) major isomer), 26.4 (C(21) or C(22) minor isomer), 19.3 (C(21) or C(22) major isomer), 19.1 (C(21) or C(22) minor isomer); *m/z* (-ve ion electrospray) 620 ([M-H]⁻, (³⁷Cl), 25%), 618 ([M-H]⁻, (³⁵Cl), 100%); (Found 642.1488, C₂₉H₂₆³⁵ClNaN₇O₇, ([M+Na]⁺), requires 642.1474).

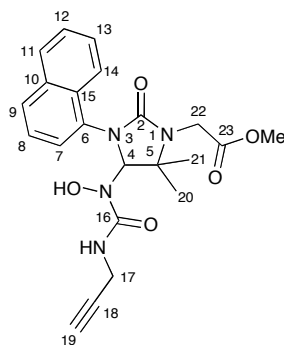
Methyl 2-(4-(hydroxyamino)-5,5-dimethyl-3-(naphthalen-1-yl)-2-oxoimidazolidin-1-yl)acetate. (95)



A solution of 1-naphthyl isocyanate (846 mg, 5 mmol) in freshly distilled THF (6 mL) was added drop-wise, under nitrogen, at 0°C, to a solution of oxime, **67** (870 mg, 5 mmol) in freshly distilled THF (44 mL). The reaction mixture was stirred at rt overnight and then concentrated to afford a mixture of compounds **96** and **72** (1.5:1 ratio; ¹H NMR). This was then purified by flash column chromatography PE:EtOAc 2:1 yielding title compound as a white solid (750 mg, 44%). Mp 127–129 °C; ν_{\max} (evaporated film)/cm⁻¹ 3323 (brm, O-H), 3272 (m, N-H), 2969 (w, C-H), 1751 (s, C=O), 1677 (s, C=O), 1597 (w, C=C), 1559 (w, C=C), 1533 (w, C=C), 1508 (w, C=C), 1499 (w, C=C); ¹H NMR (400 MHz, CDCl₃) δ 7.97 (1H, d, *J* 7.8 Hz, Ar-CH), 7.88 (1H, d, *J* 8.9 Hz, Ar-CH), 7.82 (1H, d, *J* 8.3 Hz, Ar-CH), 7.55–7.47 (4H, m, 4 × Ar-CH), 5.30 (1H, brs, NH or OH), 5.05 (1H, brs, NH or OH), 4.48 (1H, s, C(4)H), 4.17 (1H, d, *J* 17.7 Hz, C(18)H_aH_b), 3.92 (1H, d, *J* 17.7 Hz, C(18)H_aH_b), 3.75 (3H, s, CO₂CH₃), 1.51 (3H, s, C(16)H₃ or C(17)H₃), 1.41 (3H, s, C(16)H₃ or C(17)H₃); ¹³C NMR (100 MHz, CDCl₃) δ 170.8 (C(19)), 157.5 (C(2)), 134.2 (Ar-C), 133.6 (Ar-C), 131.8 (Ar-C), 128.2 (Ar-CH), 127.9 (Ar-CH), 126.3 (2 × Ar-CH), 125.7 (Ar-CH), 125.4 (Ar-CH), 120.7 (Ar-CH), 81.9 (C(4)), 58.9 (C(5)), 52.0 (CO₂CH₃), 40.4 (C(18)), 26.3 (C(16) or C(17)), 19.8 (C(16) or C(17)); *m/z* (+ve ion

electrospray) 366.1 ($[M+Na]^+$, 100%); (Found 366.1419, $C_{18}H_{21}NaN_3O_4$, ($[M+Na]^+$), requires 366.1424).

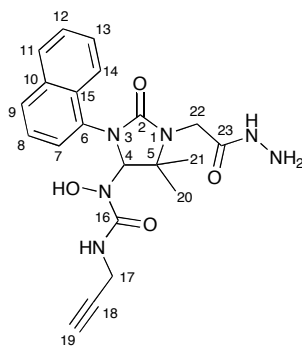
Methyl 2-(4-(1-hydroxy-3-(prop-2-ynyl)ureido)-5,5-dimethyl-3-(naphthalen-1-yl)-2-oxoimidazolidin-1-yl)acetate. (96)



1,1-Carbonyldiimidazole (477 mg, 2.94 mmol) was added under nitrogen to a solution of propargyl amine (162 mg, 2.94 mmol) in freshly distilled THF (6 mL). The reaction mixture was stirred at 50 °C for 1.5 h then mono-adduct, **96** (504 mg, 1.47 mmol) was added. The reaction mixture was stirred overnight at 50 °C then cooled down to rt. Et₂O (6 mL) was added to favour further precipitation. The solid was then filtered, washed with Et₂O and pentane and dried yielding the crude product as a cream solid. Product was purified by flash column chromatography (SiO₂, 2:1 PE:EtOAc) yielding title compound as a white solid (271 mg, 44%). Mp 83–84 °C; ν_{\max} (evaporated film)/cm⁻¹ 3412 (m, O-H), 3291 (brm, N-H), 3055 (m, C-H), 2971 (m, C-H), 2951 (m, C-H), 2920 (m, C-H), 2858 (m, C-H), 1752 (m, C=O), 1675 (s, C=O), 1597 (m, C=C), 1574 (w, C=C), 1516 (s, C=C); ¹H NMR (400 MHz, CDCl₃) δ 8.12 (1H, brs, OH), 7.92 (1H, d, *J* 8.2 Hz, Ar-CH), 7.79 (1H, d, *J* 7.9 Hz, Ar-CH), 7.71 (1H, d, *J* 8.2 Hz, Ar-CH), 7.59 (1H, d, *J* 7.0 Hz, Ar-CH), 7.48–7.39 (2H, m, 2 ×

Ar-CH), 7.27 (1H, t, *J* 7.9 Ar-CH), 6.14 (1H, brt, *J* 5.7 NH), 5.83 (1H, s, C(4)H), 4.14 (1H, d, *J* 18.1 Hz, C(22)H_aH_b), 3.82 (1H, d, *J* 18.1 Hz, C(22)H_aH_b), 3.63 (3H, s, CO₂CH₃), 3.57 (2H, m, C(17)H₂), 2.02 (1H, s, C(19)H), 1.50 (3H, s, C(20)H₃ or C(21)H₃) 1.23 (3H, s, C(20)H₃ or C(21)H₃); ¹³C NMR (100 MHz, CDCl₃) δ 172.0 (C(30)), 158.6 (C(2) or C(16)), 158.3 (C(2) or C(16)), 134.2 (Ar-C), 132.2 (Ar-C), 130.7 (Ar-C), 128.3 (Ar-CH), 128.0 (Ar-CH), 126.4 (Ar-CH), 125.8 (2 × Ar-CH), 125.3 (Ar-CH), 122.2 (Ar-CH), 79.9 (C(18)), 77.7 (C(4)), 70.5 (C(19)), 59.7 (C(5)), 52.4 (CO₂CH₃), 40.6 (C(22)), 29.1 (C(17)), 26.1 (C(20) or C(21)), 19.5(C(20) or C(21)); *m/z* (-ve ion electrospray) 423 ([M-H]⁻, 100%), (+ve ion electrospray) 447 ([M+Na]⁺; (Found 447.1651, C₂₂H₂₄NaN₄O₅, ([M+Na]⁺), requires 447.1639).

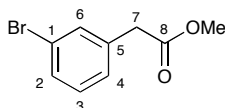
1-(1-(2-Hydrazinyl-2-oxoethyl-5,5-dimethyl-3-(naphthalen-1-yl)-2-oxoimidazolidin-4-yl)-1-hydroxy-3-(prop-2-ynyl)urea. (97)



An aqueous solution of hydrazine (62%, 0.621 mL, 12.80 mmol) was added to a solution of methyl ester, **96** (271 mg, 0.640 mmol) in anhydrous MeOH (2 mL). The reaction mixture was stirred at rt for 2.5 h. Then EtOAc (20 mL) and water (10 mL) were added and two phases were separated. The product was extracted further from

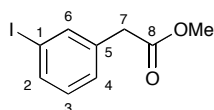
the aqueous layer using EtOAc (2 x 20 mL). The combined organic layers were washed with water several times and dried over Na₂SO₄ then filtered and concentrated under reduced pressure. This yielded the title product (250 mg, 92%) as a white solid. Mp 141–143 °C; ν_{max} (evaporated film)/cm⁻¹ 3296 (brs, O-H), 3056 (s, N-H), 2978 (m, C-H), 2929 (m, C-H), 2868 (m, C-H), 1669 (s, C=O), 1597 (m, C=C), 1520 (s, C=C); ¹H NMR (400 MHz, CD₃OD) δ 7.91 (1H, d, *J* 8.1 Hz, Ar-CH), 7.78 (1H, d, *J* 8.1 Hz, Ar-CH), 7.73 (1H, d, *J* 8.1 Hz Ar-CH), 7.60 (1H, d, *J* 7.0 Hz), 7.46–7.34 (2H, m, 2 × Ar-CH), 7.12–7.08 (1H, m, Ar-CH), 5.80 (1H, s, C(4)H), 3.97 (1H, d, *J* 17.2 Hz, C(22)H_aH_b), 3.75 (1H, d, *J* 17.2 Hz, C(22)H_aH_b), 3.53 (2H, m, C(17)H₂), 3.18 (1H, brt, NH or OH), 2.36 (1H, brs, C(19)H), 1.47 (3H, s, C(20)H₃ or C(21)H₃), 1.32 (3H, s, C(20)H₃ or C(21)H₃); ¹³C NMR (100 MHz, CD₃OD) δ 171.6 (C(23)), 161.9 (C(2) or C(16)), 160.5 (C(2) or C(16)), 136.7 (Ar-C), 136.0 (Ar-C), 132.4 (Ar-C), 130.2 (Ar-CH), 129.6 (2 × Ar-CH), 128.0 (Ar-CH), 127.3 (Ar-CH), 126.7 (Ar-CH), 123.6 (Ar-CH), 81.3 (C(18)), 79.4 (C(4)), 72.0 (C(19)), 61.6 (C(5)), 41.9 (C(22)), 30.1 (C(17)), 26.5 (C(20) or C(21)), 20.1 (C(20) or C(21)); *m/z* (-ve ion electrospray) 423 ([M-H]⁻, 100%), (+ve ion electrospray) 447 ([M+Na]⁺, 100%); (Found 423.1774, C₂₁H₂₃N₆O₄, ([M-H]⁻), requires 423.1781).

Methyl 2-(3-bromophenyl)acetate. (102)



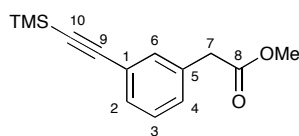
3-Bromophenylacetic acid (1.0 g, 4.7 mmol) was dissolved in MeOH (10 mL), concentrated sulphuric acid (0.1 mL, 3.6 mmol) was added, and the resulting solution was heated under reflux for 16 h. The reaction mixture was concentrated under reduced pressure and the residue was partitioned with DCM (10 mL) and saturated sodium hydrogen carbonate solution (10 mL) and layers separated. The organic layer was dried over MgSO₄, filtered and concentrated under reduced pressure and the resulting oil was purified by flash column chromatography (EtOAc/PE 1:1) to yield the title compound as a colourless oil (1.05 g, 99%) [Lit⁸² oil]; ν_{\max} (evaporated film/cm⁻¹) 3061 (w, C-H), 2998 (w, C-H), 2952 (m, C-H), 2841 (w, C-H), 2153 (w, C-H), 1739 (s, C=O), 1596 (m, C=C), 1570 (s, C=C); ¹H NMR (400 MHz, CDCl₃) δ 7.45 – 7.44 (1H, brs, C(6)H), 7.41 (1H, dt, *J* 7.1 & 1.9, Ar-CH), 7.23 – 7.17 (2H, m, 2 × Ar-CH), 3.70 (3H, s, OCH₃), 3.60 (2H, s, C(7)H₂); ¹³C NMR (125 MHz, CDCl₃) δ 171.3 (C(8)), 136.0 (Ar-C), 132.3 (Ar-CH), 130.2 (Ar-CH), 130.0 (Ar-CH), 127.9 (Ar-CH), 122.4 (Ar-C), 52.14 (CH₃), 40.6 (C(7)); *m/z* (GC/MS) 230 ([M]⁺, (⁷⁹Br), 80%), 232 ([M]⁺, (⁸¹Br), 79%); (Found 227.9786, C₉H₉⁷⁹BrO₂, ([M]⁺), requires 227.9780).

Methyl 2-(3-iodophenyl)acetate. (105)



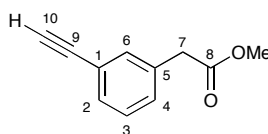
3-Iodophenylacetic acid (500 mg, 1.9 mmol) was dissolved in MeOH (5 mL), concentrated sulphuric acid (0.08 mL, 1.5 mmol) was added, and the resulting solution was heated under reflux for 16 h. The reaction mixture was concentrated under reduced pressure and the residue was partitioned between DCM (5 mL) and saturated sodium hydrogen carbonate solution (5 mL) and layers separated. The organic layer was dried over MgSO₄, filtered and concentrated under reduced pressure and the resulting oil was purified by flash column chromatography (EtOAc/PE 1:1) to yield the title compound as a colourless oil (527 mg, 95%). ν_{\max} (evaporated film/cm⁻¹) 3054 (w, C-H), 2998 (w, C-H), 2949 (m, C-H), 2840 (w, C-H), 1739 (s, C=O), 1590 (s, C=C), 1565 (s, C=C); ¹H NMR (400 MHz, CDCl₃) δ 7.56 (1H, brs, C(6)H), 7.52 (1H, d, *J* 7.7 Hz C(2)H), 7.16 (1H, d, *J* 7.7 Hz, C(4)H), 6.97 (1H, t, *J* 7.7, C(3)H), 3.61 (3H, s, OCH₃), 3.48 (2H, s, C(7)H₂); ¹³C NMR (100 MHz, CDCl₃) δ 171.4 (C(8)), 138.2 (C(6)), 136.2 (C(2)), 136.1 (C(5)), 130.2 (C(3)), 128.6 (C(4)), 94.4 (C(1)), 52.2 (CH₃), 40.5 (C(7)); *m/z* (GC/MS) 276 ([M⁺, 100%]; (Found 275.9648, C₉H₉IO₂, ([M]⁺), requires 275.9642).

Methyl (2-(3-(2-(trimethylsilyl)ethynyl)phenyl)acetate. (103)



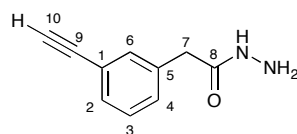
To a solution of **105** (250 mg, 0.91 mmol) and ethynyltrimethylsilane (133 mg, 1.36 mmol) in freshly distilled THF (2.5 mL) under an atmosphere of nitrogen, freshly distilled triethylamine (2.5 mL, 2.16 mmol) was added followed by bis(triphenylphosphine)palladium(II) dichloride (64 mg, 0.091 mmol) and copper(I) iodide (17 mg, 0.091 mmol). The reaction mixture was stirred at rt for 18 h then filtered and concentrated under reduced pressure. The product was extracted with EtOAc (55 mL) washed with saturated NaHCO₃ (3 × 25 mL) and brine (3 × 25 mL) and dried over MgSO₄. The product was purified by flash column chromatography (SiO₂: 20:1 Hexane:DCM then increasing polarity to 5:1 Hexane:DCM, R_f 0.16) to give the title compound as a colourless oil (216 mg, 97%). ν_{\max} (evaporated film/cm⁻¹) 3094 (w, C-H), 3057 (w, C-H), 3024 (w, C-H), 2992 (w, C-H), 2956 (s, C-H), 2898 (w, C-H), 2841 (w, C-H), 2154 (s, C≡C), 1740 (s, C=O), 1602 (m, C=C), 1579 (w, C=C); ¹H NMR (400 MHz, CDCl₃) δ 7.17 (1H, brs, C(6)H), 7.15 (1H, dt, *J* 7.1 & 1.8 Hz, Ar-CH), 7.05 – 6.99 (2H, m, 2 × Ar-CH), 3.46 (3H, s, OCH₃), 3.36 (2H, s, C(7)H₂), 0.02 (9H, s, (CH₃)₃Si); ¹³C NMR (100 MHz, CDCl₃) δ 171.6 (C(8)), 134.0 (Ar-CH), 132.8 (Ar-CH), 130.6 (Ar-CH), 129.5 (Ar-C), 128.4 (Ar-CH), 123.4 (Ar-C), 104.7 (C(9)), 94.4 (C(10)), 52.1 (OCH₃), 40.8 (C(7)), -0.09 ((CH₃)₃Si); *m/z* (+ve ion electrospray) 269 ([M+Na]⁺, 100%); (Found 269.0974, C₁₄H₁₈NaO₂Si, ([M+Na]⁺), requires 269.0968).

Methyl 2-(3-ethynylphenyl)acetate. (106)



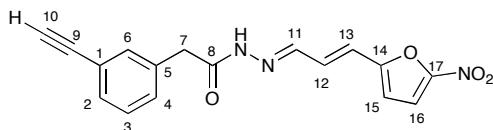
To a stirred solution of **103** (289 mg, 1.17 mmol) in freshly distilled MeCN (6 mL) under an atmosphere of nitrogen, TBAF (1.5 mL of a 1 M solution in THF, 5.05 mmol) was added. The solution was stirred at rt for 18 h then concentrated under reduced pressure. The residue was partitioned between water (40 mL) and EtOAc (40 mL) and layers separated. The organic layer was washed with water (3 × 20 mL) and brine (3 × 20 mL), dried over MgSO₄ and concentrated under reduced pressure to yield a crude product. Purification by flash column chromatography (SiO₂: 5:1 Hexane:DCM, R_f 0.20) gave the title compound as a colourless oil (150 mg, 74%). ν_{\max} (evaporated film/cm⁻¹) 3288 (s, C-H), 3030 (w, C-H), 2997 (w, C-H), 2952 (m, C-H), 2922 (w, C-H), 2846 (w, C-H), 2102 (w, C≡C), 1734 (w, C=O), 1600 (w, C=C), 1580 (w, C=C); ¹H NMR (400 MHz, CDCl₃) δ 7.35 (1H, brs, C(6)H), 7.35 – 7.32 (1H, m, Ar-CH), 7.24 – 7.20 (2H, m, 2 × Ar-CH), 3.63 (3H, s, OCH₃), 3.54 (2H, s, C(7)H₂), 3.00 (1H, s, C(10)H); ¹³C NMR (100 MHz, CDCl₃) δ 171.5 (C(8)), 134.1 (Ar-C), 133.0 (Ar-CH), 130.9 (Ar-CH), 129.8 (Ar-CH), 128.6 (Ar-CH), 122.4 (Ar-C), 83.3 (C(9)), 77.40 (C(10)), 52.1 (OCH₃), 40.8 (C(7)); *m/z* (+ve ion electrospray) 175 ([M+H]⁺, 100%); (Found 197.0581, C₁₁H₁₀NaO₂, ([M+Na]⁺), requires 197.0573).

2-(3-Ethynylphenyl)acetohydrazide. (107)



To a solution of **106** (150 mg, 0.862 mmol) in MeOH (4 mL), an aqueous solution of hydrazine (62%, 1.045 mL, 21.55 mmol) was added. The reaction was stirred at rt for 2 h then concentrated under reduced pressure. The residue was partitioned between water (20 mL) and EtOAc (20 mL) and the layers separated. The organic layer was further washed with water (3 × 20 mL), dried over MgSO₄ and concentrated under reduced pressure to give a crude product. Purification by flash column chromatography (SiO₂: EtOAc:PE 4:1, R_f 0.24) gave the title compound as colourless crystals (115 mg, 77%). Mp 79 – 81 °C; ν_{\max} (evaporated film/cm⁻¹) 3299 (s, N-H or alkyne C-H), 3284 (s, N-H or alkyne C-H), 3239 (s, N-H), 3197 (s, N-H), 3030 (s, C-H), 2879 (w, C-H), 1668 (s, C=O), 1652 (m, C=C), 1637 (s, C=C), 1616 (s, C=C), 1575 (m, C=C), 1557 (m, C=C); ¹H NMR (500 MHz, CD₃OD) δ 7.40 (1H, brs, C(6)H), 7.33 (1H, dt, Ar-CH), 7.29 – 7.24 (2H, m, 2 × Ar-CH), 3.48 (1H, s, C(10)H), 3.43 (2H, s, C(7)H₂); ¹³C NMR (125 MHz, CD₃OD) δ 172.7 (C(8)), 137.2 (Ar-C), 133.7 (C(6)), 131.6 (Ar-CH), 130.7 (Ar-CH), 129.8 (Ar-CH), 124.0 (Ar-C), 84.4 (C(9)), 79.0 (C(10)), 41.5 (C(7)); *m/z* (GC/MS) 174 ([M]⁺, 20%); (Found 174.0783, C₁₀H₁₀N₂O, ([M]⁺), requires 174.0788).

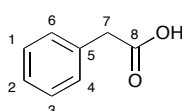
(12E)-2-(3-Ethynylphenyl)-N'-((E)-3-(5-nitro-2-furyl)allylidene)acetohydrazide. (99)



To a stirred solution of **107** (72 mg, 0.621 mmol) in freshly distilled MeOH (3 mL) under an atmosphere of nitrogen, (*E*)-3-(5-nitro-2-furyl)acrylaldehyde (114 mg, 0.683 mmol) was added. The reaction solution was stirred at rt for 18 h until a precipitate was formed. The solid was filtered and washed with cold MeOH (3 × 10 mL) and Et₂O (3 × 10 mL) to give the title compound as a yellow solid (70 mg, 53%). Mp 192 °C (dec); ν_{\max} (evaporated film/cm⁻¹) 3030 (w, N-H), 2933 (w, C-H), 2911 (w, C-H), 2857 (w, C-H), 2836 (w, C-H), 1663 (s, C=O), 1659 (s, C=C), 1575 (w, C=C) 1559 (m, C=C), 1505 (w, C=C); ¹H NMR (400 MHz, CDCl₃) δ 8.83 (1H, brs, NH), 7.51 – 7.47 (2H, m, C(11)H & Ar-CH), 7.42 – 7.30 (4H, m, C(16)H & 3 × Ar-CH), 7.15 (1H, dd, *J* 16.4 & 9.1 Hz, C(12)H), 6.66 (1H, d, *J* 16.4 Hz, C(13)H), 6.64 (1H, brs, C(15)H), 4.01 (2H, s, C(7)H₂), 3.08 (1H, s, C(10)H); ¹³C NMR (100 MHz, *d*₆-DMSO, two isomers, some signals are coincident) δ 172.1 (C=O), 166.4 (C=O), 154.9 (Ar-C), 154.9 (Ar-C), 151.3 (Ar-C), 146.8 (Ar-CH), 143.6 (Ar-CH), 136.0 (Ar-C), 135. (Ar-C), 132.8 (Ar-CH), 132.4 (Ar-CH), 130.5 (Ar-CH), 130.4 (Ar-CH), 130.2 (Ar-CH), 130.0 (Ar-CH), 129.9 (Ar-CH), 129.8 (Ar-CH), 129.0 (Ar-CH), 128.7 (Ar-CH), 128.6 (Ar-CH), 128.2 (Ar-CH), 126.8 (Ar-CH), 125.9 (Ar-CH), 123.8 (Ar-CH), 123.2 (Ar-CH), 121.7 (Ar-C), 121.5 (Ar-C), 115.4 (C(16) major isomer), 115.4 (C(16) minor isomer), 113.4 (C(15) minor isomer), 113.4 (C(15))

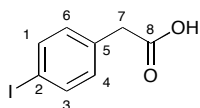
major isomer), 83.5 (C(9) major isomer), 83.4 (C(9) minor isomer), 80.8 (C(10) minor isomer), 80.7 (C(10) major isomer), 40.6 (C(7) minor isomer), 38.1 (C(7) major isomer); m/z (+ve ion electrospray) 346 ($[M+Na]^+$, 100%); (Found 346.0802, $C_{17}H_{13}N_3NaO_4$, ($[M+Na]^+$), requires 346.0799).

2-Phenylacetic acid. (109)



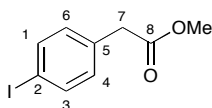
To a solution of methylphenylacetate (5.00 g, 33 mmol) in THF (100 mL) under an atmosphere of nitrogen, LiOH (100 mL of a 1 M solution in water, 100 mmol) was added. The solution was stirred at rt for 4 h then concentrated under reduced pressure. The residue was partitioned between water (100 mL) and DCM (100 mL) and the layers separated. To the aqueous layer 1M HCl (~50 mL) was added until a precipitate was formed, which was filtered and dried under vacuum to give the title compound as colourless crystals (3.76 g, 83%). Mp 76 – 79 °C (Lit¹⁰⁵ 76 – 76.5 °C); ν_{\max} (evaporated film/cm⁻¹) 3089 (brm, O-H), 3062 (m, C-H), 3032 (m, C-H), 2976 (m, C-H), 2922 (m, C-H), 2733 (w, C-H), 2652 (w, C-H), 2555 (w, C-H), 1699 (s, C=O), 1602 (w, C=C), 1497 (m, C=C); ¹H NMR (400 MHz, CDCl₃) δ 9.76 (1H, brs, CO₂H), 7.38 – 7.30 (5H, m, 5 × Ar-CH), 3.67 (2H, s, C(7)H₂); ¹³C NMR (100 MHz, CDCl₃) δ 178.0 (C(8)), 133.2 (C(5)), 129.4 (2 × Ar-CH), 128.6 (2 × Ar-CH), 127.3 (Ar-CH), 41.0 (C(7)); m/z (-ve ion electrospray) 135 ($[M-H]^-$, 100%); (Found 135.0457, $C_8H_7O_2$, ($[M-H]^-$), requires 135.0452).

2-(4-Iodophenyl)acetic acid. (110)



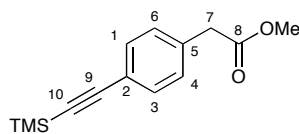
To a stirred solution of iodine (1.25 g, 4.94 mmol) and **109** (3.36 g, 24.7 mmol) in glacial acetic acid (45 mL), a mixture of HNO₃ (1.10 mL of a 70% solution) and concentrated H₂SO₄ (4.42 mL) was added drop-wise over 30 minutes. The reaction mixture was stirred at 60 °C for 1.5 h then cooled to rt and allowed to stir for a further 18 h. After the allotted time most of the iodine colour had disappeared AND the resulting solution was poured onto ice (110 g) to form a white precipitate, which was filtered under vacuum to give a crude product. Recrystallisation from hexane gave the title compound as colourless crystals (2.92 g, 45%). Mp 135 – 137 °C (Lit¹⁰⁶ 135 °C); ν_{\max} (evaporated film/cm⁻¹) 3401 (brs, O-H), 3320 (s, C-H), 3235 (m, C-H), 3186 (m, C-H), 1699 (s, C=O), 1653 (m, C=C), 1637 (w, C=C), 1616 (w, C=C), 1559 (w, C=C), 1505 (w, C=C); ¹H NMR (400 MHz, CDCl₃) δ 7.67 (2H, d, *J* 8.3 Hz, C(1)H & C(3)H), 7.04 (2H, d, *J* 8.3 Hz, C(4)H & C(6)H), 3.60 (2H, s, C(7)H₂); ¹³C NMR (100 MHz, CDCl₃) δ 176.6 (C(8)), 137.7 (C(1) & C(3)), 132.8 (C(5)), 131.3 (C(4) & C(6)), 93.0 (C(2)), 40.4 (C(7)); *m/z* (-ve ion electrospray) 261 ([M-H]⁻, 100%); (Found 260.9406, C₈H₆IO₂, ([M-H]⁻), requires 260.9418).

Methyl 2-(4-iodophenyl)acetate. (111)



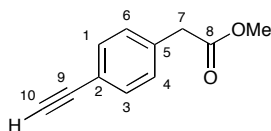
Acid, **110** (1.66 g, 6.35 mmol) was dissolved in MeOH (9 mL), concentrated sulfuric acid (0.27 mL, 1.5 mmol) was added, and the resulting solution was heated under reflux for 16 h. The reaction mixture was concentrated under reduced pressure and the residue was partitioned between DCM (20 mL) and saturated sodium hydrogen carbonate solution (20 mL) and the layers were separated. The organic layer was dried over MgSO₄, filtered and concentrated under reduced pressure giving the title product as a colourless oil (1.67 g, 95%). ν_{\max} (evaporated film/cm⁻¹) 3023 (m, C-H), 2998 (m, C-H), 2949 (s, C-H), 2840 (w, C-H), 1734 (s, C=O), 1627 (w, C=C), 1589 (w, C=C), 1565 (w, C=C), 1522 (w, C=C); ¹H NMR (400 MHz, CDCl₃) δ 7.66 (2H, d, *J* 8.0 Hz, C(1)H & C(3)H), 7.04 (2H, d, *J* 8.0, C(4)H & C(6)H), 3.70 (3H, s, OCH₃), 3.58 (2H, s, C(7)H₂); ¹³C NMR (100 MHz, CDCl₃) δ 171.4 (C(8)), 137.6 (C(1) & C(3)), 133.5 (C(5)), 131.3 (C(4) & C(6)), 92.6 (C(2)), 52.2 (OCH₃), 40.6 (C(7)); *m/z* (GC/MS) 276 ([M]⁺, 100%); (Found 275.9637, C₉H₉IO₂, ([M]⁺), requires 275.9642).

Methyl (2-(4-(2-(trimethylsilyl)ethynyl)phenyl)acetate. (112)



To a solution of **111** (500 mg, 1.81 mmol) and ethynyltrimethylsilane (266 mg, 2.72 mmol) in freshly distilled THF (5 mL) under an atmosphere of nitrogen, freshly distilled triethylamine (5 mL, 4.31 mmol) was added followed by bis(triphenylphosphine)palladium(II) dichloride (127 mg, 0.18 mmol) and CuI (34 mg, 0.18 mmol). The reaction mixture was stirred at rt for 18 h then filtered and concentrated under reduced pressure. The product was extracted with EtOAc (100 mL) washed with saturated NaHCO₃ (3 × 50 mL) and brine (3 × 50 mL) and dried over MgSO₄. The product was purified by flash column chromatography (SiO₂: 20:1 Hexane:DCM then increasing polarity to 5:1 Hexane:DCM) to give the title compound as a colourless oil (429 mg, 96%). *R_f* 0.16; ν_{\max} (evaporated film/cm⁻¹) 3024 (w, C-H), 2997 (w, C-H), 2955 (m, C-H), 2900 (w, C-H), 2836 (w, C-H), 2158 (m, C≡C), 1740 (s, C=O), 1507 (m, C=C); ¹H NMR (400 MHz, CDCl₃) δ 7.43 (2H, d, *J* 8.2 Hz, C(1)H & C(3)H), 7.22 (2H, d, *J* 8.2 Hz, C(4)H & C(6)H), 3.69 (3H, s, OCH₃), 3.62 (2H, s, C(7)H), 0.25 (9H, s, (CH₃)₃Si); ¹³C NMR (100 MHz, CDCl₃) δ 171.5 (C(8)), 134.3 (C(5)), 132.1 (C(1) & C(3)), 129.1 (C(4) & C(6)), 121.9 (C(2)), 104.7 (C(9)), 94.2 (C(10)), 52.1 (OCH₃), 41.0 (C(7)), -0.08 ((CH₃)₃Si); *m/z* (-ve ion electrospray) 245 ([M-H]⁻, 100%), (+ve ion electrospray) 269 ([M+Na]⁺, 100%); (Found 247.1156, C₁₄H₁₉O₂Si, ([M+H]⁺), requires 247.1149).

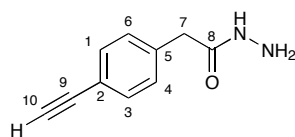
Methyl 2-(4-ethynylphenyl)acetate. (113)



To a stirred solution of **112** (429 mg, 1.74 mmol) in freshly distilled MeCN (6 mL) under an atmosphere of nitrogen, TBAF (2.19 mL of 1 M solution in THF, 7.56 mmol) was added. The solution was stirred at rt for 18 h then concentrated under reduced pressure. The residue was partitioned between water (80 mL) and EtOAc (80 mL) and layers separated. The organic layer was washed with water (3 × 40 mL) and brine (3 × 40 mL), dried over MgSO₄ and concentrated under reduced pressure to yield a crude product. Purification by flash column chromatography (SiO₂: 5:1 Hexane:DCM, R_f 0.20) gave the title compound as a colourless oil (250 mg, 83%).

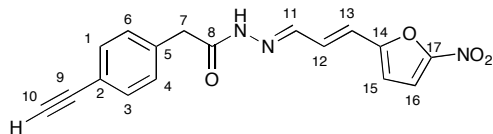
ν_{\max} (evaporated film/cm⁻¹) 3282 (s, C-H), 3032 (m, C-H), 3000 (m, C-H), 2952 (s, C-H), 2843 (w, C-H), 2108 (w, C≡C), 1737 (s, C=O), 1610 (w, C=C), 1565 (w, C=C), 1509 (s, C=C); ¹H NMR (400 MHz, CDCl₃) δ 7.46 (2H, d, *J* 8.1 Hz, C(1)H & C(3)H), 7.25 (2H, d, *J* 8.1 Hz, C(4)H & C(6)H), 3.70 (3H, s, OCH₃), 3.64 (2H, s, C(7)H), 3.08 (1H, s, C(10)H); ¹³C NMR (100 MHz, CDCl₃) δ 171.5 (C(8)), 134.7 (C(5)), 132.3 (C(1) & C(3)), 129.3 (C(4) & C(6)), 120.9 (C(2)), 83.4 (C(9)), 77.4 (C(10)), 52.1 (OCH₃), 41.0 (C(7)); *m/z* (+ve ion electrospray) 175 ([M+H]⁺, 45%), 197 ([M+Na]⁺, 100%); (Found 175.0756, C₁₁H₁₁O₂, ([M+H]⁺), requires 175.0754).

2-(3-Ethynylphenyl)acetohydrazide. (114)



To a solution of **113** (118 mg, 0.68 mmol) in MeOH (3 mL), an aqueous solution of hydrazine (62%, 0.97 mL, 1.00 g, 19.97 mmol) was added. The reaction was stirred at rt for 2 h then concentrated under reduced pressure. The residue was partitioned between water (15 mL) and EtOAc (15 mL) and the layers were separated. The organic layer was further washed with water (3 × 15 mL), dried over MgSO₄ and concentrated under reduced pressure to give a crude product. Purification by flash column chromatography (SiO₂: EtOAc:PE 3:1, R_f 0.24) gave the title compound as colourless crystals (117 mg, 99%). Mp 79 – 81 °C; ν_{\max} (evaporated film/cm⁻¹) 3333 (s, N-H or alkyne C-H), 3294 (m, N-H or alkyne C-H), 3202 (w, N-H), 3030 (w, C-H), 2954 (w, C-H), 1736 (w, C=O), 1651 (m, C=C), 1642 (s, C=C), 1616 (s, C=C), 1525 (m, C=C), 1505 (w, C=C); ¹H NMR (300 MHz, CD₃OD) δ 7.38 (2H, d, *J* 7.9 Hz, C(1)H & C(3)H), 7.25 (2H, d, *J* 7.9 Hz, C(4)H & C(6)H), 3.44 (2H, s, C(7)H₂), 3.43 (1H, s, C(10)H); ¹³C NMR (100 MHz, CD₃OD) δ 172.6 (C(8)), 137.5 (C(5)), 133.1 (C(1) & C(3)), 130.2 (C(4) & C(6)), 122.4 (C(2)), 85.6 (C(9)), 78.7 (C(10)), 41.6 (C(7)); *m/z* (GC/MS) 175 ([M+H]⁺, 20%); (Found 174.0788, C₁₀H₁₀N₂O, ([M]⁺), requires 174.0788).

(12E)-2-(4-Ethynylphenyl)-N'-((E)-3-(5-nitro-2-furyl)-2-allylidene)acetohydrazide. (100)

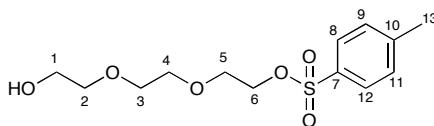


To a stirred solution of **114** (81 mg, 0.462 mmol) in freshly distilled MeOH (2 mL) under an atmosphere of nitrogen, (*E*)-3-(5-nitro-2-furyl)acrylaldehyde (85 mg, 0.509 mmol) was added. The reaction solution was stirred at rt for 18 h until a precipitate was formed. The solid was filtered and washed with cold MeOH (3 × 10 mL) and Et₂O (3 × 10 mL) to give the title compound as a yellow solid (50 mg, 34%). Mp 202 °C (dec); ν_{\max} (evaporated film/cm⁻¹) 3391 (brs, N-H), 3283 (s, C-H), 2938 (w, C-H), 1663 (s, C=O), 1581 (w, C=C), 1556 (w, C=C), 1505 (w, C=C); ¹H NMR (400 MHz, CDCl₃) δ 8.73 (1H, brs, NH), 7.49 (1H, d, *J* 8.8 Hz, C(11)H), 7.47 (2H, d, *J* 7.6 Hz, C(1)H & C(3)H), 7.37 (1H, d, *J* 3.5 Hz, C(16)H), 7.33 (2H, d, *J* 7.6 Hz, C(4)H & C(6)H), 7.15 (1H, dd, *J* 16.2 & 8.8 Hz, C(12)H), 6.66 (1H, d, *J* 16.2 Hz, C(13)H), 6.64 (1H, d, *J* 3.5 Hz, C(15)H); ¹³C NMR (100 MHz, *d*₆-DMSO, two isomers, some signals are coincident) δ 172.0 (C=O), 166.3 (C=O), 154.9 (Ar-C), 154.6 (Ar-C), 151.3 (Ar-C), 146.8 (Ar-CH), 143.6 (Ar-CH), 136.7 (Ar-C), 136.5 (Ar-C), 136.4 (Ar-C), 136.4 (Ar-C), 136.3 (Ar-C), 131.7 (Ar-CH), 131.6 (Ar-CH), 131.6 (Ar-CH), 131.5 (Ar-CH), 130.5 (Ar-CH), 130.2 (Ar-CH), 129.9 (Ar-CH), 129.5 (Ar-CH), 123.8 (Ar-CH), 123.2 (Ar-CH), 120.1 (Ar-C), 119.9 (Ar-C), 115.4 (C(15) major isomer), 115.4 (C(15) minor isomer), 113.5 (C(16) major isomer), 113.4

(C(16) minor isomer), 83.5 (C(9) major isomer), 83.4 (C(9) minor isomer), 80.7 (C(10) minor isomer), 80.5 (C(10) major isomer), 40.9 (C(7) minor isomer), 38.4 (C(7) major isomer); m/z (+ve ion electrospray) 246 ($[M+Na]^+$, 100%); (Found 322.0833, $C_{17}H_{12}N_3O_4$, ($[M-H]$), requires 322.0851).

5.2.5 Click chemistry

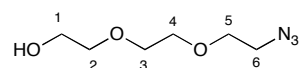
2-[2-(2-Hydroxyethoxy)ethoxy]ethyl 4-methylbenzenesulfonate. (116)



Triethylene glycol (1.00 g, 6.66 mmol) was dissolved in anhydrous pyridine (10 mL) and cooled to 0 °C. *p*-Toluenesulfonyl chloride (1.26 g, 6.66 mmol) in anhydrous pyridine (5 mL) was then added drop-wise to the stirred solution. The reaction solution was stirred for 4 h then ice water (15 mL) was added and the mixture was stirred for a further 1 h. The product was extracted with chloroform (3 x 20 mL), washed with water (3 x 20 mL), dried over magnesium sulfate and concentrated under reduced pressure. Flash column chromatography (EtOAc) gave the title product as a colourless oil (1.244 g, 61%). R_f 0.48; ν_{max} (evaporated film)/ cm^{-1} 3421 (brm, O-H), 2875 (m, C-H), 1718 (w), 1653 (w, C=C), 1646 (w, C=C), 1597 (m, C=C); 1H NMR (400 MHz, $CDCl_3$) δ 7.72 (2H, d, J 7.03 Hz, C(8)H and C(12)H), 7.28 (2H, d, J 7.03 Hz, C(9)H and C(11)H), 4.08–4.07 (2H, m, TEG CH₂), 3.62–3.61 (4H, m, 2 x TEG

CH_2), 3.52 (4H, m, 2 \times TEG CH_2), 3.49–3.48 (2H, m, TEG CH_2), 2.74 (1H, brs, OH), 2.37 (3H, s, C(13) H_3); ^{13}C NMR (100 MHz, CDCl_3 , some signals are coincident) δ 144.72 (C(10)), 132.58 (C(7)), 129.66 (C(8) and C(12)), 127.72 (C(9) and C(11)), 72.29 (TEG CH_2), 70.47 (TEG CH_2), 70.00 (TEG CH_2), 69.04 (TEG CH_2), 68.40 (TEG CH_2), 61.38 (TEG CH_2), 21.40 (C(13)); m/z (+ve ion electrospray) 305 ($[\text{M}+\text{H}]^+$, 100%); (Found 305.1060, $\text{C}_{13}\text{H}_{21}\text{O}_6\text{S}$, ($[\text{M}+\text{H}]^+$), requires 305.1053).

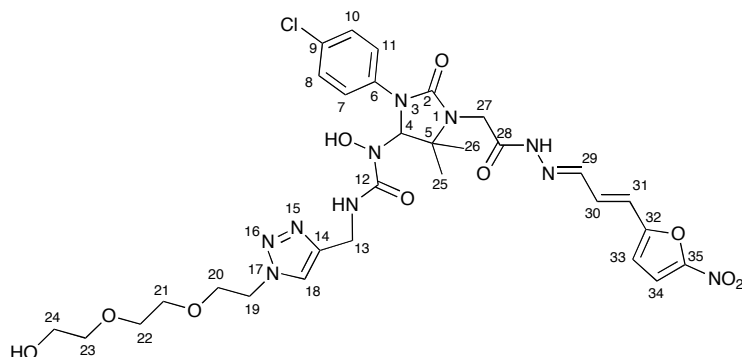
2-[2-(2-Azidoethoxy)ethoxy]ethanol. (117)



Monotosylated triethylene glycol, **116** (500 mg, 1.646 mmol) was dissolved in dry DMF (25 mL). Sodium azide (535 mg, 8.231 mmol) was added under nitrogen and the mixture heated to 70 °C for 17 h. Water (12 mL) was added and the reaction mixture cooled to rt. The product was extracted with EtOAc (3 \times 15 mL), organic layer was washed with water (3 \times 15 mL) dried over magnesium sulphate and concentrated under reduced pressure. Crude oil was purified by flash column chromatography (EtOAc) to give title product as a colourless oil (167 mg, 54%). R_f 0.45; ν_{max} (evaporated film)/ cm^{-1} 3433 (brs, O-H), 2920 (s, C-H), 2876 (s, C-H), 2103 (s, N_3), 1646 (m); ^1H NMR (400 MHz, CDCl_3) δ 3.70 (2H, t, J 4.6 Hz, TEG CH_2OH), 3.66–3.64 (6H, m, 3 \times TEG CH_2), 3.58 (2H, t, J 4.6 Hz, TEG $\text{CH}_2\text{CH}_2\text{N}_3$), 3.37 (2H, t, J 5.1 Hz, CH_2N_3), 2.69 (1H, brs, OH); ^{13}C NMR (100

(m, C-H), 2876 (m, C-H), 1752 (m, C=O), 1701 (s, C=O), 1653 (s, C=O), 1596 (w, C=C), 1521 (m, C=C), 1500 (s, C=C); ^1H NMR (400 MHz, CDCl_3) δ 7.70 (1H, s, C(18)H), 7.53 (2H, d, J 8.9 Hz, 2 \times Ar-CH), 7.14 (2H, d, J 8.9 Hz, 2 \times Ar-CH), 6.75 (1H, brt, J 5.8 Hz, NH), 6.03 (1H, s, C(4)H), 4.42 (2H, m, TEG CH₂), 4.35 (2H, m, partly obscured by multiplet at 4.42, C(13)H₂), 4.06 (1H, d, J 17.7 Hz, C(27)H_aH_b), 3.82 (1H, d, partly obscured by triplet at 3.78, C(27)H_aH_b), 3.78 (2H, t, J 4.9 Hz TEG CH₂), 3.68 (3H, s, CO₂CH₃), 3.59 (2H, m, TEG CH₂) 3.54 (4H, m, 2 \times TEG CH₂), 3.43 (2H, m, TEG CH₂), 1.29 (3H, s, C(25)H₃ or C(26)H₃), 1.27 (3H, s, C(25)H₃ or C(26)H₃); ^{13}C NMR (100 MHz, CDCl_3 , some signals are coincident) δ 170.9 (C(28)), 159.0 (C(2) or C(12)), 156.4 (C(2) or C(12)), 145 (C(14)), 137.1 (Ar-C), 128.5 (2 \times Ar-CH), 128.1 (Ar-C), 123.4 (C(18)), 120.6 (2 \times Ar-CH), 75.0 (C(4)), 72.2 (TEG CH₂), 70.2 (TEG CH₂), 69.9 (TEG CH₂), 69.0 (TEG CH₂), 61.3 (TEG CH₂), 58.9 (C(5)), 52.4 (CO₂CH₃), 50.0 (TEG CH₂), 40.6 (C(27)), 35.1 (C(13)), 26.1 (C(25) or C(26)), 19.3 (C(25) or C(26)); m/z (-ve ion electrospray) 584 ([M-H]⁻, (^{37}Cl), 40%), 582 ([M-H]⁻, (^{35}Cl), 100%), (+ve ion electrospray) 608 ([M+Na]⁺, (^{37}Cl), 30%), 606 ([M+Na]⁺, (^{35}Cl), 100%); (Found 584.2235, $\text{C}_{24}\text{H}_{35}^{35}\text{ClN}_7\text{O}_8$, ([M+H]⁺), requires 584.2230).

1-(3-(4-Chlorophenyl)-5,5-dimethyl-1-(2-((E)-2-((E)-3-(5-nitrofuran-2-yl)allylidene)hydrazinyl)-2-oxoethyl)-2-oxoimidazolidin-4-yl)-1-hydroxy-3-((1-(2-(2-(2-hydroxyethoxy)ethoxy)ethyl)-1H-1,2,3-triazol-4-yl)methyl)urea. (119)

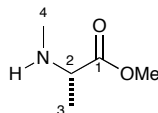


Alkyne ES, **91** (10 mg, 0.018 mmol) and triethylene glycol azide (3 mg, 0.017 mmol) were suspended in a solution of tert-butanol:water 1:1 (1.5 mL). A freshly made up solution of sodium ascorbate (1.8 μ L of a 1 M solution) followed by a freshly made up solution of copper sulphate (0.6 μ L of a 0.3 M solution) were the added to the stirring mixture. The mixture was stirred for 36 h and the product was extracted with chloroform (3 x 5 mL) and washed with brine (5 mL and water (5 mL). The organic layer was dried over MgSO₄ and concentrated under reduced pressure to yield the product as an orange oil (12.9mg, 96%). ν_{\max} (evaporated film)/cm⁻¹ 3384 (brm, O-H), 2929 (m, C-H), 2868 (m, C-H), 2101, (m, -N-N=N-), 1696 (m, C=O), 1684 (s, C=O), 1675 (m, C=O), 1653 (s, C=C), 1559 (m, C=C), 1522 (m, C=C), 1507 (m, C=C); m/z (-ve ion electrospray) 733 ([M-H]⁻, (³⁷Cl), 50%), 731 ([M-H]⁻, (³⁵Cl), 100%), (+ve ion electrospray) 757 ([M+Na]⁺, (³⁷Cl), 50%), 755 ([M+Na]⁺, (³⁵Cl), 100%); (Found 755.2288, C₃₀H₃₇³⁵ClNaN₁₀O₁₀, ([M+Na]⁺), requires 755.2275).

5.3 Synthesis of Cotransin

5.3.1 Solution phase synthesis of Cotransin

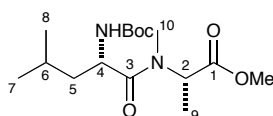
(S)-Methyl 2-(methylamino)propanoate-N-MeAla-OMe. (130)



To a solution of Boc-Ala-OH (1 g, 5.29 mmol) stirring in THF/DMF (10:1, 11 mL) was added MeI (4.28 g, 30.15 mmol) followed by sodium hydride dispersion (60% dispersion in oil) pre-washed with PE (0.543 g, 11.31 mmol) slowly. A reflux condenser fitted with a drying tube containing Drierite™ was attached and the reaction mixture was stirred at 80 °C for 24 h. The solvent was removed under vacuum from the resulting yellow mixture then ether (20 mL) was added and evaporation repeated to remove MeI. The product was extracted with ether (3 × 20 mL), washed with water (3 × 20 mL) dried over MgSO₄ and concentrated under vacuum to give the corresponding methyl ester. This crude product was immediately treated with a 37% solution of HCl in acetic acid for 2 h at rt and concentrated under reduced pressure. The crude product was dissolved in water (25 mL), washed with ether (2 × 10 mL) then evaporated to dryness and stored overnight under vacuum over P₂O₅ to yield the title compound as pale yellow oil (776 mg, 96%). $[\alpha]_D^{21} +7.20$ (*c* 1.0 in MeOH); ν_{\max} (evaporated film)/cm⁻¹ 3370 (brw, N-H), 2947 (brm, C-H), 2736 (brm, C-H), 2457 (brw, C-H), 1733 (s, C=O), 1628 (w), 1571 (w); ¹H NMR (400 MHz, CDCl₃) δ 9.96 (1H, brs, NH), 9.72 (1H, brs, NH), 3.97 (1H, q, *J* 5.8, 12.9 Hz, C(2)H), 3.84 (3H, s, CO₂CH₃), 2.8 (3H, t, *J* 7.4 Hz, C(4)H), 2.88 (3H, d, *J* 7.4

Hz, C(3)H); ^{13}C NMR (100 MHz, CDCl_3) δ 169.0 (C(1)), 56.1 (C(2)), 53.3 (CO₂CH₃), 30.8 (C(4)), 14.2 (C(3)); m/z (+ve ion electrospray) 118 ([M+H]⁺, 100%); (Found 118.0875, C₅H₁₁NO₂, ([M+H]⁺), requires 118.0863).

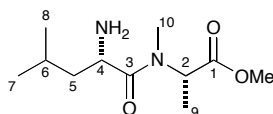
(S)-Methyl 2-((S)-2-((tert-butoxycarbonyl)amino)-N,4-dimethylpentanamido)propanoate. (131)



To a solution of Boc-Leu-OH monohydrate (497 mg, 1.99 mmol) and **130** (350 mg, 2.99 mmol) in DCM/DMF (5:1, 15 mL, 0.1 M) at 0 °C was added HOAt (407 mg, 2.99 mmol), EDCI (765 mg, 3.99 mmol) and NaHCO₃ (251 mg, 2.99 mmol). The ice bath was removed and the reaction allowed to warm to rt and then stirred overnight. The reaction mixture was quenched with HCl (1 M, 20 mL), the organic layer diluted with EtOAc (25 mL) and layers separated. The organic layer was washed with HCl (1 M, 20 mL), saturated NaHCO₃ (2 × 20 mL) and brine (2 × 20 mL) then dried over MgSO₄, filtered and concentrated under reduced pressure. Purification by flash column chromatography (SiO₂, 4:1, PE:EtOAc) gave the title compound as a white crystalline solid (457 mg, 72%). R_f 0.28; Mp 141.9 – 142.4 °C; ν_{max} (solid state)/cm⁻¹ 3296 (brw, N-H), 2958 (brw, C-H), 2871 (brw, C-H), 1746 (m, C=O), 1721 (s, C=O), 1711 (s, C=O), 1503 (m); ^1H NMR (400 MHz, CDCl_3 , major isomer) δ 5.27 – 5.21 (2H, m, NH & C(2)H), 4.67 (1H, m, C(4)H), 3.69 (3H, s, CO₂CH₃), 2.99 (3H, s, C(10)H₃), 1.80 -1.70 (1H, m, C(6)H), 1.46 – 1.39 (14H, m, C(CH₃)₃, C(9)H₃ & C(5)H₂), 0.99 (3H, d, J 6.7 Hz, C(7)H₃ or C(8)H₃), 0.93 (3H, d, J 6.7 Hz, C(7)H₃ or

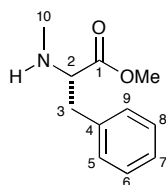
C(8)H₃); ¹³C NMR (100 MHz, CDCl₃) δ 173.4 (CON(CH₃)CH), 172.1 (CO₂CH₃), 155.6 (CO₂C(CH₃)₃), 79.4 (CO₂C(CH₃)₃), 52.2 (CO₂CH₃), 52.0 (C(2)), 48.9 (C(4)), 42.2 (C(5)), 30.9 (C(10)), 28.3 (CO₂C(CH₃)₃), 24.5(C(6)), 23.4 (C(7) or C(8)), 21.7 (C(7) or C(8)), 14.2 (C(9)); *m/z* (+ve ion electrospray) 353 ([M+Na]⁺, 100%); (Found 353.2044, C₁₆H₃₀N₂NaO₅, ([M+Na]⁺), requires 353.2047).

(S)-Methyl 2-((S)-2-amino-N,4-dimethylpentanamido)propanoate. (132)



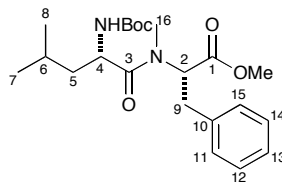
HCl-EtOAc (4 M, 7 mL) was added to neat methyl ester, **131** (239 mg, 0.75 mmol) at 0 °C for 1.5 h. Volatiles were removed with a stream of nitrogen and the sample was further dried under high vacuum to yield the title compound as colourless crystals (166 mg, 96%). This compound can be used in the subsequent reactions without further purification.

(S)-Methyl 2-(methylamino)-3-phenylpropanoate-N-MePhe-OMe. (134)



By using the similar procedure described for **130**, Boc-Phe-OH (1.0 g, 3.77 mmol) provided the title compound as a pale yellow oil (0.770 g, 89%). $[\alpha]_D^{21} +24.0$ (*c* 1.0 in MeOH) [lit¹⁰⁷ $[\alpha]_D^{20} +24.9$ (*c* 0.3 in CHCl₃)]; ν_{\max} (evaporated film)/cm⁻¹ 3366 (brw, N-H), 3027 (brw, C-H), 2955 (brw, C-H) 2747 (brm, C-H), 2692 (brm, C-H), 2434 (brm, C-H), 1737 (s, C=O), 1633 (w, C=C), 1604 (w, C=C), 1569 (w, C=C); ¹H NMR (400 MHz, CDCl₃) δ 10.44 (1H, brs, NH), 9.47 (1H, brs, NH), 7.38 – 7.27 (5H, m, 5 × Ar-H), 4.02 (1H, brs, C(2)H), 3.68 (3H, s, CO₂CH₃), 3.59 (1H, d, *J* 12.2 Hz, C(3)H_aH_b), 3.37 (1H, q, *J* 5.8, 12.2 Hz, C(3)H_aH_b), 2.76 (3H, brs, C(10)H₃); ¹³C NMR (100 MHz, CDCl₃) δ 168.1 (C(1)), 133.9 (C(4)), 129.2 (2 × Ar-CH), 128.9 (2 × Ar-CH), 127.7 (C(7)), 62.6 (C(2)), 53.1 (CO₂CH₃), 35.8 (C(3)), 32.3 (C(10)); *m/z* (+ve ion electrospray) 194 ([M+H]⁺, 100%); (Found 194.1179, C₁₁H₁₆NO₂, ([M+H]⁺), requires 194.1176).

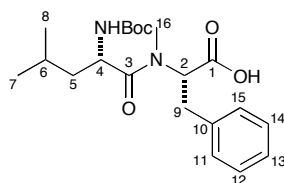
(S)-Methyl 2-((S)-2-((tert-butoxycarbonyl)amino)-N,4-dimethylpentanamido)-3-phenylpropanoate. (135)



To a solution of Boc-Leu-OH monohydrate (120 mg, 0.482 mmol) and **134** (102 mg, 0.530 mmol) in DCM/DMF (5:1, 5 mL, 0.1M) at 0 °C was added HOAt (72 mg, 0.530 mmol), EDCI (185 mg, 0.964 mmol) and NaHCO₃ (45 mg, 0.530 mmol). The ice bath was removed and the reaction allowed to warm to rt and then stirred overnight. The reaction mixture was quenched with HCl (1 M, 10 mL), the organic layer was diluted with EtOAc (15 mL) and the layers separated. The organic layer was washed with HCl (1 M, 10 mL), saturated NaHCO₃ (2 × 10 mL) and brine (2 × 10 mL) then dried over MgSO₄, filtered and concentrated under reduced pressure. Purification by flash column chromatography (SiO₂, 3:1, PE:EtOAc) gave the title compound as a white crystalline solid (371 mg, 76%). *R_f* 0.35; Mp 117.5 – 119.5 °C; ν_{max} (solid state)/cm⁻¹ 3383 (w, N-H), 3028 (w, C-H), 2977 (w, C-H), 2949 (w, C-H), 2917 (w, C-H), 2874 (w, C-H), 1730 (m, C=O), 1703 (s, C=O), 1644 (s, C=O), 1584 (m, C=C), 1516 (w, C=C); ¹H NMR (400 MHz, CDCl₃, major isomer) δ 7.24 – 7.09 (5H, m, 5 x Ar-CH), 5.11 (1H, dd, *J* 10.1 & 5.3 Hz, C(2)H), 4.97 (1H, brd, *J* 9.5 Hz, NH), 4.45 (1H, ddd, *J* 9.5, 9.5 & 4.1 Hz, C(4)H), 3.65 (3H, s, CO₂CH₃), 3.30 (1H, dd, *J* 14.5 & 5.3 Hz, C(9)H_aH_b), 2.97 (1H, dd, *J* 14.5 & 10.1, C(9)H_aH_b), 2.83 (3H, s, C(16)H), 1.67 – 1.57 (1H, m, C(6)H), 1.37 – 1.34 (11H, m, C(CH₃)₃ & C(5)H₂), 0.88 (3H, dd, *J* 6.3 Hz, C(7)H₃ or C(8)H₃), 0.84 (3H, dd, *J* 6.3 Hz, C(7)H₃ or C(8)H₃); ¹³C

NMR (100 MHz, CDCl₃ major isomer) δ 173.4 (CON(CH₃)CH), 171.0 (CO₂OCH₃), 155.4 (CO₂C(CH₃)₃), 136.7 (C(10)), 128.8 (2 \times Ar-CH), 128.4 (2 \times Ar-CH), 126.7 (C(13)), 79.3 (CO₂C(CH₃)₃), 58.8 (C(2)), 52.2 (C(4)), 48.7 (CO₂OCH₃), 42.2 (C(5)), 34.4 (C(16)), 32.9 (C(9)), 28.2 (CO₂C(CH₃)₃), 24.5 (C(6)), 23.3 (C(7) or C(8)), 21.6 (C(7) or C(8)); m/z (+ve ion electrospray) 429 ([M+Na]⁺, 100%); (Found 429.2363, C₂₂H₃₄N₂NaO₅, ([M+Na]⁺), requires 429.2360).

(S)-2-((S)-2-((Tert-butoxycarbonyl)amino)-N,4-dimethylpentanamido)-3-phenylpropanoic acid. (136)



Methyl ester **135** (200 mg, 0.49 mmol) was dissolved in t-BuOH:H₂O (2:1, 0.1 M) and cooled to 0 °C. Lithium hydroxide monohydrate (24 mg, 0.99 mmol) was added and the mixture was stirred for 1.5 h after which HCl (1 M) was added until pH reached 1-2. The product was extracted with EtOAc (3 \times 10 mL) and the combined extracts dried over MgSO₄, filtered and concentrated under reduced pressure to yield the free acid as colourless crystals (190 mg, 98%). This compound can be used in the subsequent reactions without further purification.

5.4 Biochemical experiments.

5.4.1 General methods

Materials

α 1-Antitrypsin antibody was purchased from Calbiochem, anti- α -tubulin antibody was obtained from Abcam and the anti-ubiquitin P4D1 monoclonal antibody was obtained from Santa Cruz Biotechnology inc. (Santa Cruz, CA, USA) and secondary antibodies were purchased from Licor Biosciences. Proteasome inhibitor II (ZLLF-CHO; Benzyloxycarbonyl)-Leu-Leu-phenylalaninal) was obtained from Merck Biosciences. Alexa488 azide was obtained from Invitrogen. T7 and SP6 RNA polymerases, rNTPs, RNasin ribonuclease inhibitor, amino acids and nuclease treated rabbit reticulocyte lysate were obtained from Promega. DNA and RNA purification kits were obtained from Qiagen. All other reagents were obtained from Sigma.

The linear transcription template for ppCec was provided by Nick Johnson in the High lab in the pTNT vector and the mRNA transcript of pPL was provided by Quentin in the High lab. Canine pancreatic ER microsomes and mRNA for pre-procecropin and pre-prolactin were prepared by the High lab according to published protocols.^{108,109} All ES compounds were synthesised as previously described and solubilised at a concentration of 10 mM in DMSO giving a stock solution and stored at $-80\text{ }^{\circ}\text{C}$ prior to use.

Cell Culture

HeLa cells were cultured in DMEM (Sigma) supplemented with 10% fetal bovine serum (FBS) and 2 mM L-glutamine. HepG2 cells were cultured in DMEM supplemented with 10% FBS only.

Splitting cells

Growth media was aspirated and replaced with warm phosphate buffered saline (PBS, 10 mL) then aspirated again. Warm trypsin (3 mL) was then added and the flask returned to 37 °C for 5-15 mins. Gentle tapping every few minutes dislodged cells from the surface. Complete media (7 mL) was added to the trypsinised cells and the solution resuspended to break up any cell clumps by pipetting against the side of the flask 3 times. The cells were split at a 1:3 or 1:4 dilution into 6 or 12 well dishes for use in experiments or 1:10 into a new flask for maintenance.

Semi-intact cell preparation

HeLa cells in a 12-well dish were washed twice with ice-cold PBS then incubated in ice-cold 1× KHM buffer (110 mM KOAc, 2 mM Mg(OAc)₂, 20 mM HEPES, pH 7.2; 0.5 mL per well) containing digitonin (40 µg/mL) for 10 mins. The cells were washed twice with 1× KHM buffer (0.5 mL per well) then incubated in ice-cold 1× HEPES buffer (238 g/L HEPES in H₂O, pH 7.5, 0.5 mL per well) on ice for 10 mins. The cells were washed again with 1× KHM buffer and incubated with 1× KHM buffer (0.2 mL/well) containing CaCl₂ (1 mM) and calcium-dependant monococcal nuclease (10 µg/mL) at RT for 12 mins. The solution was aspirated and the cells incubated in 1× KHM buffer (0.2 mL/well) containing ethylene glycol tetraacetic acid (EGTA, 4 mM) to chelate Ca²⁺ and inactivate the nuclease.

TCA precipitation

1/10 of the total volume of 100% trichloroacetic acid (TCA) was added to each sample, mixed thoroughly and left on ice for 30 mins. Each sample was centrifuged at 4 °C for 30 minutes at 14,000 rpm in a microfuge and the supernatant removed. Each pellet was washed with 1 mL of acetone, centrifuged for 15 mins at 14,000 rpm in a microfuge and the supernatant removed. The pellets were dried at 95 °C for 5 mins then 1× SDS-PAGE sample buffer (100 µL) and DTT (1 M, 10 µL) were added.

SDS-PAGE and sample analysis

SDS-PAGE gels were performed using the Laemmli method¹¹⁰, which involved the solubilisation of samples in 1× SDS sample buffer and denaturation at 37 °C for 1 h before electrophoresis with 8, 10, 12 or 18% tris-glycine acrylamide separating gels. For radiolabelled samples, gels were dried and exposed to phosphorimager plate (Fuji), then scanned using a Fujifilm LAS-3000 system. Quantitative analysis of pixel intensity on phosphorimages was carried out using AIDA v4.0 software.

Western Blotting

Proteins were transferred to a nitrocellulose membrane (Licor Biosciences) in 1× transfer buffer (0.025 M Tris-HCl, pH 8.3, 0.192 M glycine and 0.0013 M SDS, 20% (V/V) MeOH) at 30 mAmps for required time (2.5 h for ubiquitin, 1 h for all other). After this time the membrane was blocked for 1 h at rt in a solution containing 4.5 mL of 1× TBS (0.02 M Tris-HCl, pH 7.6, and 0.15 M NaCl) and 500 µL of 10× blocking buffer (Sigma). The membrane was then blotted with a relevant antibody for 18 h at 4 °C (P4D1 mouse ubiquitin was used 1:500, α -tubulin, albumin and α 1-

AT were used 1:3000) in a solution containing 1× TBS (4.5 mL) and 10× blocking buffer (500 µL). The membrane was then washed four times with 1× TBS (5 mL) and then the blot was incubated for 1 h at rt in a solution containing 1× TBS (4.5 mL), 10× blocking buffer (500 µL) and the corresponding secondary antibody (all secondary antibodies were used 1:5000). The membrane was washed with 1× TBS four times and bands visualised using an Odyssey-SA (Licor Biosciences) infra-red scanner. Bands were quantified using Odyssey software.

Data analysis and statistics

Graphs and statistical analyses were prepared using Microsoft Excel 2004 for Macintosh.

5.4.2 Measurement of Cell Viability (MTT assay)

Approximately 10,000 HeLa cells were plated into each well of a 96 well plate and grown for 24 h. Old media was aspirated and replaced with 200 µL of media containing 2, 4, 8, 16, 32 and 64 µM concentrations of ES compounds or DMSO solvent control in triplicate (i.e. 3 wells per treatment condition) or in triplicate with fresh media in the blanks. The cells were incubated for a further 16 h then the media was aspirated and the cells washed twice with PBS. A 0.05 µg/mL solution of MTT (Sigma) was prepared in 9 mL of DMEM (without phenol red) was added (100 µL per well) and the cells incubated for 2 h. The MTT media was aspirated and DMSO (100 µL) was added to each well and the plate was agitated for 15 minutes. The absorbance of the DMSO solubilised product was measured at 570 nm using a Synergy H1 hybrid reader spectrophotometer (BioTek, USA) and the data compiled

using Gen5 software (Biotek, USA). Cell viability was determined measuring the absorption at 570 nm and calculating the mean of triplicate samples and expressing as a percentage against the mean absorption of DMSO treated cells. Standard deviation for ESI and ES35 was calculated from three sets of data.

5.3.3 Vacuolisation and accumulation of polyubiquitin conjugates

HeLa cells were plated into 6-well dishes and left to grow until 60-70% confluent.

Cells were treated with PSII (10 μ M), ESI, ES35, ES40, ES326, ES328, ES47, ES24, ES24 Click para or ES24 Click meta at 8 μ M or ES47 at 16 μ M at 37°C for 8 h. An Olympus IX51 Inverted microscope was used to take pictures of live cells. Cells were then washed with PBS twice and then lysed 1 \times SDS sample buffer (62.5 mM Tris-HCl, pH 6.8, 10% glycerol, 2% SDS, 0.0025% Bromophenol blue; 100 μ l per well of a 6 or 12-well dish). Cells were solubilised at RT overnight and insoluble material was sonicated using a Diagenode bioruptor at high speed for 5 mins at 4°C. Denaturation of proteins was performed at 37 °C for 1 hour or at 70 °C for 10 minutes and samples centrifuged at 14800 rpm in a microfuge for 5 mins. Samples were analysed by SDS-PAGE and western blotting.

5.4.4 *In vitro* translocation assay

The analysis of translocation inhibition involved two types of assay post-translational translocation and co-translational translocation:

Post-translational translocation: Cell free translation was performed by taking 240 μ l of a translation mixture (200 μ L rabbit reticulocyte lysate supplemented with 6.25 μ L of amino acids (–methionine), 2.5 μ L of RNasin, 25 μ L of water and 19 μ L of

³⁵S Methionine/Cysteine (22 µCi/mL)) and incubating at 30 °C for 15 mins in the presence of an *in vitro* synthesised mRNA transcript of ppCec (24 µL). Translation was stopped upon the addition of puromycin (1 mM, 12 µL) and further incubation for 5 mins, this generated the ³⁵S labelled ppCec. The translation mixture was added to a 12 well dish (20 µL per well) containing freshly prepared semi-permeabilised HeLa cells that had been treated with 10 µM PSII, 8 µM ESI, ES35, ES326, ES328, ES47, ES40, ES24, ES24 Click para, ES24, Click meta or 16 µM ES47 for 1 h. Cells were then incubated at 30 °C for 1 h to allow post-translational translocation of ppCec across the ER membrane of the semi-permeabilised cells.

Co-translational translocation: Translation reactions were assembled as above but on ice to prevent translation and the *in vitro* synthesised mRNA transcript of pre-prolactin (pPL) was added. This mixture was then added to freshly prepared semi-permeabilised HeLa cells that had been treated with PSII (10 µM), ES35, ESI, ES40, ES24 Click para or ES24 Click meta at 8 µM for 1 h. Cells were then incubated with the translation reaction for 1 h at 30 °C to allow co-translational translocation of pPL to occur.

In both post- and co-translational translocation assays the translation mixture was aspirated and the cells were washed with 1× KHM buffer. The cells and associated radiolabelled proteins were then solubilised in 2× SDS-PAGE sample buffer (40 µL) and incubated at 37 °C for 30 min. The samples were analysed by SDS-PAGE using 18% acrylamide gels followed by dried gel phosphorimaging.

5.4.5 Protein secretion from HepG2 cells

Normal media was aspirated from each well of a 6-well dish and washed twice with PBS and cells incubated with starvation media (DMEM lacking methionine and cysteine supplemented with 2 mM glutamine) containing ESI, ES35, ES40, ES326, ES328, ES47, ES24, ES24 Click para, ES24 Click meta at 8 μ M, DMSO 10 μ M, or Brefeldin A (5 μ g/mL, Sigma) for 30 mins at 37 °C. The starvation media was aspirated and replaced with 1 mL pulse media per well (Starvation media containing 2 μ L/mL, 22 μ Ci/mL, 35 S methionine/cysteine) containing the same compounds. The cells were incubated for a further 1 h at 37 °C to allow metabolic labelling of cellular proteins (“Pulse” period). The pulse media was then aspirated and the cells washed twice with PBS and then incubated with chase media (1 mL per well, normal DMEM without FBS) containing the same compounds for a further 1.5 h at 37 °C. During this ‘Chase’ period, the radiolabelled secretory proteins synthesised during the pulse period, were transported along the secretory pathway and released into the media. The chase medium was collected and centrifuged at 4 °C for 5 mins at 10,000 rpm in a microfuge and the supernatant TCA precipitated. The samples were analysed by SDS-PAGE using a 10% acrylamide gel and radioactive proteins were visualised by phosphorimaging. The cells were harvested in 1 \times SDS-PAGE sample buffer (200 μ L), and analysed as above. Cell lysates were also analysed by SDS-PAGE using an 8% acrylamide gel and immunoblotting with α -tubulin and ubiquitin antibodies of the cell samples. The secretion of α 1-anti-trypsin and albumin into the media was specifically analysed by SDS-PAGE using a 12% acrylamide gel and immunoblotting of the TCA precipitation samples.

5.4.6 Click chemistry

ESI Click, ES35 Click, ES47 Click or ESIB Click (250 μM) were incubated with canine pancreatic rough microsomes (10 μL) at 0 $^{\circ}\text{C}$ for 1 h. To ES-treated microsomes the following reagents were added in order: 1% SDS (10% stock in H_2O), Alexa 488- N_3 (50 μM), tris(carboxyethyl)phosphine (TCEP, 1 mM), TBTA (100 μM in 4:1 *tert*-BuOH/ H_2O) and lastly CuSO_4 (1 mM). Reactions were mixed gently and incubated at rt for 2 h. 6 \times SDS-PAGE sample buffer (5 μL) was added, the samples were incubated at 70 $^{\circ}\text{C}$ for 10 minutes and the reactions resolved by SDS-PAGE on 12% acrylamide gels (BioRad). The gels were scanned for fluorescence (480 nm) using a Fujifilm LAS-3000 system.

REFERENCES

1. J. M. Berg, J. L. Tymoczko and L. Stryer, *Biochemistry*, 5th edn., W H Freeman and Company, New York, 2002.
2. B. Alberts, A. Johnson, J. Lewis, M. Raff, K. Roberts and P. Walter, *Molecular Biology Of The Cell*, 4th edn., Garland Publishing Inc., New York, 2002.
3. OpenWetWare, Wellesley College, 2011, http://openwetware.org/wiki/BISC220/S11:_Mod_2_Background.
4. T. Jung, B. Catalgol and T. Grune, *Mol. Aspects. Med.*, 2009, **30**, 191-296.
5. U. Schubert, L. C. Anton, J. Gibbs, C. C. Norbury, J. W. Yewdell and J. R. Bennink, *Nature*, 2000, **404**, 770-774.
6. K. Römisch, *Annu. Rev. Cell. Dev. Biol.*, 2005, **21**, 435-456.
7. K. Römisch, *Traffic*, 2004, **5**, 815-820.
8. S. Vashist and D. T. W. Ng, *J. Cell Biol.*, 2004, **165**, 41-52.
9. A. Sayeed and D. T. W. Ng, *Crit. Rev. Biochem. Mol. Biol.*, 2005, **40**, 75-91.
10. B. Meusser, C. Hirsch, E. Jarosch and T. Sommer, *Nat. Cell. Biol.*, 2005, **7**, 766-772.
11. A. E. Johnson and M. A. van Waes, *Annu. Rev. Cell. Dev. Biol.*, 1999, **15**, 799-842.
12. T. A. Rapoport, *Nature*, 2007, **450**, 663-669.
13. B. C. S. Cross, I. Sinning, J. Luirink and S. High, *Nat. Rev. Mol. Cell. Biol.*, 2009, **10**, 255-264.

14. T. A. Rapoport, *FEBS J.*, 2008, **275**, 4471-4478.
15. S. High, S. S. Andersen, D. Görlich, E. Hartmann, S. Prehn, T. A. Rapoport and B. Dobberstein, *J. Cell. Biol.*, 1993, **121**, 743-750.
16. S. High and B. Dobberstein, *Curr. Opin. Cell Biol.*, 1992, **4**, 581-586.
17. H. P. Wessels and M. Spiess, *Cell*, 1988, **55**, 61-70.
18. T. A. Rapoport, B. Jungnickel and U. Kutay, *Annu. Rev. Biochem.*, 1996, **65**, 271-303.
19. S.-i. Nishikawa, J. L. Brodsky and K. Nakatsukasa, *J. Biochem.*, 2005, **137**, 551-555.
20. R. S. Hegde and H. L. Ploegh, *Curr. Opin. Cell Biol.*, 2010, **22**, 437-446.
21. M. Aebi and A. Helenius, *Annu. Rev. Biochem.*, 2004, **73**, 1019-1049.
22. B. Tsai, Y. Ye and T. A. Rapoport, *Nat. Rev. Mol. Cell. Biol.*, 2002, **3**, 246-255.
23. R. Y. Hampton, *Curr. Opin. Cell Biol.*, 2002, **14**, 476-482.
24. S. S. Vembar and J. L. Brodsky, *Nat. Rev. Mol. Cell. Biol.*, 2008, **9**, 944-957.
25. G. C. Flynn, J. Pohl, M. T. Flocco and J. E. Rothman, *Nature*, 1991, **353**, 726-730.
26. J. B. J. Huppa, T. R.; Story, C. M.; Tortorella, D.; Wiertz, E. J. , *J. Cell. Biol.*, 1998, **142**, 365-376.
27. A. Ciechanover, A. Hershko and I. Rose, "Popular Information", 2004, http://www.nobelprize.org/nobel_prizes/chemistry/laureates/2004/public.html.
28. G. Goldstein, M. Scheid, U. Hammerling, D. H. Schlesinger, H. D. Niall and E. A. Boyse, *Proc. Nat. Acad. Sci.*, 1975, **72**, 11-15.

29. A. Hershko and A. Ciechanover, *Annu. Rev. Biochem.*, 1998, **67**, 425-479.
30. E. J. H. J. Wiertz, D. Tortorella, M. Bogyo, J. Yu, W. Mothes, T. R. Jones, T. A. Rapoport and H. L. Ploegh, *Nature*, 1996, **384**, 432-438.
31. M. Pilon, R. Schekman and K. Römisch, *EMBO J*, 1997, **16**, 4540-4548.
32. Y. Yoshida, *J. Biochem.*, 2003, **134**, 183-190.
33. Y. Ye, Y. Shibata, C. Yun, D. Ron and T. A. Rapoport, *Nature*, 2004, **429**, 841-847.
34. S. Braun, S. Jentsch, K. Matuschewski, M. Rape and S. Thoms, *EMBO J.*, 2002, **21**, 615-621.
35. C. Hirsch, R. Gauss, S. C. Horn, O. Neuber and T. Sommer, *Nature*, 2009, **458**, 453-460.
36. E. Jarosch, C. Taxis, C. Volkwein, J. Bordallo, D. Finley, D. H. Wolf and T. Sommer, *Nat. Cell. Biol.*, 2002, **4**, 134-139.
37. Y. Ye, H. H. Meyer and T. A. Rapoport, *Nature*, 2001, **414**, 652-656.
38. R. Ernst, J. H. L. Claessen, B. Mueller, S. Sanyal, E. Spooner, A. G. van der Veen, O. Kirak, C. D. Schlieker, W. A. Weihofen and H. L. Ploegh, *PLoS Biol*, 2011, **8**, e1000605.
39. R. Ernst, B. Mueller, H. L. Ploegh and C. Schlieker, *Mol. Cell*, 2009, **36**, 28-38.
40. Q. Wang, L. Li and Y. Ye, *J. Cell Biol.*, 2006, **174**, 963-971.
41. Q. Wang, L. Li and Y. Ye, *J. Biol. Chem.*, 2008, **283**, 7445-7454.
42. A. A. McCracken and J. L. Brodsky, *BioEssays*, 2003, **25**, 868-877.
43. R. J. Kaufman, *J. Clin. Invest.*, 2002, **110**, 1389 - 1398.
44. J. Adams, *Cancer Cell*, 2004, **5**, 417-421.

45. E. A. Obeng, L. M. Carlson, D. M. Gutman, W. J. Harrington, K. P. Lee and L. H. Boise, *Blood*, 2006, **107**, 4907-4916.
46. D. R. Fels, J. Ye, A. T. Segan, S. J. Kridel, M. Spiotto, M. Olson, A. C. Koong and C. Koumenis, *Cancer Res.*, 2008, **68**, 9323-9330.
47. R. Z. Orlowski and D. J. Kuhn, *Clin. Cancer. Res.*, 2008, **14**, 1649-1657.
48. D. J. Newman and G. M. Cragg, *J. Nat. Prod.*, 2007, **70**, 461-477.
49. F. Tokunaga, C. Brostrom, T. Koide and P. Arvan, *J. Biol. Chem.*, 2000, **275**, 40757-40764.
50. D. Tortorella, C. M. Story, J. B. Huppa, E. J. H. J. Wiertz, T. R. Jones and H. L. Ploegh, *J. Cell Biol.*, 1998, **142**, 365-376.
51. E. Fiebigler, C. Hirsch, J. M. Vyas, E. Gordon, H. L. Ploegh and D. Tortorella, *Mol. Biol. Cell*, 2004, **15**, 1635-1646.
52. Q. Wang, B. A. Shinkre, J.-g. Lee, M. A. Weniger, Y. Liu, W. Chen, A. Wiestner, W. C. Trenkle and Y. Ye, *PLoS ONE*, 2010, **5**, e15479.
53. B. C. S. Cross, C. McKibbin, A. C. Callan, P. Roboti, M. Piacenti, C. Rabu, C. M. Wilson, R. Whitehead, S. L. Flitsch, M. R. Pool, S. High and E. Swanton, *J. Cell Sci.*, 2009, **122**, 4393-4400.
54. C. McKibbin, Unpublished work, University of Manchester, Manchester, 2008.
55. M. Piacenti, Unpublished work The University of Manchester, Manchester, 2006.
56. H. Harant, N. Lettner, L. Hofer, B. Oberhauser, J. E. de Vries and I. J. D. Lindley, *J. Biol. Chem.*, 2006, **281**, 30492-30502.

57. H. Harant, B. Wolff, E. P. Schreiner, B. Oberhauser, L. Hofer, N. Lettner, S. Maier, J. E. de Vries and I. J. Lindley, *Mol. Pharm.*, 2007, **71**, 1657-1665.
58. J. L. Garrison, E. J. Kunkel, R. S. Hegde and J. Taunton, *Nature*, 2005, **436**, 285-289.
59. J. Besemer, H. Harant, S. Wang, B. Oberhauser, K. Marquardt, C. A. Foster, E. P. Schreiner, J. E. de Vries, C. Dascher-Nadel and I. J. D. Lindley, *Nature*, 2005, **436**, 290-293.
60. A. L. MacKinnon, J. L. Garrison, R. S. Hegde and J. Taunton, *J. Am. Chem. Soc.*, 2007, **129**, 14560-14561.
61. D. L. Boger, H. Keim, B. Oberhauser, E. P. Schreiner and C. A. Foster, *J. Am. Chem. Soc.*, 1999, **121**, 6197-6205.
62. Y. Chen, M. Bilban, C. A. Foster and D. L. Boger, *J. Am. Chem. Soc.*, 2002, **124**, 5431-5440.
63. I. Coin, M. Beerbaum, P. Schmieder, M. Bienert and M. Beyermann, *Org. Lett.*, 2008, **10**, 3857-3860.
64. U. Hommel, H.-P. Weber, L. Oberer, H. Ulrich Naegeli, B. Oberhauser and C. A. Foster, *Febs Lett.*, 1996, **379**, 69-73.
65. R. K. Olsen, *J. Org. Chem.*, 1970, **35**, 1912-1915.
66. J. R. Coggins and N. L. Benoiton, *Can. J. Chem.*, 1971, **49**, 1968-1971.
67. B. H. Lee, G. J. Gerfen and M. J. Miller, *J. Org. Chem.*, 1984, **49**, 2418-2423.
68. A. L. MacKinnon, J. L. Garrison, R. S. Hegde and J. Taunton, *J. Am. Chem. Soc.*, 2007, **129**, 14560-14561.

69. B. L. Kieffer, M. P. Goeldner and C. G. Hirth, *J. Chem. Soc. Chem. Commun.*, 1981, 398-399.
70. H. C. Kolb, M. G. Finn and K. B. Sharpless, *Angew. Chem. Int. Ed.*, 2001, **40**, 2004-2021.
71. V. V. Rostovtsev, L. G. Green, V. V. Fokin and K. B. Sharpless, *Angew. Chem. Int. Ed.*, 2002, **41**, 2596-2599.
72. A. D. Moorhouse and J. E. Moses, *Chem. Med. Chem.*, 2008, **3**, 715-723.
73. X. Fu, C. Albermann, C. Zhang and J. S. Thorson, *Org. Lett.*, 2005, **7**, 1513-1515.
74. T. R. Chan, R. Hilgraf, K. B. Sharpless and V. V. Fokin, *Org. Lett.*, 2004, **6**, 2853-2855.
75. L. J. Beckham, W. A. Fessler and M. A. Kise, *Chem. Rev.*, 1951, **48**, 319-396.
76. A. F. Rukasov, S. P. Epshtein, V. P. Tashchi, Yu. A. Baskakov and Y. G. Putsykin, *Chem. Heterocycl. Comp.*, 1984, 323-325.
77. L. Grehn, B. Fransson and U. Ragnarsson, *J. Chem. Soc., Perkin Trans. 1*, 1987, 529-535.
78. J. Clayden, N. Greeves, S. Warren and P. Wothers, *Organic Chemistry*, OUP, New York, 2001.
79. G. Asato, *US Pat.*, 4154740, 1979.
80. V. Bhowruth, A. K. Brown, R. C. Reynolds, G. D. Coxon, S. P. Mackay, D. E. Minnikin and G. S. Besra, *Bioorg. Med. Chem. Lett.*, 2006, **16**, 4743-4747.
81. K. Sonogashira, Y. Tohda and N. Hagihara, *Tetrahedron Lett.*, 1975, **16**, 4467-4470.

82. J. R. Davies, P. D. Kane and C. J. Moody, *J. Org. Chem.*, 2005, **70**, 7305-7316.
83. E. J. Iwanowicz, S. H. Watterson, T. G. M. Dhar, W. J. Pitts, H. H. Gu, *US Pat.*, WO 0181340, 2001.
84. M. S. Mohamed Ahmed, A. Sekiguchi, K. Masui and A. Mori, *Bull. Chem. Soc. Jap.*, 2005, **78**, 160-168.
85. A. Klapars and S. L. Buchwald, *J. Am. Chem. Soc.*, 2002, **124**, 14844-14845.
86. S. R. Nagarajan, B. Devadas, M. E. Zupec, S. K. Freeman, D. L. Brown, H.-F. Lu, P. P. Mehta, N. S. Kishore, C. A. McWherter, D. P. Getman, J. I. Gordon and J. A. Sikorski, *J. Med. Chem.*, 1997, **40**, 1422-1438.
87. S. M. Waybright, C. P. Singleton, K. Wachter, C. J. Murphy and U. H. F. Bunz, *J. Am. Chem. Soc.*, 2001, **123**, 1828-1833.
88. H. A. Rajapakse, P. G. Nantermet, H. G. Selnick, S. Munshi, G. B. McGaughey, S. R. Lindsley, M. B. Young, M.-T. Lai, A. S. Espeseth, X.-P. Shi, D. Colussi, B. Pietrak, M.-C. Crouthamel, K. Tugusheva, Q. Huang, M. Xu, A. J. Simon, L. Kuo, D. J. Hazuda, S. Graham and J. P. Vacca, *J. Med. Chem.*, 2006, **49**, 7270-7273.
89. G. Noble and S. Webb, University of Manchester, 2008.
90. T. Feizi, H. C. Gooi, P. G. Sinay, *US Pat.*, 4563445, 1986.
91. K. Barlos, D. Gatos, J. Kallitsis, G. Papaphotiu, P. Sotiriu, Y. Wenqing and W. Schäfer, *Tetrahedron Lett.*, 1989, **30**, 3943-3946.
92. <http://www.2-chlorotriptylresins.com/>, aapptec.
93. N. L. Benoiton, *Pept. Sci.*, 1996, **40**, 245-254.

94. C. Kay, O. E. Lorthioir, N. J. Parr, M. Congreve, S. C. McKeown, J. J. Scicinski and S. V. Ley, *Biotechnol. Bioeng.*, 2000, **71**, 110-118.
95. T. Mosmann, *J. Immunol. Methods.*, 1983, **65**, 55-63.
96. S. Sperandio, I. de Belle and D. E. Bredesen, *Proc. Nat. Acad. Sci.*, 2000, **97**, 14376-14381.
97. S. Tardito, C. Isella, E. Medico, L. Marchio, E. Bevilacqua, M. Hatzoglou, O. Bussolati and R. Franchi-Gazzola, *J. Biol. Chem.*, 2009, **284**, 24306-24319.
98. A. Vinitzky, C. Michaud, J. C. Powers and M. Orlowski, *Biochemistry*, 1992, **31**, 9421-9428.
99. R. Wilson, A. J. Allen, J. Oliver, J. L. Brookman, S. High and N. J. Bulleid, *Biochem. J.*, 1995, **307**, 679-687.
100. G. Schlenstedt, G. H. Gudmundsson, H. G. Boman and R. Zimmermann, *J. Biol. Chem.*, 1990, **265**, 13960-13968.
101. J. Beger, T. T. Luong, C. Thielemann and P. D. Thong, *J. Prakt. Chem.*, 1978, **320**, 433-451.
102. K. Venters, S. Hillers, V. Cirule, *UK Pat.*, GB 1109417, 1968.
103. I. Saikawa, S. Takano and T. Maeda, *Yakugaku Zasshi*, 1967, **87**, 1514-1520.
104. T. Curtius and E. Boetzelen, *J. Prakt. Chem.*, 1901, **64**, 314-323.
105. R. Adams and A. F. Thal, *Org. Synth.*, 1922, **2**, 59.
106. J. T. Plati, W. H. Strain and S. L. Warren, *J. Am. Chem. Soc.*, 1943, **65**, 1273-1276.
107. J. D. Park, K. J. Lee and D. H. Kim, *Bioorg. Med. Chem.*, 2001, **9**, 237-243.

108. P. Walter, I. Ibrahimi and G. Blobel, *J. Cell. Biol.*, 1981, **91**, 545-550.
109. V. V. Gurevich, I. D. Pokrovskaya, T. A. Obukhova and S. A. Zozulya, *Anal. Biochem.*, 1991, **195**, 207-213.
110. U. K. Laemmli, *Nature*, 1970, **227**, 680-685.